GEOLOGIJA

2013 | št.: **56/1**

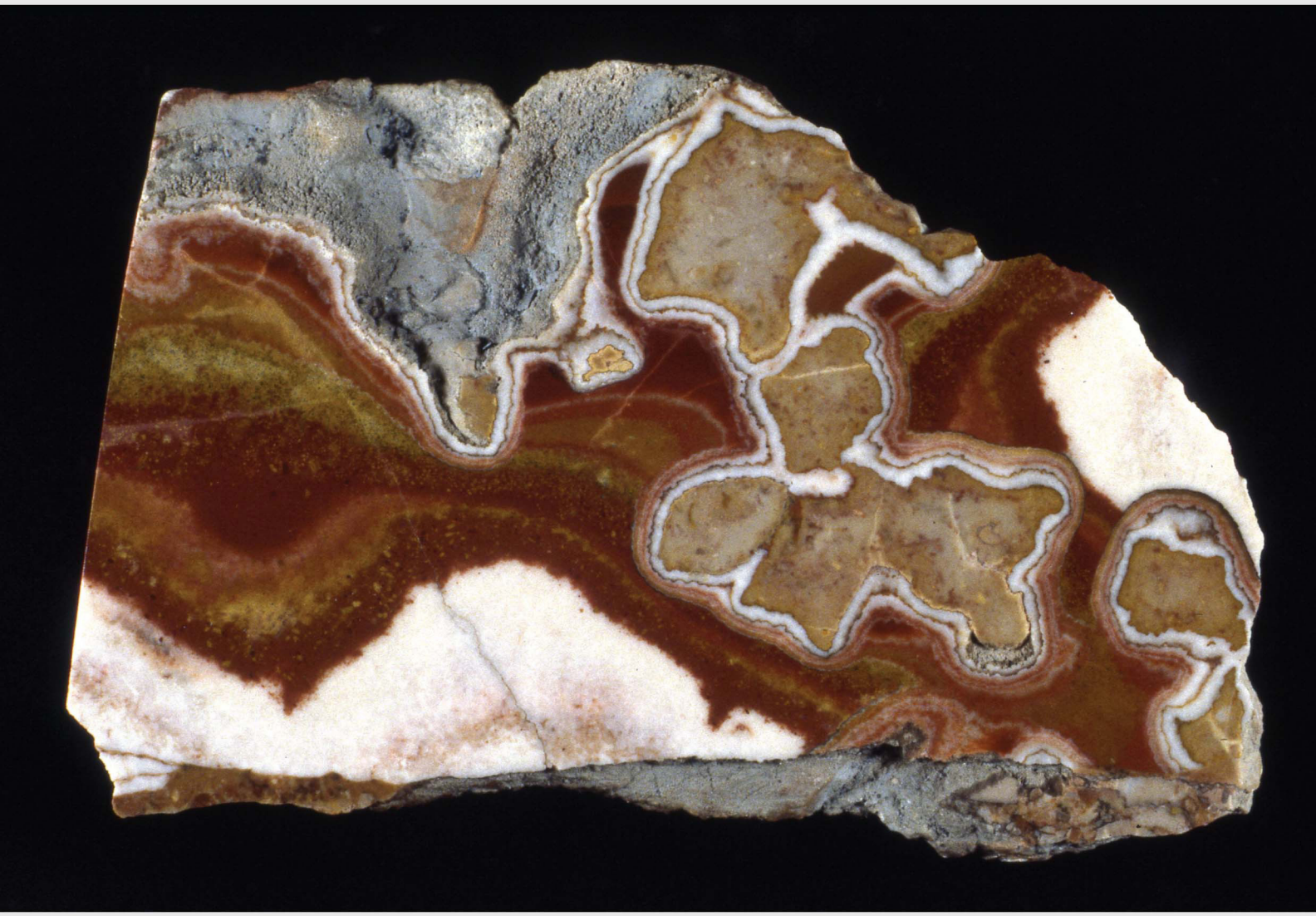

Geološki zavod Slovenije
Geological Survey of Slovenia

ISSN 0016-7789
ISSN 1854-620X

GEOLOGIJA

56/1 – 2013

V spomin dolgoletnemu uredniku prof. dr. Bojanu Ogorelcu
Dedicated to the memory of prof. dr. Bojan Ogorelec

GEOLOGIJA	2013	56/1	1–144	Ljubljana

GEOLOGIJA
ISSN 0016-7789

Izdajatelj: Geološki zavod Slovenije, zanj direktor Marko Komac
Publisher: Geological Survey of Slovenia, represented by Director Marko Komac
Financirata Javna agencija za knjigo Republike Slovenije in Geološki zavod Slovenije
Financed by the Slovenian Book Agency and the Geological Survey of Slovenia

Vsebina številke 56/1 je bila sprejeta na seji Uredniškega odbora, dne 2. 7. 2013.
Manuscripts of the Volume 56/1 accepted by Editorial and Scientific Advisory Board on July 2, 2013.
Glavna in odgovorna urednica / Editor-in-Chief: Mateja Gosar
Tehnična urednica / Technical Editor: Bernarda Bole

Naslov uredništva / Editorial Office: GEOLOGIJA Geološki zavod Slovenije /
Geological Survey of Slovenia, Dimičeva ulica 14, SI-1000 Ljubljana, Slovenija
Tel.: +386 (01) 2809-700, Fax: +386 (01) 2809-753, e-mail: urednik@geologija-revija.si
URL: http://www.geologija-revija.si/

GEOLOGIJA izhaja dvakrat letno. / GEOLOGIJA is published two times a year.
GEOLOGIJA je na voljo tudi preko medknjižnične izmenjave publikacij. /
GEOLOGIJA is available also on exchange basis.

Baze, v katerih je Geologija indeksirana / Indexation bases of Geologija: Directory of Open Access Journals, GeoRef, Zoological Record, Geoscience e- Journals

Cena / Price

Posamezni izvod / Single Issue	Letna naročnina / Annual Subscription
Posameznik / Individual: 15 €	Posameznik / Individual: 25 €
Institucija / Institutional: 25 €	Institucija / Institutional: 40 €

Tisk / Printed by: Tiskarna Formatisk d.o.o.

Slika na naslovni strani: Paleokraška kokardna tekstura v zgornjetriasnem Dachsteinskem apnencu s Krna (Julijske Alpe). Mikrofacies Dachsteinskega apnenca je bil ena glavnih raziskovalnih tematik prof. dr. Bojana Ogorelca. (arhiv: B. Ogorelec)

Cover page: Paleokarstic cockade structure in the Upper Triassic Dachstein Limestone from Mt. Krn (Julian Alps, Slovenia). Microfacies of Dachstein Limestone has been one of the main research interests of prof. dr. Bojan Ogorelec. (archive: B. Ogorelec)

GEOLOGIJA *56/1*, 001–144, Ljubljana 2013

VSEBINA - CONTENTS

GEOLOGIJA *56/1*, 005–018, Ljubljana 2013

doi:10.5474/geologija.2013.001

Accuracy and precision of EDS analysis for identification of metal-bearing minerals in polished and rough particle samples

Točnost in natančnost EDS analize pri prepoznavanju mineralov s kovinami v poliranih vzorcih in grobih delcih

Miloš MILER[1] & Breda MIRTIČ[2]

[1]Geological Survey of Slovenia, Dimičeva ulica 14, Ljubljana, Slovenia;
e-mail: milos.miler@geo-zs.si
[2]Faculty of Natural Sciences and Engineering, Department of Geology, Aškerčeva ulica 12,
SI-1000 Ljubljana, Slovenia;
e-mail: breda.mirtic@guest.arnes.si
Prejeto / Received 27.11. 2012; Sprejeto / Accepted 20. 2. 2013

Key words: EDS analysis, accuracy, precision, polished samples, rough particle samples, metal-bearing phases, mineral identification
Ključne besede: EDS analiza, točnost, natančnost, polirani vzorci, grobi delci, faze s kovinami, identifikacija mineralov

Abstract

The study was carried out in order to estimate reliability of EDS analysis for identification of various natural and anthropogenic metal-bearing phases in polished and rough particle samples of stream sediments. For this purpose, the accuracy and precision of EDS analysis were assessed. Results of the precision measurements showed that the overall relative standard deviation of EDS measurements was 8 % for polished samples and 24 % for rough particle samples and was within acceptable limits for most of major elements and some of the elements present in minor or trace contents in the analysed metal-bearing phases. The random analytical fluctuations were considered negligible and phase compositions could be determined with sufficient reliability in individual grains of each phase. The overall average relative error for all elements amounted to about 12 %, which was within acceptable limits for accuracy in EDS analysis of polished samples. Chemical formulae and identification of mineral species of metal-bearing phases were thus calculated from atomic ratios between constituent elements with sufficient accuracy. A comparison between EDS measurements in polished and rough particle samples using the Welch's t-test showed that about 38 % of studied metal-bearing phases could be identified with sufficient reliability by EDS analysis of rough particle samples. The results of this study demonstrated that elemental composition of metal-bearing phases in polished and rough particle samples was mostly determined with sufficient precision and accuracy using EDS analyses.

Izvleček

Raziskava je bila izvedena z namenom oceniti zanesljivost EDS analize pri identifikaciji raznovrstnih naravnih in antropogenih fazah s kovinami v poliranih vzorcih in vzorcih grobih delcev rečnih sedimentov. V ta namen sta bili ocenjeni točnost in natančnost EDS analize. Rezultati meritev natančnosti so pokazali, da je celotni relativni standardni odklon EDS meritev znašal 8 % za polirane vzorce in 24 % za grobe delce ter je bil znotraj sprejemljivih meja za večino glavnih elementov in nekatere sledne elemente v analiziranih fazah. Naključna analitična nihanja so bila zanemarljiva, tako da je bilo možno z zadostno zanesljivostjo določiti sestavo faz v posameznih kristalnih zrnih. Celotna povprečna relativna napaka za vse elemente je znašala okrog 12 %, kar je bilo znotraj sprejemljivih meja točnosti EDS analize poliranih vzorcev. Kemijske formule in identifikacija mineralnih vrst faz s kovinami so bile z zadovoljivo točnostjo preračunane iz atomskih razmerij med sestavnimi elementi. Primerjava EDS meritev v poliranih vzorcih in grobih delcih z uporabo Welch-evega t-testa je pokazala, da je bilo okrog 38 % faz s kovinami identificiranih z zadostno zanesljivostjo iz analize grobih delcev. Rezultati raziskave so pokazali, da je bila elementarna sestava faz s kovinami v poliranih vzorcih in grobih delcih določena z ustrezno natančnostjo in točnostjo z uporabo EDS analize.

Introduction

In environmental geochemistry, analysed samples or metal-bearing phases are frequently very diverse and may be natural or anthropogenic by origin. This results in limited pre-knowledge of the sample's elemental composition and its identity and thus difficult selection of suitable standards for quantitative EDS analysis. Because suitable standards of natural minerals are often not available for all analysed metal-bearing phases, pre-measured universal fitted standards

included in the EDS software are commonly used instead.

Samples of environmental media that are commonly used in environmental geochemistry are usually so friable that their surface morphologies, important for their characterisation, are destroyed during preparation of polished sections. In these cases, samples with rough, randomly oriented surfaces are analysed, which may introduce severe spectral artifacts and interferences due to significant X-ray absorption and fluorescence effects and consequently affects quantification of elements and identification of their mineral species.

Usefulness of fitted-standards EDS analysis for identification and characterisation of minerals in stony meteorites by their stoichiometry calculated from atomic ratios of constituent elements was demonstrated in a study of mineral composition of chondritic meteorite (Miler et al., 2009). Obtained results were the main motive to perform similar study on genetically various metal-bearing phases in stream sediments, which is presented in this paper. The aim of this study was to estimate reliability of EDS analysis for identification of various natural and anthropogenic metal-bearing phases in polished and rough particle samples of stream sediments. The estimation of reliability of EDS analysis was based on assessing (a) precision of EDS analysis of elemental composition in polished and rough particle samples, (b) accuracy of EDS analysis of elemental composition in polished samples and (c) agreement between EDS measurements of constituent elements in polished and rough particle samples. Partial results of the study presented in this paper were also included as a chapter in PhD thesis "Application of SEM/EDS to environmental mineralogy and geochemistry" (Miler, 2012).

Materials and methods

Sample preparation

Stream sediments, collected at different locations along the Meža River and its tributaries and the Drava River in 2005 (Fux, 2007; Fux & Gosar, 2007), were used for this study. Stream sediments were air dried and sieved to a fraction smaller than 0.063 mm, which was considered the most suitable for SEM/EDS analysis, due to its grain size. Polished-sections of individual metal-bearing phases were prepared for EDS analysis by embedding sediments in araldite resin, followed by fine polishing using a diamond suspension fluid and coating with carbon for conductivity (Miler, 2012). Rough particle samples were prepared by mounting sediment particles on a double-sided carbon tape and coating them with a thin layer of gold for conductivity instead of carbon (Miler, 2012) to obtain more detailed morphological features of the particle surface. Gold coating, however, introduces Au characteristic lines and reduces intensities of some light element peaks due to absorption of their characteristic X-rays and may thus influence the EDS analysis.

SEM/EDS analysis

SEM/EDS analysis was carried out in a high vacuum using a JEOL JSM 6490LV scanning electron microscope (SEM) coupled with an Oxford INCA energy dispersive spectroscopy (EDS) system, comprising Oxford INCA PentaFETx3 Si(Li) detector and INCA Energy 350 processing software, at 20 kV accelerating voltage, spot size 50 and 10 mm working distance (Miler, 2012). Each analysed metal-bearing phase was characterised by its chemical composition measured by the EDS point analysis with acquisition times of 30 s for polished samples and 60 s for rough particle samples. Longer times for rough particle samples were chosen in order to improve signal-to-noise ratios and assure sufficient signal for quantification of minor elements (Reed, 2005). Mineral species of 16 analysed metal-bearing phases were assessed by calculating stoichiometric ratios from atomic % of constituent elements, acquired by the EDS analysis (Gonzalez et al., 2007; Vanek et al., 2008), and comparison with atomic proportions of constituent elements in known stoichiometric minerals, obtained from mineral databases (Anthony et al., 2009; Barthelmy, 2010). The software was calibrated for quantification using pre-measured universal standards included in the EDS software, which is a basic standardisation procedure in fitted-standards EDS analysis (Goldstein et al., 2003), referenced to a Co optimisation standard. The correction of EDS data was performed on the basis of the standard ZAF-correction procedure included in the INCA Energy software (Oxford Instruments, 2006).

Precision

Precisions of EDS analyses of rough particle and polished samples were assessed for constituent elements in 16 different metal-bearing phases. The upper precision threshold level for EDS analysis of polished samples was set at ≤ 12 % relative, which is in accordance with accepted precision levels for fitted standards EDS analysis (Statham, 2002). Since no reported data on precision levels for EDS analysis of rough particle samples were found, the precision threshold level was adapted from the accepted precision for standardless EDS analysis (Statham, 2002) and was arbitrarily set at ≤ 30 % relative. EDS data sets consisted of 20 replicate measurements made at random locations on each metal-bearing grain. The precisions of EDS measurements of element contents in metal-bearing phases were expressed as Relative Standard Deviations (RSD):

$$RSD\ (\%) = \left(\frac{\sigma^{at}}{X_{av}}\right) \cdot 100\%$$

where σ^{at} is standard deviation of replicate measurements (in at%), X_{av} is mean content of constituent element (in at%).

Compositional homogeneity

Compositional homogeneity of metal-bearing phases in polished sections was assessed by determining scatter in intensity (number of counts) of spectrum peaks of constituent elements, not corrected for background, obtained by analyses of random points on a metal-bearing phase. The level of homogeneity was expressed as (Goldstein et al., 2003):

$$Homogeneity\ (\%) = \frac{3 \cdot \sqrt{\overline{N}}}{\overline{N}} \cdot 100\%$$

where $\overline{N}$ is mean uncorrected intensity (number of counts) in spectrum peaks of constituent elements.

Criterion for homogeneity is that the scatter in number of counts should be within limits of $\overline{N} \pm 3 \cdot \sqrt{\overline{N}}$ (Goldstein et al., 2003; Reed, 2005).

Accuracy

Theoretical accuracy for EDS analysis of metal-bearing phases was also assessed. The upper accuracy threshold level for EDS analysis of metal-bearing phases in polished samples was set at ≤ 25 % relative to the composition of fitted standards, which is in accordance with the accepted accuracy for standardless quantitative analysis of flat-polished bulk samples using fitted standards procedures (Newbury, 1998; Goldstein et al., 2003). EDS measurements were carried out at 20 random locations on surface of each grain. Accuracy of EDS analysis of element contents in metal-bearing phases were estimated by calculation of relative error:

$$Relative\ error\ (\%) = \frac{|X_{av} - X_{st}|}{X_{st}} \cdot 100\%$$

where X_{av} is mean content of constituent element in analysed metal-bearing phase (in at%), X_{st} is content of constituent element in known stoichiometric mineral (in at%).

Comparison of mean element contents in polished and rough particle samples (Welch's t-test)

Mean element contents in metal-bearing phases in polished and rough particle samples were compared using Welch's t-test at the 95 % confidence level, since the population variances and number of measurements were mostly unequal in both samples. The following equation was used:

$$t = \frac{\overline{X}_1 - \overline{X}_2}{S_{\overline{X}_1 - \overline{X}_2}}$$

where

$$S_{\overline{X}_1 - \overline{X}_2} = \sqrt{\frac{S_1^{\,2}}{n_1} + \frac{S_2^{\,2}}{n_2}}$$

Welch-Satterthwaite equation was used for the calculation of degrees of freedom (d.f.):

$$d.f. = \frac{\left(\frac{S_1^{\,2}}{n_1} + \frac{S_2^{\,2}}{n_2}\right)}{\frac{S_1^{\,4}}{n_1^{\,2} \cdot (n_1 - 1)} + \frac{S_2^{\,4}}{n_2^{\,2} \cdot (n_2 - 1)}}$$

Where $\overline{X}_1$ and $\overline{X}_2$ are mean element contents (in at%) in analysed metal-bearing phases in rough particle and polished samples, respectively, $s_1^{\,2}$ and $s_2^{\,2}$ are variances in rough particle and polished samples, respectively and n_1 and n_2 are number of measurements in rough particle and polished samples, respectively.

Results and discussion

Precision of EDS analyses of metal-bearing phases in polished and rough particle samples

The EDS microanalysis depends on several variable factors, such as the number of detected characteristic X-rays emitted from constituent elements in a sample and effects of spectral interferences and spectral background. These factors may vary from analysis to analysis. Other factors that also influence the analysis are related to sample preparation and elemental composition of the sample. Precision was determined in order to assess repeatability of measurements, thus taking into account all deviations that arise due to variations in compositional homogeneity of analysed phases and random nature of X-ray generation and emission. Precisions of EDS analyses of constituent element contents were calculated for different metal-bearing phases and are given in Table 1.

The precision measurements in polished samples showed that EDS relative standard deviations (RSD) were within acceptable limits for quantitative EDS analysis (< 12 %) for 85 % of all measured elements in 16 analysed phases, while they exceeded the upper limit value for 15 % of all elements. The average RSD amounted to 3 % for elements within acceptable limits and 34 % for elements that exceeded the upper limit value. The precision was in acceptable limits for all major constituent elements, while it exceeded the upper limit values for 73 % of minor or trace elements. The average RSD was thus 3 % for major constituent elements and 27.2 % for minor or trace elements. High RSD values for minor and trace elements were ascribed to inhomogeneous distribution of these elements throughout analysed phases.

Tab. 1. Elemental composition of 16 metal-bearing phases in rough particle and polished sediment samples coated with carbon, determined by EDS analysis; n - number of measurements on individual grains, (X_{av} (at%)) - mean elemental composition with standard deviation in atomic %, Acq. t. - spectrum acquisition time, Level of homogeneity (%) - level of compositional homogeneity of phases (lower values suggest higher degree of homogeneity), Peak intensity - intensity of X-ray lines. Upper values of precision threshold level were arbitrarily set at ≤ 12 % for polished and at ≤ 30 % for rough particle samples.

Tab. 1. Elementarna sestava 16 kovinskih faz v grobih delcih in poliranih vzorcih sedimentov naparjenih z ogljikom, določena z EDS analizo; n - število meritev na posameznih zrnih, (X_{av} (at%)) - aritmetična sredina elementarne sestave s standardnim odklonom v atomskih %, Acq. t. - čas zajema spektra, Level of homogeneity (%) - stopnja homogenosti sestave faz (nižje vrednosti pomenijo višjo stopnjo homogenosti), Peak intensity - intenziteta linij rtg-žarkov. Izbrana mejna vrednost natančnosti je ≤ 12 % za polirane vzorce in ≤ 30 % za grobe delce.

	Rough particle sample		Polished sample			
Element	**X_{av} (at%)**	**Precision (RSD %)**	**X_{av} (at%)**	**Precision (RSD %)**	**Level of homogeneity (%)**	**Peak intensity**
Ba-S-O	**n=8, Acq. t.=60 s**		**n=20, Acq. t.=30 s**			
O	74.08 ± 5.03	6.79	70.55 ± 0.95	1.35	7.57	1572.5
S	14.00 ± 2.29	16.39	15.23 ± 0.47	3.08	7.75	1498.4
Sr	0.28 ± 0.21	**73.52**	0.98 ± 0.11	11.26	20.62	211.7
Ba	11.63 ± 2.68	23.07	13.24 ± 0.58	4.37	8.59	1220.9
Ti-O	**n=10, Acq. t.=60 s**		**n=20, Acq. t.=30 s**			
O	74.85 ± 5.68	7.59	72.06 ± 0.63	0.88	11.42	689.9
Ti	25.15 ± 5.68	22.58	27.94 ± 0.63	2.26	5.13	3423.0
Fe-Ti-O	**n=10, Acq. t.=60 s**		**n=20, Acq. t.=30 s**			
O	78.04 ± 3.92	5.02	66.74 ± 0.68	1.02	10.28	851.2
Ti	11.53 ± 1.60	13.86	16.96 ± 0.35	2.09	7.16	1757.1
Mn	0.58 ± 0.39	**67.52**	0.90 ± 0.18	**20.59**	32.39	85.8
Fe	9.86 ± 2.40	24.38	15.40 ± 0.46	2.97	9.89	920.6
Ca-Ti-Si-O	**n=10, Acq. t.=60 s**		**n=20, Acq. t.=30 s**			
O	72.58 ± 3.09	4.26	69.39 ± 0.74	1.07	7.68	1526.2
Al	0.67 ± 0.17	25.89	0.79 ± 0.11	**13.73**	15.92	355.1
Si	9.79 ± 0.96	9.85	11.13 ± 0.28	2.54	4.98	3623.6
Ca	8.64 ± 1.04	12.05	9.72 ± 0.29	2.96	5.56	2909.9
Ti	8.33 ± 1.34	16.11	8.97 ± 0.26	2.93	6.71	1996.5
Zr-Si-O	**n=10, Acq. t.=60 s**		**n=20, Acq. t.=30 s**			
O	71.41 ± 2.48	3.47	71.05 ± 0.86	1.22	9.73	950.0
Si	13.92 ± 1.10	7.90	14.10 ± 0.44	3.09	5.97	2521.3
Zr	14.68 ± 1.45	9.88	14.85 ± 0.48	3.27	5.88	2599.5
Ce-P-O	**n=10, Acq. t.=60 s**		**n=20, Acq. t.=30 s**			
O	71.61 ± 6.10	8.51	72.20 ± 0.60	0.83	7.74	1500.6
P	15.22 ± 2.84	18.63	15.58 ± 0.39	2.50	8.40	1274.8
La	3.77 ± 0.95	25.28	3.12 ± 0.18	5.85	16.81	318.5
Ce	6.98 ± 1.78	25.55	6.39 ± 0.29	4.54	12.80	549.5
Nd	2.12 ± 0.63	29.59	2.38 ± 0.22	9.33	14.11	451.9
Th	0.30 ± 0.32	**104.63**	0.38 ± 0.39	**101.84**	25.65	136.8
Pb-(C)-O	**n=10, Acq. t.=60 s**		**n=20, Acq. t.=30 s**			
O	85.88 ± 2.73	3.17	78.63 ± 0.68	0.86	13.18	517.8
Pb	14.13 ± 2.73	19.30	21.37 ± 0.68	3.17	21.42	196.2
Zn-S	**n=10, Acq. t.=60 s**		**n=20, Acq. t.=30 s**			
S	54.28 ± 2.27	4.19	52.91 ± 0.68	1.29	5.26	3252.9
Zn	45.52 ± 2.44	5.37	46.65 ± 0.67	1.45	10.47	821.2
Cd	0.20 ± 0.42	**211.93**	0.44 ± 0.24	**55.25**	30.37	97.6
Zn-(C)-O	**n=10, Acq. t.=60 s**		**n=20, Acq. t.=30 s**			
O	82.08 ± 2.63	3.21	74.40 ± 0.67	0.90	7.55	1579.8
Zn	17.92 ± 2.63	14.69	25.60 ± 0.67	2.61	12.39	586.4

Tab. 1 (continued)

	Rough particle sample		Polished sample			
Element	**X_{av} (at%)**	**Precision (RSD %)**	**X_{av} (at%)**	**Precision (RSD %)**	**Level of homogeneity (%)**	**Peak intensity**
Fe-S	**n=8, Acq. t.=60 s**		**n=20, Acq. t.=30 s**			
S	68.57 ± 3.06	4.46	68.83 ± 0.28	0.41	3.70	6561.9
Fe	31.43 ± 3.06	9.73	31.17 ± 0.28	0.90	8.07	1383.5
Pb-Mo-O	**n=10, Acq. t.=60 s**		**n=20, Acq. t.=30 s**			
O	83.01 ± 4.49	5.41	71.72 ± 1.39	1.94	13.59	487.6
Mo	9.19 ± 2.46	26.71	14.97 ± 0.80	5.33	5.71	2757.2
Pb	7.80 ± 2.07	26.50	13.31 ± 0.67	5.05	24.45	150.6
Pb-Zn-V-O	**n=6, Acq. t.=60 s**		**n=20, Acq. t.=30 s**			
O	76.68 ± 3.59	4.68	61.88 ± 3.45	5.58	13.79	473.4
V	7.53 ± 1.21	16.10	12.53 ± 1.19	9.50	12.23	601.5
Zn	7.38 ± 1.54	20.82	12.76 ± 1.37	10.74	19.56	235.4
Pb	8.42 ± 1.51	17.96	12.84 ± 1.00	7.76	26.18	131.3
Zn-Si-O	**n=8, Acq. t.=60 s**		**n=20, Acq. t.=30 s**			
O	73.13 ± 5.84	7.99	64.91 ± 0.67	1.03	7.79	1484.3
Si	10.45 ± 1.43	13.65	12.16 ± 0.16	1.35	9.21	1060.0
Zn	16.42 ± 4.52	27.54	22.93 ± 0.64	2.79	11.85	641.3
Pb-S	**n=7, Acq. t.=60 s**		**n=20, Acq. t.=30 s**			
S	55.70 ± 1.38	2.47	54.27 ± 0.58	1.07	4.83	3850.6
Pb	44.30 ± 1.38	3.10	45.73 ± 0.58	1.27	18.53	262.1
Fe-Si	**n=10, Acq. t.=60 s**		**n=20, Acq. t.=30 s**			
Si	33.85 ± 1.92	5.66	27.20 ± 0.45	1.64	7.98	1413.9
Fe	66.15 ± 1.92	2.90	72.80 ± 0.45	0.61	6.10	2417.5
Fe-O (Pb,Zn)	**n=10, Acq. t.=60 s**		**n=20, Acq. t.=30 s**			
O	73.19 ± 5.93	8.11	71.43 ± 2.81	3.94	6.05	2459.5
Si	2.64 ± 1.15	**43.74**	0.92 ± 0.20	**21.27**	23.04	169.6
Ca	1.31 ± 0.61	**46.09**	0.38 ± 0.08	**20.01**	30.39	97.5
Fe	19.84 ± 4.25	21.41	26.23 ± 2.61	9.95	7.38	1654.0
Zn	1.77 ± 1.22	**69.31**	0.53 ± 0.13	**23.71**	54.96	29.8
Pb	1.27 ± 0.77	**60.87**	0.50 ± 0.08	**16.76**	71.11	17.8

values exceeding upper limits are in bold

However, since minor and trace elements produce low intensity spectral lines, their RSD values may also result from poor counting statistics. The lowest average RSD values calculated for all constituent elements in each individual phase were obtained for Fe-S, Fe-Si, Pb-S, Ti-O and Zn-Si-O, and the highest for trace element containing Ce-P-O, Zn-S and Fe-O (Pb,Zn), in which the RSD upper limit value of 12 % was exceeded. The RSD values for all measured elements ranged from 0.4 % to 101.8 %, with an average of 8 %, which was well within the acceptable limits.

Precision was also calculated for elements in 16 phases identified in rough particle samples (Table 1). The RSD values were below the upper limit value for EDS analysis of rough particle samples, set at 30 %, for 85 % of all measured elements in all analysed phases, while they exceeded the upper limit value for 15 % of all elements. The precision was within acceptable limits for all major constituent elements, while it exceeded the upper limit values for 73 % of elements present in phases in minor or trace contents. These results were in good agreement with those of EDS analysis of polished samples. The average RSD for major constituent elements in these phases was 12.2 %, which is well below the upper limit value for EDS analysis of rough particle samples. However, the average RSD for minor and trace constituent elements was 68.9 %. The lowest average RSD values for all constituent elements were calculated for Pb-S, Fe-Si, Zr-Si-O, Fe-S and Zn-(C)-O, while they exceeded the upper limit value of 30 % in phases containing trace elements, such as Ce-P-O, Zn-S and Fe-O (Pb,Zn). The RSD values for all elements including major, minor and trace elements ranged from 2.5 % to 211.9 %, with an average of 24 %.

Most of RSD values for minor and trace elements exceeded the upper limit values in both polished and rough particle samples. The exceptions were Sr in Ba-S-O, for which RSD upper limit was exceeded in rough particle samples, and Al in Ca-Ti-Si-O, where RSD limit for Al was exceeded in polished samples.

RSD values were generally much higher and much more variable in rough particle samples than RSD for elements in polished samples. The main reason for such differences in RSD values are geometry effects, arising during rough particle EDS analysis due to surface morphology and orientation of particle surfaces. Comparison between ratios of RSD values for individual phases in rough particle and polished samples showed greatest differences for Zn-Si-O, Ti-O and Fe-S, while the best correspondence was observed for Ce-P-O, Pb-Zn-V-O and also Pb-S, Fe-O (Pb,Zn), Zr-Si-O and Ca-Ti-Si-O.

Precision measurements thus showed that the overall repeatability of EDS analyses of polished and rough particle samples, under applied analytical conditions, was within acceptable limits for all major elements and smaller part of the elements present in minor or trace contents in analysed metal-bearing phases. This indicated that the random analytical fluctuations were mostly negligible and that composition of phases could be determined with sufficient reliability in individual grains of each phase.

Compositional homogeneity of metal-bearing phases in polished samples

Compositional homogeneity provides information on the degree of element distribution in an analysed phase. Homogeneity of chemical composition of analysed metal-bearing phases affects the repeatability of EDS analysis. For this reason, homogeneity of analysed grains in polished samples was assessed. Calculated levels of compositional homogeneity (in %) of different metal-bearing phases are given in Table 1.

Levels of compositional homogeneity ranged between 3.7 % and 71 % with an average value of 14.3 %, which considerably exceeded the desired homogeneity level of < 1 %, according to Goldstein et al. (2003). The results of the homogeneity test were generally in agreement with precision RSD values for elements in different phases, however these relations seemed to be more complicated in more complex phases, especially those containing minor and trace elements, which is mostly due to low number of counts in spectrum peaks and consequently higher counting errors. Less complex metal-bearing phases, such as Fe-S, Fe-Si and Zr-Si-O exhibited the most homogeneous compositions, while Fe-O (Pb,Zn) was the least homogeneous phase, primarily on the account of minor and trace elements. The calculated average level of homogeneity for major constituent elements was about 10 % and for minor and trace elements 30.5 %. This could suggest that elements present in a phase in minor or trace contents are generally distributed more heterogeneously than major constituent elements. However, the calculated level of homogeneity for minor and trace elements could also be ascribed to low intensities of their spectra and counting errors. Zn and Pb were the most common elements that occurred either as major constituents or as minor and trace elements. The average level of homogeneity for Zn and Pb when they occurred as major elements was 18 %, but when they were present in minor contents, the homogeneity level was above 63 %. There were also some exceptions. The distributions of Pb and Zn in Pb-Zn-V-O, Pb-C-O, Pb-Mo-O and Pb-S were inhomogeneous despite the fact that Pb and Zn occurred as major elements.

Where precision and homogeneity coincided, repeatability of measurements depended on the distribution of constituent elements. In 8 phases (Ba-S-O, Pb-C-O, Zn-S, Zn-C-O, Fe-S, Zn-Si-O, Pb-S and Fe-Si) distributions of constituent elements agreed with calculated RSD values, while in 4 phases (Ti-O, Zr-Si-O, Pb-Mo-O and Pb-Zn-V-O) the repeatability of measurements could not be explained by compositional homogeneity. Since determination of compositional homogeneity is based on measuring the intensities of uncorrected element peaks, it is directly subjected to various factors related to spectra acquisition conditions. The result of homogeneity test thus depended, besides on distribution of constituent elements, also on the quantity of contaminant gases, adsorbed on the surface of the phase, ratio between the volume of the analysed phase and the electron beam interaction area, on signal variations and instrumental factors and also intensity of spectral lines. The latter usually occurred due to changes in SEM/EDS operating conditions, such as the intensity of electron beam and drift of the sample position.

Mineral composition of metal-bearing phases and accuracy of their identification

Because suitable standards of natural minerals were not available, the accuracy was used to define the degree of concordance between elemental compositions of analysed individual metal-bearing phases with corresponding stoichiometric mineral species obtained from mineral databases (Anthony et al., 2009; Barthelmy, 2010).

Accuracies were obtained by comparing elemental composition of measured phases to the elemental composition of corresponding minerals. Elemental compositions of most common metal-bearing phases and their possible corresponding mineral analogues and relative errors of EDS analysis of constituent element contents are given in Table 2.

The EDS relative errors were within acceptable limits (< 25 %) for 90 % of all measured elements in 16 analysed phases and exceeded the upper limit value for 10 % of all elements. The average relative error for elements within acceptable limits was 8.6 % and 45.1 % for elements above the limit, which are values presented in bold in Table 2. The overall average relative error for all elements in all phases, relative to the underlined mineral analogues in Table 2, ranged from 0.2 % to 69.2 % and amounted to 12.3 %, which was within acceptable limits for accuracy in quantitative EDS analysis. The calculated overall relative error was relatively high mostly because some of analysed metal-bearing phases contained minor and trace elements, whose contents are usually extremely variable and may substitute for major constituent elements in analysed phases and their mineral analogues. Furthermore, contents of

Tab. 2 Comparison between elemental composition of metal-bearing phases in carbon-coated polished sediment samples and elemental composition of corresponding stoichiometric minerals; (X_{av} (at%)) - mean elemental composition of 20 measurements in atomic %, (X_{st} (at%)) - elemental composition of stoichiometric mineral, (Rel. err. (%)) - relative error in %; (+) - positive values, (-) - negative values. Elemental composition of stoichiometric minerals, except those marked with *, was obtained from mineral databases (Anthony et al., 2009; Barthelmy, 2010) and recalculated to atomic %, considering only elements that were also identified in analysed phases. Upper value of accuracy threshold level was set at ≤ 25 %.

Tab. 2 Primerjava elementarne sestave kovinskih faz v poliranih vzorcih sedimentov naparjenih z ogljikom in elementarno sestavo možnih stehiometričnih mineralov; (X_{av} (at%)) - aritmetična sredina elementarne sestave 20 meritev v atomskih %, (X_{st} (at%)) - elementarna sestava stehiometričnega minerala v atomskih %, (Rel. err. (%)) - relativna napaka v %; (+) - pozitivne vrednosti, (-) - negativne vrednosti. Elementarna sestava stehiometričnih mineralov, razen tistih označenih z *, je bila povzeta iz podatkovnih baz mineralov (Anthony et al., 2009; Barthelmy, 2010) in preračunana v atomske %, glede na elemente določene v analiziranih fazah. Izbrana mejna vrednost točnosti je ≤ 25 %.

	Phase	**Stoichiometric mineral**		**Stoichiometric mineral**	
Element	**X_{av} (at%)**	**X_{st} (at%)**	**Rel. err. (%)**	**X_{st} (at%)**	**Rel. err. (%)**
	Ba-S-O	**Barite**			
O	70.55	66.66	5.83 (-)	n.d.	n.d.
S	15.23	16.67	8.66 (+)	n.d.	n.d.
Sr	0.98	n.d.	n.d.	n.d.	n.d.
Ba	13.24	16.67	20.54 (+)	n.d.	n.d.
Σ Ba,Sr	14.22	16.67	14.69 (+)	n.d.	n.d.
	Ti-O	**Rutile-anatase-brookite**			
O	72.06	66.68	8.08 (-)	n.d.	n.d.
Ti	27.94	33.32	16.16 (+)	n.d.	n.d.
	Fe-Ti-O	**Ilmenite**		**Pseudorutile**	
O	66.74	60.00	11.23 (-)	64.29	3.81 (-)
Ti	16.96	20.00	15.20 (+)	21.42	20.81 (+)
Mn	0.90	n.d.	n.d.	n.d.	n.d.
Fe	15.40	20.00	23.00 (+)	14.29	7.78 (-)
Σ Fe,Mn	16.30	20.00	18.51 (+)	14.29	14.06 (-)
	Ca-Ti-Si-O	**Sphene**			
O	69.39	62.82	10.45 (-)	n.d.	n.d.
Al	0.79	2.57	**69.21** (+)	n.d.	n.d.
Si	11.13	12.82	13.20 (+)	n.d.	n.d.
Ca	9.72	12.18	20.19 (+)	n.d.	n.d.
Ti	8.97	9.61	6.65 (+)	n.d.	n.d.
Σ Al,Ti	9.76	12.18	19.83 (+)	n.d.	n.d.
	Zr-Si-O	**Zircon**			
O	71.05	67.80	4.80 (-)	n.d.	n.d.
Si	14.10	16.95	16.80 (+)	n.d.	n.d.
Zr	14.85	15.25	2.66 (+)	n.d.	n.d.
	Ce-P-O	**Monazite**		**Rhabdophane**	
O	72.20	66.66	8.30 (-)	71.43	1.08 (-)
P	15.58	16.66	6.49 (+)	14.29	9.08 (+)
La	3.12	4.17	**25.24** (+)	3.57	12.78 (+)
Ce	6.39	8.34	23.37 (+)	10.72	**40.39** (+)
Nd	2.38	3.33	**28.73** (+)	n.d.	n.d.
Th	0.38	0.83	**54.54** (+)	n.d.	n.d.
Σ La,Ce,Nd,Th	12.26	16.67	**26.47** (+)	14.29	14.21 (+)
	Pb-(C)-O	**Cerussite**		**Hydrocerussite**	
O	78.63	75.00	4.85 (-)	72.72	8.12 (-)
Pb	21.37	25.00	14.54 (+)	27.28	21.66 (+)

Tab. 2 (continued)

	Phase	Stoichiometric mineral		Stoichiometric mineral	
Element	**X_{av} (at%)**	**X_{st} (at%)**	**Rel. err. (%)**	**X_{st} (at%)**	**Rel. err. (%)**
	Zn-S	**Sphalerite**			
S	52.91	51.29	3.16 (-)	n.d.	n.d.
Zn	46.65	48.71	4.23 (+)	n.d.	n.d.
Cd	0.44	n.d.	n.d.	n.d.	n.d.
Σ Zn,Cd	47.09	48.71	3.33 (+)	n.d.	n.d.
	Zn-(C)-O	**Smithsonite**		**Hydrozincite**	
O	74.40	75.00	0.81 (+)	70.59	5.39 (-)
Zn	25.60	25.00	2.43 (-)	29.41	12.94 (+)
	Fe-S	**Pyrite-marcasite**		**Pyrite***	
S	68.83	66.67	3.24 (-)	68.25	0.84 (-)
Fe	31.17	33.33	6.47 (+)	31.75	1.82 (+)
	Pb-Mo-O	**Wulfenite**			
O	71.72	66.66	7.59 (-)	n.d.	n.d.
Mo	14.97	16.67	10.20 (+)	n.d.	n.d.
Pb	13.31	16.67	20.16 (+)	n.d.	n.d.
	Zn-Si-O	**Hemimorphite**		**Willemite**	
O	64.91	62.50	3.85 (-)	57.15	13.58 (-)
Si	12.16	12.50	2.69 (+)	14.28	14.83 (+)
Zn	22.93	25.00	8.29 (+)	28.57	19.75 (+)
	Pb-Zn-V-O	**Descloizite**			
O	61.88	62.50	1.00 (+)	n.d.	n.d.
V	12.53	12.50	0.21 (-)	n.d.	n.d.
Zn	12.76	12.50	2.06 (-)	n.d.	n.d.
Pb	12.84	12.50	2.71 (-)	n.d.	n.d.
	Pb-S	**Galena**			
S	54.27	50.00	8.54 (-)	n.d.	n.d.
Pb	45.73	50.00	8.54 (+)	n.d.	n.d.
	Fe-Si	**Gupeiite**			
Si	27.20	25.00	8.80 (-)	n.d.	n.d.
Fe	72.80	75.00	2.93 (+)	n.d.	n.d.
	Fe-O (Pb,Zn)	**Goethite-lepidocrocite**		**Bernalite**	
O	71.43	66.67	7.14 (-)	75.00	4.76 (+)
Si	0.92	n.d.	n.d.	1.75	**47.54** (+)
Ca	0.38	n.d.	n.d.	n.d.	n.d.
Fe	26.23	33.33	21.30 (+)	22.25	17.90 (-)
Zn	0.53	n.d.	n.d.	0.50	6.55 (-)
Pb	0.50	n.d.	n.d.	0.50	0.24 (-)
Σ Fe,Zn,Pb	27.27	33.33	18.20 (+)	23.25	17.28 (-)

n.d. - not determined
*values of reference standards measured by EDS analysis
underlined data were used in calculation of average relative errors
values exceeding upper limits are in bold

some of these elements in certified minerals were not provided in mineral databases and thus they could not be included in calculation of relative errors. On the basis of their elemental composition, mineral species of all analysed metal-bearing phases were designated with sufficient accuracy. The relative error for those phases ranged from 1.5 % to 24.4 % with an average amounting to 10.3 %, which was within acceptable limits. The best results were obtained for Pb-Zn-V-O and Zn-C-O, while the highest relative errors were observed for more complex metal-bearing phases containing variable minor and trace elements, such as Ce-P-O and Ca-Ti-Si-O. Obtained results also showed that EDS

analysis of polished samples provided data with sufficient accuracy for calculation of chemical formulae of metal-bearing minerals based on the atomic ratios between constituent elements but not their absolute contents. The atomic ratios between light elements and other constituent elements in most of analysed metal-bearing phases, however, were always somewhat higher than the ratios in corresponding stoichiometric minerals, although relative errors for light elements, especially O, were generally low and mostly well within the acceptable limits. Average relative errors calculated for light elements were biased negatively (Table 2), while they were positively biased for metals. This confirmed that measured contents of light elements were generally higher than those in stoichiometric minerals and measured contents of metals were mostly lower than in stoichiometric minerals. This was ascribed to the fact that quantification of light elements in EDS analysis is strongly subjected to matrix effects (Oxford Instruments, 2006). Thus, matrix corrections and consequently errors in quantification are always much greater for light elements.

Elemental composition and calculated relative errors for constituent elements in Ba-S-O showed good agreement with barite stoichiometry. High relative error was observed for Ba, which is most probably due to minor contents of Sr substituting for Ba in barite (Brower, 1973), forming a solid solution between barite and celestine. For this reason and since contents of Sr were not given for stoichiometric barite, the sum of Ba and Sr was also considered in calculation of relative error and mineral formula, which provided much better results. By chemical composition and calculated relative errors for constituent elements, Ti-O corresponded best to TiO_2 (Table 2), which has several natural mineral polymorphs: rutile, anatase and brookite and a few anthropogenic forms differing by their oxidation states and atomic coordination. These, however, could not be distinguished from each other merely on the basis of EDS analysis. According to its elemental composition, analysed Fe-Ti-O has two possible mineral analogues, ilmenite and pseudorutile. Based on calculated relative errors, Fe-Ti-O agreed better with pseudorutile, however the ratio between Ti and Fe showed good correspondence with ilmenite. Moreover, minor content of Mn, which was measured in Fe-Ti-O and also applied to calculation of Ti/Fe ratio, is consistent with ilmenite of metamorphic origin (Cassidy et al., 1988). Elemental composition of Ca-Ti-Si-O corresponded in stoichiometry well to mineral sphene, which was also confirmed by relative errors calculated for major constituent elements, with the exception of Al, which is a minor element substituting for Ti in sphene. Contents of major constituent elements in Zr-Si-O corresponded only to mineral zircon. The calculated relative errors were well within accepted limits, but reached the highest values for Si although atomic ratios between Zr and Si agreed well with zircon stoichiometry. Elemental composition of Ce-P-O, obtained by EDS analysis, corresponded to two possible Ce-bearing mineral series according to data in mineral databases (Anthony et al., 2009; Barthelmy, 2010); monazite and rhabdophane. Mean relative errors were greater for Ce-monazite than for Ce-rhabdophane. However, much better agreement with monazite was observed for major constituents Ce and P. Moreover, Ce/P atomic ratio and presence of Th and Nd, which are very variable trace elements in Ce-monazite (Barthelmy, 2010), conformed better in stoichiometry to Ce-monazite rather than Ce-rhabdophane (Table 2). Compositionally, Pb-C-O agreed with minerals cerussite and hydrocerussite (Table 2). However, calculation of relative errors and O/Pb atomic ratio confirmed that the analysed Pb-C-O is cerussite. Elemental composition of Zn-S and stoichiometric ratio between Zn and S, corresponded very well to mineral sphalerite (Table 2) and so did the calculated relative errors. Minor contents of Cd were also detected in Zn-S, which is in agreement with the fact that Cd frequently occurs as a trace element in Zn ore minerals (Štrucl, 1984). Considering its elemental composition, Zn-C-O could correspond to two possible Zn-bearing carbonate minerals; smithsonite and hydrozincite (Table 2). Though, atomic ratios between O and Zn and calculated relative errors were consistent with stoichiometric smithsonite. Relative errors and atomic ratios between Fe and S corresponded to stoichiometry of pyrite or marcasite (Table 2). For comparison, a polished pyrite standard was also analysed with EDS analysis and the results showed perfect match. However, based solely on EDS analysis it is impossible to determine whether analysed Fe-S is either pyrite or marcasite. Constituent elements in Pb-Mo-O were difficult to identify due to overlaps between the S Kα (2.307 keV), Pb Mα (2.342 keV) and Mo Lα (2.293 keV) energy lines, which are below the energy resolution of the EDS, thus Pb-Mo-O could easily be mistaken for Pb-S-O. There is also no difference in Mo/O atomic ratios in wulfenite and S/O in anglesite. The peak overlaps were resolved by comparing acquired spectra with synthesized spectra of possible minerals with ideal compositions and presence of Mo was also confirmed by exciting its non-overlapping high-energy X-ray lines at 30 kV accelerating voltage. The obtained elemental composition and relative errors for Pb-Mo-O, which were in acceptable limits, corresponded well to wulfenite. Analysed Zn-Si-O has two possible mineral analogues; hemimorphite and willemite. The calculated atomic ratios and relative errors indicated that Zn-Si-O agreed best with mineral hemimorphite. According to mineral databases (Anthony et al., 2009; Barthelmy, 2010), descloizite was the only possible analogue containing elements that were also present in the analysed Pb-Zn-V-O. Atomic ratios and relative errors showed that in stoichiometry Pb-Zn-V-O perfectly corresponded to mineral descloizite, although the measured O contents were slightly lower than in stoichiometric descloizite. Pb-S corresponded to mineral galena, which was also confirmed by calculated relative errors and atomic ratios. However, measured contents of S were somewhat higher than in stoichiometric galena, while Pb contents were consequently somewhat

lower. The calculated relative errors and atomic ratios between constituent elements in analysed Fe-Si corresponded in stoichiometry perfectly to mineral gupeiite. Natural occurrences of gupeiite are very rare in nature though and may be either of extraterrestrial or anthropogenic origin (Reller et al., 2000). Fe-O (Pb,Zn) corresponded to three different mineral species, goethite or lepidocrocite and bernalite according to its elemental composition. Since Pb and Zn may also substitute for Fe in goethite and lepidocrocite, a sum of Fe, Pb and Zn was also considered in the calculation of relative errors. Si and Ca, which were also identified in analysed Fe-O (Pb,Zn), most probably co-precipitated with Fe-O (Pb,Zn). Relative errors calculated for constituent elements showed best agreement between the chemical composition of Fe-O (Pb,Zn) and mineral bernalite. However, considering the fact that O contents, obtained by EDS analysis, are commonly a little bit higher than those in stoichiometric minerals, it could be assumed that the mineral analogue of Fe-O (Pb,Zn) was more probably goethite or lepidocrocite and not bernalite. In addition to that, bernalite is considered a very rare mineral.

Comparison between elemental compositions of metal-bearing phases in rough particle and polished samples

Identification of phases in rough particle samples is considered difficult and unreliable mostly due to sample geometry effects and matrix correction, which are not suited to rough surface analyses (Reed, 2005). To assure that EDS measurements of phases in rough particle samples are reliable and representative, a comparison between average contents of elements in phases in rough particle samples and average element contents in polished samples was made using Welch's t-test and calculating the X_{av}^{u}/X_{av}^{p} ratio. The results of this comparison are presented in Table 3.

Welch's t-test was carried out in order to show differences in elemental composition of metal-bearing phases measured in rough particle and polished samples. The t-test showed that there were no statistically significant differences between mean element contents in 6 metal-bearing phases (Ti-O, Zr-Si-O, Ce-P-O, Zn-S, Fe-S and Pb-S) measured in rough particle

Tab. 3. Comparison between elemental composition of metal-bearing phases in rough particle and polished sediment samples; n - number of measurements on different grains, (X_{av}^{u} (at%)) - mean elemental composition of rough particle samples with standard deviation in atomic %, (X_{av}^{p} (at%)) - mean elemental composition of polished samples in atomic %.

Tab. 3. Primerjava med elementarno sestavo kovinskih faz v grobih delcih in poliranih vzorcih sedimentov; n - število meritev na različnih zrnih, (X_{av}^{u} (at%)) - aritmetična sredina elementarne sestave grobih delcev s standardnim odklonom v atomskih %, (X_{av}^{p} (at%)) - aritmetična sredina elementarne sestave poliranih vzorcev v atomskih %.

	Rough particle sample	**Polished sample**	**Comparison**		
Element	**X_{av}^{u} (at%)**	**X_{av}^{p} (at%)**	**Welch's t-test**		**X_{av}^{u}/X_{av}^{p} ratio**
Ba-S-O	**n=8**	**n=10**	**t (0.05,22) = 2.074**		
O	74.08 ± 5.03	70.25 ± 0.31	**2.150**	**different**	1.05
S	14.00 ± 2.29	15.38 ± 0.19	1.693	equal	0.91
Sr	0.28 ± 0.21	0.61 ± 0.45	2.010	equal	0.46
Ba	11.63 ± 2.68	13.76 ± 0.47	**2.213**	**different**	0.85
Ti-O	**n=10**	**n=10**	**t (0.05,30) = 2.042**		
O	74.85 ± 5.68	72.82 ± 0.78	1.123	equal	1.03
Ti	25.15 ± 5.68	27.19 ± 0.78	1.123	equal	0.93
Fe-Ti-O	**n=10**	**n=10**	**t (0.05,17) = 2.110**		
O	78.04 ± 3.92	68.46 ± 1.32	**7.326**	**different**	1.14
Ti	11.53 ± 1.60	15.98 ± 0.62	**8.211**	**different**	0.72
Mn	0.58 ± 0.39	0.82 ± 1.01	0.698	equal	0.71
Fe	9.86 ± 2.40	14.74 ± 1.08	**5.860**	**different**	0.67
Ca-Ti-Si-O	**n=10**	**n=10**	**t (0.05,9) = 2.262**		
O	72.58 ± 3.09	69.28 ± 0.58	**3.315**	**different**	1.05
Al	0.67 ± 0.17	0.65 ± 0.45	0.073	equal	1.02
Si	9.79 ± 0.96	11.04 ± 0.18	**4.003**	**different**	0.89
Ca	8.64 ± 1.04	9.89 ± 0.27	**3.698**	**different**	0.87
Ti	8.33 ± 1.34	9.14 ± 0.45	1.810	equal	0.91
Zr-Si-O	**n=10**	**n=10**	**t (0.05,6) = 2.447**		
O	71.41 ± 2.48	70.43 ± 0.61	1.220	equal	1.01
Si	13.92 ± 1.10	14.35 ± 0.26	1.209	equal	0.97
Zr	14.68 ± 1.45	15.23 ± 0.44	1.153	equal	0.96

Tab. 3 (continued)

	Rough particle sample	Polished sample	Comparison		
Element	**X_{av}^{u} (at%)**	**X_{av}^{p} (at%)**	**Welch's t-test**		**X_{av}^{u}/X_{av}^{p} ratio**
Ce-P-O	**n=10**	**n=10**	**t (0.05,34) = 2.032**		
O	71.61 ± 6.10	72.68 ± 0.74	0.551	equal	0.99
P	15.22 ± 2.84	15.38 ± 0.33	0.171	equal	0.99
La	3.77 ± 0.95	3.14 ± 0.43	1.897	equal	1.20
Ce	6.98 ± 1.78	6.27 ± 0.24	1.235	equal	1.11
Nd	2.12 ± 0.63	2.23 ± 0.22	0.538	equal	0.95
Th	0.30 ± 0.32	0.29 ± 0.28	0.060	equal	1.03
Pb-(C)-O	**n=10**	**n=10**	**t (0.05,8) = 2.306**		
O	85.88 ± 2.73	78.57 ± 0.85	**8.092**	**different**	1.09
Pb	14.13 ± 2.73	21.43 ± 0.85	**8.092**	**different**	0.66
Zn-S	**n=10**	**n=10**	**t (0.05,6) = 2.447**		
S	54.28 ± 2.27	53.62 ± 0.68	0.890	equal	1.01
Zn	45.52 ± 2.44	46.39 ± 0.68	1.076	equal	0.98
Zn-(C)-O	**n=10**	**n=10**	**t (0.05,7) = 2.365**		
O	82.08 ± 2.63	76.49 ± 0.80	**6.419**	**different**	1.07
Zn	17.92 ± 2.63	23.51 ± 0.80	**6.419**	**different**	0.76
Fe-S	**n=8**	**n=10**	**t (0.05,10) = 2.228**		
S	68.57 ± 3.06	69.12 ± 1.02	0.488	equal	0.99
Fe	31.43 ± 3.06	30.88 ± 1.02	0.488	equal	1.02
Pb-Mo-O	**n=10**	**n=10**	**t (0.05,24) = 2.064**		
O	83.01 ± 4.49	71.70 ± 1.78	**7.410**	**different**	1.16
Mo	9.19 ± 2.46	15.15 ± 0.94	**7.166**	**different**	0.61
Pb	7.80 ± 2.07	13.15 ± 0.94	**7.456**	**different**	0.59
Pb-Zn-V-O	**n=6**	**n=4**	**t (0.05,11) = 2.201**		
O	76.68 ± 3.59	60.78 ± 0.40	**10.762**	**different**	1.26
V	7.53 ± 1.21	13.06 ± 0.23	**10.889**	**different**	0.58
Zn	7.38 ± 1.54	12.86 ± 0.57	**7.967**	**different**	0.57
Pb	8.42 ± 1.51	13.31 ± 0.30	**7.687**	**different**	0.63
Zn-Si-O	**n=8**	**n=4**	**t (0.05,37) = 2.026**		
O	73.13 ± 5.84	65.87 ± 1.36	**3.338**	**different**	1.11
Si	10.45 ± 1.43	12.12 ± 0.13	**3.301**	**different**	0.86
Zn	16.42 ± 4.52	22.01 ± 1.39	**3.204**	**different**	0.75
Pb-S	**n=7**	**n=8**	**t (0.05,4) = 2.776**		
S	55.70 ± 1.38	54.50 ± 1.05	1.886	equal	1.02
Pb	44.30 ± 1.38	45.50 ± 1.05	1.886	equal	0.97
Fe-Si	**n=10**	**n=4**	**t (0.05,43) = 2.016**		
Si	33.85 ± 1.92	28.59 ± 1.96	**4.564**	**different**	1.18
Fe	66.15 ± 1.92	71.41 ± 1.96	**4.564**	**different**	0.93
Fe-O (Pb,Zn)	**n=10**	**n=10**	**t (0.05,33) = 2.035**		
O	73.19 ± 5.93	71.00 ± 0.76	1.153	equal	1.03
Si	2.64 ± 1.15	0.92 ± 0.43	**4.421**	**different**	2.87
Ca	1.31 ± 0.61	0.35 ± 0.15	**4.906**	**different**	3.81
Fe	19.84 ± 4.25	25.73 ± 1.91	**4.002**	**different**	0.77
Zn	1.77 ± 1.22	1.37 ± 0.64	0.901	equal	1.29
Pb	1.27 ± 0.77	0.64 ± 0.45	**2.237**	**different**	1.99

and polished samples. This indicated that these phases could be identified with sufficient reliability using the data obtained by EDS analysis of rough particle samples. For other 6 phases (Pb-C-O, Zn-C-O, Pb-Mo-O, Pb-Zn-V-O, Zn-Si-O and Fe-Si), there were significant differences in element contents obtained from polished and rough particle samples. In 4 phases (Ba-S-O, Fe-Ti-O, Ca-Ti-Si-O and Fe-O (Pb,Zn)), which are among the most complex phases according to their elemental composition, t-test showed significant differences mostly for major constituent elements, while for most of minor and trace elements no significant differences were observed. The differences between contents of constituent elements measured in rough particle and polished samples were ascribed to geometry effects due to the surface morphology and orientation of particle surfaces, to variations in analytical conditions and homogeneity level of individual phases.

The comparison using X_{av}^{u}/X_{av}^{p} ratios showed that contents of light and some other non-metallic elements (O, Si, P and S) in most of metal-bearing phases measured in rough particle samples were generally higher than those measured in polished samples, while contents of metals, especially Ti, Fe, Zn and Pb, were mostly lower in rough particle than in polished samples. These ratios were quite different in Ce-P-O and Pb-S, in which contents of metals were higher and contents of light elements were lower in rough particle samples. In other metal-bearing phases, the X_{av}^{u}/X_{av}^{p} ratios were relatively constant and did not change considerably from phase to phase. They appeared to be mostly independent of different combinations of elements but were dependent on their contents. Thus, in more complex phases, such as Fe-O (Pb,Zn), contents of minor and trace elements were higher in rough particle samples, while in simple phases, such as Zn-S, Pb-S, Ti-O and Fe-S, better ratios between element contents were observed. In metal-bearing phases, in which elements were present as major constituents, the X_{av}^{u}/X_{av}^{p} ratios were lower than 1. However, when they occurred as minor or trace elements, the X_{av}^{u}/X_{av}^{p} ratios became more variable and were generally higher than 1. Thus, the X_{av}^{u}/X_{av}^{p} ratios for major constituent light elements ranged between 0.86 and 1.26, with an average value of 1.04 ± 0.10. The average values of X_{av}^{u}/X_{av}^{p} ratios for major constituent metals were 0.80 ± 0.16 and 1.53 ± 1.06 for metals and light elements present in minor or trace contents in analysed metal-bearing phases.

EDS measurements of rough particle samples thus proved as sufficiently reliable for identification of most of analysed natural and anthropogenic metal-bearing phases, as compared to EDS analysis of polished samples. However, all established characteristics, relations between elements and phases and X_{av}^{u}/X_{av}^{p} ratios need to be considered in calculation of mineral formulae and identification of metal-bearing phases.

Conclusions

The results of this study demonstrated that elemental and mineral compositions of metal-bearing phases in polished and rough particle samples were mostly determined with sufficient precision and accuracy using EDS analyses. Precision measurements showed that the overall average repeatability of EDS analyses under applied analytical conditions amounted to 8 % for polished samples and 24 % for rough particle samples, which was within acceptable limits for most of major elements and some of the elements present in minor or trace contents in the analysed metal-bearing phases. The random analytical fluctuations were considered negligible and phase composition could be determined with sufficient reliability in individual grains of each phase. The homogeneity test showed that metal-bearing phases with minor or trace elements were least homogeneous. The precisions were thus explained by homogeneity level of constituent element distributions throughout phases for 50 % of all analysed phases. The overall average relative error for all elements amounted to about 12 %, which was within acceptable limits for accuracy in quantitative EDS analysis. This allowed calculation of chemical formulae and identification of mineral species of metal-bearing phases based on atomic ratios between constituent elements, determined with sufficient accuracy. All analysed individual phases were thus identified with sufficient accuracy. A comparison between average contents of elements in rough particle and polished samples (the X_{av}^{u}/X_{av}^{p} ratio) showed that the ratios were mostly constant in different phases and depended on atomic number and contents of constituent elements. Light elements and trace metals thus have higher ratios than major metals. However, the t-test showed that only about 38 % of studied metal-bearing phases could be identified with sufficient reliability using the data obtained by EDS analysis of rough particle samples, while for 62 % of phases mineral composition could not be reliably determined. EDS measurements of rough particle samples were sufficiently reliable for identification of most of analysed natural and anthropogenic metal-bearing phases, however, relations between elements and phases and X_{av}^{u}/X_{av}^{p} ratios needed to be considered in calculation of mineral formulae and identification of metal-bearing phases in rough particle samples.

Acknowledgements

The authors acknowledge the financial support from the state budget by the Slovenian Research Agency obtained through the research project "Environmental geochemistry of metal contaminated sites" (No. J1-2065) and research programme "Groundwater and geochemistry" (No. P1-0020).

References

Anthony, J. W., Bideaux, R. A., Bladh, K. W. & Nichols, M. C. 2009: The Handbook of Mineralogy [online]. Mineralogical Society of America. Internet: http://www.handbookofmineralogy.org/ (11. 8. 2011).

Barthelmy, D. 2010: The Mineralogy Database [online]. Internet: http://webmineral.com/ (11. 8. 2011).

Brower, E. 1973: Synthesis of barite, celestite and barium-strontium sulfate solid solution crystals. Geochimica et Cosmochimica Acta, 37/1: 155-156, doi:10.1016/0016-7037(73)90253-6.

Cassidy, K. F., Groves, D. I. & Binns, R. A. 1988: Manganoan ilmenite formed during regional metamorphism of archean mafic and ultramafic rocks from Western Australia. Canadian Mineralogist, 26: 999-1012.

Fux, J. 2007: Težke kovine v sedimentih reke Meže in pritokov kot posledica 300-letnega rudarjenja na območju Mežiške doline. Diploma thesis. University of Ljubljana, Faculty of Natural Sciences and Engineering, Ljubljana: 95 p.

Fux, J. & Gosar, M. 2007: Vsebnosti svinca in drugih težkih kovin v sedimentih na območju Mežiške doline. Geologija, 50/2: 347-360, doi:10.5474/geologija.2007.025.

Goldstein, J., Newbury, D., Joy, D., Lyman, C., Echlin, P., Lifshin, E., Sawyer, L. & Michael, J. R. 2003: Scanning electron microscopy and x-ray microanalysis, 3rd edition. Kluwer Academic/Plenum Publishers, New York: 689 p.

Gonzalez, I., Jordan, M. M., Sanfeliu, T., Quiroz, M. & de la Fuente, C. 2007: Mineralogy and heavy metal content in sediments from Rio Gato, Carelmapu and Cucao, Southern Chile. Environmental Geology, 52/7: 1243-1251, doi: 10.1007/s00254-006-0562-0.

Miler, M., Curk, U. & Mirtič, B. 2009: The use of SEM/EDS method in mineralogical analysis of ordinary chondritic meteorite. Geologija, 52/2: 183-192, doi:10.5474/geologija.2009.018.

Miler, M. 2012: Application of SEM/EDS to environmental mineralogy and geochemistry. Ph.D. thesis. University of Ljubljana, Faculty of Natural Sciences and Engineering, Ljubljana: 169 p.

Newbury, D. E. 1998: Standardless Quantitative Electron-Excited X-ray Microanalysis by Energy-Dispersive Spectrometry: What Is Its Proper Role? Microscopy and Microanalysis, 4/6: 585-597, doi:10.1017/S1431927698980564.

Oxford Instruments 2006: INCA Energy Operator Manual. Oxford Instruments Analytical Ltd., High Wycombe: 84 p.

Reed, S. J. B. 2005: Electron Microprobe Analysis and Scanning Electron Microscopy in Geology, 2nd edition. Cambridge University Press, New York: 189 p.

Reller, A., Braungart, M., Soth, J. & Uexküll, O. 2000: Silicone-eine vollsynthetische Materialklasse macht Geschichten. Gaia, 9/1: 13-24.

Statham, P. J. 2002: Limitations to accuracy in extracting characteristic line intensities from X-ray spectra. Journal of Research of the National Institute of Standards and Technology, 107/6: 531-546.

Štrucl, I. 1974: Formation of carbonate rocks and zinc-lead ore in Anisian beds of Topla. Geologija, 17: 299-397.

Vanek, A., Ettler, V., Grygar, T., Boruvka, L., Šebek, O. & Drabek, O. 2008: Combined chemical and mineralogical evidence for heavy metal binding in mining- and smelting-affected alluvial soils. Pedosphere, 18/4: 464-478, doi:10.1016/S1002-0160(08)60037-5.

doi:10.5474/geologija.2013.002

Structure of the chondrules and the chemical composition of olivine in meteorite Jesenice

Tekstura hondrul in kemijska sestava olivina v meteoritu Jesenice

Bojan AMBROŽIČ[1], Sašo ŠTURM[2], Miha JERŠEK[3] & Breda MIRTIČ[1]

[1]Faculty of Natural Sciences and Engineering,
Aškerčeva 12, 1000 Ljubljana, e-mail: ambrozicbojan@hotmail.com

[2]Jožef Stefan Institute, Jamova 39, 1000 Ljubljana
[3]Slovenian Museum of Natural History, Prešernova 20, 1000 Ljubljana

Prejeto / Received 20. 3. 2013; Sprejeto / Accepted 8. 5. 2013

Key words: quantitative EDS analysis, chondrules, olivine, ordinary chondrite, meteorite Jesenice
Ključne besede: kvantitativna EDS analiza, hondrule, olivin, navadni hondrit, meteorit Jesenice

Abstract

This paper presents a mineralogical analysis of various chondrule types and chemical analysis of olivine in different parts of meteorite Jesenice. Quantitative energy-dispersive X-ray spectroscopy with a scanning electron microscope was used in the analyses. The results showed that the chemical composition of the olivine was homogeneous throughout the meteorite with an average olivine composition of Fa 26.4 ± 0.6. The results of this study were in agreement with previous study of the meteorite, which showed that the meteorite Jesenice was an equilibrated L chondrite.

Izvleček

V prispevku so predstavljene mineraloške raziskave različnih tipov hondrul ter kemijske raziskave olivina v različnih delih meteorita Jesenice. Pri raziskavah smo uporabili točkovno kvantitativno energijsko disperzijsko spektroskopijo rentgenskih žarkov z vrstičnim elektronskim mikroskopom. Rezultati so potrdili, da je kemična sestava preiskanih olivinovih zrn v različnih delih meteorita Jesenice homogena s povprečno sestavo olivina Fa 26,4 ± 0,6. To potrjuje rezultate dosedanjih raziskav, ki so pokazale, da meteorit Jesenice sodi med homogenizirane L hondrite.

Introduction

Chondrites are the most common type of stony meteorites, representing 70 % of all falls (Norton, 2002). Meteorite Jesenice is the first known Slovenian chondritic meteorite. It fell on the Mežakla plateau, near the town of Jesenice, in April 2009 (Spurný et al., 2010).

The classification of stony meteorites is based on their chemical and mineralogical composition. Stony meteorites are divided into two classes: chondrites, i.e. meteorites containing chondrules, and achondrites, i.e. meteorites without chondrules (Norton, 2002).

Bischoff and coworkers (2011) were the first to investigate the chemical and mineral composition of meteorite Jesenice. They determined the composition of the olivine to be $Fa_{25.1 \pm 0.4}$ with a compositional range from 23.9 to 25.8 mole % of iron. Based on these criteria Bischoff and coworkers (2011) classified meteorite Jesenice as a weakly shocked (S3), low total iron (L) ordinary chondrite of petrologic type 6. Bischoff and coworkers (2011) claim that meteorite Jesenice is an equilibrated chondrite, which means the chemical composition of minerals in meteorite Jesenice is homogenous in all parts of the meteorite.

EDS (quantitative and/or semi-quantitative) is considered a standard method petrographic and mineralogical characterization of meteorites and was also used in similar studies of meteorites (Bischoff et al., 2010, 2011; Greshake et al., 1998; Horstmann et al., 2010; Sokol et al., 2005, 2007; Keil et al., 2008; Llorca et al., 2010; Metzler et al., 2011). In addition, Sepp and coworkers (2001) used WDX in the chemical analysis of a meteorite. Some authors performed their chemical analyses of chondrites using averaged samples (Bischoff et al., 2011) such as INAA and XRF (Greshake et al., 1998; Metzler et al., 2011). Although this method gives reliable information about the chemical composition, the major drawback is that it provides an average, i.e. the bulk chemical composition. On the other hand some authors (Šmit et al.,

2011) used single-point analyses by PIXE. Some authors (Greshake et al., 1997; Keil et al., 2008; Metzler et al., 2011; Simon et al., 2011; Sokol et al., 2005; Llorca et al., (2010), found the zonal composition in mineral grains and in chondrules by using EMPA alone/and LA ICP MS.

Prior to the quantitative EDS analysis of meteorite Jesenice the microstructures of different types of chondrules and chondrule rims were investigated to understand the genesis of the chondrules and consequently the possible differences in the chemical composition of the olivines. On the basis of these results locations in the sample for chemical analysis were chosen.

Our goal was to determine the exact degree of homogeneity of meteorite Jesenice. In this study the mineral olivine was chosen, because it is by far the most common mineral found in the meteorite Jesenice. Olivine is a solid solution between forsterite (Mg_2SiO_4) and fayalite (Fe_2SiO_4). Consequently, even small changes in the crystallization conditions in different parts of the meteorite can result in a variation of the chemical composition of the mineral olivine, which can give valuable information about the crystallization history of the whole meteorite body. For this reason the composition of the olivine was studied in detail in relations to the following criteria:

- the homogeneity of the olivine inside the individual mineral grains,
- the differences in the olivine composition between the chondrules and the matrix,
- the compositional variations of the olivine between the rim and the core, within the individual chondrules,
- the compositional variations of the olivine between different types of chondrules,
- the compositional differences of the olivine between relict olivine grain, porphyritic and olivine chondrule.

This paper follows the classification of meteorites, the classification of chondrules, the genesis and the structure of chondrules which were summarized in the paper *Classification of stony meteorites and chondrules – the case of meteorite Jesenice* (Ambrožič et al., 2012) after different authors.

Samples and methods

To investigate the interior of the meteorite, the mineral phases and the structure of the chondrules, small fragments of the meteorite were cut into slices. From these slices a few polished thin sections were prepared. Thin sections were observed with a Zeiss Axio Z1- polarized optical microscope in reflected and transmitted light. The thin sections were additionally coated with a 3 nm thick layer of amorphous carbon to ensure the conductivity of samples for further scanning electron microscopy/energy-dispersive X-ray spectroscopy (SEM/EDS) analyses.

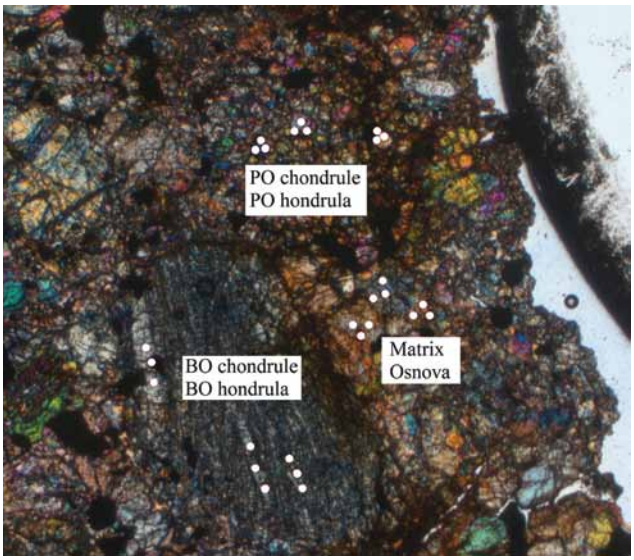

Fig. 1. Scheme of selection of locations for EDS analyses
Sl. 1. Shema izbire lokacij za EDS analizo

The optical microscopy was used mainly for identifying different minerals in meteorite Jesenice. However, a second benefit of this method, compared with electron microscopy, is large field of view, which allows us to observe an entire chondrule. In addition, the places damaged by oxidation were identified with an optical microscope and were later excluded from the SEM/EDS analysis. The data obtained with the optical microscopy were later used to select the best areas for chemical EDS analyses in the SEM.

Prior to the quantitative EDS analysis the microstructures of different types of chondrules and chondrule rims were investigated to understand the genesis of the chondrules and consequently the possible differences in the chemical composition of the olivines. On the basis of these results regions in the sample were chosen for chemical analysis.

In order to distinguish between the areas with different mineral composition we used a scanning electron microscope (SEM) and backscattered electrons (BSE). The signal in BSE mode is dependent on the average atomic number (Z) of a certain mineral. Minerals with higher Z-number appear brighter than minerals with a lower Z-number (Goldstein et al., 2003). Unfortunately, when using BSE the oxidized areas related to iron-bearing minerals were difficult to distinguish.

In order to perform a detailed quantitative analysis of the olivine composition, scanning electron microscopy (SEM) combined with quantitative energy-dispersive X-ray spectroscopy (EDS) was chosen. Different mineral reference materials were used as the calibration standards for the quantitative EDS analysis. The chemical analyses of the olivine in the meteorite were made with a Jeol JSM 5800 scanning electron microscope equipped with an EDS system (Oxford instruments ISIS 300). The analyses were performed at an accelerating voltage of 20 kV (Greshake et al., 1998; Sokol et al., 2005; Metzler et al., 2011) and

a working distance of 10 mm. The spectra acquisition time was set to 100 s and the beam current was adjusted to reach the value of dead time between 25 and 30 %. Every 20 min of analysis the instrument was calibrated and optimized for quantification with a cobalt standard. The spectra

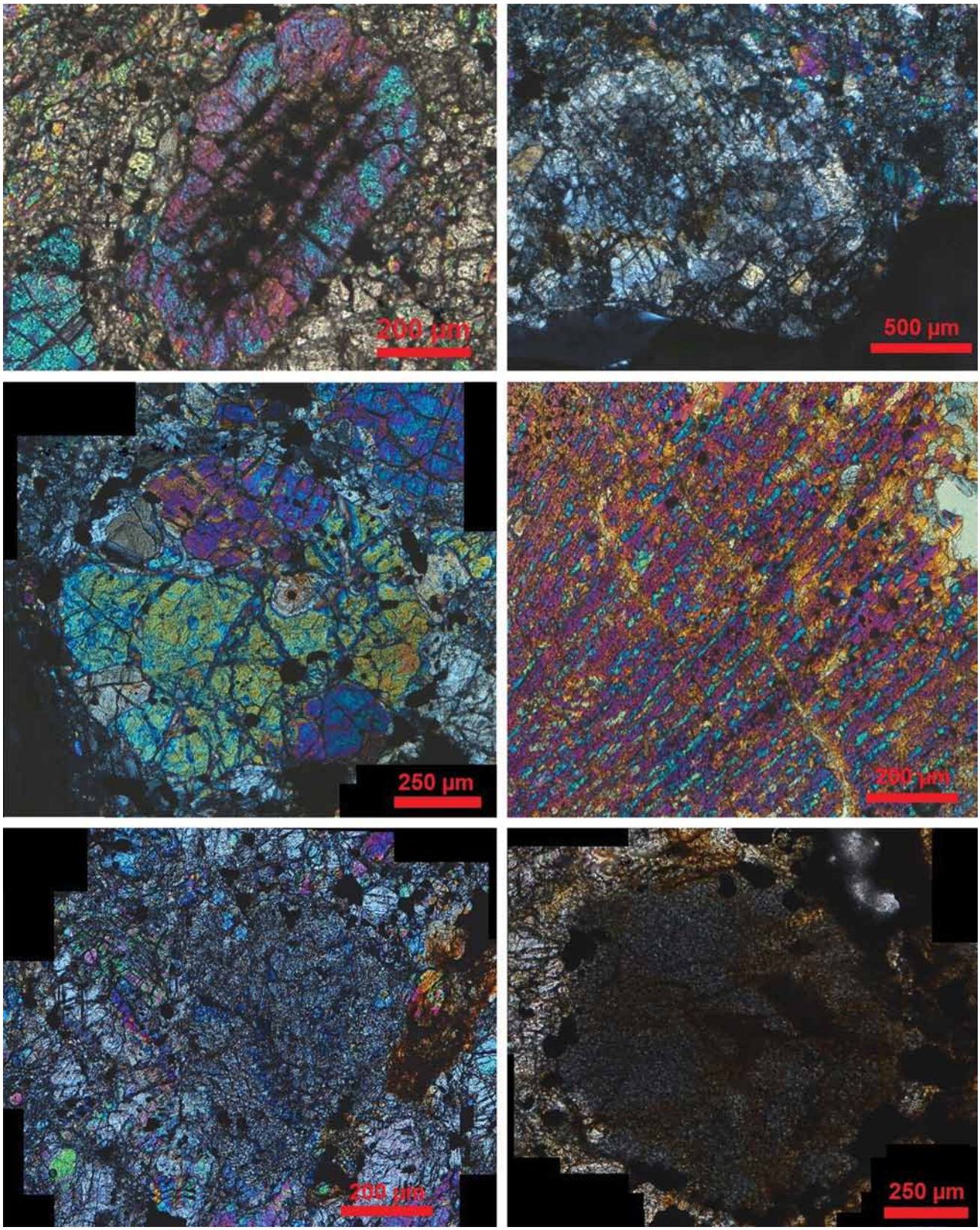

Fig. 2. Various different types of chondrules in meteorite Jesenice. Plane-polarized light, x nicols. A) barred olivine chondrule (BO), B) porphyritic pyroxene chondrule (PP), C) porphyritic olivine chondrule (PO), D) radial pyroxene chondrule (RP), E) porphyritic pyroxene chondrule, F) cryptocrystalline chondrule (C)

Sl. 2. Različni tipi hondrul v meteoritu Jesenice. Presevna polarizirana svetloba, x nikoli. A) lamelarna olivinova hondrula (BO), B) porfirska piroksenova hondrula (PP), C) porfirska olivinova hondrula (PO), D) pahljačasta piroksenova hondrula (RP), E) kriptokristalna hondrula (C).

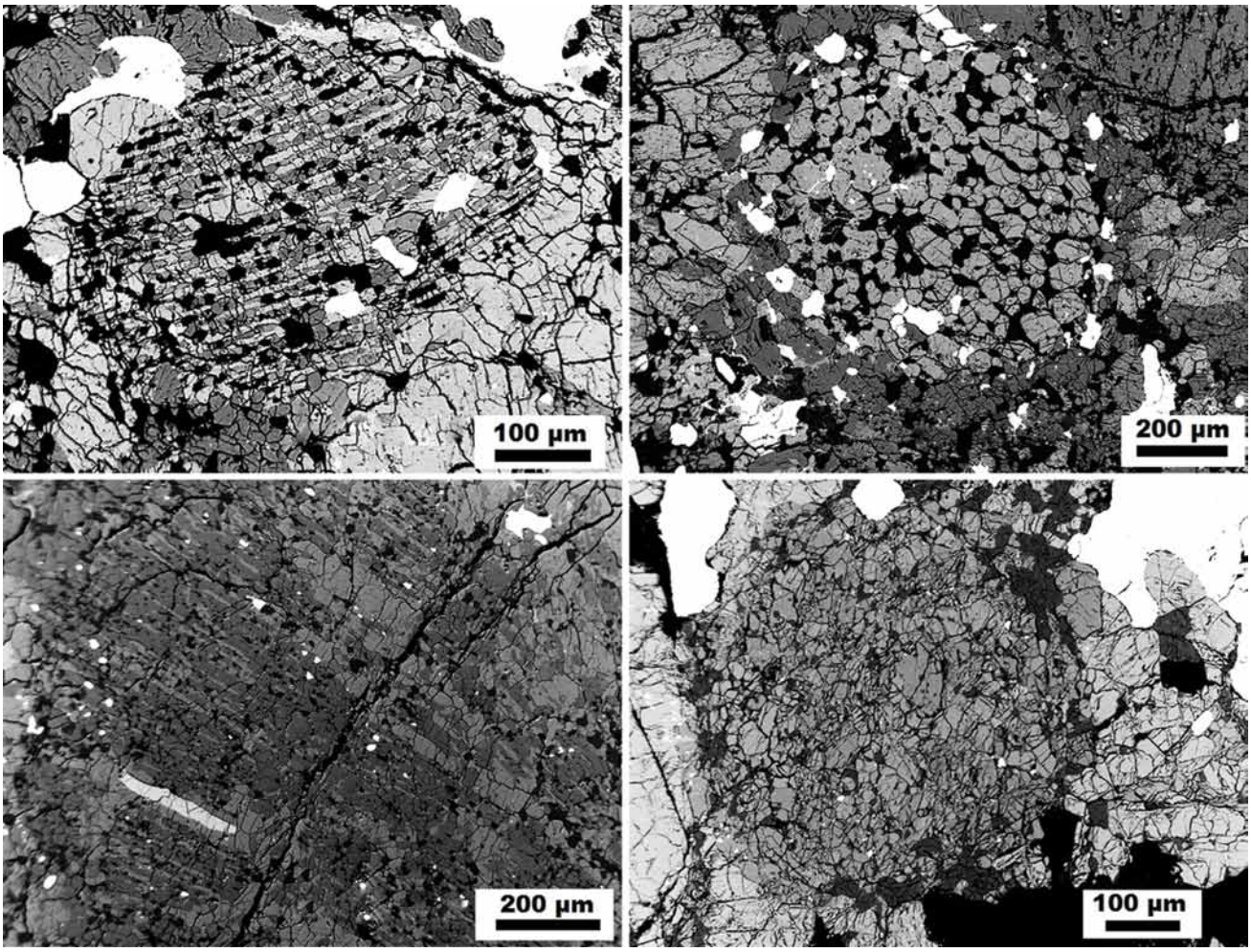

Fig. 3. Various types of chondrules in meteorite Jesenice. SEM, BSE. A) Barred olivine chondrule, B) Porphyritic olivine chondrule, C) Radial pyroxene chondrule, D) Porphyritic pyroxene chondrule

Sl. 3. Različni tipi hondrul v meteoritu Jesenice. SEM, BSE. A) lamelarna olivinova hondrula , B) porfirska olivinova hondrula, C) pahljačasta piroksenova hondrula, D) porfirska piroksenova hondrula

were quantified using reference materials with a well-defined chemical composition obtained from C. M. Taylor Company. The following mineral reference materials were used: α-quartz (SiO_2) for silicon, almandine ($(Fe, Mg, Mn)_3 Al_2(SiO_4)_3$) for iron and manganese and diopside ($MgCaSi_2O_6$) for magnesium. Bischoff and coworkers (2011) used olivine (Mg, Fe, Si), jadeite (Na), plagioclase (Al), sanidine (K), diopside (Ca), rutile (Ti), chromite (Cr), rhodonite (Mn) and pentlandite (Ni).

Prior to the EDS analysis of the olivine in the meteorite, spectra from the reference materials were acquired. The calibration factors for the quantitative EDS analysis were calculated by assigning a given composition of the reference materials to the related reference spectra. The oxygen concentration was calculated from the stoichiometry. This procedure was performed using Link ISIS computer software (Oxford Instrument Limited, 1995). Since this instrument does not have the capability to measure the absolute current values and in order to minimize the influence of the random fluctuations of the microscope's instabilities on the reliability of the EDS analysis, this procedure was repeated every time prior to the EDS measurements on a daily basis.

The percentage of the unknown mass concentration (C_i) of the chemical element i in the sample was calculated using the equation:

$$C_i = C_i^* \cdot (I_i / I_i^*) \cdot [ZAF]_i = C_i^* \cdot k_i \cdot [ZAF]_i$$

where C_i^* is known mass concentration of element i in reference material, I_i and I_i^* are the intensities of emitted X-ray radiation of a certain spectral line of element i in the sample and in the reference material, respectively, and k_i is the k-ratio for the element i in the sample. $[ZAF]_i$ is the product of matrix-correction factors Z, A and F. Z is an atomic correction factor, A is an absorption factor and F is a secondary fluorescence correction factor (Reed, 1996). ZAF corrections are commonly applied in the EDS analyses of meteorites (e.g. Greshake et al., 1998; Sokol et al., 2005; Metzler et al., 2011).

In each of eight examined chondrules we picked three olivine mineral grains and within each grain we chose three spots where the EDS analyses were performed (Fig. 1). Similar procedures were also used in the analyses of the matrix, the chondrule rims and in the relict olivine grain. All studied chondrules are displayed in Table 1.

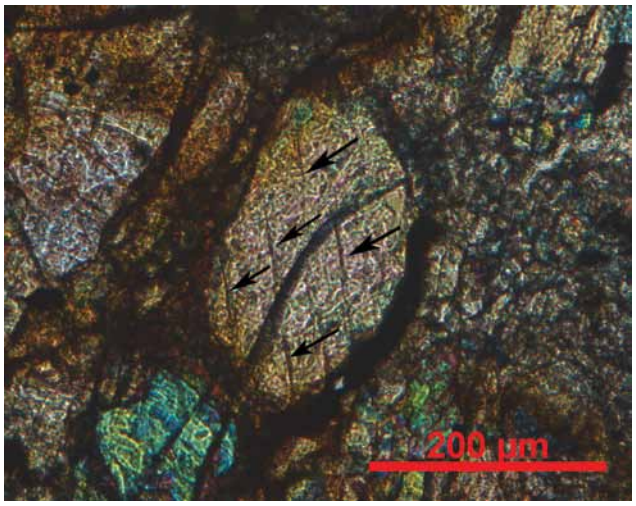

Fig. 4. Planar deformations in olivine grain marked by arrows. Plane-polarized light, x nicols.

Sl. 4. Planarne razpoke v olivinu, označene s puščicami. Presevna polarizirana svetloba, x nikoli.

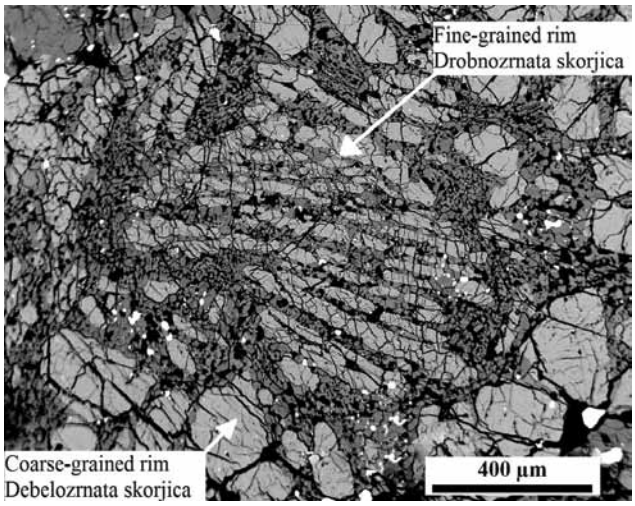

Fig. 5. Barred olivine chondrule with coarse-grained and fine-grained rim. SEM, BSE.

Sl. 5. Lamelarna olivinova hondrula z drobnozrnato skorjico znotraj debelozrnate skorjice. SEM, BSE.

Results

Chondrules and their structure

Meteorite Jesenice contains a variety of different chondrule groups and types. The texture of meteorite Jesenice is highly recrystallized, as a result of the large degree of thermal metamorphosis (Bischoff et al., 2011). The rims of the chondrules are often very deformed and mixed with the surrounding matrix. The chondrules are usually surrounded by a thin rim of metal grains. The smallest measured cross-section of the chondrules measures about 200 µm and the largest around 7000 µm.

In meteorite Jesenice, chondrules that belong to the groups of porphyritic chondrules, nonporphyritic chondrules and granular chondrules were found (Ambrožič et al., 2012; Ambrožič, 2012).

Porphyritic chondrules are the most abundant chondrule group in meteorite Jesenice. This group of chondrules usually contains a large number of olivine and pyroxene crystals, which were weakly resistant to processes during the thermal metamorphosis. Consequently, many porphyritic chondrules lack a rim. In meteorite Jesenice all three types of porphyritic chondrules were found (Ambrožič et al., 2012): porphyritic olivine (PO) chondrules, porphyritic olivine-pyroxene (POP) chondrules and porphyritic pyroxene (PP) chondrules. Out of these, the PO chondrules are by far the most common. They are composed of euhedral to subhedral olivine crystals. The olivine grains in most of the PO chondrules seem to have a random arrangement. However, several PO chondrules show olivine grains oriented in a few dominant directions. Inside one of the PO chondrules a relict olivine grain (R) was found. The relict is a possible remnant of a previous generation of chondrules. PP chondrules are rare, but, on the other hand, they are easily spotted because they are formed mostly out of large pyroxene phenocrysts. POP chondrules are composed of both pyroxene and olivine crystals; however, in most cases olivine is dominant over pyroxene (Figs. 2 and 3).

Nonporphyritic chondrules or droplet chondrules are chondrules that formed from the melt. Barred olivine (BO) chondrules were the most common type found in meteorite Jesenice. They are easily recognized under crossed-polarized light by their characteristic structure. BO chondrules are formed out of a series of alternating bars of olivine and plagioclase. Olivine crystals are monosomatic and can be observed in the same optical orientation under a polarized optical microscope. Olivine bars are more resistant to thermal metamorphosis in comparison to the surrounding chondrule rim. Consequently, many chondrules in meteorite Jesenice lack a rim, whereas their morphology is defined as irregular polygonal forms instead of spheres. BO chondrules with a different orientation of olivine bars (or so called polysomatic BO chondrules) are also present. Some BO chondrules occur with bended olivine bars, while radial pyroxene (RP) chondrules are made of fan-shaped pyroxene and plagioclase crystals. The fan shape is a consequence of the crystallization of minerals from one eccentric point. There are also chondrules with more than one crystallization point. In meteorite Jesenice the RP chondrules are almost all without a rim, which is why their outer parts are chemically corroded into a shape of a sea shell (Figs. 2 and 3).

Granular olivine-pyroxene (GOP) chondrules are composed of a tight package of very small olivine and pyroxene crystals. These minerals are too small to be distinguished using an optical microscope. On average, the mineral grains in the GOP chondrules in meteorite Jesenice measure around 10 µm. On the other hand, the metal grains in GOP chondrules are significantly larger – measuring 20 –100 µm. All the metal grains are of an anhedral shape. Cryptocrystalline (C) chondrules are also present; they are composed of mineral grains, which are too small to be individually observable using an optical microscope (Fig. 2).

Besides the previously noted, more common types of chondrules, we also found some rarer

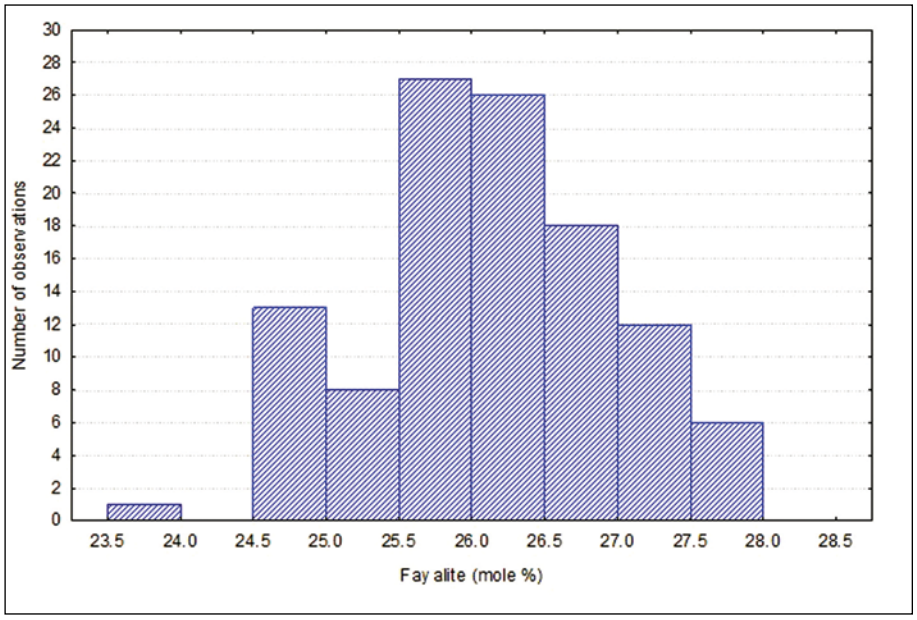

Fig. 6. Histogram of average composition of olivine in meteorite Jesenice, in mole % of fayalite (N=93).

Slika 6. Histogram povprečne sestave olivina v meteoritu Jesenice, v mol. % fayalite (N=93).

types of chondrules in meteorite Jesenice. One such example are metal (M) chondrules. The M chondrules in meteorite Jesenice are composed of euhedral metal grains embedded in feldspar. The metal grains are concentrated in a thick ring around the centre of the chondrule, while the feldspar embeds the rest of the chondrule. In optical microscope these chondrules look like black flakes. Compound chondrules are another interesting group of chondrules found in meteorite Jesenice. These chondrules are composed of two chondrules joined together. Compound chondrules that have both the same structure and mineralogy are called sibling compound chondrules or independent compound chondrules. Sometimes one chondrule can envelop another. These chondrules are called enveloping chondrules. In Jesenice we found independent compound chondrule composed of PO and POP chondrule.

Shock metamorphosis

Some olivine and pyroxene crystals show shock lamellae or planar deformations (Fig. 4), which were only observed on a few larger grains at higher magnifications. Most grains lack planar deformations. We also found several sets of planar deformations in a relict grain inside a porphyritic olivine chondrule. The olivine and plagioclase also show undulatory extinction. The shock features observed in this study were in agreement with S3 shock stage determined by Bischoff and coworkers (2011).

Weathering of the meteorite

Meteorite Jesenice had lain on the ground atop of Mežakla plateau for 39 days before it was found in April 2009 (Spurný et al., 2010). The meteorite fragment (later named BOJO) was found in shallow impact pit partially covered with a mixture of snow and leaves (Bischoff et al., 2011). The severe weather conditions of the Mežakla plateau had already partially altered the meteorite. The meteorite fusion crust, in some places, seems "rusty". Rust is a mix of secondary iron minerals as a result of the oxidation of metallic iron. The meteorite's interior is also partially weathered. There are oxide rims around the metal and around the major cracks and veins. Olivine and pyroxene grains are unaltered.

Chondrule rims

In meteorite Jesenice most of the chondrules lack chondrule rims due to the high degree of thermal metamorphosis. Nevertheless, all the observed porphyritic chondrules have coarse grained rims with an average thickness of 150 µm. It is also possible that some porphyritic chondrules once had fine-grained rims, which were later destroyed by the process of thermal metamorphosis.

Of the nonporphyritic chondrules most BO chondrules have a fine-grained rim with an average thickness between 50 and 100 µm (Figs. 2 and 3). We also found a BO chondrule with a fine-grained rim inside of a larger, coarse-grained rim (Fig. 5). The BO chondrule rims in meteorite Jesenice are chemically classified as high-FeO rims (Bischoff et al, 2011). On the other hand, we did not find a single RP chondrule with at least part of its rim preserved (Figs. 2 and 3).

Chemical composition of olivine

Chemical composition of olivine in various areas of meteorite Jesenice was determined by EDS using a spot-mode technique. These areas were located within three BO chondrules, three PO chondrules, one BO chondrule rim, one PO chondrule rims, the matrix, an olivine relict grain and a PO chondrule that contains a relict grain and are marked in Table 1. The concentrations of magnesium, silicon, iron and manganese were determined. The measured chemical composition

Table 1. Chemical composition of olivine at different spots of the analyses, in wt.%
Preglednica 1. Kemična sestava olivina po posameznih mestih preiskav, v mas.%

Spots of the analyses	Labels	Number of analyses	MgO (wt.%)	SiO_2 (wt.%)	FeO (wt.%)	MnO (wt%)
Barred olivine chondrule 1	BO 1	9	37.3 ± 0.2	39.0 ± 0.2	23.1 ± 0.3	0.6 ± 0.1
Barred olivine chondrule 2	BO 2	9	37.4 ± 0.1	38.9 ± 0.2	23.2 ± 0.1	0.6 ± 0.1
Barred olivine chondrule 3	BO 3	9	37.5 ± 0.3	38.9 ± 0.2	22.9 ± 0.2	0.6 ± 0.1
Average of barred olivine chondrules	Average BO	27	37.4 ± 0.2	38.9 ± 0.2	23.1 ± 0.2	0.6 ± 0.1
Rim of Barred olivine chondrule 1	BO S	9	36.9 ± 0.3	38.9 ± 0.2	23.7 ± 0.4	0.5 ± 0.1
Porphyritic olivine chondrule 1	PO 1	9	36.8 ± 0.2	39.1 ± 0.2	23.7 ± 0.2	0.4 ± 0.1
Porphyritic olivine chondrule 2	PO 2	9	36.8 ± 0.3	39.0 ± 0.3	23.8 ± 0.4	0.4 ± 0.1
Porphyritic olivine chondrule 3	PO 3	9	36.7 ± 0.3	38.8 ± 0.2	24.0 ± 0.3	0.5 ± 0.1
Porphyritic olivine chondrule 4	PO 4	9	36.5 ± 0.3	38.7 ± 0.3	24.3 ± 0.5	0.4 ± 0.1
Average of porphyritic olivine chondrules	Average PO	36	36.5 ± 0.2	38.8 ± 0.2	24.2 ± 0.3	0.5 ± 0.1
Rim of Porphyritic olivine chondrule 1	PO S	9	37.3 ± 0.1	38.8 ± 0.2	23.4 ± 0.2	0.6 ± 0.1
Matrix of the meteorite	M	9	36.5 ± 0.2	38.8 ± 0.2	24.2 ± 0.3	0.5 ± 0.0
Relict grain in porphyritic olivine chondrule	R	3	37.1 ± 0.1	38.8 ± 0.2	23.5 ± 0.2	0.6 ± 0.1
Olivine grains around relict grain in porphyritic olivine chondrule	R-o	9	37.1 ± 0.1	38.8 ± 0.1	23.5 ± 0.1	0.7 ± 0.1
Average	/	/	**37.0 ± 0.4**	**38.9 ± 0.2**	**23.6 ± 0.5**	**0.5 ± 0.1**

in wt.% of oxides is shown in Table 1. In addition, the fayalite content in the olivine was also quantified. The results are shown in Fig. 6. All the gathered data show a Gaussian distribution.

The calculated average composition of the analyzed olivine grains is $Fa_{26.4 \pm 0.6}$ with a compositional range from 23.9 to 27.7 mole% (Fig. 6). No statistically significant deviations were found in the composition of the olivine between the different spots of the analyses in chondrules (Tab. 1) and between the different parts of the meteorite (Tab. 1). On average, the olivine in meteorite Jesenice contains 37.2 ± 0.7 wt.% MgO, 18.2 % ± 0.6 wt. % FeO, 38.8 ± 0.3 wt.% SiO_2 and 0.5 ± 0.1 wt.% MnO.

Discussion

There are many different types and groups of chondrules in meteorite Jesenice, which were classified according to the Gooding-Keil classification (Gooding & Keil, 1981). Among porphyritic chondrules we found the POP, PP and PO

chondrules in meteorite Jesenice, of which the PO chondrules were the most common. The group of nonporphyritic chondrules is represented by BO and PO chondrules in meteorite Jesenice. We also found some rarer types of chondrules, like granular olivine-pyroxene chondrules and independent compound chondrules. Knowledge about the different chondrule types was necessary for the subsequent EDS analyses. We used this knowledge to locate suitable olivine grains and the appropriate spots for the EDS analyses. Different types and groups of chondrules have very different origins (Norton, 2002), which could imply differences between the chondrule types and groups.

The rims of the chondrules are often very deformed and mixed with the surrounding matrix or are completely missing. For this reason it is sometimes hard to distinguish between the matrix and some of the chondrule types. There are two basic types of chondrule rims: fine-grained and coarse-grained (Norton, 2002). Fine-grained chondrule rims in meteorite Jesenice formed with accretion from the nebular dust after the chondrules were already formed. On the other hand, the coarse-grained rims formed partially from the host chondrule and partially out of the solar nebula dust. In meteorite Jesenice the coarse-grained chondrules are more common in the porphyritic chondrules and the fine-grained chondrules in the non-porphyritic (BO) chondrules. There are also chondrules with both coarse- and fine-grained rims (concentric to each other), which implies the chondrules were exposed to multiple heating and dusting events (Norton, 2002).

We could not successfully determine the average size of the chondrules in meteorite Jesenice because it was difficult to deduce the exact cross-section geometry of the chondrules inside the thin section and because most chondrules are destroyed due to high grade of thermal metamorphosis.

The presence of planar deformations in the pyroxene and olivine and undulatory extinction in the olivine grains indicates that meteorite Jesenice is a weakly shocked (S3) (Bischoff et al., 2011) ordinary chondrite according to classification by Wlotzka (1993). The presence of planar deformation in relict grain indicates that relict had been a part of meteorite Jesenice before the shock metamorphosis took place.

The presence of oxide rims around the metal, major cracks and veins indicate that meteorite Jesenice is a weakly weathered meteorite (W1) (Bishoff et al., 2011) according to classification by Wlotzka (1993). The low degree of oxidation was crucial for the successful EDS analysis. In order to prevent further oxidation our samples are kept in a vacuum chamber.

Chemically, the chondrules are divided according to the Scott-Taylor-Jones (Scott & Taylor, 1983; Jones & Scott, 1989; Jones, 1990, 1994) scheme into FeO rich and FeO poor. The chondrules in meteorite Jesenice are FeO rich or Type-II, which is typical for an ordinary chondrite. Type-II chondrules are further divided in Type-IIA, Type-IIB and Type-IIAB. Meteorite Jesenice contains all these types of chondrules; however, type Type-IIA is the most common. The dominant mineral in meteorite Jesenice is olivine, which is a direct consequence of being chemically L chondrite. Besides olivine, the major minerals are low Ca-pyroxene, plagioclase (oligoclase) and iron-nickel minerals. The average fayalite content in the olivine put meteorite Jesenice into the upper boundary of L ordinary chondrites according to Bischoff and coworkers (2011) (Tab. 2) and into the lower boundary of LL chondrites according to Norton (2002) (Tab. 2).

Table 2. Classification of ordinary chondrites by fayalite composition. Adopted by Bischoff et al., (2011) and Sears (2002).
Preglednica 2. Klasifikacija navadnih hondritov glede na sestavo fayalita. Povzeto po Bischoff et al. (2011) in Sears (2002).

Group of ordinary chondrites	Fa (mole %)	
	According to Bischoff et al., (2011)	According to Norton (2002)
H	16-20.5	16-20
L	21-26.5	21-25
LL	27-31	26-32

The results show meteorite Jesenice is homogeneous inside the individual grains. There is also no statistically significant difference in the composition of the olivine inside the chondrule or in the matrix (Tab. 1). We carried out analyses in several different types of chondrules. The results (Tab. 1) show no difference in the composition of the olivine between the different chondrule types. Also, the chondrule rim has the same composition as the chondrule itself. What came as a surprise was the fact that the composition of the relict olivine grain is exactly the same as that of all the other analyzed olivine grains. If we sum up, the olivine in meteorite Jesenice is homogeneous, which confirms the claim of Bischoff and coworkers (2011). The extreme degree of homogeneity implies that the relict grain was part of meteorite Jesenice long before the thermal metamorphosis event took place. This thermal metamorphosis was strong enough to cause ion migration and homogenization of the whole meteorite.

The standard errors in the detection of the elements using our EDS analyses are similar to those obtained by Metzler and coworkers (2011) using similar method (Tab. 3). The results shown in Tab. 3 indicate that quantitative EDS is one of the most accurate methods, combining a high spatial resolution and a reliable quantitative analysis, making it extremely suitable for analyses of heterogeneous meteorite bodies.

EDS analyses are also subject to the counting error of the detector. This error is therefore related to the quantity of a certain element in the sample, if we assume the same acquisition time for all the elements. A higher quantity of a certain element

Table 3. Accuracy of EDS / EMP / PIXE analysis by different authors

Preglednica 3. Natančnost EDS / EMP/ PIXE analiz na meteoritih po različnih avtorjih

Oxide	Reference	Method	Error (wt. %)
MgO	Llorca et al. (2008)	EMP	1-5
	Janots et al. (2010)	EMP	1-5
	Šmit et al. (2011)	PIXE	4.6
	Metzler et al. (2011)	EDS	0.37
	This study	EDS	0.4
SO_2	Llorca et al. (2008)	EMP	1-5
	Janots et al. (2010)	EMP	1-5
	Šmit et al. (2011)	PIXE	4.9
	Metzler et al. (2011)	EDS	0.32
	This study	EDS	0.2
FeO	Llorca et al. (2008)	EMP	1-5
	Janots et al. (2010)	EMP	1-5
	Šmit et al. (2011)	PIXE	6.55
	Metzler et al. (2011)	EDS	0.39
	This study	EDS	0.5

in the samples results in a lower counting error and vice versa. The lowest counting error was detected with Si (0.5 %), followed by Mg (0.6 %) and Fe (1.3 %). On the other hand, Mn was at the limit of detection for our quantitative EDS method. For this reason the counting error was as large as 21 %.

Conclusions

Present study of the meteorite Jesenice showed that olivine in meteorite has a composition of Fa 26.4 ± 0.6 and confirmed conclusions made by Bischoff and coworkers (2011) that it is an ordinary L chondrite of petrologic type 6. The planar deformation and the undulatory extinction of the mineral grains, determined also in this study, indicate that meteorite Jesenice is a weakly shocked (S3) meteorite. Analyses with quantitative energy-dispersive X-ray spectroscopy proved that the olivine in meteorite Jesenice is homogeneous. We did not notice any anomalies in the composition of the different chondrule types, the chondrule rims, the relict grain and the matrix. All this confirms that meteorite Jesenice is an equilibrated meteorite.

Acknowledgments

We would like to thank the Department for Nanostructured Materials, Jožef Stefan Institute, Ljubljana, for providing access to the scanning electron microscope. We are also very grateful to dr. Paul J. McGuiness for proofreading of the paper.

References

Ambrožič, B., Šturm, S., Jeršek, M. & Mirtič, B. 2012: Klasifikacija kamnitih meteoritov in hondrul – primer meteorita Jesenice = Classification of stony meteorites and chondrules – the case of meteorite Jesenice. Geologija, 55/2: 163-180, doi:10.5474/geologija.2012.011.

Ambrožič, B. 2012: Mineralogija meteorita Jesenice: diplomsko delo. Ljubljana: 38 p.

Bischoff, A., Horstmann, M., Pack, A., Laubenstein, M. & Haberer, S. 2010: Asteroid 2008 TC_3 –Almahata Sitta: A spectacular breccia containing many different ureilitic and chondritic lithologies. Meteoritics & Planetary Science, 45/10-11: 1638–1656, doi: 10.1111/j.1945-5100.2010.01108.x.

Bischoff, A., Jeršek, M., Grau, T., Mirtič, B., Ott, U., Kučera, J., Horstmann, M., Laubenstein, M., Hermann, S., Řanda, Z., Weber, M. & Heusser, G. 2011: Jesenice – A new meteorite fall from Slovenia. Meteoritics & Planetary Science, 46/6: 793–804, doi:10.1111/j.1945-5100.2011.01191.x.

Goldstein, J. I., Newbury, D. E., Echlin, P., Joy, D. C., Lyman, C. E., Lifshin, E., Sawyer, L. & Michael, J. R. 2003: Scanning Electron Microscopy and X-Ray Microanalysis. Third edition, Kluwer Academic/Plenum Publishers (Boston): 689 p.

Gooding, J. L. & Keil, K. 1981: Relative abundances of chondrule primary textural types in ordinary chondrites and their bearing on conditions of chondrule formation. Meteoritics, 16: 17–43.

Greshake, A., Wolfgang, K., Arndt, P., Maetz, M., Flynn, G. J. & Bischoff, A. 1998: Heating experiments simulating atmospheric entry heating of micrometeorites: Clues to parent body sources. Meteoritics & Planetary Science, 33/2: 267-290.

Horstmann, M., Bischoff, A., Pack, A. & Laubenstein, M. 2010: Almahata Sitta-Fragment MS-CH. Meteoritics & Planetary Science, 45/10-11: 1657–1667, doi:10.1111/j.1945-5100.2010.01107.x.

Jones, R. H. 1990: Petrology and mineralogy of type II chondrules in Semarkona (LL3.0): Origin of closed-system fractional crystallization, with evidence for supercooling. Geochim.Cosmochim. Acta, 54: 1785–802.

Jones, R. H. 1994: Petrology of FeO-poor, porphyritic pyroxene chondrules in the Semarkona chondrite. Geochim.Cosmochim. Acta, 58: 5325–40.

Jones, R. H. & Scott, E. R. D. 1989: Petrology and thermal history of type IA chondrules in the Semarkona (LL3.0) chondrite. Proc. 19th Lunar Planet. Sci. Conf. Lunar and Planetary Institute, 523–36.

Llorca, J., Casanova, I., Pack, A., Trigo-Rodríguez. J., Maideo, J., Bischoff, A., Ott, U., Franch, I. A., Greenwood, R.C. & Laubenstein, M. 2009: The Puerto Lápice eucrite. Meteoritics & Planetary Science (2010), 44/2: 159–174.

Metzler, K., Bichoff, A., Greenwood, R. C., Palme,

H., Gellisen, M., Hopp, J., Franhi, I. A. & Trieloff, M. 2011: The L3-6 chondritic regolith breccia Northwest Afrca (NWA) 869: (I) Petrology, chemistry, oxygen isotopes, and Ar-Ar age determinations. Meteoritics & Planetary Science, 46/5: 652-680.

Norton, R. 2002: The Cambridge Encyclopedia of the Meteorites. Cambridge: Press Syndicate of the University of Cambridge: 354 p.

Oxford instrument limited. Microanalyses group: Link ISIS operatoržs manual, 1995.

Reed, S. J. B. 1996: Electron Microprobe Analysis and Scanning Electron Microscopy in Geology. Cambridge University Press: 215 p.

Scott, E. R. D. & Taylor, G. J. 1983: Chondrules and other components in C, O, and E chondrites; Similarities in their properties and origins. Proc. 14th Lunar Planet. Sci. Conf. J. Geophys. Res. 88, B275–B286.

Sears, D. 2004: The Origin of Chondrules and Chondrites. Cambridge University Press: 209 p.

Sepp, B., Bischoff, A. & Bosbach, D. 2001: Low-temperature phase decomposition in iron-nickel metal of the Portales Valley meteorite. Meteoritics & Planetary Science, 36/5: 587–595.

Simon, S. B., Beckett, J.R., Vaughan, W.M., Sutton, S.R & Grosman, L. 2011: Chondrule –composition melts: Response of Fe and Ti valence to changing redox conditions. 42nd Lunar and Planetary Science Conference. Contribution No. 1608, p.1271

Sokol, A., & Bischoff, A. 2005: Meteorites from Botswana. Meteoritics & Planetary Science, 40/9: A177–A184.

Sokol, A., Bischoff, A., Marhas, K.K., Mezeger, K & Zinner, E. 2007: Late accretion and lithification of chondritic parent bodies: Mg isotope studies on fragments from primitive chondrites and chondritic breccias. Meteoritics & Planetary Science, 42/7: 1291–1308.

Spurný, P., Borovnička, J., Kac, J., Kalenda, P., Atanackov, J., Kladnik, G., Heinlein, D. & Grau, T. 2010: Analysis of instrumental observations of the Jesenice meteorite fall on April 9, 2009. Meteoritics & Planetary Science, 45/8: 1392–1407, doi:10.1111/j.1945-5100.2010.01121.

Šmit, Ž., Jezeršek, D., Pelicon, P., Vavpetič, P., Jeršek, M., Mirtič, B. 2011: Analysis of a chondrite meteorite from Slovenia. X-ray spectrom: 40/3: 205-209, doi:10.1002/xrs.1307.

Wlotzka, F. A. 1993: Weathering scale for the ordinary chondrites. Meteoritics, 28/3: 460-460.

GEOLOGIJA *56/1*, 029–046, Ljubljana 2013

doi:10.5474/geologija.2013.003

The origin of emeralds embedded in archaeological artefacts in Slovenia

Izvor smaragdov v arheoloških predmetih na Slovenskem

Albina KRŽIČ[1], Žiga ŠMIT[2,3], Helena FAJFAR[3], Matej DOLENEC[4], Breda ČINČ JUHANT[5] & Miha JERŠEK[1,5]

[1] Višja strokovna šola Šolskega centra Srečka Kosovela, Kraška ulica 4, Sežana
[2] Fakulteta za matematiko in fiziko, Univerza v Ljubljani, Jadranska 19, SI – 6210 Ljubljana
[3] Inštitut Jožef Stefan, Jamova 39, SI – 1000 Ljubljana
[4] Oddelek za geologijo Naravoslovnotehniške fakultete Univerze v Ljubljani, Aškerčeva 20, SI – 1000 Ljubljana
[5] Prirodoslovni muzej Slovenije, Prešernova 20, SI – 1000 Ljubljana

Prejeto / Received 20. 3. 2013; Sprejeto / Accepted 8. 5. 2013

Key words: emerald, beryl, PIXE/PIGE, Egypt, Habachtal, Afghanistan, Ptuj,
Ključne besede: smaragd, beril, PIXE/PIGE, Egipt, Habachtal, Afganistan, Ptuj

Abstract

Roman gold jewellery, which was excavated in Ptuj (Poetovio) and consists of a necklace, earrings and a bracelet with embedded emeralds, is part of the Slovenian archaeological artefacts collections. Crystallographic characteristics, inclusions, luminous phenomena and geological characteristics were determined in order to establish the origin of the emeralds. Chemical composition of the emeralds was determined non-destructively using the methods of proton-induced X-rays and gamma rays (PIXE/PIGE). The results were compared with reference emeralds from Habachtal in Austria and with green beryls from the Ural Mts. Literature data for emeralds from Egypt and modern-day Afghanistan area were used to interpret the results. Specifically, these sites were known for emeralds being mined for jewellery in Roman times. It was assumed that emeralds from archaeological artefacts originated from Habachtal in Austria, given that this site was the nearest to the place where found. But the emeralds from the necklace and earrings in fact came from Egyptian deposits. The origin of emeralds from the bracelet could not have been determined absolutely reliably due to the lack of comparative materials; they may originate from a site in modern-day Afghanistan or from Egypt, but certainly not from the same site as the previously mentioned emeralds in the necklace and earrings.

Izvleček

V zbirkah arheoloških predmetov na Slovenskem hranimo zlat rimski nakit, ki je bil najden na Ptuju (Poetovio); verižico, uhana in zapestnico, ki imajo okovane smaragde. Da bi določili njihov izvor, smo poskušali ugotoviti kristalografske značilnosti ter določiti vključke, luminiscenčne pojave in geokemične značilnosti smaragdov. Kemijsko sestavo smaragdov smo izmerili nedestruktivno z metodama protonsko vzbujenih rentgenskih žarkov in žarkov gama (PIXE/PIGE). Dobljene rezultate smo primerjali z referenčnimi smaragdi iz Habachtala v Avstriji in zeleno obarvanim berilom iz Urala, medtem ko smo za interpretacijo rezultatov uporabili še literaturne podatke za smaragde iz Egipta in iz območja današnjega Afganistana. Ta nahajališča so bila namreč v času izdelave rimskega nakita znana po izkopavanju smaragdov. Domnevali smo, da so smaragdi iz arheoloških predmetov iz Habachtala v Avstriji, saj je bilo to nahajališče najbližje mestu najdbe, nazadnje pa ugotovili, da so smaragdi iz verižice in uhanov iz nahajališč v Egiptu. Kar zadeva smaragde iz zapestnice, zaradi pomanjkanja primerjalnega gradiva nismo mogli povsem zanesljivo določiti njihovega izvora; lahko so iz nahajališča v današnjem Afganistanu ali pa iz Egipta, vendar ne z istega nahajališča kot prej omenjeni smaragdi iz verižice in uhanov.

Introduction – emeralds and people through time

The human race has been associated with emeralds for more than 4,000 years. As early as in the Antiquity, they were the symbol of the magic wisdom of God Hermes. The Egyptian Queen Cleopatra was a great lover of jewels, particularly emeralds. Her legendary emerald mines remained a mystery for ages, and it was only about a century ago that they were rediscovered in the vicinity of the Red Sea (Finlay, 2006).

In the Ancient Greece, Pliny often wondered whether anything in this world could be at all greener than a genuine emerald. The Greeks believed that jewels had a healing power and brought luck at the same time. Nero, the dissolute

arsonists of Ancient Rome, simply loved watching gladiator fights through emerald sunglasses (Henn, 1990).

The Holy Grail, too, was made of emerald which, however, has remained a mystery till this very day. Through history, people have been attributing various properties to the emerald, such as preventing carnality, invigorating memory, and helping us, when put on the tongue, during the summoning of spirits and conversation with them. In the end it was the Blessed Hildegard from Bingen who claimed that the emerald grows in the morning, when green meadows are the freshest, which evaluates emerald green colour (Jeršek & Dobnikar, 2005).

In Islamic tradition, the Muslims, too, highly esteemed emeralds and their green colour. Emerald green was allegedly the cloak and turban of the Prophet Muhammad. Green colour thus became also the colour of Islam, as can be noted on their national flags. The colour symbolises the posthumous paradise promised to people by Muhammad. Outwardly, the Muslim rulers showed, by wearing emeralds, not only that they were immensely rich but that they were protected by God Allah himself (Finlay, 2006).

The Celts and Romans mined these gemstones at the historic site of Habachtal in the Hohe Tauern in Austria at an altitude between 2,000 and 2,200 m (Henn, 1990). Historically significant emerald sites are also located in Egypt and Afghanistan (Henn, 1990), as well as in the Ural Mts according to some data (Calligaro et al., 2000). Through discovery of increasingly new sites, emeralds became more and more accessible, and after their discovery in Columbia in 1545 AD, they became one of the most precious gems (Bauer, 1968). As natural emeralds are still relatively scarce, they are produced in laboratories as well (Henn, 1990).

In archaeological artefacts from the Roman period, particularly in gold jewellery, a necklace, earrings and a bracelet with embedded emeralds have been found in sites in Ptuj Slovenia (Tušek, 1985). The origin of these emeralds, however, has not been researched in detail as yet. Owing to the relative proximity of the emerald site at Habachtal in Austria it seemed most likely that they originated from this very upland site. This is why we studies crystallographic, physical and geochemical characteristics of emeralds embedded in archaeological artefacts in Slovenia and compared them with reference emeralds from Habachtal. A green coloured beryl from the Ural Mts was also part of our analyses, whereas reference emeralds from Egypt and Afghanistan were not available, forcing us to rely on literature sources in the interpretation of results (Jennings et al., 1993; Calligaro et al., 2000).

Historically significant emerald sites

The largest site of emerald crystals in Europe is located in Austria at Habachtal in the area of Hohe Tauern National Park. The first mention of emerald finds reaches back to the Celtic-Roman times (Henn, 1990). Emerald mining was resumed as late as in the 18th century. Under the Legbachscharte Pass, several pits were dug. Through centuries, their owners changed and, together with them, the rules as to who and under what conditions may mine these gemstones. Entrance to the pits is prohibited mainly for safety reasons, while searchers are allowed to look for emeralds on the dump in front of the mine. Beryl crystals are located in black and green biotite-actinolite slate and, less often, in magnesite-actinolate slate (Rečnik et al., 1994).

Major rocks in the wider area of Habachtal are serpentinites. In the narrower area, where emeralds occur, a series of serpentinites and magnesite slates runs parallel to the tectonic border, which separates central gneisses from the formation composed predominantly of garnet schists and amphibole gneisses. Minerals in serpentinites are enriched with chrome, while minerals in schists and amphibolites are the carriers of beryllium and aluminium. At the contact between serpentinites and schists, magnesite, actinolite, chlorite and biotite were extracted as reaction products. About some 65 million years ago, at the beginning of alpidic regional metamorphism, chrome enriched beryl began to extract at their contacts (Rečnik et al., 1994).

All Habachtal emeralds crystallize in the form of hexagonal prism that ends with pinacoid. Their cleavage takes place perpendicularly to the longitudinal axis c. Emerald crystals are dark green, more often pale green and of various green-white tints. Totally transparent crystals are very rare indeed. Quite often, they are cloudy to partially transparent and untransparent. White and light coloured crystals are usually larger and more transparent than green crystals (Bauer, 1968). Crystals are often cracked on basal planes owing to the tectonic events taking place during their origin. Emeralds contain inclusions of mica, tourmaline, titanite, epidote, apatite, and rutile. Emerald excavation in the Habachtal area is very poor in comparison with other sites across the world (Henn, 1990).

Emerald deposits in Egypt are considered historic, as precious stones were dug in this area more than 1,650 years BC ago. Egypt allegedly represented one of the three sources of emerald sites for Europe and Africa in the Greek-Roman times. Well known for those times were the following sites with chronological order of the carried out excavations: Gimal Valley A and B (4th-5th centuries), Nuqrus Valley and Sikait Valley (6th-9th centuries) and Zubara (12th-16th centuries) (Shaw et al., 1999).

Today, emerald sites are known from the island of Zabargad in the Red Sea and a place some 100 km south of modern-day Cairo in the Sikait-Zubara Valley. Through the excavations carried out in the 19th century, the British establish on the basis of discovered tools that emeralds had been dug in this area more than 1,650 years BC ago. For those particular times, Egypt was an important source of emeralds that were highly appreciated both in India and Europe (Finlay, 2006).

The emeralds from Egypt crystallized in mica slate at the contact with granite. They are pale green, full of inclusions and often very small (Finlay, 2006). Most important among inclusions are the fluid inclusions, while growth tube are uniquely characteristic (Jennings et al., 1993).

Once upon a time, emeralds were also dug in the area of the Panjshir Valley on the edge of Hindukush Mts in Afghanistan. In the Antiquity, this area was called Bactrian, as reported by Theophrastus, and was known already from the time of Alexander the Great between the 3rd and 1st centuries BC (Calligaro et al., 2000). Digging was resumed at the beginning of 1970 (Jennings et al., 1993).

Some people believe that the sites in the Ural Mts, too, are a possible source of emeralds in the times of the Romans (Calligaro et al., 2000), while the great majority of data on emeralds originate from the period after 1830 (Bauer, 1968), when they were found near the Tokowaya River. Those from historically significant sites, on the other hand, were supposed to be dug from 1500 BC onwards, which means that emerald mines existed as early as in the Antiquity. Pliny the Elder, too, writes about Ural emeralds from Scythia site in his work Historia Naturalis (Calligaro et al., 2000). The Ural emeralds contain inclusions of brownish to almost colourless actinolite crystals, which are independent or occur in tiny clusters, as well as biotite and three-phase inclusions, while tourmaline is a rare inclusion (Henn, 1990).

Crystallographic characteristics of emeralds

One of the emeralds' characteristic feature is their prismatic habitus, which is stipulated by hexagonal prisms of the first order a(100). Separate crystals end with the basic pinacoid c(001), while their morphological diversity is created by additional crystal surfaces, among which hexagonal bipyramid of the first order d(101), hexagonal bipyramid of the first order e(111), dihexagonal prism f(210) and hexagonal prism of the second order g(110) are found. Separate crystal surfaces can be more or less pronounced on crystal surfaces, which means that totally short prismatic crystals can also be found, or the peaks of crystals are fairly rounded at first sight due to the mass of crystal surfaces (Jeršek & Vidrih, 2009).

Crystallogenetic trend reveals the sequence of crystallization from the very short prismatic to short prismatic, medium prismatic and long prismatic crystals, depending on the presence of different alkaline elements (Kostov & Kostov, 1999).

Inclusions in emeralds

Owing to the manner of crystallization, emeralds contain a very high number of inclusions, which is the reason why experts decided to name them emerald garden. Frequent inclusions in emeralds are fluid inclusions, whereas solid inclusions are often chromite, spinel, picotite, actinolite, biotite, pyrite, calcite and dolomite (Gübelin & Koivula, 1986). Inclusions in emeralds are characteristic due to the location and also very important for their identification. Characteristic inclusions in emeralds from Habachtal are biotite, talk, actinolite and tremolite (Henn, 1990), in emeralds from Ural crystals we can find phlogopite (Henn, 1990) and for emeralds and green beryl's from Egypt are typical growth tubes (Jennings et al., 1993). In gemological practice, the emerald is the only gemstone in which its quality regarding the purity and thus the presence and type of inclusions is evaluated by naked eye and not with a 10x magnifying loupe.

Green coloured beryl as a gemstone

Emeralds are gem quality of a beryl with a green colour caused by the presence of chromium. There are two other green beryl's used as a gem; green beryl and vanadium beryl. Green beryl is green because of a presence of iron and vanadium beryl because of a presence of vanadium.

Material

In Slovenia, only a few artefacts with embedded emeralds have been found by archaeologists (Table 1). A well known is the gold jewellery of a lady from Roman Poetovio with light emerald crystals set in it. It was found in 1982 in Mežanova ulica in Ptuj – archaeological site Hajdina (EŠD 581) – stored in a brick chest, which contained a skeleton grave with a double burial of mother and child. The gold necklace (Fig. 1) (Inv. No. A 164) is composed of 31 golden parts, three emerald crystals (V-1, V-2, V-3) and clip. The necklace is kept by the Institute for the Protection of Cultural Heritage of Slovenia, Preventive Archaeology Centre, Regional Department Ptuj (Tušek, 1985).

Two gold earrings (Fig. 2) (Inv. Nos. 80CP001/002 and 80CP001/003) were found in 1980 within the area of the Secondary School Centre on Volkmerjeva cesta in Ptuj. They were located in grave No. 1, where a female skeleton lay. Both earrings have an emerald crystal set in them (U-1, U-2) and are kept by the Archaeological Department of the Regional Museum Ptuj-Ormož (Tušek, 1985).

The third archaeological artefact is a bracelet in two fragments (Fig. 3). It was found in 2009 in the area of Ljudski vrt Primary School, grave No. 154 (Inv. No. PN 627). It contains three emerald crystals (Z-1, Z-2, Z-3) and is kept by the Archaeological Department of the Regional Museum Ptuj-Ormož.

As comparative material, ten emerald crystals from Habachtal in Austria (Fig. 4) (Inv. Nos. 623-a, 623-b, 623-c, 627, 628, 1475, 1478, 1488, M-1, M-2) and green beryl from the Ural Mts (Fig. 5) (Inv. No. 1470) were chosen; all of them, with the exception of samples M1 and M2 (private collection), are from the renowned Zois Mineral Collection (Table 1) (Činč Juhant & Jeršek, 2005).

Fig. 1. The golden necklace (A 164) with three emeralds (V1-3). Collection of Institute for the Protection of Cultural Heritage of Slovenia, Preventive Archaeology Centre, Regional Department Ptuj Photo: Miha Jeršek

Sl. 1. Zlata verižica (A 164) s tremi smaragdi (V1-3). Zbirka Zavoda za varstvo kulturne dediščine Slovenije, Center za preventivno arheologijo, Regionalni oddelek Ptuj Foto: Miha Jeršek

Fig. 2. Gold earrings (80CP001/002, 80CP001/003) with emeralds U2,3), collection of Regional Museum Ptuj-Ormož. Photo: Miha Jeršek

Sl. 2. Zlata uhana (80CP001/002, 80CP001/003) s smaragdi U2,3), zbirka Pokrajinskega muzeja Ptuj-Ormož. Foto: Miha Jeršek

Fig. 3. The golden bracelet in two fragments (PN 627) with three emeralds (Z1-3), collection of Regional Museum Ptuj-Ormož. Photo: Miha Jeršek

Sl. 3. Zlata zapestnica v dveh delih (PN 627) s tremi smaragdi (Z1-3), zbirka Pokrajinskega muzeja Ptuj-Ormož. Foto: Miha Jeršek

Fig. 4. Emerald from Habachtal, collection of Slovenian Museum of Natural History (Inv. No. 623, c). Photo: Miha Jeršek

Sl. 4. Habachtalski smaragd, zbirka Prirodoslovnega muzeja Slovenije (inv. št. 623, c). Foto: Miha Jeršek

Fig. 5. Green coloured beryl from Ural, collection of Slovenian Museum of Natural History (Inv. No. 1470). Photo: Miha Jeršek

Sl. 5. Zeleno obarvani beril iz Urala, zbirka Prirodoslovnega muzeja Slovenije (inv. št. 1470). Foto: Miha Jeršek

Methods

Macroscopic description

The emeralds were initially observed with naked eye and a 10x magnifying loupe. Crystallographic characteristics, inclusions and colour were determined. With the aid of a calliper, the emeralds' size was measured.

Gemmological microscope

The emeralds were studied with gemmological microscope (model KSW 63/11434.3), which is in fact a stereomicroscope with 10x to 80x magnification.

UV lamp

With standard ultraviolet lamp, the luminous phenomena in the samples (fluorescence and phosphorescence) were studied with shortwave and longwave UV light.

Table 1. Samples of emeralds and green beryls in this study
Tabela 1. Vzorci smaragdov in zelenih berilov v tej raziskavi

Object / Predmet	Inv. Nos. / Inv. št.	Collection / Zbirka	Mark / Oznaka
Golden necklace	A 164	Institute for the Protection of Cultural Heritage of Slovenia, Preventive Archaeology Centre, Regional Department Ptuj	V1, V2, V3
Golden earings	80CP001/002 80CP001/003	Regional Museum Ptuj-Ormož	U1, U2
Golden bracelet	PN 627	Regional Museum Ptuj-Ormož	Z1, Z2, Z3
Emerald, Habachtal	623-a, 623-b, 623-c, 627, 628, 1475, 1478, 1488	Slovenian Museum of Natural History	623-a, 623-b, 623-c, 627, 628, 1475, 1478, 1488
Emerald, Habachtal	M-1, M-2	Private collection	M-1, M-2
Green beryl, Ural	1470	Slovenian Museum of Natural History	1470

PIXE and PIGE methods

The PIXE and PIGE methods are based on the irradiation of samples with high energy ions, which induce the characteristic X-rays and gamma rays in the matter. Protons with the energy of a few MeV penetrate up to 100 μm deep into the matter, so that the measurements show the condition not only on the surface but a few 10 μm deep as well, for it has to be considered that the protons slow down whilst passing through the matter, whereas the reaction cross sections are quickly reduced with energy. In a sample, the created X-rays are also absorbed, while for the much harder gamma rays the absorption effects are negligible. The measuring procedure is non-destructive, given that the radiation with protons does not cause visible traces, which means that the methods are suitable for the analysis of valuable objects, including precious stones.

Measurements with the PIXE – PIGE method were carried out at the Tandetron accelerator of the Jožef Stefan Institute in Ljubljana. Measuring was executed with the proton beam in the air, as this enables a simple setting of sample and selection of the place for irradiation. The protons' nominal energy was 2.5 MeV, and while passing through a 2 μm thick window made of tantalum foil and 1 cm wide air gap this energy was reduced to approximately 2.2 MeV. The beam profile was Gaussian, with 0.8 mm full-width at half maximum. To the X-ray detector, which was placed under the angle of 45° with regard to the proton beam, the induced X-rays also travelled through a 5.7 cm wide air gap. Due to the absorption in the air gap, we were able to detect with X-rays only the elements heavier than silicon. At each selected point, two measurements were made. With the first one we measured the low energy spectrum of elements between silicon and iron, while during the second measurement the proton current was increased to a few nA; at the same time, we measured the high energy X-ray spectrum of elements heavier than iron, and gamma spectra. For this purpose, the X-ray detector was equipped with additional absorber made of 0.1 mm thick aluminium foil. From the gamma spectra, the elemental concentrations of Na, Mg and Al were determined. In the spectra, lines of lithium and fluorine also appeared, but they were not taken into account in the quantification of results, as no suitable standards were at hand. The concentrations of beryllium, too, were considered only mathematically.

The uncertainties in concentrations of the major elements are of the order ± 5%, while in elements in concentrations below 0.1% they can be greater, i.e. 10-15 %. Measuring uncertainties are greater also during measurements made on natural beryls, which have tiny mineral impurities on their surface, usually flakes of mica, owing to which higher concentrations of potassium and aluminium were determined.

Results

Macroscopic description

Emerald crystals from Habachtal are mostly translucent and not transparent. Their crystal surfaces seem like being etched and are seldom smooth. This "etchy" appearance is the result of their growth in parent rock or of partial dissolution. The colour of emeralds is not uniform. Some are colourless (Inv. No. 628), others of different green shades. They have several mica inclusions. General ratio between the crystals' width and length ranges from 1:3 to 1:6.

Table 2. The size of emeralds in archaeological artefacts (V-1, V-2, V-3 – emeralds from the necklace, U-2 and U-3 emeralds from the earrings, and Z-1, Z-2 and Z-3 the emeralds from the bracelet).

Tabela 2. Velikost smaragdov v arheoloških predmetih (V-1, V-2, V-3 – smaragdi iz verižice, U-2 in U-3 smaragda iz uhanov ter Z-1, Z-2 in Z-3 smaragdi v zapestnici).

Sample	Dimensions (mm)	Sample	Dimensions (mm)
V-1	V= 4.2; Š= 3.65 V= 4.2; Š= 4 V= 4.2; Š= 4.45	**Z-1**	V= 3.1; Š= 2.85 V= 3.1; Š= 2.9 V= 3.1 . Š= 3
V-2	V= 4.4; Š= 4.15 V= 4.4; Š= 4.15 V= 4.4; Š= 4.55	**Z-2**	V= 4.95; Š= 2.6 V= 4.95; Š= 2.65 V= 4.95; Š= 2.95
V-3	V= 4.2; Š= 4 V= 4.2; Š= 4.45 V= 4.2; Š= 5.7	**Z-3**	V= 0.9; Š= 2.35 V= 0.9; Š= 2.4 V= 0.9; Š= 2.55
U-2	V= 3.75; Š= 2.55	**U-3**	V= 3; Š= 4.65

PLATE 1 – TABLA 1

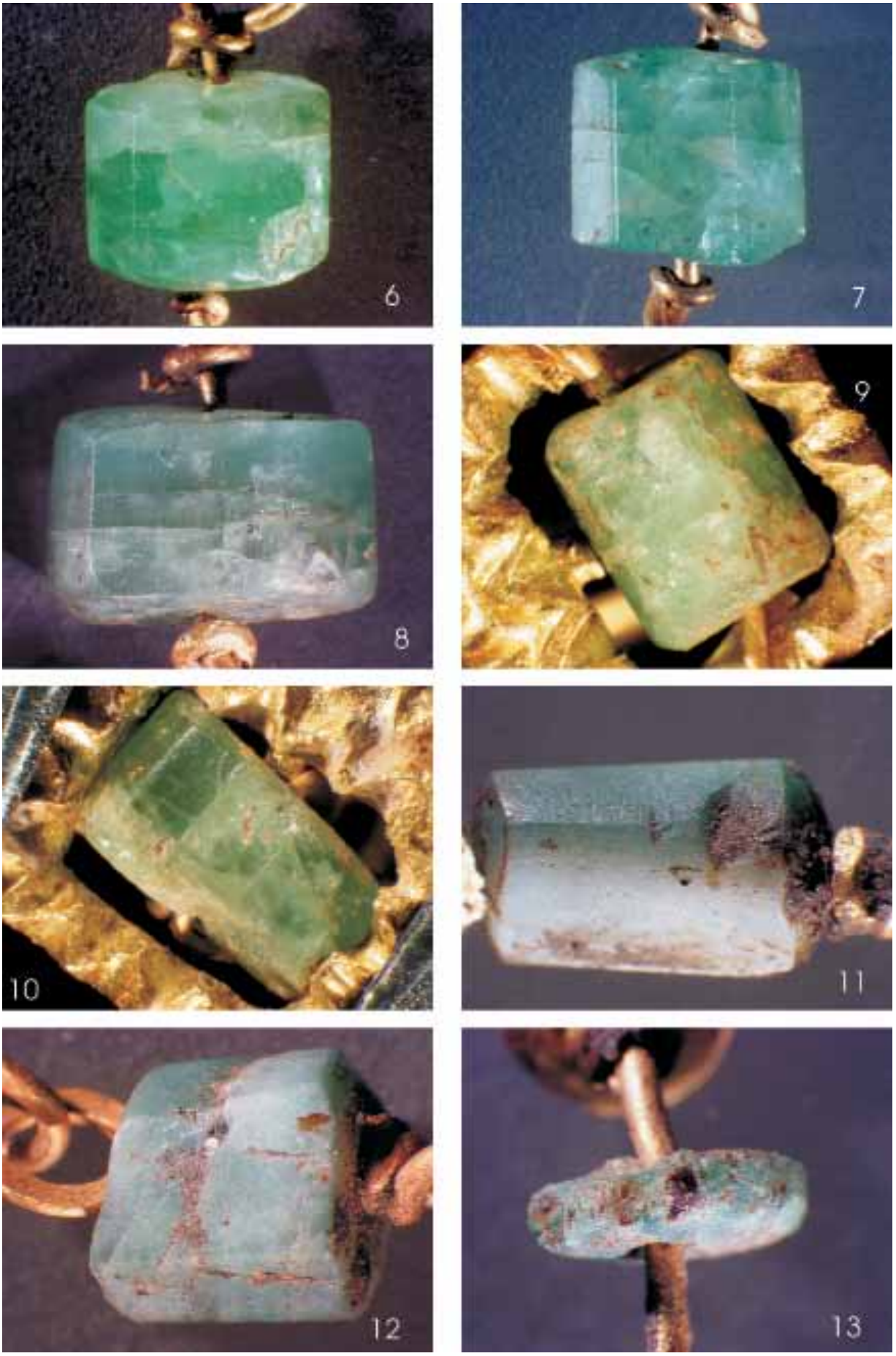

The emeralds embedded in archaeological artefacts apparently differ from each other. Those in the bracelet are apparently opaque and of different colour shade (bluish green), with a fairly large amount of mica. The emeralds in the necklace and earrings are translucent to transparent, of green colour with numerous fluid inclusions and relatively little amount of mica (Pl.1, figs. 6 to 13).

The size of emeralds in archaeological artefacts was ascertained by measuring the distances between two opposite surfaces of the hexagonal prism (Š) and the height of emerald between two pinacoids (V). Results of the measurements are given in Table 2.

Crystallographic characteristics of the emeralds

The crystals of Habachtal emeralds have a characteristic prismatic habitus, which is stipulated by the surfaces of the hexagonal prism of the first order a (100), and end with pinacoid c surface (001) (Fig. 14). The green beryl from the Ural Mts also has a distinct prismatic habitus with developed surfaces of hexagonal prism of the first order a(100) and pinacoid c(001). The three crystal surfaces of the first order prism are sanded and polished.

The emeralds from the archaeological artefacts have, apart from the hexagonal prism of the first order a(100) and pinacoid c(001), other crystal surfaces developed as well. We determined the hexagonal bipyramid of the first order d(101), hexagonal bipyramid of the second order e(111)

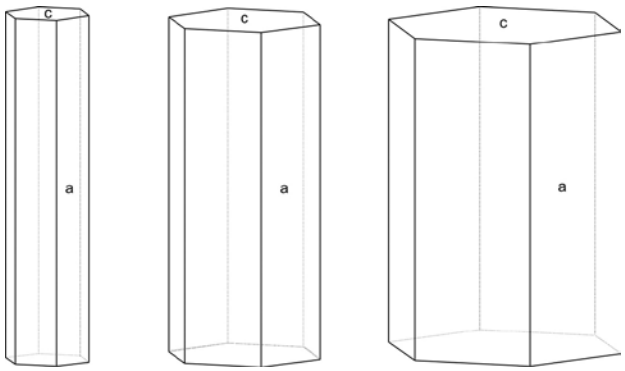

Fig. 14. Crystallographic characteristics of the emeralds from Habachtal. Only hexagonal prisms of the first order a(100) and pinacoid c(001) crystal surfaces are developed. Drawing: Miha Jeršek

Sl. 14. Kristalografske značilnosti smaragdov iz Habachtala. Razvite so samo kristalne ploskve heksagonalne prizme I. reda a(100) in pinakoid c(001). Risba: Miha Jeršek

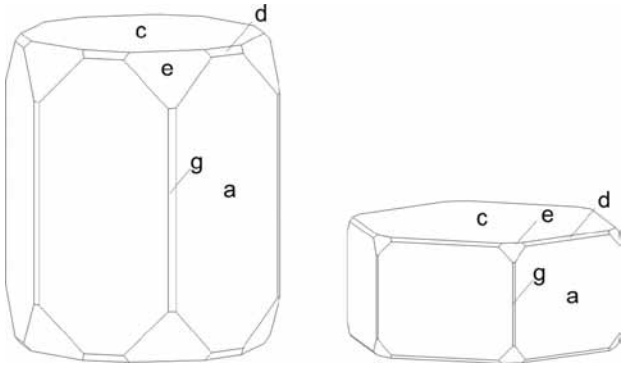

Fig. 15. Crystallographic characteristics of the emeralds from the earrings. In addition to hexagonal prisms of the first order a(100) and pinacoid c(001), emerald crystals have hexagonal bipyramid of the first order d(101), hexagonal bipyramid of the second order e (111) and hexagonal prism of the second order g(110). Drawing: Miha Jeršek.

Sl. 15. Kristalografske značilnosti smaragdov v uhanih (U-2, U-3). Kristali smaragda imajo poleg heksagonalne prizme I. reda a(100) in pinakoida c(001) razvite še heksagonalno bipiramido I. reda d(101), heksagonalno bipiramido II. reda e(111) in heksagonalno prizmo II. reda g(110). Risba: Miha Jeršek

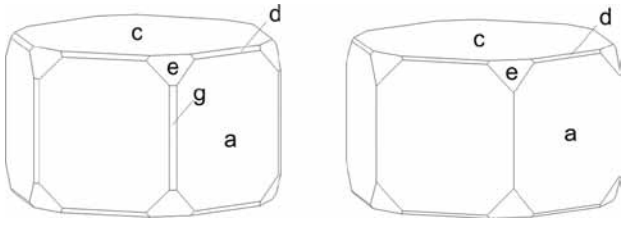

Fig. 16. Crystallographic characteristics of the emeralds from the archaeological artefacts – the necklace (V1-3). In addition to the hexagonal prism of the first order a(100) and pinacoid c(001), the emerald crystals have hexagonal bipyramid of the first order d(101), hexagonal bipyramid of the second order e (111) and hexagonal prism of the second order g(110) developed as well. Drawing: Miha Jeršek

Sl. 16. Kristalografske značilnosti smaragdov v arheoloških predmetih – verižica (V1-3). Kristali smaragda imajo poleg heksagonalne prizme I. reda a(100) in pinakoida c(001) razvite še heksagonalno bipiramido I. reda d(101), heksagonalno bipiramido II. reda e(111) in heksagonalno prizmo II. reda g(110). Risba: Miha Jeršek

---

PLATE 1 – TABLA 1

6 Emerald from the necklace (V-1)
Smaragd v verižici (V-1)

7 Emerald from the necklace (V-2)
Smaragd v verižici (V-2)

8 Emerald from the necklace (V-3)
Smaragd v verižici (V-3)

9 Emerald from the earring (U-2)
Smaragd v uhanu (U-2)

10 Emerald from the earring (U-3)
Smaragd v uhanu (U-3)

11 Emerald from the bracelet (Z-1)
Smaragd v zapestnici (Z-1)

12 Emerald from the bracelet (Z-2)
Smaragd v zapestnici (Z-2)

13 Emerald from the bracelet (Z-3)
Smaragd v zapestnici (Z-3)

Photos (fotografije): Miha Jeršek

and the hexagonal prism of the second order g(110) (Figs. 15 and 16). The crystal (V-1) on the necklace has no surfaces of the hexagonal prism of the second order g(110), but these are present in the other (V-2) crystal in the necklace. Although the crystals

Fig. 17. Detail from the bracelet's emerald shows that emeralds from this jewellery have, in addition to the hexagonal prism of the first order a(100) and pinacoid c(001), have other crystal surfaces developed as well, but owing to their unclear position or poor condition the surfaces could not have been determined in a greater detail. Photo: Miha Jeršek

Sl. 17. Detajl smaragda iz zapestnice nam razkriva, da imajo smaragdi v tem nakitu poleg heksagonalne prizme I. reda a(100) in pinakoida c(001) razvite še nekatere druge dodatne kristalne ploskve, ki pa jih zaradi nejasne lege oziroma slabše ohranjenosti nismo mogli natančneje določiti. Foto: Miha Jeršek

in the bracelet (Z1-3) are not so well preserved, it can still be noted that that crystal has similar crystallographic characteristics as the emeralds in the necklace (V1-3) and in the earrings (U-2, U-3). The emeralds in the bracelet are partially preserved as natural crystals, but are partly sanded, given that the surfaces that supposedly belong to the hexagonal prism are explicitly unparallel between each other. In some places, we furthermore determined additional crystal surfaces of the hexagonal bipyramid (Fig. 17).

On the basis of the crystallographic characteristics we can conclude that the crystals of the Habachtal emeralds and of the Ural beryl are characteristically prismatic and that they developed, apart from pinacoid surface, only surfaces of the hexagonal prism, while the emeralds from the archaeological artefacts have other crystal surfaces developed as well. Apart from it, the Habachtal emeralds are medium to long prismatic, whereas the crystals of the emeralds from the archaeological artefacts are short to medium prismatic and, in general, more barrel-shaped, with several developed types of crystal surfaces. This leads us to the fact that the emeralds under consideration were formed under different conditions (Kostov & Kostov, 1999), which could indicate that they originate from different sites.

Luminescent phenomena

While studying samples with UV lamp, i.e. with short- and long-wave UV light, the tested samples did neither fluoresce nor phosphoresce, which means that chromium is not the only or most significant colouring ion.

Inclusions

The Habachtal emeralds are not translucent to transparent and contain numerous fluid and mica inclusions both in crystals themselves and partly on the surface of emerald crystals. The Ural green beryl has, similarly, numerous fluid inclusions and

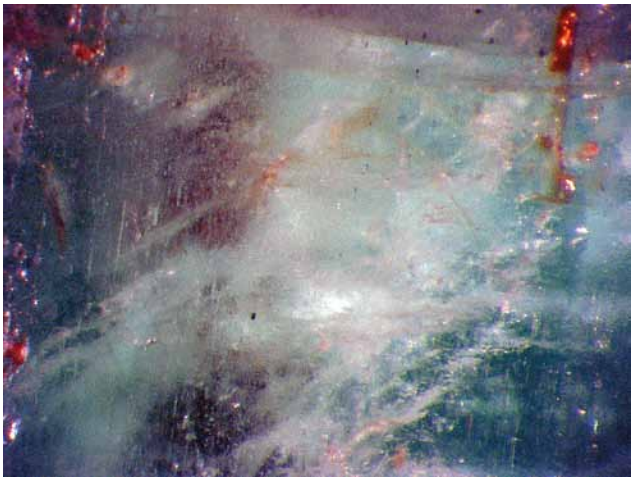

Fig. 18. Fluid inclusions in sample V-3, 40 x magnification. This type of inclusions were found in all emerald samples except in the emeralds from the bracelet, where inclusions could not be defined due to the emeralds' opacity. Photo: Miha Jeršek

Sl. 18.Tekočinski vključki v vzorcu V-3, 40-kratna povečava. Tovrstne vključke smo našli v vseh vzorcih smaragdov razen v smaragdih v zapestnici, ker so le ti neprozorni in jih zato ne moremo določiti. Foto: Miha Jeršek

Fig. 19. Growth tube from sample V-3, 30x magnification. This type of inclusions were found in emeralds from the necklace, while those from earrings are less developed and look more like normal liquid inclusions. In emeralds from the bracelet, no such inclusions were found. Photo: Miha Jeršek

Sl. 19. Tekočinski kanali v vzorcu V-3, 30-kratna povečava. Tovrstne vključke smo našli v smaragdih v verižici, medtem ko so v uhanih manj izraziti in so bolj podobni običajnim tekočinskim vključkom. V smaragdih v zapestnici jih nismo našli. Foto: Miha Jeršek

exhibit zonal colours, which change from light to dark green, and mica inclusions.

The emeralds from the archaeological necklace and earrings contain fluid inclusions (Fig. 18). Parallel growth tube were found in all emeralds from the necklace (V1-3) (Fig. 19), while in the earrings they were not so distinct or could generally be attributed to fluid channels. The emeralds from the bracelet (Z1-3) contain a great amount of mica both on the surface and in the interior (Fig. 20). Other inclusions were not found owing to the opacity of the samples.

Emeralds are known to contain numerous inclusions, which has also been ascertained by us from the studied samples, both the emeralds embedded in the archaeological artefacts and reference emeralds. In the emeralds from the archaeological artefacts, inclusions in the form of parallel growth tube were particularly salient. We found them in the emeralds embedded in the necklace and earrings, but not in the bracelet's emeralds. Neither were they found in reference emeralds. According to the literature data (Jennings et al., 1993), it is the very parallel growth tube that are characteristic of the Egyptian emeralds, which has also been confirmed by other researchers (Hyršl, 2012). We presume that differences would be visible between micas as well, considering that they occur as inclusions in all samples and that they differ among each other already when samples are examined under a gemmological microscope. This is why it would be reasonable to analyse them in greater detail in the near future.

PIXE/PIGE method

Twelve samples were analysed with the PIXE/PIGE method. As reference material, samples from Inv. Nos. 628, 1470, 1488, M-1 and M-2 were taken. Emerald samples from archaeological artefacts were V-1, V-2, V-3, U-2, U-3, Z-1 and Z-2. During data analysis, statistical error was below 5 % in Mg, while total error in Mg was about 10 %. In other elements, total error could be taken as 5 %, except for the smallest concentrations, where it was again about 10 %. Measurements are given in Table 3.

Table 3 presents results of the analyses of emeralds in the archaeological artefacts, reference emeralds and literature data (Austria, Afghanistan, Egypt, India, Roman-Gaul) as to the content of selected oxides that are significant in determining their origin (Calligaro et al.,2000).

Characteristic grouping of the measured data was tested by principal component analysis (PCA) using the oxides of Na, Mg, Al, K, and Ca; the concentrations were transformed according to c´=ln(1+c) following the method of Duewer et al., 1975. As shown in Figure 21, the emeralds for particular artefacts are nicely grouped, indicating that each artefact contains emeralds from an individual source. According to Calligaro et al., 2000, more precise locations can be determined from the Na_2O/MgO and Na_2O/Al_2O_3 bivariate plots.

Fig. 20. In emerald samples from the bracelet, mica could be found as an inclusion (on the right in brown) or as an enclosing rock on emerald crystal (left), where crystal structure is expressed. Photo: Miha Jeršek

Sl. 20. Sljuda v smaragdih je v vzorcih smaragdov iz zapestnice ohranjena kot vključek (na desni strani v rjavi barvi) ali kot prikamnina na kristalu smaragda (levo), kjer je prepoznavna še kristalna oblika. Foto: Miha Jeršek

The Na_2O/MgO relationship shows certain data grouping (Fig. 22), which leads us up to the same or at least very similar environment in which green beryls were formed. The Ural green beryl's MgO and Na_2O values completely differ from others, which means that the emeralds from the archaeological artefacts do not originate from

Table 3. Comparison of oxides from emeralds in archaeological artefacts, reference emeralds and literature data (Calligaro et al., 2000) (Austria, Afghanistan, Egypt, India, Roman-Gaul).

Tabela 3. Primerjava oksidov v smaragdih v arheoloških predmetih, primerjalnih smaragdih in podatkih iz literature (Calligaro et al., 2000) (Avstrija, Afganistan, Egipt, Indija, Rimska-Galija).

	Sample	Na_2O	MgO	Al_2O_3	K_2O	CaO
1	V-1	1.93	2.54	14.9	0.04	0.16
2	V-2	2.25	2.60	15.3	0.07	0.30
3	V-3	1.93	2.59	15.9	0.04	0.17
4	U-2	1.85	2.27	14.3	0.18	0.66
5	U-3	2.14	2.89	13.0	0.12	0.95
6	Z-2	1.54	2.70	14.5	1.42	0.17
7	Z-1	1.29	2.85	12.7	1.67	0.19
8	1488 (Habachtal)	2.00	4.10	14.6	0.39	0.31
9	628 (Habachtal)	1.85	4.56	15.2	0.33	0.21
10	M-2 (Habachtal)	1.86	7.36	12.1	0.11	2.94
11	M-1 (Habachtal)	1.77	3.07	14.6	0.05	2.00
12	1470 (Ural)	0.06	0.11	19.7	0	0
13	Habachtal	2.10	2.70	15.4	0.04	0.06
14	Afghanistan (Panshir)	1.50	1.80	16.6	0.05	0.00
15	Egypt (D. Zabara)	2.60	2.90	15.4	0.06	0.03
16	India (Adjmer)	1.80	1.80	16.8	0.04	0.03
17	Roman-Gaul (found in Paris)	2.20	2.50	15.1	0.13	0.09

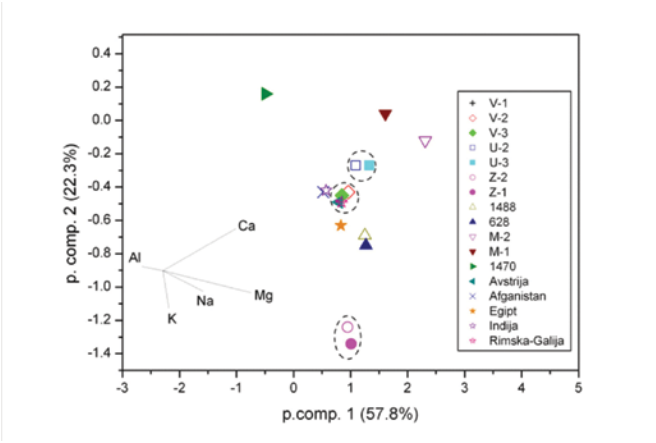

Fig. 21. Characteristic grouping of archaeological and reference emeralds according to principal component analysis (PCA).

Sl. 21. Razdelitev arheoloških in referenčnih smaragdov v skupine z metodo glavnih osi (PCA).

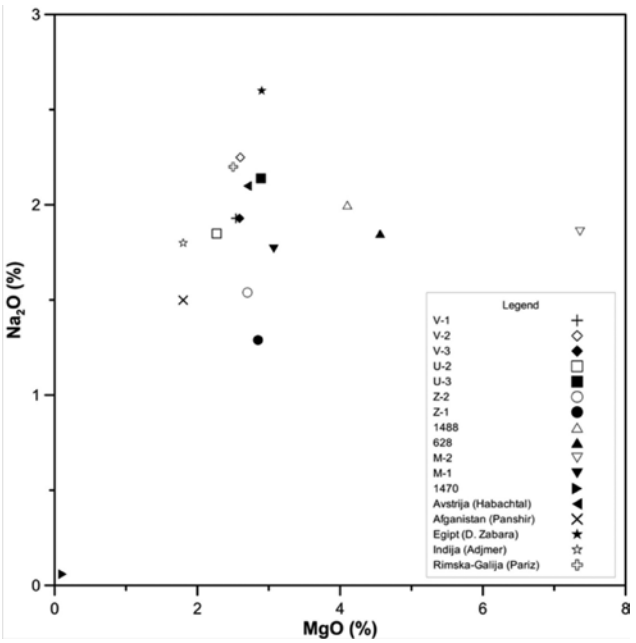

Fig. 22. Graphical representation of Na_2O/MgO concentrations in emeralds from archaeological artefacts, reference emeralds and literature data (Calligaro et al., 2000) (Austria, Afghanistan, Egypt, India, Roman-Gaul).

Sl. 22. Koncentraciji Na_2O in MgO v smaragdih v arheoloških predmetih, primerjalnih smaragdih in podatkih iz literature (Calligaro et al., 2000) (Avstrija, Afganistan, Egipt, Indija, Rimska-Galija).

this historically significant site in the Ural Mts. Similarly, the data of given relationship between sodium and magnesium oxide for Habachtal emeralds are grouped. Characteristic of them is the changeable magnesium oxide content, which is also a result of the numerous mica inclusions, whereas the sodium oxide content is more or less constant. For the emeralds from the archaeological bracelet, however, we can say with certainty that they do not originate from the sites at Habachtal. Their relationship of oxides is very near the literature data (Calligaro et al., 2000) for emeralds from Afghanistan.

The magnesium oxide content in other emeralds from the archaeological artefacts (V1-3, U2, U3)

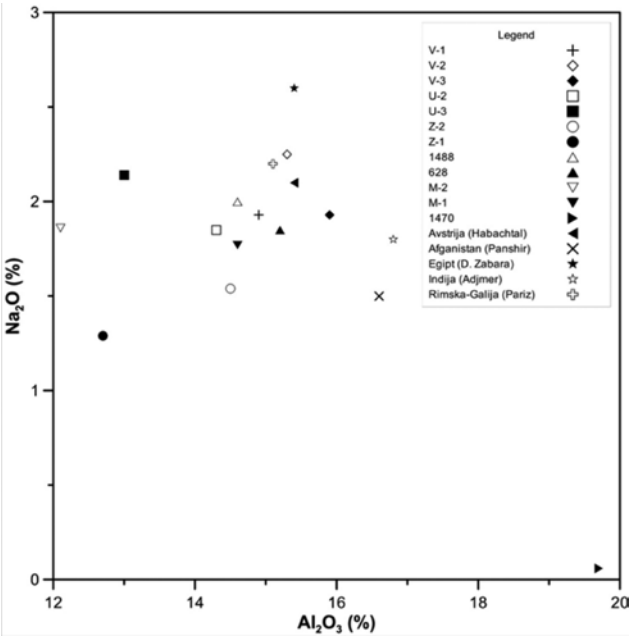

Sl. 23. Koncentraciji Na_2O in Al_2O_3 v smaragdih v arheoloških predmetih, primerjalnih smaragdih in podatkih iz literature (Calligaro et al., 2000) (Avstrija, Afganistan, Egipt, Indija, Rimska-Galija).

Fig. 23. Graphical representation of the Na_2O/ Al_2O_3 concentrations in emeralds from the archaeological artefacts, reference emeralds and literature data (Calligaro et al., 2000) (Austria, Afghanistan, Egypt, India, Roman-Gaul).

is fairly constant, while the sodium oxide content changes. Part of this data "cluster" is also the investigated Roman-Gaul sample, which is kept by the Carnavalet Museum (Paris) and originates from African sites (Calligaro et al., 2000). If compared with literature data (Calligaro et al., 2000), we can conclude that they have somewhat higher magnesium oxide content than Indian emeralds and lower sodium oxide content than the single emerald from Egypt. Given that the values of relationship between magnesium and sodium oxide for the samples of emeralds from the necklace and earrings is still near enough, we believe that they originate from a common site which, after all, has been confirmed by the value of the mentioned relationship for the single sample (Roman-Gaul). The differences between given samples and, above all, the difference towards other literature data for Egyptian emerald may lie in the fact that we are dealing with some other microlocation, as there were several mines in Egypt (Shaw et al., 1999).

The Na_2O/ Al_2O_3 relationship (Fig. 23) shows, similar as the Na_2O /MgO relationship, certain data grouping, which leads us up to the same or at least very similar environment in which green beryls were formed. For the Ural green beryl we can reiterate that we are again dealing with a completely different story, which additionally confirms that the emeralds from the archaeological artefacts were not formed under same conditions as the Ural green beryl. For other samples we can generally establish, the same as for samples from literature data (Calligaro et al., 2000), that Al_2O_3 content changes to a relatively

lesser extent than Na_2O content. Regarding the Z1-2 samples, we can confirm once again that in view of Na_2O content they are the nearest to the emeralds from Afghanistan, while in connection with Al_2O_3 content this fact leads us to believe that they might be from some other site – from Egypt, perhaps – but certainly not from the same microlocation. Particularly salient is one literature datum (Egypt) (Calligaro et al., 2000) for the emerald from Egypt, while the other (Roman-Gaul) is from the cluster of data for emeralds from the archaeological artefacts in Slovenia. These data are grouped in the central part of the diagram, where Habachtal, Indian and studied emeralds in the arhaeological artefacts belong. A certain groupation can indeed be detected, i.e. that the Habchtal emeralds have lower Na_2O and Al_2O_3 content, and that Indian emeralds have relatively more Al_2O_3, while the emeralds from the archaeological artefacts have relatively more Na_2O and average Al_2O_3 content.

On the basis of geochemical analyses of emerald samples we may thus conclude that the emeralds from archaeological necklace and earrings (V1-3, U2, U3) most probably originate from sites in Egypt (the valleys of Gimal del A and B, Nuqrus, Sikait, Zubara), whereas the emeralds from the bracelet (Z1-2) originate from sites in the region of modern-day Afghanistan (Panjshir valley) or from Egypt, although from a different microlocation than the emeralds embedded in the bracelet and earrings.

Conclusions

So far, the origin of emeralds from the archaeological artefacts in Slovenia has not been researched from the aspect of geochemical (Calligaro et al., 2000) and mineralogical characteristics (Bauer, 1968; Henn, 1990), while in archaelogical respect the finds have been appropriately described (Tušek, 1985).

As the emeralds from the archaeological artefacts have preserved their crystal surfaces, we decided to compare the forms of crystals from Habachtal with those in the archaeological jewellery. The Habachtal emeralds have a characteristic and simple prismatic habitus, which is stipulated by the surfaces of hexagonal prism of the first order a(100) and pinacoid c(001). The emeralds from archaeological artefacts have, apart from hexagonal prism of the first order a(100) and pinacoid c(001), other crystal surfaces as well, i.e. surfaces of hexagonal bipyramid of the first order d(101), hexagonal bipyramid of the second order e(111) and hexagonal prism of the second order g(110). It was established that the crystallographic characteristics of emeralds from Habachtal (Henn, 1990) differ from the crystallographic characteristics of emeralds from the archaeological artefacts in Slovenia, which can of course be associated with different conditions during their origin and therefore other sites.

The geochemical characteristics that can reveal the origin of emeralds were studied already by Calligaro and his associates (2000). On the basis of relations between Na_2O and MgO and Na_2O and Al_2O_3, he tried to establish the origin of emeralds, comparing them with reference emeralds from various sites. On the basis of our results and literature data (Calligaro et al., 2000), we concluded that the green beryl from the Ural Mts is a completely different story, that emerald samples from the bracelet originate from the region of modern-day Afghanistan, whereas emerald samples from the necklace could possibly originate either from Egypt or Habachtal. The geochemical characteristics of emeralds from Habachtal and Egypt do not differ enough to be able to stipulate the site merely on the basis of their characteristic chemical composition. If, however, the crystallographic characteristics (Henn, 1990) and the characteristic inclusions in the form of growth tube (Jennings, 1993) are also taken into account, then the samples of emeralds from the archaeological artefacts (necklace and earrings) originate from Egyptian sites. The differences in geochemical characteristics can be attributed to the microlocation inside Egyptian sites.

At the beginning we set up a working hypothesis that the emeralds embedded in the archaeological artefacts in Slovenia originated from the Habchtal site in Austria. On the basis of geochemical and crystallographic characteristics as well as characteristic inclusions, however, it was established that the emeralds from the necklace and earrings originated from Egypt (the valleys of Gimal A and B, Nuqrus, dolina Sikait, Zubara). As far as emeralds from the bracelet are concerned, on the other hand, their origin could not have been determined with utmost certainty owing to the lack of reference material; they may be from a site in modern-day Afghanistan or from Egypt, but certainly not from the same site as the previously mentioned emeralds from the necklace and earrings.

Acknowledgement

Our sincere thanks are due to: Marija Lubšina Tušek, BSc in Archaeology, curator at the Institute for the Protection of Cultural Heritage of Slovenia, Preventive Archaeology Centre, Ptuj Regional Office, who kindly lent us the necklace and thus enabled us to carry out the necessary analyses; Mojca Vomer Gojkovič, BSc in Archaeology, curator at the Archaeology Dept. of the Regional Museum Ptuj-Ormož, who supplied us with the earrings and bracelet for the necessary analyses.

Uvod - smaragd in ljudje skozi čas

Ljudje smo s smaragdi povezani že več kot 4.000 let. Že v antičnem času so predstavljali simbol magične modrosti boga Hermesa. Egipčanska vladarica Kleopatra je izredno cenila dragulje, še posebno smaragde. Njeni legendarni rudniki smaragdov so dolgo ostali skrivnost, šele pred približno sto leti so jih znova odkrili v bližini Rdečega morja (Finlay, 2006).

V Stari Grčiji se je Plinij spraševal, ali je sploh lahko karkoli bolj zeleno od pristnega smaragda. Grki so verjeli, da imajo dragulji zdravilno moč in da prinašajo srečo. Razvratni požigalec starega Rima, Neron, je skozi smaragdna sončna očala najraje opazoval boje gladiatorjev (Henn, 1990).

Tudi sveti Gral je narejen iz smaragda, njegova vrsta pa ostaja še dandanes neznanka. Ljudje so v zgodovini smaragdu pripisovali lastnosti, da preprečuje poltenost, krepi spomin, položen na jezik pomaga pri klicanju duhov in pogovoru z njimi. Nazadnje je še blažena Hildegarda iz Bingena trdila, da smaragd raste zjutraj, ko so zelene livade najbolj sveže, kar ovrednoti njihovo smaragdno zeleno barvo (Jeršek & Dobnikar, 2005).

Muslimani so prav tako v islamski tradiciji cenili smaragde in njihovo zeleno barvo. Smaragdno zelen naj bi bil plašč in turban preroka Mohameda. Tako je zelena barva postala tudi barva Islama in jo lahko opazimo na njihovih zastavah. Barva simbolizira posmrtni paradiž, ki ga je Mohamed obljubljal vernikom. Muslimanski vladarji so z nošenjem smaragdov navzven kazali ne le, da so neizmerno bogati in politično močni, ampak da jih varuje sam bog Alah (Finlay, 2006).

Kelti in Rimljani so kopali smaragde v zgodovinskem nahajališču Habachtal v Visokih Turah v Avstriji, na nadmorski višini med 2.000 in 2.200 m (Henn, 1990). Zgodovinsko pomembna nahajališča smaragdov so še v Egiptu in Afganistanu (Henn, 1990) po nekaterih podatkih tudi na Uralu (Calligaro et al., 2000). Z odkrivanjem vedno novih in novih nahajališč so smaragdi postali vse bolj dostopni. Z odkritjem nahajališč smaragdov v Kolumbiji so postali eni najbolj cenjenih draguljev (Bauer, 1968). Ker je naravnih še vedno premalo, jih izdelujejo tudi v laboratorijih (Henn, 1990).

Med arheološkimi predmeti iz rimskega obdobja, predvsem v zlatem nakitu, so na Slovenskem našli verižico, uhana in zapestnico z vgrajenimi smaragdi (Tušek, 1985). Izvor teh smaragdov še ni bil podrobneje raziskan. Zaradi relativne bližine nahajališča smaragdov v Habachtalu v Avstriji se je zdelo najverjetneje, da je njihov izvor prav v tem visokogorskem nahajališču. Zato smo raziskali kristalografske, fizikalne in geokemične značilnosti smaragdov v arheoloških predmetih na Slovenskem in jih primerjali z referenčnimi smaragdi iz Habachtala. V analize smo vključili še zeleno obarvan beril iz Urala, medtem ko referenčnih vzorcev smaragdov iz Egipta in Afganistana nismo imeli na razpolago in smo se pri interpretaciji rezultatov oprli na literaturne vire (Jennings et al.,1993; Calligaro et al., 2000).

Zgodovinsko pomembna nahajališča smaragdov

V Avstriji, na območju narodnega parka v Visokih Turah, je največje evropsko nahajališče kristalov smaragda, v dolini Habachtal. Prve omembe o najdbah smaragda segajo v keltsko-rimski čas (Henn, 1990). Kasneje so s kopanjem nadaljevali v 18. stoletju. Pod prelazom Legbachscharte so izkopali kar nekaj rovov. Lastniki so se skozi stoletja menjavali in z njimi tudi pravila o tem, kdo in pod kakšnimi pogoji lahko koplje smaragde. Vstop v rove je prepovedan predvsem iz varnostnih razlogov. Iskalci lahko iščejo smaragde na odvalu pred rudnikom. Kristali berila so v črno zelenem biotitno-aktinolitnem in redkeje v lojevčevo-aktinolitnem skrilavcu (Rečnik et al., 1994).

Glavne kamnine v širšem območju Habachtalu so serpentiniti. Na ožjem področju, kjer se pojavljajo smaragdi, poteka serija serpentinitov in lojevčevih skrilavcev vzporedno s tektonsko mejo, ki loči centralne gnajse od formacije, ki jo v večini sestavljajo granatovi blestniki in amfibolovi gnajsi. Minerali v serpentinitih so obogateni s kromom, medtem ko so minerali v blestnikih in amfibolitih nosilci berilija in aluminija. Na stiku med serpentiniti in blestniki so se kot reakcijski produkti izločili lojevec, aktinolit, klorit in biotit, nato pa se je na njihovih stikih pred približno 65 milijoni let, z začetkom alpidske regionalne metamorfoze, začel izločati beril, ki je obogaten s kromom. (Rečnik et al., 1994).

Vsi smaragdi iz Habachtala kristalizirajo v obliki heksagonalne prizme, ki je zaključena s pinakoidom. Njihova razkolnost poteka pravokotno po vzdolžni osi c. Kristali smaragdov so temno zelene barve, pogosteje bledo zelene ter vse do zeleno belih odtenkov. Popolnoma prosojni kristali so prava redkost. Pogosto so motni do delno prosojni in neprosojni. Beli in svetlo obarvani kristali so navadno večji in bolj prosojni od zelenih (Bauer, 1968). Kristali so pogosto napokani po bazalnih ravninah zaradi tektonskega dogajanja ob nastanku. Smaragdi vsebujejo vključke sljude, turmalina, titanita, epidota, apatita in rutila. Količina izkopanih smaragdov na Habachtalskem območju je zelo majhna v primerjavi s količino smaragdov, ki jo izkopljejo v drugih nahajališčih po svetu (Henn, 1990).

Nahajališča smaragdov v Egiptu veljajo za zgodovinska, saj so na tem območju kopali drage kamne že več kot 1650 let pr.n.št.. Egipt naj bi predstavljal enega od treh virov smaragdnih nahajališč za Evropo in Afriko v grško- rimskem času. Za takratni čas so bila znana naslednja nahajališča s kronološkim redom izkopavanj: Dolina Gimal del A in B (4.-5. stol.), dolina Nuqrus in dolina Sikait (6.- 9. stol.) in Zubara (12.-16. stol.) (Shaw et al., 1999)

Danes so znana nahajališča smaragdov na otoku Zabargad v Rdečem morju in 100 km južno od današnjega Kaira v dolini Sikait-Zubara. Z izkopavanji v 19. stoletju so Angleži na podlagi najdenega orodja ugotovili, da so tu smaragde kopali že več kot 1650 let pr.n.št.. Za takratni čas je bil Egipt pomemben vir smaragdov, ki so bili

cenjeni tako v Indiji kot tudi v Evropi (Finlay, 2006).

Smaragdi iz Egipta so kristalizirali v sljudnem skrilavcu na stiku z granitom. Smaragdi so bledo zeleni, polni vključkov in pogosto zelo majhni (Finlay, 2006). Med najpomembnejšimi vključki so tekočinski vključki, posebno značilni pa so tekočinski kanali (Jennings et al.,1993).

Smaragde so nekoč kopali na tudi območju doline Panjshir, na robu gore Hindukuš v Afganistanu. V antičnem času se je to področje imenovalo baktrijsko, kot poroča Theophrastus in je znano še za časa Aleksandra Velikega od 3.-1. stol. p.n.št. (Calligaro et al., 2000). S ponovnim kopanjem so pričeli na začetku leta 1970 (Jennings et al.,1993).

Nekateri menijo, da so tudi nahajališča na Uralu v Sibiriji možen vir smaragdov v času Rimljanov (Calligaro et al., 2000), velika večina podatkov o smaragdih iz Urala pa izvira iz obdobja po letu 1830 (Bauer, 1968), ko so jih našli v bližini reke Tokowaya. Tiste iz zgodovinsko pomembnih nahajališč pa naj bi kopali že od leta 1.500 pr. n. št. Tako, da so rudniki smaragdov znani še iz antičnih časov. Tudi Plinij starejši navaja v svojem delu Historia Naturalis legendo o uralskih smaragdih iz nahajališča Scythia (Calligaro et al., 2000). Smaragdi iz Urala vsebujejo vključke rjavkastih do skoraj brezbarvnih aktinolitnih kristalov, ki so samostojni ali v drobnih skupkih, biotit in trofazne vključke, redko pa je vključek turmalin (Henn, 1990).

Kristalografske značilnosti smaragdov

Za smaragde je značilen prizmatski habitus, ki ga določajo heksagonalne prizme I. reda a (100). Posamezni kristali so zaključeni z osnovnimi pinakoidom c (001), morfološko pestrost kristalov smaragda pa ustvarijo dodatne kristalne ploskve, med katerimi najdemo heksagonalno bipiramido I. reda d (101), heksagonalno bipiramido I. reda e (111), diheksagonalno prizmo f (210) in heksagonalno prizmo II. reda g (110). Posamezne kristalne ploskve so lahko na kristalih bolj ali manj izrazite, tako da lahko najdemo tudi povsem kratkoprizmatske kristale, ali pa so vrhovi kristalov zaradi množice drobnih kristalnih ploskev na prvi pogled precej zaobljeni. (Jeršek & Vidrih, 2009).

Kristalogenetski trend razkriva zaporedje kristalizacije od zelo kratko prizmatskih, do kratko prizmatskih, srednje prizmatskih in dolgo prizmatskih kristalov v odvisnosti od prisotnosti različnih alkalnih prvin (Kostov & Kostov, 1999).

Vključki v smaragdih

Smaragdi vsebujejo zaradi načina kristalizacije zelo veliko število vključkov, zato so jim strokovnjaki nadeli ime smaragdni vrt (francosko jardin). Pogosti vključki v smaragdih so tekočinski vključki, med trdnimi pa so pogosti kromit, kromov spinel, picotit, aktinolit, biotit, pirit, kalcit in dolomit (Gübelin & Koivula, 1986). Vključki v smaragdih so značilni za posamezna nahajališča in zato je njihova določitev pomembna za ugotovitev njihovega izvora. Značilni vključki za smaragde iz Habachtala so biotit, lojevec, aktinolit in tremolit (Henn, 1990), v smaragdih iz Urala najdemo flogopit (Henn, 1990), za smaragde in zelene berile iz Egipta pa so še posebej značilni tekočinski kanali (Jennings et al., 1993). V gemološki praksi je smaragd edini dragulj, pri katerem se njihova kakovost glede na čistost in s tem na prisotnost ter vrsto vključkov, vrednoti s prostim očesom in ne z lupo 10x povečave.

Zeleno obarvani berili kot dragulji

Smaragdi so zeleno obarvani berili draguljarske kakovosti. Poznamo pa še dva zeleno obarvana berila, ki sta uporabna kot draga kamna; zeleni beril, ki je obarvan zaradi primesi železa in vanadijev beril, ki je obarvan zaradi primesi vanadija.

Material

Arheologi so na Slovenskem našli samo nekaj predmetov s smaragdi (tab. 1). Poznan je zlat nakit dame iz rimske Petovione, ki ima vdelane svetle kristale smaragda. Najden je bil leta 1982, na Mežanovi ulici na Ptuju, na arheološkem najdišču Hajdina (EŠD 581). Nahajal se je v opečnati skrinji, v kateri je bil skeletni grob, z dvojnim pokopom matere in otroka. Zlata verižica (sl. 1) (inv. št.: A 164) je sestavljena iz 31 delov, treh smaragdnih kristalov (V-1, V-2, V-3) in sponke. Ogrlico hrani Zavod za varstvo kulturne dediščine Slovenije, Center za preventivno arheologijo, Regionalni oddelek Ptuj (Tušek, 1985).

Dva zlata uhana (sl. 2) (inv. št. 80CP001/002 in 80CP001/003) sta bila najdena leta 1980, iz območja Srednješolskega centra, na Volkmerjevi cesti, na Ptuju. Nahajala sta se v grobu številka 1, kjer se je v sledeh nahajal ženski skelet. Uhana imata vkovana kristala smaragda (U-1, U-2). Hrani ju Arheološki oddelek Pokrajinskega muzeja Ptuj-Ormož (Tušek, 1985).

Kot tretji arheološki predmet je zapestnica v dveh delih (sl. 3). Najdena je bila leta 2009, na območju Osnovne šole Ljudski vrt, grob 154 (inv. št. PN 627). Vsebuje tri smaragdne kristale (Z-1, Z-2, Z-3). Hrani jo Arheološki oddelek Pokrajinskega muzeja Ptuj-Ormož.

Kot primerjalni material smo izbrali deset kristalov smaragda iz Habachtala v Avstriji (sl. 4) (inv. št. 623-a, 623-b, 623-c, 627, 628, 1475, 1478, 1488, M1, M2) in zeleno obarvan beril iz Urala (sl. 5) (inv. št. 1470), vsi, razen vzrorcev M1 in M2, pa so iz znamenite Zoisove zbirke mineralov (tab. 1) (Činč Juhant & Jeršek, 2005).

Metode

Makroskopski opis

Vzorce smo najprej opazovali s prostim očesom in lupo 10x povečave. Določali smo kristalografske značilnosti, vključke in barvo. S pomočjo kljunastega merila smo izmerili velikost smaragdov.

Gemološki mikroskop

Smaragde smo pregledali z gemološkim mikroskopom, ki je pravzaprav stereolupa s povečavami od 10 do 80x. Model gemološkega mikroskopa je bil KSW 63/11434.3.

UV svetilka

S standardno ultravijolično svetilko smo preiskovali luminiscenčne pojave pri vzorcih (fluorescenca in fosforescenca) s kratko in dolgovalovno ultravijolično svetlobo.

Metodi PIXE in PIGE

Metodi PIXE in PIGE temeljita na obsevanju vzorca z visokoenergijskimi ioni, ki v snovi vzbudijo karakteristične rentgenske žarke in žarke gama. Protoni z energijo nekaj MeV prodrejo do 100 µm globoko v snov, tako da meritve ne kažejo le stanja na površini, ampak nekaj 10 µm globoko - upoštevati moramo namreč, da se protoni pri prehajanju skozi snov upočasnjujejo, reakcijski preseki pa se z energijo hitro manjšajo. Nastali rentgenski žarki se v vzorcu tudi absorbirajo, medtem ko so učinki absorpcije pri veliko trših žarkih gama zanemarljivi. Merilni postopek je nedestruktiven, saj obsevanje s protoni ne povzroča vidnih sledov, tako da sta metodi posebno primerni za analizo dragocenih predmetov, med katere spadajo tudi dragi kamni.

Meritve z metodo PIXE - PIGE smo opravili na tandemskem pospeševalniku Instituta Jožef Stefan v Ljubljani. Merili smo s protonskim žarkom v zraku, ker omogoča enostavno nameščanje vzorca in izbiro mest za obsevanje. Nominalna energija protonov je bila 2,5 MeV, pri prehodu skozi 2 µm debelo okence iz tantalove folije in 1 cm široko zračno režo se je ta energija zmanjšala na približno 2,2 MeV. Profil žarka je bil Gaussov, s širino 0,8 mm na polovični višini. Vzbujeni rentgenski žarki so do detektorja rentgenskih žarkov, ki je bil postavljen pod kotom 45° glede na protonski žarek, prepotovali še 5,7 cm široko zračno režo. Zaradi absorpcije v zračni reži smo lahko z rentgenskimi žarki zaznali le elemente, težje od silicija. V vsaki izbrani točki smo opravili dve meritvi. S prvo smo merili nizkoenergijski spekter elementov med silicijem in železom, pri drugi pa smo tok protonov povečali na nekaj nA in merili hkrati visokoenergijski rentgenski spekter elementov, težjih od železa, in spekter gama. Detektor rentgenskih žarkov smo v ta namen opremili z dodatnim absorberjem iz 0,1 mm debele aluminijeve folije. V spektrih gama smo zajeli elemente Na, Mg in Al. V spektrih se sicer pojavljajo tudi črte litija in fluorja, vendar jih pri kvantifikaciji rezultatov nismo upoštevali, ker nismo imeli ustreznih standardov. Prav tako smo koncentracije berilija upoštevali le računsko.

Negotovosti pri koncentracijah večinskih elementov so reda ± 5 %, pri elementih v koncentracijah pod 0,1 % pa so lahko večje, in sicer 10-15 %. Merilne negotovosti so večje tudi pri meritvah na naravnih berilih, ki imajo na površini drobne mineralne nečistoče, navadno lističe sljude, zaradi katerih smo z meritvami določili večje koncentracije kalija in aluminija.

Rezultati

Makroskopski opis

Habachtalski kristali smaragdov so večinoma prosojni in ne prozorni. Kristalne ploskve imajo videz, kot da bi bile najedkane, redko so gladke. Videz je posledica rasti v kamnini ali pa je najedkanost posledica delnega raztapljanja. Smaragdi so barvno neenoviti. Nekateri so brezbarvni (inv. št. 628), drugi različnih odtenkov zelene barve. Imajo veliko vključkov sljude. Splošno razmerje med širino in dolžino kristalov je v razmerju od 1 : 3 do 1 : 6.

Smaragdi v arheoloških predmetih se navidezno med seboj ločijo. In sicer so smaragdi v zapestnici na videz neprozorni, imajo tudi drugačen barvni odtenek (modrikasto zelen) in vsebujejo veliko sljude.

Smaragdi v verižici in uhanih so prosojni do prozorni, zelene barve s številnimi tekočinskimi vključki in relativno malo sljude (tabla 1, sl. 6 do 13).

Velikost smaragdov v arheoloških predmetih smo izmerili tako, da smo izmerili razdalje med dvema nasprotnima si ploskvama heksagonalne prizme (Š) in višino smaragda med dvema pinakoidoma (V). Rezultati meritev so podani v tabeli 2.

Kristalografske značilnosti smaragdov

Kristali smaragdov iz Habachtala imajo značilen prizmatski habitus, ki ga določajo ploskve heksagonalne prizme I. reda a (100) in so zaključeni s ploskvijo pinakoida c (001) (sl. 14). Zeleno obarvan beril iz Urala ima prav tako izrazit prizmatski habitus z razvitimi ploskvami heksagonalne prizme I. reda a (100) in pinakoida c (001). Tri kristalne ploskve heksagonalne prizme I. reda so zbrušene in spolirane.

Smaragdi v arheoloških predmetih imajo poleg heksagonalne prizme I. reda a (100) in pinakoida c (001) razvite še druge kristalne ploskve. Določili smo heksagonalno bipiramido I. reda d (101), heksagonalno bipiramido II. reda e (111) in heksagonalno prizmo II. reda g (110) (sl. 15 in 16). Kristal (V-1) na verižici nima ploskev heksagonalne prizme II. reda g (110), medtem ko jih drugi (V-2) kristal v verižici ima. Kristali na zapestnici (Z1-3) so slabše ohranjeni, a se še vedno da opaziti, da ima kristal podobne kristalografske značilnosti kot jih imajo smaragdi na verižici (V1-3) in uhanih (U-2, U-3). Smaragdi v zapestnici so deloma ohranjeni kot naravni kristali, deloma pa so obrušeni, saj so ploskve, ki naj bi pripadale heksagonalni prizmi, med seboj izrazito nevzporedne. Poleg tega smo na nekaterih mestih določili dodatne kristalne ploskve heksagonalne bipiramide (sl. 17).

Na osnovi kristalografskih značilnosti lahko zaključimo, da so kristali smaragdov iz Habachtala in berila iz Urala značilno prizmatski in imajo poleg ploskve pinakoida razvite samo še ploskve heksagonalne prizme, medtem ko imajo smaragdi v arheoloških predmetih razvite še druge kristalne ploskve. Poleg tega so smaragdi iz

Habachtala srednje do dolgo prizmatski, medtem ko so kristali smaragdov iz arheoloških predmetov kratko do srednje prizmatski in v splošnem bolj sodčkasti in imajo razvitih več vrst kristalnih ploskev. To nas navaja na dejstvo, da so obravnavani smaragdi nastali pri različnih razmerah (Kostov & Kostov, 1999), kar lahko pomeni, da so tudi iz različnih nahajališč.

Luminiscenčni pojavi

Pri pregledu vzorcev z ultravijolično svetilko, s kratko in dolgovalovno ultravijolično svetlobo, preiskovani vzorci niso fluorescirali in tudi niso fosforescirali.

Vključki

Smaragdi iz Habachtala niso prosojni do prozorni in vsebujejo veliko tekočinskih vključkov in vključkov sljud tako v samih kristalih kot deloma na površini kristalov smaragda. Podobno ima zeleno obarvan beril iz Urala številne tekočinske vključke, conarno obarvanost, ki se spreminja od svetlo do temno zelene ter vključke sljud.

Smaragdi iz arheoloških predmetov, iz verižice in uhanov, vsebujejo tekočinske vključke (sl. 18). Tekočinske kanale smo našli v vseh smaragdih v verižici (V1-3) (sl. 19), medtem ko le ti v uhanih niso tako izraziti oziroma jih lahko pripišemo splošno tekočinskim vključkom. Smaragdi v zapestnici (Z1-3) imajo veliko sljude tako na površini kot v notranjosti (sl. 20) medtem ko drugih vključkov zaradi neprozornosti vzorcev nismo našli.

Za smaragde je znano, da vsebujejo veliko vključkov, kar smo ugotovili tudi v preiskovanih vzorcih in sicer tako v smaragdih iz arheoloških predmetov kot v primerjalnih smaragdih. V smaragdih iz arheoloških predmetov posebno izstopajo vključki v obliki tekočinskih kanalov. Našli smo jih v smaragdih v verižici in v uhanih medtem ko v smaragdih v zapestnici ne. Prav tako jih nismo našli v primerjalnih smaragdih. Po literaturnih podatkih (Jennings et al., 1993), so prav tekočinski kanali značilni za smaragde iz Egipta in so jih določili tudi drugi raziskovalci (Hyršl, 2012). Predvidevamo tudi, da bi bile razlike vidne med sljudami, saj se le te pojavljajo kot vključki v vseh vzorcih in so že pri pregledu vzorcev z gemološkim mikroskopom med seboj drugačne. Zato jih bo smiselno v prihodnosti podrobneje analizirati.

Metoda PIXE/PIGE

Z metodo PIXE/PIGE smo analizirali 12 vzorcev. Za primerjalno gradivo smo izbrali vzorce z inv. št. 628, 1470, 1488, M-1 in M-2. Vzorci smaragdov iz arheoloških predmetov so bili V1, V2, V-3, U-2, U-3, Z-1 in Z-2. Pri analizi podatkov je bila statistična napaka pri Mg pod 5 %, celotna napaka pri Mg pa je bila okoli 10 %. Pri drugih elementih lahko vzamemo celotno napako 5 %, razen pri najmanjših koncentracijah, kjer lahko doseže 10-15 %. Rezultati meritev so podani v tabeli 3.

V tabeli 3 so zbrani rezultati analiz smaragdov v arheoloških predmetih, v primerjalnih smaragdih in po podatkih iz literature (Avstrija, Afganistan, Egipt, Indija, Rimska Galija) glede na vsebnost izbranih oksidov, ki so pomembni za določitev njihovega izvora (Calligaro et al., 2000).

Izmerjene podatke smo najprej poskusili razdeliti v skupine z metodo glavnih osi (PCA), tako da smo upoštevali okside Na, Mg, Al, K in Ca; pri tem smo uporabili logaritemsko transformacijo c'=ln(1+c) po Duewerju et al., 1975. Na sliki 21 smaragdi iz posameznih arheoloških predmetov jasno nastopajo skupaj, kar kaže, da so pri vsakem predmetu uporabili smaragde iz izbranega individualnega vira. Po Calligaru et al., 2000, lahko podrobneje določimo lokacije virov iz dvojnih diagramov Na_2O/MgO in Na_2O/Al_2O_3.

Razmerje med Na_2O in MgO nam kaže določeno grupiranje podatkov (sl. 22), kar nas navaja na enako ali pa vsaj zelo podobno okolje, v katerem so zeleno obarvani berili nastali. Zeleno obarvani beril iz Urala ima vrednosti MgO in Na_2O povsem drugačne od ostalih, tako da so zgodba zase. To pomeni, da smaragdi iz arheoloških predmetov ne izvirajo iz tega zgodovinsko pomembnega nahajališča na Uralu. Podobno se grupirajo podatki danega razmerja med natrijevim in magnezijevim oksidom za smaragde iz Habachtala. Zanje je sicer značilno, da se spreminja vsebnost magnezijevega oksida, kar je tudi posledica številnih vključkov sljude, medtem ko je vsebnost natrijevega oksida bolj ali manj stalna. Zato pa lahko za smaragda iz zapestnice iz arheoloških predmetov (Z1-2) ugotovimo, da ne izvirata iz nahajališč v Habachtalu. Njuno razmerje oksidov je zelo blizu literaturnemu podatku (Calligaro et al., 2000) za smaragde iz Afganistana.

Preostali smaragdi iz arheoloških predmetov (V1-3, U2, U3) imajo dokaj stalno vsebnost magnezijevega oksida, medtem ko se vsebnost natrijevega oksida spreminja. V ta »oblak« podatkov sodi tudi preiskovani vzorec Rimska Galija, ki ga hranijo v muzeju Carnavalet (Pariz), ki izhaja iz severno afriških nahajališč (Calligaro et al., 2000). Če jih primerjamo z literaturnimi podatki (Calligaro et al., 2000), lahko ugotovimo, da imajo nekoliko višjo vsebnost magnezijevega oksida kot smaragdi iz Indije in nižjo vsebnost natrijevega oksida kot en smaragd iz Egipta. Ker so vrednosti razmerja med magnezijevim oksidom in natrijevim oksidom za vzorce smaragdov iz verižice in uhanov vendarle dovolj skupaj, menimo, da izvirajo iz skupnega nahajališča, kar potrjuje tudi vrednost omenjenega razmerja za en vzorec (Rimska Galija). Razlike med danimi vzorci in predvsem različnost drugega literaturnega podatka za smaragd iz Egipta nakazujejo, da gre morda za drugo mikrolokacijo, saj je bilo rudnikov v Egiptu več (Shaw et al, 1999).

Razmerje med Na_2O in Al_2O_3 (sl. 23) nam podobno kot razmerje med Na_2O in MgO kaže določeno grupiranje podatkov, kar nas navaja na enako ali pa vsaj zelo podobno okolje, v katerem so zeleno obarvani berili nastali. Za zeleni beril

iz Urala lahko ponovno ugotovimo, da je tudi v tem primeru zgodba zase, kar nam dodatno potrjuje, da smaragdi iz arheoloških predmetov niso nastali v enakih razmerah kot zeleni beril iz Urala. Na splošno lahko za druge vzorce, kakor tudi za vzorce iz literaturnih podatkov (Calligaro et al., 2000) ugotovimo, da se vsebnost Al_2O_3 spreminja relativno manj kot vsebnost Na_2O. Za vzorca (Z1-2) lahko ponovno potrdimo, da sta glede na vsebnost Na_2O še najbližje smaragdom iz Afganistana, medtem ko nas v povezavi z vsebnostjo Al_2O_3 to dejstvo navaja, da so morda iz kakega drugega nahajališča; morda iz Egipta, vendar ne iz iste mikro lokacije. Posebej izstopa en literaturni podatek (Egipt) (Calligaro et al., 2000) za smaragd iz Egipta, medtem ko je drugi (Rimska Galija) znotraj oblaka podatkov za smaragde iz arheoloških predmetov na Slovenskem. Ti podatki se grupirajo v osrednjem delu diagrama, kamor sodijo habachtalski, indijski in preiskovani smaragdi v arheoloških predmetih. Zaznamo lahko določeno grupacijo, in sicer da imajo smaragdi iz Habachtala nižjo vsebnost tako Na_2O kot Al_2O_3, indijski imajo relativno več $Al_2O_{3,}$ medtem ko imajo smaragdi iz arheoloških predmetov relativno več Na_2O in povprečno vsebnost Al_2O_3.

Na osnovi geokemičnih analiz vzorcev smaragdov lahko zaključimo, da so smaragdi iz arheoloških predmetov, verižice in uhanov (V1-3, U2, U3) zelo verjetno iz nahajališč v Egiptu (dolina Gimal del A in B, dolina Nuqrus, dolina Sikait, Zubara) medtem ko so smaragdi iz zapestnice (Z1-2) iz nahajališč na območju današnjega Afganistana (dolina Panjshir) ali pa iz Egipta, vendar druge mikro lokacije kot smaragdi iz verižice in uhanov.

Zaključek

Izvor smaragdov v arheoloških predmetih na Slovenskem do sedaj ni bil raziskan s stališča geokemičnih (Calligaro et al., 2000) in mineraloških značilnosti (Bauer, 1968; Henn, 1990) medtem ko so v arheološkem pogledu najdbe opisane (Tušek, 1985).

Smaragdi v arheoloških predmetih imajo večinoma ohranjene kristalne ploskve in zato smo primerjali oblike kristalov iz Habachtala in tiste v arheološkem nakitu. Smaragdi iz Habachtala imajo značilen in preprost prizmatski habitus, ki ga določajo ploskve heksagonalne prizme I. reda a (100) in pinakoida c (001). Smaragdi v arheoloških predmetih imajo poleg heksagonalne prizma I. reda a (100) in pinakoida c (001), še druge kristalne ploskve in sicer ploskve heksagonalne bipiramide I. reda d (101), heksagonalne bipiramide II. reda e (111) in heksagonalne prizme II. reda g (110). Ugotovili smo, da se kristalografske značilnosti smaragdov iz Habachtala (Henn, 1990) razlikujejo od kristalografskih značilnosti smaragdov iz arheoloških predmetov na Slovenskem, kar lahko povezujemo z drugačnimi razmerami pri njihovem nastanku in s tem na drugo nahajališče.

Geokemične značilnosti, ki nam lahko pokažejo izvor smaragdov, je raziskoval že Calligaro s sodelavci (2000). Na osnovi razmerij med Na_2O in MgO ter Na_2O in Al_2O_3 je ugotavljal izvor smaragdov in jih primerjal z referenčnimi smaragdi iz različnih nahajališč. Na osnovi naših rezultatov in podatkih iz literature (Calligaro et al., 2000) smo ugotovili, da je zeleni beril iz Urala povsem svoja zgodba, vzrorci smaragdov iz zapestnice izvirajo iz območja današnjega Afganistana, medtem ko bi vzorci smaragdov iz verižice lahko izvirali iz Egipta, kot tudi iz Habachtala.

Geokemične značilnosti smaragdov iz Habachtala in Egipta se ne razlikujejo dovolj, da bi določili nahajališče samo na osnovi značilne kemijske sestave. Če pa upoštevamo še kristalografske značilnosti (Henn, 1990) in značilne vključke v obliki tekočinskih kanalov (Jennings, 1993), pa so vzorci smaragdov iz arheoloških predmetov (verižica in uhana) iz nahajališč v Egiptu. Razlike v geokemičnih značilnostih lahko pripišemo mikrolokaciji znotraj nahajališč v Egiptu.

Na začetku smo postavili delovno hipotezo, da so smaragdi v arheoloških predmetih na Slovenskem iz nahajališča Habachtal v Avstriji. Na osnovi geokemičnih in kristalografskih značilnosti ter značilnih vključkov, pa smo ugotovili, da so smaragdi iz verižice in uhanov iz nahajališč v Egiptu (dolina Gimal del A in B, dolina Nuqrus, dolina Sikait, Zubara). Za smaragde iz zapestnice zaradi pomanjkanja primerjalniega gradiva nismo mogli povsem zanesljivo določiti izvora; lahko so iz nahajališča v današnjem Afganistanu ali pa iz Egipta, vendar ne iz istega nahajališča, kot prej omenjeni smaragdi iz verižice in uhanov.

Zahvala

Mariji Lubšini Tušek, univ. dipl. arheologinji, konservatorki, na Zavodu za varstvo kulturne dediščine Slovenije, Center za preventivno arheologijo, Regionalni oddelek Ptuj, ki nam je posodila verižico in tako omogočila analize.

Mojci Vomer Gojkovič, univ. dipl. arheologinji, kustodinji na arheološkem oddelku Pokrajinskega muzeja Ptuj-Ormož, ki nam je zaupala izposojo uhanov in zapestnice za analizo.

Literatura - References

Bauer, M. 1968: Precious Stones. Dover Publications, 2: 226 p.

Calligaro, T., Dran, J. C., Poirot, J. P., Querre, G., Salomon, J. & Zwaan, J. C. 2000: PIXE/PIGE characterisation of emeralds using an external micro-beam, Nuclear Instruments and Methods in Physics Research B, Elsevier Science B.V., B 161–163: 769-774

Činč Juhant, B. & Jeršek, M. 2005: Dragulji iz zgodovinskih mineraloških zbirk Prirodoslovnega muzeja Slovenije. V: Jeršek, M. (ed.): Dragulji: v kamen ujeta barva. Olševek: Narava; Ljubljana: Prirodoslovni muzej Slovenije, 32-35.

Duewer, D.L., Kowalski, B.R. & Schatzki, T.F. 1975: Source identification of oil spills by pattern recognition analysis of natural elemental composition, Anal. Chem., 47: 1573-1583.

Finlay, V. 2006: Jewels: A secret history, Ballantine Books, ZDA: 496 p.

Gübelin, E. J. & Koivula, J. I. 1986: Photoatlas of Inclusions in Gemstones, ABC Edition, Zurich, 244-260 p.

Henn, U. 1990: Gemmologisches Praktikum, Eine Sonderveröffentlichung von gold, silber, uhren, schmuck, Deutche Stiftung Edelsteinforschung (DSEF), Idar-Oberstein: 86 p.

Hyršl, J. 2012: Gemmological study of the St. Wenceslas crown in Prague. http://www.korunovacniklenoty.cz/en/other/gemmological-study-of-the-st-wenceslas-crown-in-prague.html (10.12.2012)

Jennings, R.H., Kammerling, R.C., Kovaltchouk, A., Calderon, G.P., Mohamed, K.E.B. & Koivula, J.I. 1993: Emeralds and Green Beryls of Upper Egypt. Gems & Gemology, 29/2: 100–115.

Jeršek, M. & Dobnikar, M. 2005: Dragulji, v kamen ujeta barva. Olševek: Narava, Prirodoslovni muzej Slovenije, Ljubljana: 168 p.

Jeršek, M. & Vidrih, R. 2009: Smaragdi, Življenje in tehnika, 60/5: 30–37.

Kostov, I & Kostov, R.I. 1999: Crystal habits of minerals. Prof. Marin Drinov Academic Publishing House & Pensoft Publishers, Sofia, 231–243.

Rečnik, A., Podgornik, A. & Marjetič, R. 1994: Nahajališča smaragda v Habachtalu in Untersulzbachtalu v Avstriji, Proteus, 56/9: 322–326.

Shaw, I., Bunbury, J. & Jameson, R. 1999: Emerald mining in Roman and Byzantine Egypt. Journal of Roman Archaeology, 12: 203–205.

Tušek I. 1985: Zlati nakitni predmeti v rimskih grobovih na Ptuju. Ptujski zbornik, Skupščina občine Ptuj, 5: 405–417.

GEOLOGIJA *56/1*, 049–056, Ljubljana 2013

doi:10.5474/geologija.2013.004

Minerals of Pohorje marbles

Minerali pohorskih marmorjev

Miha JERŠEK[1], Sabina KRAMAR[2], Simona SKOBE[3], Nina ZUPANČIČ[3,4] & Viljem PODGORŠEK[5]

[1]Slovenian Museum of Natural History, Prešernova 20, SI-1000 Ljubljana
[2]Slovenian National Building and Civil Engineering Institute, Dimičeva ul.12, SI-1000 Ljubljana
[3]University of Ljubljana, Faculty of Natural Sciences and Engineering, Department of Geology, Aškerčeva 12, SI-1000 Ljubljana, Slovenia

[4]Ivan Rakovec Institute of Palaeontology, ZRC SAZU, Novi trg 2, SI-1000 Ljubljana, Slovenia
[5]Kraigherjeva ulica 17, SI-2250 Ptuj, Slovenia

Prejeto / Received 4. 4. 2013; Sprejeto / Accepted 17. 6. 2013

Key words: marble, Pohorje, accessory minerals, tremolite, vesuvianite, diopside
Ključne besede: marmor, Pohorje, akcesorni minerali, tremolit, vezuvianit, diopsid

Izvleček

Na Pohorju izdanjajo pretežno kalcitni marmorji, ki ponekod prehajajo v dolomitne. Karbonatne kamnine, iz katerih so nastali, so vsebovale tudi detritične minerale, ki so se med metamorfozo ohranili ali pa prešli v nove minerale. Raziskali smo minerale v marmorjih s Pohorja, ki so kot kristali vidni s prostim očesom ali z lupo 10 x povečave in s pomočjo binokularnega mikroskopa. Z ramansko mikrospektroskopijo, SEM-EDS analizo in na osnovi morfoloških značilnosti smo določili 17 različnih mineralov, med katerimi so, poleg kalcita, najpogostejši in obenem tudi najbolj značilni tremolit, diopsid, grosular in epidot. Prvič sta v pohorskih marmorjih opisana vezuvianit in skapolit. Ploskovno bogati so kristali kremena, ki vsebujejo igličaste vključke amfibola. Drugi minerali, ki dopolnjujejo mineralno paragenezo marmorjev, so različni minerali sljud, minerali kloritove skupine, glinenci, magnetit, titanit, pirit in grafit. Določena mineralna združba nam razkriva mineralno pestrost pohorskih marmorjev in nam ponuja nove izzive za raziskovanje značilnosti in razmer pri nastanku te plemenite kamnine, ki so jo cenili in izkoriščali že Rimljani, danes pa ponovno dobiva svojo veljavo in prepoznavnost.

Abstract

In the Pohorje Mts, mostly outcrops of calcite marble can be found, which in places turn into dolomite marbles. The protolith carbonate rocks contained also detritical minerals, which remained unchanged or formed new minerals during metamorphosis. Minerals in the Pohorje marbles that can be seen as crystals with the naked eye or 10x magnifying loupe and with binocular microscope were investigated. With the aid of Raman microspectroscopy, SEM-EDS analysis and on the basis of morphological characteristics, the presence of 17 different minerals or group of minerals was confirmed. The most numerous and also the most significant were, apart from calcite, tremolite, diopside, grossular and epidote. For the first time, vesuvianite and scapolite were described in the Pohorje Mts. Particularly rich, as far as crystal faces are concerned, were the crystals of quartz that contained needle-like amphiboles. Other minerals that well supplemented the mineral paragenesis were different minerals of mica and chlorite group, feldspars, magnetite, titanite, pyrite and graphite. The determined mineral association revealed the mineral diversity of Pohorje marbles, offering us a new challenge for the investigation of the characteristics and conditions during the origin of this noble rock, which was highly esteemed already by the Romans, while today it is regaining its value and recognisability.

Introduction

The thick Pohorje forests still hide many interesting mineral associations. This is also the case of Pohorje marbles. Thanks to various collectors, particularly Viljem Podgoršek and Franci Golob, who carried out extensive field sampling, we have been given an opportunity to analyse the macroscopically visible crystals in the marble. The Pohorje marbles, which were highly esteemed already by the Romans, have thus been supplemented by some new minerals, which may contribute to the characterization of this rock.

Metamorphism of relatively pure limestone and dolomite yields generally marble and dolomarble (Best, 2007). Impure carbonate protoliths that contain variable amounts of quartz grains and shaly material may include, in addition to calcite, dolomite and quartz, as well as diopside, tremolite, talc, phlogopite, wollastonite, calcic plagioclase, vesuvianite, forsterite and grossular-andradite (Best, 2007). Therefore, the presence of the minor content of non-carbonate minerals corresponds to the chemistry and mineralogy of the protolith and its metamorphic history. Mineral

assemblages, and therefore accessory minerals, provide crucial information on temperature and pressure during metamorphism, i.e. metamorphic facies (Best, 2007). Some mineral species are particularly good traces since, alone, they may point to the provenance of the host marble (Capedri et al., 2004; Origlia et al., 2011; Taelman et al., 2012). For example, fluorite points at Anatolian marbles, in particular to Marmara, Mugla/Salkim, or Balikesir/Kocoglu; zoisite to Naxos, and rare earth-containing epidote to Mugla/Golkuc; aspidolite is unique to Marmara, whereas margarite occurs at Marmara and Samos, and paragonite at Marmara, Aydin and Iraklia. Plogopite occurs at Marmara and Mugla/Salkim among the Anatolian marbles, and at Thasos, Naxos, Paros and Penteli among the Greek marbles; it may be worth noting that phlogopite is absent from Carrara marble (Capedri et al., 2004). By contrast, plagioclase is typical of Carrara and Aydin among the white marbles, and of Mani and Mugla/Golkuc among the red coloured marbles (Capedri et al., 2004).

On the other hand, some authors argue (Lazzarini et al., 1980) that the accessory minerals themselves do not seem to have much diagnostic value owing to the wide distribution and frequent occurrences of common minerals like quartz, epidote and mica, and because of the absence of rare or special minerals. They may be used successfully in combination with other parameters for the characterisation of the marbles (Capedri et al., 2004), e. g. geographical distribution as well as metamorphic history of the marble (Bucher & Frey, 2002).

Within this study we focused only on determination of minerals, which are large enough to be seen macroscopically or with a 10x magnifying loupe.

Geological setting

The Pohorje Mts represent the south-eastern margin of the Eastern Alps. From the west to the south, Pohorje is bounded by the Labot fault and by the Periadriatic zone (Mioč, 1978, 1983; Mioč & Žnidarčič, 1977, 1983, 1989), whereas on the northern side the mid-Miocene Ribnica through separates Pohorje from the mountains of similar lithology and structure. On the eastern side, Pohorje gently dips below Plio-Quaternary sediments.

The Eastern Alps consist of a system of large nappes formed during the Eoalpine orogeny (Frank, 1987; Schmid et al., 2004, Fodor et al., 2008). Pohorje Mts are part of the Austroalpine nappe (Placer, 2008). The deepest tectonic unit, the Pohorje nappe (Janak et al., 2006), is mainly composed of medium- to high-grade (HP) metamorphic rocks – gneisses, mica schists and amphibolites with marble and quartzite. These rocks form a strongly foliated matrix along sporadic eclogite lenses and two main serpentinite bodies (Hinterlechner-Ravnik, 1971, 1973; Mioč, 1978). The evidence of ultra-high-pressure (UHP) metamorphism in eclogites was confirmed by Janak et al., 2004. The timing of HP/UHP metamorphism in the Pohorje nappe is Cretaceous (Thöni, 2002; Miller et al., 2005; Cornell et al., 2007) and Tertiary – Early to Middle Miocene (Fodor et al., 2002). The Pohorje nappe is overlain by a nappe of weakly metamorphosed Paleozoic rocks, mainly low-grade metamorphic slates and phyllites (Hinterlechner-Ravnik, 1971, 1973; Vrabec, 2010). The upper nappe is built up of Permo-Triassic clastic sedimentary rocks, prevailingly sandstones and conglomerates (Hinterlechner-Ravnik, 1971, 1973; Vrabec, 2010). The entire nappe stack is overlain by early Miocene sediments, which belongs to the syn-rift basin fill of the Pannonian Basin (Fodor et al., 2003).

Also, a large granodiorite body with a smaller dacite part in its north-western section (Dolar Mantuani, 1935; Faninger, 1970; Zupančič, 1994a, b) is intruded into the central part of the massif. It is of the Miocene age (18–19 Ma; Trajanova et al., 2008; Fodor et al., 2008). The boundary of the pluton is locally tectonized, but the original magmatic contact is marked by a thin contact aureole (Mioč & Žnidarčič, 1977; Žnidarčič & Mioč, 1988; Mioč & Žnidarčič, 1989). In the contact with muscovite micashist, the contact aureole is missing as the rocks have already been crystallised in almadine amphibolites facies (Hinterlechner-Ravnik, 1973).

Germovšek (1954) distinguished three genetic marble types. The major type present in SE Pohorje was described as dynamometamorphic marbles and associated them with micashists. In the northern part of Pohorje, there are small outcrops of metamorphosed Upper Cretaceous limestones, while in the NW part of Pohorje marbles in contact with dacite are present. According to Hinterlechner-Ravnik & Moine (1977), the marble level occurs in two separated areas in the southern and eastern parts of the massif, clearly exposed between the Oplotniščica and Dravinja brooks, and north of Šmartno, towards Ruše. Here, marbles occur between biotite ± muscovite schists and gneiss and flaser gneiss with ± almandine ± kyanite and amphibolite varieties (Hinterlechner-Ravnik & Moine, 1977). Marble is more abundant in the southern part of the massif, where it represents up to 30% of the horizon, than in its northern part (Hinterlechner-Ravnik & Moine, 1977; Jarc & Zupančič, 2009). The marble is coarse grained, rarely fine grained; in contacts with phyllite schists it is poorly crystallized and brecciated (Hinterlechner-Ravnik, 1971). The marble is white, or coloured due to accessory minerals, such as graphite and pyrite (grey colour) or silicate minerals, such as amphiboles and biotite (greenish and brownish to violet coloured). The dolomite marble is also present (Hinterlechner-Ravnik, 1971).

The textures of marbles are granoblastic, sutured and blastomillonitic. Calcite crystals exhibit twin lamellae, rhombohedral cleavage and undulatory extinction, which indicates the growth under pressure (Hinterlechner-Ravnik, 1971). The accessory minerals are quartz, Na-rich plagio-

clase, tremolite, green hornblende, diopside, forsterite, mica (muscovite and biotite group), rarely garnets, graphite, pyrite, and the products of retrograde metamorphism: chlorite, epidote, clinozoisite, serpentine over forsterite and limonite (Hinterlechner-Ravnik, 1971; Jarc & Zupančič, 2009). From the vicinity of Zreče, Germovšek (1954) reported on wollastonite rich marble with transition to wollastonite-bearing rock.

Materials and methods

Marble samples from different Pohorje quarries were collected by Viljem Podgoršek and Franc Golob, who registered several mineral sites in the period between August 12th 2011 and July 24th 2012. We have selected, examined and analysed 16 marble samples from the area of Bojtina quarry, three from the Skomarje quarry, two from the marble quarry at Gorenja vas near Zreče, two from Planica, and one from Frajhajm near Pregel and Čadram.

Raman spectroscopy has been used successfully in nearly all geoscience disciplines and virtually all kinds of samples have been studied using this technique (Nasdala et al., 2004). Raman spectroscopy is a technique based on inelastic scattering of monochromatic light - sample is illuminated with a laser beam. Scattered light results in Raman spectrum that is characteristic of a certain mineral. Raman microspectroscopy does not require special preparation of samples for analyses, but enables us to identify minerals even non-destructively. Furthermore, tiny crystals that due to the impossibility of separation or preparation of such diminutive amounts could not be analysed by other techniques, such as X-ray diffraction analysis, could be identified. Raman spectra of samples were obtained with a Horiba Jobin Yvon LabRAM HR800 Raman spectrometer equipped with an Olympus BXFM optical microscope. Measurements were made using a 785 nm laser excitation line, and the Leica 50´ objective was used. The spectral resolution was about 1 cm^{-1}.

The morphology and chemical compositions of the selected samples were additionally examined using Scanning Electron Microscopy (SEM) JEOL 5500 LV SEM equipped with the Energy Dispersive X-Ray spectrometry (EDS), at accelerating voltage 20 kV and working distance 20 mm. Prior to the analyses, samples were carbon coated. X-ray spectra were optimized for quantification using cobalt optimization standard, and the correction of EDS data was performed on basis of the standard ZAF-correction procedure included in the INCA Energy software.

Results and discussion

The identified minerals in marble with their localities are given in Table 1. All of the collected samples have more or less fully developed crystals of different minerals, which could have been established already with the naked eye, a 10x magnifying loupe, or with the aid of a binocular microscope.

A total of 17 different minerals were identified in marbles from the Pohorje Mts. The largest crystals are secondary calcite crystals of younger generation that occur in nests of calcite marbles. The most abundant and also the larger crystals found are pyroxene diopside and amphibole tremolite. Significant minerals are grossular, scapolite, epidote and vesuvianite. Among micas, quite frequently group of minerals, biotite and muscovite were identified. Also, some minerals of chlorite group were detected. Quartz (sometimes with inclusions of amphibole), magnetite, titanite and pyrite that is sometimes limonitised are less abundant among minerals easily seen with the naked eye. We also identified some feldspars; plagioclase and orthoclase. Small inclusions in calcite are identified as graphite.

Hereinafter, macroscopic characteristics of selected minerals will be given.

Calcite

Calcite crystals in nests of marbles are white, colourless and slightly yellow coloured. Dominant crystal face is a step rhombohedron, modified by other rhombohedrons (Figs. 1 and 2). Calcite crystals are up to 1 cm high. Calcite crystals with step rhombohedrons are characteristic of the final stage of crystallisation in metamorphic rocks, referred to as a continuous drop of temperature or a successive change in the solutions' pH (Kostov & Kostov, 1999).

Fig. 1. Corroded calcite crystals in a rare nest in marbles from Bojtina, 10 x 6 cm. Franc Golob's Collection

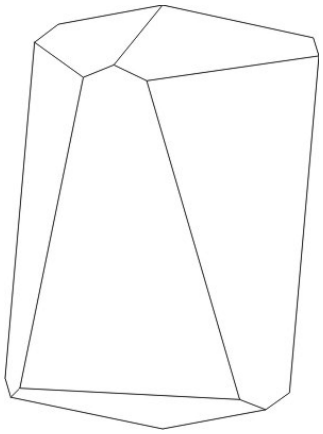

Fig. 2. Crystals of calcite from Bojtina marble have developed step rhombohedron faces (≈071) and rhombohedron (021).

Diopside

Apart from calcite, diopside is very common mineral found in the Pohorje marbles (Figs. 3 and 4). It is usually green, olive green to dark green or even colourless (Fig. 3). For the most part, the crystals are seemingly opaque, and it is only rare smaller samples that are transparent. Exceptions are the utterly colourless and transparent diopside crystals from Frajhajm near Pregel. Here and there, diopside is finely granulated and massive. Individual olive green crystals with glassy shine are more than 20 mm long. The largest diopside crystal is dark green and 50 mm high. On the parts, where crystal planes have been preserved, the crystal has silky lustre.

Fig. 3. 10 mm high crystals of dark green diopside in the Bojtina marble. Viljem Podgoršek's Collection

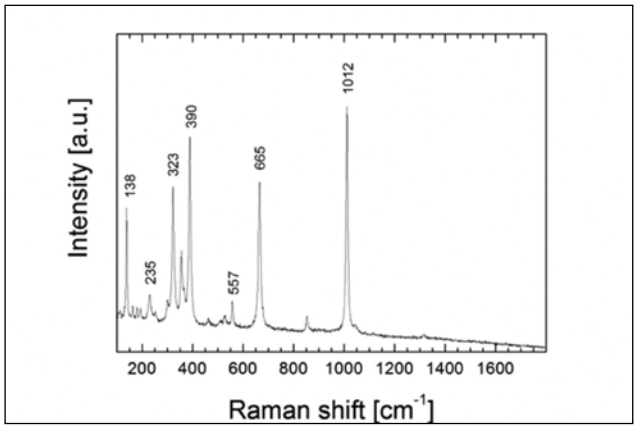

Fig. 4. Raman spectrum of diopside from Bojtina marble

Tremolite

Tremolite (Fig. 5) occurs in prismatic elongated crystals. They are colourless to white and form up

Fig. 6. Radial clusters of tremolite from Bojtina marble, 10 x 6 cm. Viljem Podgoršek's Collection

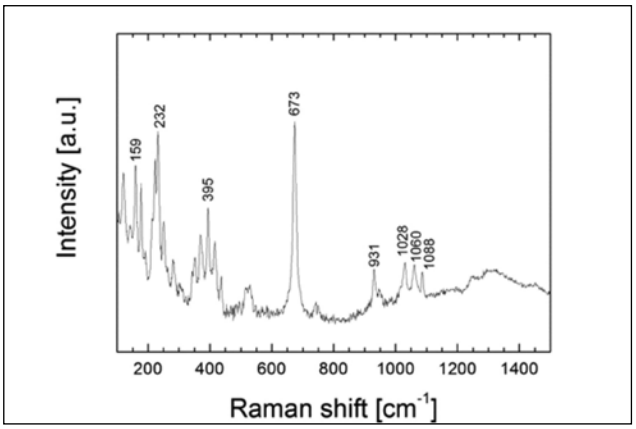

Fig. 5. Raman spectrum of tremolite from Skomarje marble

to 25 mm long crystals. They can develop as separate crystals or form radial clusters with a diameter of up to 40 mm (Fig. 6).

Grossular

The honey-brown crystals of garnet mineral grossular (Fig. 7) occur in marble alongside to epidote, biotite and pyrite. Grossular is partially massive and without apparently developed crystal surfaces, or in separate crystals that do not exceed 1 mm in size (Fig. 8). On separate crystals, surfaces of rhombic dodecahedron can be determined (Fig. 9). The tiny crystals are transparent with high lustre.

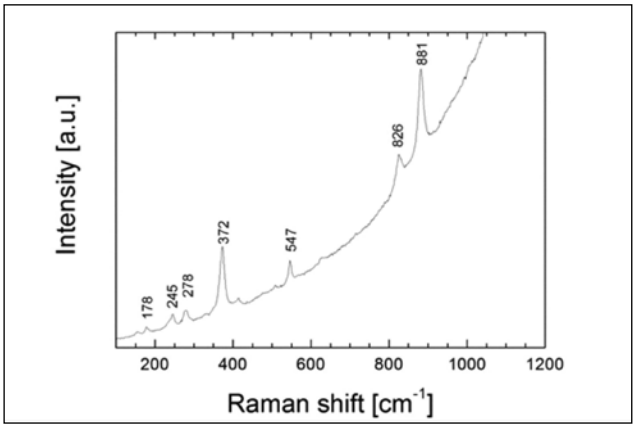

Fig. 7. Raman spectrum of grossular from Bojtina marble

Fig. 8. Honey-brown crystals of grossular from Bojtina marble measure up to 1 mm in diameter. Viljem Podgoršek's Collection

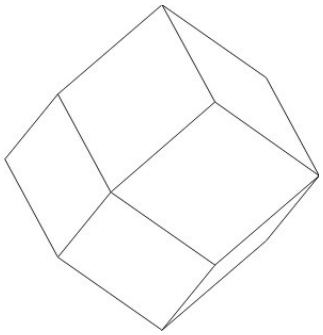

Fig. 9. The grossular in Bojtina marble has well-developed rhombic dodecahedron crystal faces (101).

Epidote

Epidote (Fig. 10) occurs in characteristic green, or less frequently in green-brownish crystals up to 15 mm in size. They are mostly translucent, less often transparent. The epidote crystals are explicitly prismatic, some have etched figures on crystal faces (Fig. 11).

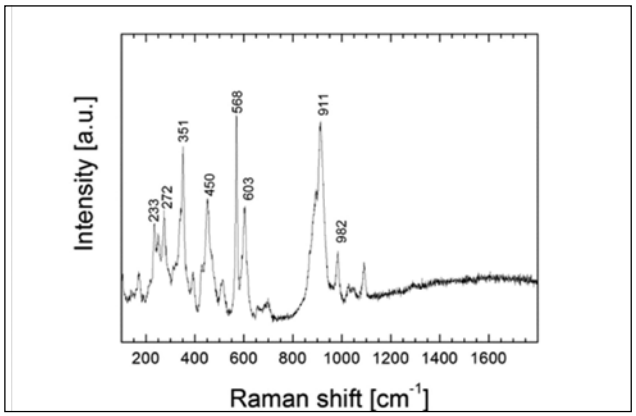

Fig. 10. Raman spectrum of epidote from Bojtina marble

Fig. 11. Epidote crystals in the Bojtina marble, 2.0 x 0.5 mm. Viljem Podgoršek's Collection

Vesuvianite

Vesuvianite crystals occur in hatches between calcite crystals. They are translucent to transparent and brown. The tiny up to a few mm long crystals are well-developed with crystal faces, where glassy lustre can be well seen. The crystals are medium to long prismatic (Figs 12 and 13) and have well-developed crystal faces of tetragonal prism of first (110) and second order (100), tetragonal pyramid of second order (1.0.14.), and basal pinacoid (001).

According to the crystalogenetic trend of vesuvianite (Kostov & Kostov, 1999), the vesuvianite prismatic crystals from Pohorje marbles indicate that they crystallised under lower temperature.

Fig. 12. The prismatic vesuvianite crystal (height of the crystal is 3 mm) in a hatch with calcite crystals in the Bojtina marble. Viljem Podgoršek's Collection

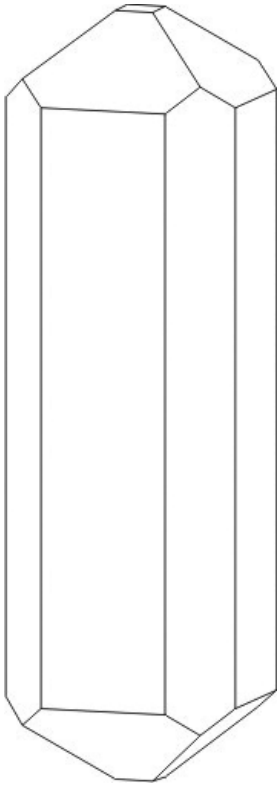

Fig. 13. Long prismatic crystal of vesuvianite from Bojtina with well-developed crystal faces of tetragonal prism of first and second order, tetragonal bipyramid of second order, and basal pinacoid.

Magnetite

Magnetite occurs in tiny up to 2 mm large crystals, together with colourless calcite crystals, sometimes as inclusions in them. They are opaque, grey and almost black with almost metallic lustre (Fig. 14). Some individual crystals have attractively developed octahedron crystal faces (Fig. 15), while the great majority of crystals are granular and of fairly irregular shapes.

Fig. 14. Tiny up to 1 mm large magnetite crystals rarely occur in crystals with well-developed crystal faces from Bojtina marble. Viljem Podgoršek's Collection

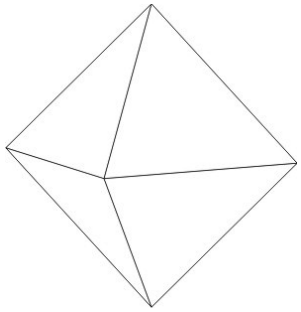

Fig. 15. Individual magnetite crystals from Bojtina have well-developed crystal faces of an octahedron (111).

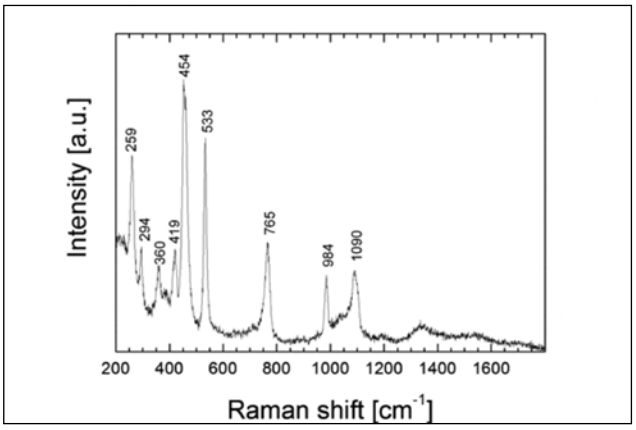

Fig. 16. Raman spectrum of scapolite from Bojtina marble

Fig. 17. Scapolite in the Bojtina marble is in white opaque crystals, the length of which does not exceed 25 mm. Viljem Podgoršek's Collection

Scapolite

Scapolite (Fig. 16) is a group of solid solution minerals with end members meionite $Ca_4Al_6Si_6O_{24}CO_3$ and marialite $Na_4Al_3Si_9O_{24}Cl$. In Pohorje marbles, scapolite occurs in white transparent, seemingly opaque crystals up to 30 mm in size (Fig. 17). The crystals are relatively rare, cracked and distinctly prismatic.

Quartz

Quartz is massive and white in the form of few tens of cm lenses in a marble. Rarely, crystals of quartz are developed in well formed colourless crystals (Fig. 18). They are mostly up to 1 cm high. The largest crystal discovered is 2 cm in length. Crystal morphology of quartz exhibits also left crystal forms (Fig. 19). Such crystals are twinned as left Douphhiné twin. Crystals have sometimes inclusions of tiny needle-like inclusions of amphibole (Fig. 20).

Fig. 18. Quartz crystal (15 mm high) with inclusion of a needle-like amphibole from Bojtina marble. Franc Golob's Collection

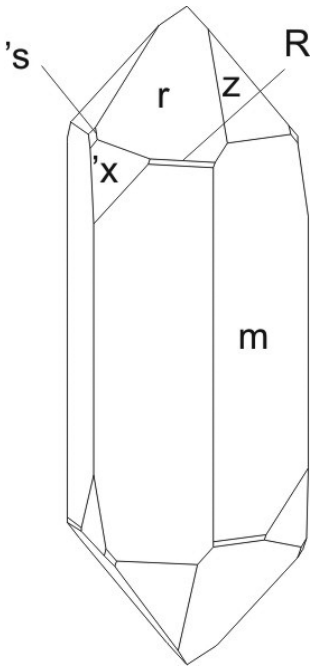

Fig. 19. Quartz crystals from Bojtina have well developed crystal faces of hexagonal prism of 1st order **m** (100), rhombohedron of 1st order **r** (101), negative rhombohedron of 1st order **z** (011), step rhombohedron **R** (≈20.0.1.), trigonal bipyramid of 2nd order **'s** (-121) and trapezohedron **z** (-561).

Pyrite

Pyrite occurs in limonitised crystals up to 5 mm in size. Smaller crystals, up to 1 mm, have well-developed crystal forms of cube and octahedron (Fig. 20). Such crystals can be found among quartz crystals (Fig. 21).

Fig. 20. Limonitised pyrite crystal among two quartz crystals with inclusion of a needle-like amphibole from Bojtina marble (5 x 4 mm). Franc Golob's Collection

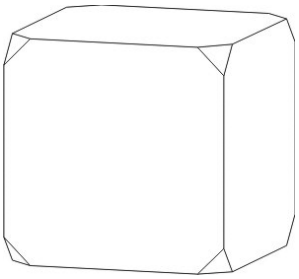

Fig. 21. Pyrite crystal with crystal faces of cube and octahedron. (Bojtina)

Other minerals

In Pohorje marbles, some other minerals were identified as well. Thus, flakes of mica can also be found, which are brownish and totally transparent (biotite group) or colourless and transparent, too (muscovite). Crystals of chlorite group minerals are green and up to 1 mm in size (Fig. 22). Titanite

Fig. 22. Bojtina minerals from chlorite group are overgrown with calcite rhombohedrons. Viljem Podgoršek's Collection

Fig. 23. Bojtina titanite crystal with crystal forms [001] and [111], 2 mm. Franc Golob's Collection.

is a yellow-coloured and wedge-shaped crystal up to 3 mm in size (Fig. 23). Amongst feldspars, plagioclases and orthoclase were determined. Graphite crystals are found only in two samples; one from Čadram and the second from Bojtina.

Based on the morphological features, Raman microspectroscopy and SEM/EDS analyses (Tab. 2), it was possible to confirm the presence of 17 different minerals or group of minerals, i.e. calcite, quartz, tremolite, grossular, vesuvianite, epidote, diopside, scapolite group, micas (muscovite and biotite group), feldspars (orthoclase and plagioclase), titanite, chlorite group, magnetite, pyrite and graphite. For the first time, vesuvianite and scapolite were observed in Pohorje Mts., whereas other minerals have already been determined also

Table 1. Identified minerals of marbles with their localities and analytical method used Legend: □ Raman microspectroscopy; ● SEM/EDS; ◊ morphology

MINERAL/ LOCALITY	Bojtina	Skomarje	Gorenja vas	Planica	Frajhajm	Čadram
Calcite	◊	◊	◊	◊ □	◊	
Tremolite	◊ □	□●	◊ □	□		
Grossular	◊ □ ●					
Vesuvianite	◊ □ ●					
Epidote	◊ □ ●				□ ◊	
Diopside	◊ □ ●	◊			□ ●	
Scapolite	◊ □ ●					
Magnetite	◊ □					
Quartz	◊					
Biotite	◊	◊	◊			
Muscovite	◊ □					
Clinochlor	◊ □ ●	●	□			
Titanite	◊ □					
Pyrite	◊	◊	◊ ●			
Orthoclase	□					
Plagioclase	□					
Graphite	□					□

by microscopical investigations (e.g. Hinterlechner-Ravnik, 1971, 1973; Mioč, 1978, 1983; Jarc & Zupančič, 2009). Both vesuvianite and scapolite are common minerals in metamorphic rocks.

All of the identified minerals could be found in marbles (Bucher & Frey, 2002; Best, 2007; Internet). Sedimentary carbonate rocks consist predominantly of carbonate minerals, but the rocks often contain variable amounts of quartz (Bucher & Frey, 2002). During metamorphism of these rocks, chemical reactions in the $CaO - MgO - SiO_2$ system are thus very common indeed and, besides calcite, dolomite and quartz, the formation of non-carbonate minerals such as talc, tremolite, diopside, forsterite, antigorite, periclase, brucite and wollastonite (Bucher & Frey, 2002) occur. Depending on the P-T conditions of metamorphism, the mineral assemblages of the above-mentioned minerals are stable and, in fact, the presence or absence of some mineral defines the conditions. The carbonate protolith usually contains some shaly material (Best, 2007), which is also the source for Fe, Mg and other components. Thus, the final mineral composition is mainly dependent of the chemistry of the source material. In Pohorje marbles, beside carbonates and quartz, tremolite and diopside are very common minerals. These mineral assemblages are typical in regional metamorphism of limestones and dolomites and also in contact metamorphism of the carbonates (Bucher & Frey, 2002). Also, other present minerals, such as garnets, vesuvianite and scapolite, could be the products of regional or contact metamorphism (Internet). Given that the minerals have been determined only by morphological feature, Raman microspectroscopy and SEM/EDS, the type of metamorphism could not be established.

Minerals, such as epidote, clinochlor, are typical products of retrograde metamorphism, which has been already established in Pohorje metamorphic rocks (Hinterlechner-Ravnik, 1971).

Therefore, numerous present non-carbonate minerals of Pohorje marbles are the result of the very complex polimetamorphic history of the Pohorje rocks with a combination of progressive and retrograde metamorphisms as interpreted by Hinterlechner-Ravnik (1971, 1973).

Table 2. Average (of two measurements) elementary compositions (wt%) of selected mineral samples from Bojtina marble, determined with EDS

O	Na	Mg	Al	Si	Cl	Ca	Fe	K	Mineral
70,83	-	2,46	6,34	15,63	1,50	1,68	1,55	-	clinochlor
63,81	-	11,01	-	20,71	-	4,47	-	-	tremolite
61,39	-	-	11,55	14,49	-	9,94	2,62	-	epidote
66,84	-	6,50	1,24	17,34	-	7,32	1,37	-	diopside
73,79	-	0,82	5,75	10,84	-	8,21	0,59	-	vesuvianite
66,90	1,88	0,73	10,33	16,40	-	4,14	-	1,69	scapolite
64,25	-	-	7,87	14,03	-	11,98	1,86	-	grossular

Conclusions

The marbles from Pohorje Mts contain numerous minerals, which could be easily seen by the naked eye. They are not very common and sometimes it is hard to see them owing to their rarity and size. Nevertheless, we managed to find, collect and study them.

Morphological features of the minerals from 25 samples were determined by 10x magnifying loupe and binocular microscope. Besides carbonate minerals (calcite), numerous silicate minerals, oxides and sulphides with graphite have been observed. A total of 17 minerals or mineral groups were identified based on the morphology observation, Raman microspectroscopy and SEM/EDS analyses. Thus the presence of calcite, quartz, tremolite, grossular, vesuvianite, epidote, diopside, scapolite group, micas (muscovite and biotite group), feldspars (potassium feldspar and plagioclase), titanite and chlorite group among silicate minerals, and magnetite, pyrite and graphite was confirmed. The calcite crystals are up to 1 cm long, quartz crystals up to 2 cm and tremolite crystals are up to 25 mm long and could form radial clusters with a diameter of up to 40 mm and epidote crystals are up to 15 mm. The biggest found minerals with clear morphological features belong to diopside (50 mm) and scapolite group. Although scapolite crystals are relatively rare, they are up to 30 mm long. The sizes of the other accessory minerals do not exceed few mm. Quartz crystals with many well developed crystal faces and inclusions of a needle- like amphibole have also been found. For the first time, vesuvianite and scapolite were observed in Pohorje Mts.

The mineral assemblages are not significant for the specific locality. Therefore, the examined mineral sites could not have been distinguished only by the presence or absence of the specified minerals.

The mineral assemblage of Pohorje marble is typical of the marble metamorphosed from carbonate rich protolith (calcite was prevailing), but with variable amounts of quartz and other shaly materials. The Pohorje marbles are predominantly calcitic, with some dolomite present as well as with some silicate minerals such as quartz, tremolite, diopside, which are typical mineral assemblages for regional metamorphosis of limestones and dolomites, and also for contact metamorphosis of carbonate rocks (Bucher & Frey, 2002). Therefore, the type and grade of metamorphosis could not have been determined from minerals determined by morphological investigations, Raman microspectroscopy and SEM/EDS analyses. The determined mineral assemblage from Pohorje marbles clearly indicates a very complex history of this area.

References

Best, M. G. 2007: Igneous and metamorphic petrology. Second Edition, Blackwell Publishing: 729 p.

Bucher, K. & Frey, M. 2002: Petrogenesis of metamorphic rocks. Seventh Edition, Springer, Berlin: 341 p.

Capedri, S., Venturelli, G. & Photiades, A. 2004: Accessory minerals and $\delta^{18}O$ and $\delta^{13}C$ of marbles from the Mediterranean area. Journal of Cultural Heritage, 5/1: 27–47, doi;10.1016/j.culher.2003.03.003.

Cornell, D., Janák, M., Froitzheim, N., Broska, I., Vrabec, M. & De Hoog, J.C.M. 2007: Ion microprobe U-Pb zircon dating of gneiss from the Pohorje, Eastern Alps and implications for deep subduction of a coherent continetal crust. In Abstract volume, 8th Workshop on Alpine Geological Studies, Davos, 10–12 October 2007: 15–16.

Dolar Mantuani, L. 1935: Tonalite and aplite ratio of Pohorje massiv. Geološki Anali Balkanskog Poluostrova, 12: 1–165.

Faninger, E. 1970: The tonalite of Pohorje and its differentiates. Geologija, 13: 35–104.

Fodor, L., Jelen, B., Márton, E., Zupančič, N., Trajanova, M., Rifelj, H., Pécskay, Z., Balogh, K., Koroknai, B., Dunkl, I., Horváth, P., Horvat, A., Vrabec, M., Kraljič, M. & Kevrič, R. 2002: Connection of Neogene basin formation, magmatism and cooling of metamorphics in NE Slovenia. Geologica Carpathica, 53 (special issue): 199–201.

Fodor, L., Balogh, K., Dunkl, I., Pécskay, Z., Koroknai, B., Trajanova, M., Vrabec, M., Vrabec, M., Horváth, P., Janák, M., Lupták, B., Frisch, W., Jelen, B. & Rifelj, H. 2003: Structural evolution and exhumation of the Pohorje-Kozjak Mts., Slovenia. Annales Universitatis Scientiarum Budapestinensis, Sectio Geologica, 35: 118–119.

Fodor, L., Gerdes, A., Dunkl, I., Koroknai, B., Pécskay, Z., Trajanova, M., Horváth, P., Vrabec, M., Jelen, B., Balogh, K. & Frisch, W. 2008: Miocene emplacement and rapid cooling of the Pohorje pluton at the Alpine-Pannonian-Dinaric juction, Slovenia. Swiss Journal of Geoscience, 101/1: 255–271, doi 10.1007/s00015-008-1286-9.

Frank, W. 1987: Evolution of the Austroalpine elements in the Cretaceous. In: Flügel, H.W. & Faupel, P. (eds.): Geodynamics of the Eastern Alps. Vienna: Deuticke: 379–406.

Germovšek, C. 1954: Petrographic research of Pohorje in 1952. Geologija, 2: 191–210.

Hinterlechner-Ravnik, A. 1971: Metamorphic rocks of Pohorje mountains. Geologija, 14: 187–226.

Hinterlechner-Ravnik, A. 1973: Metamorphic rocks of the Pohorje mountains II. Geologija, 16: 245–269.

Hinterlechner-Ravnik, A. & Moine, B. 1977: Geochemical characteristics of the metamorphic rocks of the Pohorje Mountains. Geologija, 20: 107–140.

Janák, M., Froitzheim, N., Vrabec, M. & Krogh Ravna, E.J. 2004. First evidence for ultrahigh-pressure metamorphism of eclogites in Pohorje, Slovenia: Tracing deep continental subduction in the Eastern Alps. Tectonics, 23/5, doi:10.1029/2004TC001641.

Janák, M., Froitzheim, N., Vrabec, M., Krogh Ravna, E.J & De Hoog, J.C.M. 2006: Ultrahigh-pressure metamorphism and exhumation of garnet peridotite in Pohorje, Eastern Alps. J. metamorphic Geol., 24: 19–31, doi:10.1111/j.1525-1314.2005.00619.x.

Jarc, S. & Zupančič, N. 2009: A cathodoluminescence and petrographical study of marbles from the Pohorje area in Slovenia. Chem. Erde, 69: 75–80, doi:10.1016/j.chemer.2008.01.001.

Lazzarini, L., Moschini, G. & Stievano, B. M. 1980: A contribution to identification of Italian, Greek and Anatolian marbles through a petrological study and the evaluation of Ca/Sr ratio. Archaeometry, 22/2:173–183.

Kostov, I. & Kostov, R.I. 1999: Crystak habits of mineral, Prof. Marin Drinov Academic Publishing House & Pensoft Publishers, Sofia: 415 p.

Miller, C., Mundil, R., Thöni, M. & Konzett, J. 2005: Refining the timing of eclogite metamorphism: a geochemical, petrological, Sm-Nd and U-Pb case study from the Pohorje Mountains, Slovenia (Eastern Alps). Contrib. Mineral. Petrol, 150: 70–84, doi:10.1007/s00410-005-0004-0.

Mioč, P. 1978: Osnovna geološka karta SFRJ 1:100,000. Tolmač za list Slovenj Gradec (L 33–55). Zvezni geološki zavod, Beograd: 74 p (in Slovenian with English summary).

Mioč, P. 1983: Osnovna geološka karta SFRJ 1:100,000. Tolmač za list Ravne na Koroškem (L 33–54). Zvezni geološki zavod, Beograd: 69 p.

Mioč, P. & Žnidarčič, M. 1977: Osnovna geološka karta SFRJ 1:100,000, list Slovenj Gradec (L 33–55). Zvezni geološki zavod, Beograd (in Slovenian).

Mioč, P. & Žnidarčič, M. 1983: Geološka karta 1:25.000, Vitanje, Vuzenica, Slovenska Bistrica, Ribnica na Pohorju, Oplotnica, Mislinja, Slovenj Gradec. Manuscript maps. Archive of the Geological Survey of Slovenia, Ljubljana (in Slovenian).

Mioč, P. & Žnidarčič, M. 1989: Osnovna geološka karta SFRJ 1:100,000. Tolmač za list Maribor in Leibnitz. Zvezni geološki zavod, Beograd: 60 p.

Nasdala, L., Smith, D.C., Kaindl, R. & Ziemann, M.A. 2004: Raman spectroscopy: Analythical perspectives in mineralogical research. In: Beran, A. & Libowitzky, E. (eds.): Spectroscopic Methods in Mineralogy, EMU Notes in Mineralogy, 6/7: 281-343.

Origlia, F., Gliozzo, E., Meccheri, M., Spangenberg, J.E., Memmi, I.T. & Papi, E. 2011: Minerlaogical, petrographic and geochemical characterization of White and Coloured Iberian marbles in the context of the provenancing of some artefacts from Thamusida (Kenitra, Marocco). European Journal for Minerlaogy, 23: 857-69.

Placer, L. 2008: Principles of the tectonic subdivision of Slovenia. Geologija, 51/2: 205–217, doi:10.5474/geologija.2008.021.

Schmid, S.M., Fügenschuh, E., Kissling, E. & Schuster, R. 2004: Tectonic map and overall architecture of the Alpine orogen. Eclogae Geol. Helv., 97/1: 93–117, doi 10.1007/S00015-004-1113-X.

Taelman, D., Elburg, M., Smet, I., De Paepe, P., Vanhaecke, F. & Vermeulen, F. 2012: White, veined marble form Roman Ammaia (Portugal): Provenance and use, Archaeometry, 55/3: 370-390, doi: 10.1111/j.1475-4754.2012.00691.x

Thöni, M. 2002: Sm-Nd isotope systematics in garnet from differ-ent lithologies (Eastern Alps): age results, and an evaluation of potential problems for garnet Sm-Nd chronometry. Chem. Geol., 185/3-4: 255–281, doi:10.1016/S0009-2541(01)00410-7.

Trajanova, M., Pécskay, Z. & Itaya, T. 2008: K-Ar geochronology and petrography of the Miocene Pohorje Mountains batholith (Slovenia). Geologica Carpathica, 59: 247–260

Vrabec, M. 2010: Garnet peridotites from Pohorje: petrography, geothermobarometry and metamorphic evolution. Geologija, 53/1: 21–36, doi:10.5474/geologija.2010.002.

Zupančič, N. 1994a: Petrographical characteristics and classifica-tion of magmatic rocks of Pohorje. Rudarsko-metalurški zbornik, 41: 101–112

Zupančič, N. 1994b: Geochemical characteristics and origin of magmatic rocks of Pohorje. Rudarsko-metalurški zbornik, 41: 113–128.

Žnidarčič, M. & Mioč, P. 1988: Osnovna geološka karta SFRJ 1:100,000, list Maribor in Leibnitz (L 33–56, L 33–44). Zvezni geološki zavod, Beograd).

Internet: http://www.mindat.org/ (28.3.2013)

GEOLOGIJA *56/1*, 057–072, Ljubljana 2013

doi:10.5474/geologija.2013.005

Opuščeni rudnik Remšnik z ramsbeckitom in namuwitom(?)

Abandoned Remšnik mine with ramsbeckite and namuwite(?)

Mirka TRAJANOVA[1] & Zmago ŽORŽ[2]

[1]Geološki zavod Slovenije, Dimičeva ulica 14, SI-1000 Ljubljana, e-mail: mirka.trajanova@geo-zs.si
[2]Pod Perkolico 52, 2360 Radlje ob Dravi, e-mail: zmago.zorz@gmail.com

Prejeto / Received 17. 4. 2013; Sprejeto / Accepted 8. 5. 2013

Ključne besede: ramsbeckit, namuwit, bakrovi, cinkovi in svinčevi sekundarni minerali, Remšnik, Kobansko, severna Slovenija

Key-words: ramsbeckite, namuwite, secondary minerals of copper, zinc and lead, Remšnik, Kobansko, north Slovenia

Izvleček

Polimetalno rudišče Remšnik se nahaja na Kobanskem v severni Sloveniji. Mineralizacija nastopa v narivni coni med staropaleozojskimi nizkometamorfnimi kamninami Štalenskogorske formacije, Remšniškega pokrova in retrogradno metamorfnih skrilavcev Avstroalpinske podlage. Hidrotermalno orudenje in okremenitev sledita skrilavemu klivažu v delno brečiranih lečah dolomitnih marmorjev ter podrejeno metatufitov in filitov. Najverjetneje je nastalo v povezavi z živahnim terciarnim magmatizmom, ki je ugotovljen in razkrit na območju današnjega Pohorja. Mineralno paragenezo prevladujočega Pb, Cu, Zn srebronosnega sulfidnega orudenja spremlja pestra združba sekundarnih mineralov. Med njimi se nahajata pri nas prvič opisana redka vodna sulfata bakra in cinka. Zelene, prosojne monoklinske kristale, velikosti le nekaj desetink milimetra, smo z vrstičnim elektronskim mikroskopom določili kot ramsbeckit (Cu, Zn)$_{15}$(SO$_4$)$_4$(OH)$_{22}$ · 6(H$_2$O). Zelenkaste barve so tudi lističasti, po obliki heksagonalni, cvetasti kristalni zraščenci, ki najverjetneje pripadajo namuwitu (Cu, Zn)$_4$(SO$_4$)(OH)$_6$ · 4(H$_2$O). Zaradi submikroskopske velikosti in majhne količine njegova določitev še ni zanesljiva.

Abstract

The polymetallic Remšnik ore deposit is situated at the Kobansko area in northern Slovenia. Mineralization occurs in the thrust zone of the weakly metamorphosed old Palaeozoic rocks of the Magdalensberg formation, the Remšnik nappe, onto the retrogressed schists of the Austroalpine metamorphic basement. Hydrothermal ore mineralization and silicification follow slaty cleavage in partly brecciated marmorized dolomite lenses and subordinately in metatuffites and phyllites. Its origin is most probably connected to the lively Tertiary magmatism, occurring at the Pohorje Mountains. Mineral paragenesis of the predominant Pb, Cu and Zn silver bearing sulphide ore is associated with numerous secondary minerals. Among them, two rare sulphates with H$_2$O of Cu and Zn occur, found for the first time in Slovenia. The green, transparent monoclinic crystals, only some tenth of millimetre in size were determined by SEM as ramsbeckite (Cu, Zn)$_{15}$(SO$_4$)$_4$(OH)$_{22}$ · 6(H$_2$O). Greenish in colour are also leafy, hexagonal, flowery intergrown crystals, which most probably belong to namuwite (Cu, Zn)$_4$(SO$_4$)(OH)$_6$ · 4(H$_2$O). Its submicroscopic size and small quantity did not permit reliable determination, yet.

Uvod

Dosedanje raziskave Avstroalpinika pri nas so bile usmerjene predvsem na območje Pohorja, medtem ko so bili ostali deli vključeni v manjšem obsegu. Podrobno proučevanje mineralnih surovin in mineralogije je bilo pogosto postavljeno v ozadje. Zbiralski vnemi ljubiteljev mineralov se moramo zahvaliti, da se pri nas tudi na področju odkrivanja mineralov stvari premikajo naprej.

Čeprav je rudišče Remšnik znano že dolgo časa, spoznavanje njegove mineralne združbe še ni zaključeno. Za sledenje rudnih pojavov in s tem rudišč so pogosto prvi indikatorji sekundarni minerali, ki se pojavljajo v oksidacijskih conah. Navadno najdemo le neznatne količine teh mineralov, vendar nam lahko kažejo, kaj se nahaja v njihovi okolici. Najdba ramsbeckita v remšniškem rudišču je zato pomembna tako z mineraloškega vidika, kot tudi z vidika sledenja sorodnih pojavov rudne mineralizacije na drugih območjih.

Remšnik danes kot rudno nahajališče ni več zanimiv, kljub temu pa predstavlja na širšem območju za strukturne geologe edini vpogled v tretjo dimenzijo, predvsem pa »Meko« za zbiralce redkih mineralov. Le-ti se radi pošalijo, da jih je Bog kaznoval z množico modrih in zelenih mineralov. Zato ni čudno, da tudi predstavljena najdba ramsbeckita pripada zelenim kristalčkom. Vendar pa so se že makroskopsko, še posebno pa pod lupo, razlikovali od do sedaj

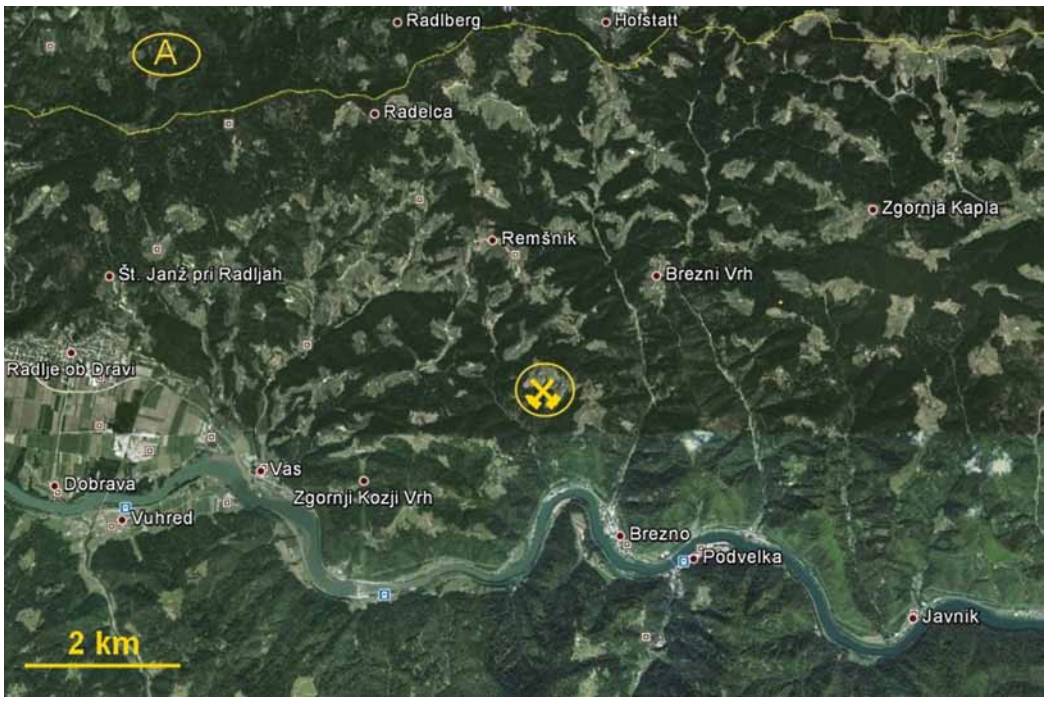

Sl. 1. Položaj vasi Remšnik in opuščenega Janičkovega rova. Izsek iz Google Earth.

Fig. 1. Location of the Remšnik village and the abandoned Remšnik mine (Janiček pit). Cut out from Google Earth.

znanih v remšniškem rudišču. Njihova določitev je predstavljala osnovo za pričujoče raziskave.

Ramsbeckit so do sedaj, razen v matičnem nahajališču pri Ramsbecku in še nekaterih mestih v Nemčiji, našli v kar nekaj rudnikih po svetu: npr. v Italiji, prvič v rudniku »La Venezia« v limonitizirani jalovini (Orlandi & Perchiazzi,1989), o najdišču poročajo iz rudnikov Ecton v Pennsylvaniji (Peacor et al, 1987), Penrhiw (Mason & Green, 1995) in drugih iz Velike Britanije, z Japonske (Ohnishi et al, 2004) i.t.d. Po sedaj znanih podatkih so ga našli v enajstih državah na različnih lokacijah. Na mnogih mestih verjetno še čaka naključnega najditelja, saj ga pred tem dobro varuje obilica drugih zelenkastih mineralov in mikroskopska velikost kristalov.

Geografski položaj

Vzporedno s Pohorjem poteka na severni strani Dravske doline hribovje, ki ga uvrščamo med sredogorja. Ker nima enotnega pogorja, so ga v preteklosti večkrat neuspešno poskušali poimenovati enotno. V nekaterih atlasih je vpisano ime Kobansko, v drugih Kozjak. V osrednjem delu tega območja se v povirju levih pritokov reke Drave (Brezniškega, Štimpaškega in Vaškega potoka) nahaja raztreseno naselje Remšnik. Na zahodnem pobočju jugo-jugovzhodno potekajočega remšniškega hrbta, se južno od naselja nahaja opuščen rudnik Remšnik (sl. 1).

Od rudarskih objektov je najdostopnejši Janičkov rov, ki je označen na sliki 1. Območje je dokaj zaraščeno, zato ga prišlekom ni lahko najti.

Nekaj podatkov o rudišču

Rudišče Remšnik je pritegnilo pozornost raziskovalcev in rudarjev že pred več kot 250 leti. V arhivskih virih (Arhiv R Slovenije) najdemo, da je baron Michelangelo Zois leta 1763 odprl rudnik in zgradil topilnico na Breznu, kar pomeni, da je bilo rudišče gotovo odkrito že prej, čeprav pisnih virov o tem nismo zasledili. Koncesija za odprtje rudnika je bila podeljena na podlagi fevdnega pisma z dne 14. junija 1850 pod št. 1937. Glasila se je na ime »Drauwalder silberhältiger Blei, Kupfer und Zink Bergbau« (srebronosni svinčev, bakrov in cinkov rudnik Dravski gozd). Prvi lastniki rudnika so bili Jakob Krušnik, Karl Kranz in Johan Baumgartner. Izdelana sta bila dva rova, ki so ju poimenovali Marija in Franz, oz. tako imenovan Zwilling Stollen (dvojčični rov). V tem času so nakopano rudo talili v Ožbaltu ob Dravi. Po podatkih graške trgovinske zbornice so leta 1853 pridobili 74,658 kg srebra, tri leta kasneje le še okoli 50 kg. Oktobra 1887 je postal lastnik Karel Wehrkan iz Litije in ga že leta 1888 prodal Litijski rudarski družbi. Ta je prenehala z odkopavanjem rude na Remšniku 22. decembra 1891. V tem času so izkopali rov pod kmetijo Dijak in ga poimenovali Janičkov rov, rudnik pa »Fressen Bergbau«. Do druge svetovne vojne se je zamenjalo še nekaj lastnikov, dokler rudnik 1946. leta ni bil nacionaliziran. Po tem obdobju so ga obiskovali le geologi in zbiralci mineralov.

V remšniškem rudniku so namesto lesenega podporja uporabljali jalovinski material, s katerim so podzidali in podpirali rove in stene večjih odkopnih mest. Prav zato je Janičkov rov, kljub temu, da je le 3 do 5 m pod površjem, v sprednjem delu še danes dostopen, v zadnjem delu pa zarušen.

Po dosedanjih podatkih se orudenje v Remšniku nahaja v staropaleozojskih nizkometamorfnih kamninah Štalenskogorske formacije. Nastopa v obliki leč v območju metatufitov in dolomitnih marmorjev ter filitov (Drovenik et al, 1980). Najstarejši nam znani članek o rudišču predstavlja objava Tornqui-

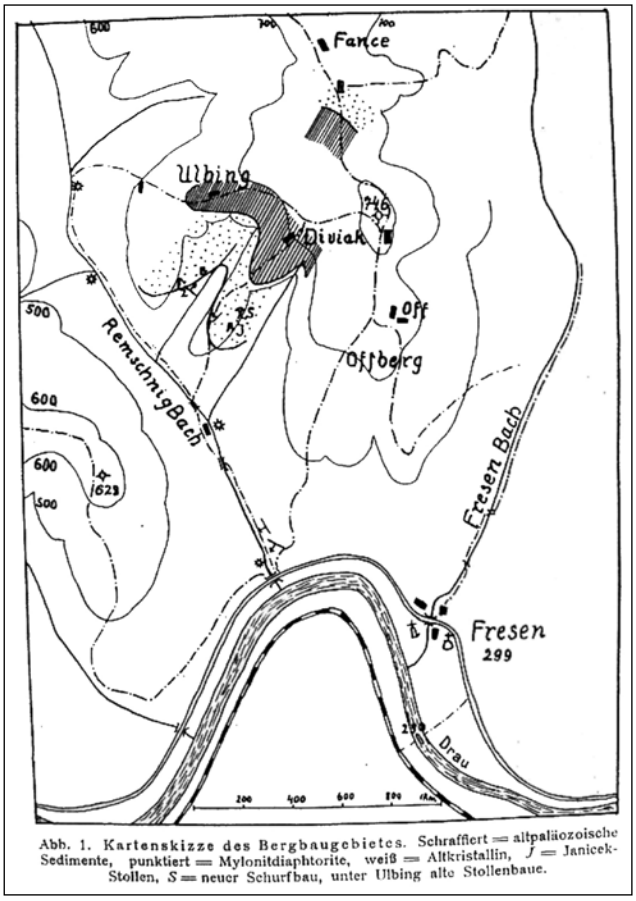

Abb. 1. Kartenskizze des Bergbaugebietes. Schraffiert = altpaläozoische Sedimente, punktiert = Mylonitdiaphtorite, weiß = Altkristallin, J = Janicek-Stollen, S = neuer Schurfbau, unter Ulbing alte Stollenbaue.

Sl. 2. Tornquistova geološka skica z označenima rovoma Janiček in Ulbing pod narivnim stikom staropaleozojskih kamnin z retrogradno spremenjenimi in milonitiziranimi kamninami. Reproducirana slika 1 (iz: Tornquist, 1929).

Fig. 2. Tornquist geological sketch with marked Janiček and Ulbing pits under the thrust contact of old-Paleozoic rocks with retrogressed and mylonitized rocks. Reproduced Figure 1 (From: Tornquist 1929).

sta (1929), kjer omenja rudarska dela pod kmetijo Ulbing. Avtor je v svoji objavi na sliki 1 označil dva rudniška rova (Janičkov in Ulbing) pod narivnim stikom staropaleozojskih kamnin (nem. altpaläozoische Sedimente) z retrogradno spremenjenimi in milonitiziranimi kamninami (nem. Mylonitdiaphtorite), ki je prikazana na sliki 2. Na manuskriptni geološki karti odkopa pod kmetijo Dijak iz arhiva rudnika Mežica (Poročila geološke službe rudnika Mežica, 1984-1989) uvrstitev kamnin med milonite ali prave filite ni opredeljena. Znana je le uvrstitev krovnih kamnin v Štalenskogorsko formacijo, ki sta jim Mioč in Ramovš (1973) na tem območju določila spodnjedevonsko starost. Zato še vedno obstaja dvom, na katero formacijo (če je samo ena) je pravzaprav vezana mineralizacija.

O genezi rudišča so mnenja deljena. Orudenje nekateri povezujejo s pohorskim (Tornquist, 1929; Duhovnik, 1956; Berce, 1963, Grafenauer, 1965), drugi pa s paleozojskim magmatizmom (Hegemann, 1960; Drovenik et al, 1980).

Polimetalno rudišče Remšnik se ponaša z raznolikostjo mineralov, ki ji kar ni videti konca. Mineralno paragenezo sestavljajo številni rudni in jalovinski minerali, katerih skupno število že presega 55. Od rudnih mineralov so bili do sedaj določeni: galenit, sfalerit, pirit in halkopirit kot prevladujoči, podrejeno pa kuprit, tetraedrit, boulangerit, bornit, halkozin, covellin, freibergit, gersdorffit, akantit in polibazit. Drovenik (1980) in Grafenauer (1966) še nista našla polibazita in akantita, zato je Drovenik domneval, da je srebro (in bizmut) vgrajen v strukturi galenita in halkopirita. Posredno namiguje, da bi bila za visoko vsebnost srebra v galenitu lahko kriva tudi neustrezna analitska metoda.

Glavni jalovinski minerali v rudi so kremen, dolomit s povišano vsebnostjo železa in podrejeno kalcit in aragonit. Posebno pestrost pa predstavljajo sekundarni minerali, ki so nastali v oksidacijski coni remšniškega rudišča. Naj naštejemo le nekatere: kuprit, tenorit, hematit, goethit, manganovi oksidi in hidroksidi, malahit, azurit, smithsonit, cerusit, hidrocinkit, brianyoungit, rosasit, aurikalcit, barit, sadra, linarit, langit, baverit, posnjakit in karbonatni cianotrihit, aragonit, piromorfit in krizokola (chrysocolla).

Nekaj pogostejših mineralov Kobanskega (predvsem kristale kremena) so prikazali Žorž in sodelavci (2007).

Material in metode preiskav

Prikazani rezultati temeljijo tako na terenskih opazovanjih, kot tudi laboratorijskih preiskavah. Vzorci so bili odvzeti ob orudeni žili iz Janičkovega rova. Pestrost sekundarnih mineralov, ki se nahajajo v razpokah, lahko vidimo pod stereolupo, vendar so premajhni za določitev. Količina najdenih vzorcev ni bila zadostna, niti pa primerna za izdelavo petrografskih preparatov in/ali obrusov, saj bi tanke prevleke z brušenjem izgubili. Izdelana je bila rentgenska difraktometrijska analiza na koščku vzorca z mikrokristalnim oprhom. Drobnih kristalčkov, ki smo jih želeli določiti, prav tako ni bilo mogoče izolirati za kemično analizo. Tako je od palete preiskovalnih metod, zaenkrat ostala le preiskava z vrstičnim elektronskim mikroskopom. Analize so izdelane s SEM znamke JEOL JSM 6490LV pri pospeševalni energiji 20 kV, na delovni razdalji 10 mm. Uporabljen je način BSE pri nizkem vakuumu, brez napraševanja. Osnovna semikvantitativna kemična sestava je določena z Oxford INCA EDS (compo način) pri enaki pospeševalni energiji.

Rezultati in diskusija

Na Osnovni geološki karti 1:100 000, list Slovenj Gradec (Mioč & Žnidarčič, 1977) je remšniško nahajališče označeno med Remšniškim pokrovom iz štalenskogorskih kamnin in talninsko Pohorsko formacijo iz retrogradno metamorfnih skrilavcev Avstroalpinske podlage. Med njima se nahaja tanek pas filitov. Določitev filitov na tem območju in vzhodno od tod je nekoliko sporna. Zaradi

večfaznih sekundarnih sprememb ni jasno, ali pripadajo pravim filitom ali pa milonitom, ki so nastali retrogradno iz dinamometamorfno spremenjenih kamnin Pohorske formacije (po Mioču, 1978 imenovane Kobanska serija). Nesporno je vanje vključenih tudi del štalenskogorskih kamnin, zajetih v narivno cono.

Tako makro-, kot tudi mikrotekstura kamnin nakazujejo več faz tektonskega delovanja, vključno z dvakrat reaktiviranim subhorizontalnim strižnim premikanjem, zaradi katerega so v vse kamnine vtisnjene dinamometamorfne spremembe. Prvo se odraža kot plastične deformacije z nastankom foliacije. Pri tem so bile kamnine intenzivno milonitizirane. Pri drugem pa je nastal skrilav klivaž, ki pretežno sledi foliaciji. Nastanek teh struktur je v širšem območju vzhodnega Avstroalpinika povezan z zgornjekrednim krovnim narivanjem in terciarnim vzhodno usmerjenim alpskim pobegom (npr. Fodor et al. 1998, 2002, 2008). Strukturni parametri širšega območja nakazujejo, da sta bila Pohorje in Kobansko/Kozjak ob vtiskanju granodioritne magme v spodnjem miocenu še enoten blok in sta se ločila šele pozneje.

Sl. 3. Razpoke in sekundarni klivaž nakazujejo delovanje desnega striga (rdeče puščice). Janičkov rov daje zavetje netopirjem. Opuščen rudnik Remšnik. Foto Z. Žorž.

Fig. 3. Fractures and secondary cleavage indicate dextral sense of shear (red arrows). The Janiček pit gives shelter to bats. Abandoned Remšnik mine. Photo Z. Žorž.

Stopnja dosedanjih raziskav ne dovoljuje enoznačne opredelitve geneze rudišča. Kljub temu pa se nakazujejo nekatere pomembne povezave, ki negirajo njegovo paleozojsko poreklo: sulfidna rudna mineralizacija in močna okremenitev, ki je prikrila teksturni značaj kamnin, sta sledili klivažu, ki je terciarnega (predvidoma miocenskega) nastanka; kobanski blok se je ločil od pohorskega verjetno v srednjem miocenu in je bil do tedaj bliže vplivnemu območju granodioritne intruzije; mineralna sestava in izotopska sestava žvepla v Remšniku in na Okoški gori na Pohorju sta sorodni (Drovenik et al. 1976, 1980). Na osnovi tega obstaja velika verjetnost, da je orudenje povezano z miocenskim pohorskim magmatizmom, kot so že domnevali Tornquist (1929), Duhovnik (1956), Berce (1963) in Grafenauer (1965). Še vedno pa ostaja vprašanje, ali je lahko povezano tudi z remobilizacijo starejše (kredne/paleozojske?) mineralizacije, saj naj bi po Droveniku in sodelavcih (1980) orudenje na Okoški gori nastalo v paleozoiku. To starost argumentirajo z blastično rastjo rudnih mineralov v času regionalne metamorfoze, kar pa ni zadosten razlog.

Prečno na foliacijo in skrilav klivaž potekajo mlajše poševne razpoke, nastale kot posledica obnovljenega strižnega premikanja. Oblikujejo sekundarne klivažne ravnine ter označujejo delovanje desnega striga (sl. 3). Te razpoke niso okremenjene in so brez primarne (sulfidne) mineralizacije. Vse

Sl. 4. Delno zarušen Janičkov rov. Vidne so subhorizontalne razpoke vzporedne starejšemu klivažu in strma prelomna površina (zgoraj). Levo spodaj je odlomljen blok brečiranega in nato še močno okremenjenega dolomita. Janičkov rov, opuščen rudnik Remšnik. Foto Z. Žorž.

Fig. 4. Partly collapsed Janiček pit. Subhorizontal fractures are parallel to the older cleavage. Steep fault surface (top of the figure) cut other structures. Fallen block of brecciated and subsequently strongly silicified dolomite can be seen at the bottom left. Abandoned Remšnik mine. Photo Z. Žorž.

Sl. 5. Modrikasti in zeleni oprhi sekundarnih mineralov na prečnih prelomnih površinah. Vzdolž klivaža po foliaciji se nahaja predvsem sulfidno svinčevo, cinkovo, bakrovo orudenje in okremenitev (sveži odlomi v sredini slike). Remšnik, Janičkov rov. Foto Z. Žorž.

Fig. 5. Bluish and green coatings of secondary minerals on transverse fault plains. Prevailingly sulphide copper zinc and lead ore mineralization and silicification occur along the cleavage parallel to foliation (fresh surfaces in the photo centre). Janiček pit, abandoned Remšnik mine. Photo Z. Žorž.

Sl. 6. Rjavi (na levi skoraj črni) do 1 mm veliki kristali beaverita na kremenu iz Janičkovega rova. Opuščen rudnik Remšnik. Najdba in zbirka Z. Žorž. Foto: B. Moser.

Fig. 6. Brown (nearly black on the left), up to 1 mm big crystals of beaverite on quartz from the Janiček pit. Abandoned Remšnik mine. Find and collection Z. Žorž, photo B. Moser.

Sl. 7. Modri rosasit ter brezbarvni in prozorni aragonitni ježki iz Janičkovega rova. Opuščen rudnik Remšnik. Velikost motiva 15 x 12 mm. Najdba, zbirka in foto Z. Žorž.

Fig. 7. Blue rosasite and colourless transparent aragonite needles from the Janiček pit. Abandoned Remšnik mine. Size of the motif 15 x 12 mm. Find, collection and photo Z. Žorž.

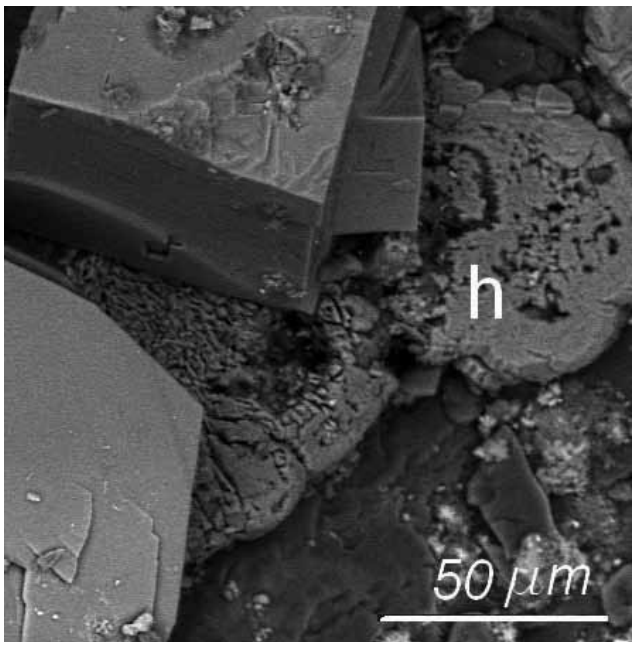

strukture sekajo genetsko najmlajši subvertikalni prelomi (sl. 4) prevladujoče smeri jugozahod-severovzhod, redkeje prečno nanje.

Razmere v Janičkovem rovu kažejo, da so orudene pretežno karbonatne leče ter delno širša porušena narivna cona, v kateri so zajete tako kamnine Štalenskogorske, kot tudi Pohorske formacije. Primarna rudna mineralizacija in okremenitev sta sledili razpoklinski poroznosti starejšega skrilavega klivaža, ki makroskopsko sovpada s foliacijo, medtem ko v dveh generacijah prečnih razpok in prelomov najdemo v glavnem sekundarno mineralizacijo (sl. 5). Brečirane kamnine so prepojene s kremenico, zato so na videz masivne.

Večino redkih sekundarnih mineralov je na Remšniku našel Z. Žorž in določil skupaj z Moserjem (Žorž & Moser, 2002). Med njimi je posebno zanimiv beaverit, svinčev-bakrov-železov-aluminijev sulfat. Po dosegljivih podatkih je bil ta mineral do najdbe Z. Žorža poznan le kot rumen oprh, tu pa se nahajajo milimetrski, karamelno rjavi, prozorni do prosojni kristali (sl. 6). Nastopa kot prevleke na kremenu.

Med karbonati je zelo slikovita parageneza rosasita in aragonita na nekoliko limonitizirani kremenovi podlagi (sl. 7).

V osnovi nekaterih sekundarnih mineralov smo s SEM določili hemimorfit (h) s kemično formulo $(Zn_4Si_2O_7(OH)_2 \cdot (H_2O)$. V vzorcih je tako mikrozrnat, da je tudi z vrstičnim elektronskim mikroskopom vidna le njegova skorjasta (natečna) struktura. Na SEM sliki 8 (levo) se nahaja ob kristalih ramsbeckita. EDS spekter hemimorfita (slika 8 desno) prikazuje glavne elemente kemične sestave Zn, Si in O.

Redki minerali, določeni v remšniškem rudišču, nastopajo v sledovih in so mikroskopske do submikroskopske velikosti, zato so do zadnjih nekaj let ostali neopaženi. Med njimi sta dve posebno lepi obliki sulfatov, ki pri nas do nedavna še nista bili najdeni. Gre za sekundarna minerala, ki nastajata v procesu pripovršinskega preperevanja bakro-

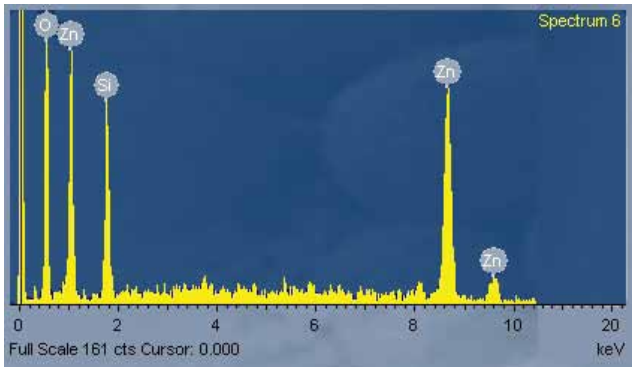

Sl. 8. Majhno svetlo sivo polje hemimorfita (h) ob dveh kristalih ramsbeckita. SEM posnetek (levo, izsek iz slike 13) in EDS spekter hemimorfita (zgoraj). Opuščen rudnik Remšnik.

Fig. 8. Small light grey field of hemimorphite (h) near two ramsbeckite crystals. Left - SEM (BSE) image (cut from fig. 12); top - EDS spectrum of hemimorphite. Abandoned Remšnik mine.

vo cinkovih rud, odvalov in žlinder. Prvi pripada ramsbeckitu, ki sta ga na kratko predstavila Žorž in Trajanova (2010).

Določitev drugega minerala je še vedno vprašljiva, saj nastopa v neznatni količini in v tako drobnih kristalih, da ga pod binokularno lupo nismo opazili in ga tudi s SEM analizo nismo uspeli enoznačno dokazati. Njegova semikvantitativna kemična sestava in kristalna oblika pa nakazujeta, da zelo verjetno pripada namuwitu.

Ramsbeckit

Značilne rudne žile v remšniškem rudišču so sestavljene predvsem iz halkopirita, galenita in sfalerita v osnovi iz kremena in karbonatov, od katerih je najpogostejši dolomit. V opuščenih rovih dosežejo v povprečju debelino med 3 in 5 cm. Debelejše žile so navadno sestavljene iz več slojev, ki so med seboj ločeni s trakovi kremena in dolomita. Slednji je videti kot pole razlistane osnovne kamnine in/ali pa remobiliziranega karbonata iz nje. Sekundarna mineralizacija se nahaja v odprtih razpokah in prelomih. Razpoke sekundarnega klivaža položno, vzdolžno sekajo rudne žile. V najmlajših, strmih prelomih in razpokah so se kot oprhi odlagali le sekundarni minerali, značilni za oksidacijsko cono.

Debelejša orudena žila z ramsbeckitom se nahaja v spodnjem (drugem) obzorju, ki je okrog 7 m pod površjem. Sestavljena je predvsem iz halkopirita, galenita in sfalerita. Med posameznimi sloji v žili je kristaliziral pirit, ki ima razvite kristalne ploskve pentagonskega dodekaedra, velikosti do enega milimetra. Oprhi bakrovo cinkovih sekundarnih mineralov so se odložili v razpoki v zgornjem delu žile. Razpoka v sredini žile je vsebovala največ linarita in langita. V spodnjem delu žile so prevladovali kristali malahita in rosasita v združbi z redkima aurihalkitom in hidrocinkitom.

Kljub večanju števila najdb, ramsbeckit še vedno spada med redke sulfate. Po Nickel-Strunzovi klasifikaciji mineralov spada med vodne sulfate z dodatnimi anioni, v prostorsko skupino P 2_1/a 2/m. Matično nahajališče je rudnik Bastenberg blizu kraja Ramsbeck v Nemčiji, po katerem je dobil svoje ime. Odkrit je bil leta 1984, IMA pa ga je potrdila 1985 (Internet 1). Prvi so ga opisali Hodenberg in sodelavci leta 1985 in zanj podali stehiometrično kemijsko formulo $(Cu, Zn)_7(SO_4)_2(OH)_{10}\cdot 5(H_2O)$. Določili so mineralno paragenezo (Hodenberg et al. 1985), ki je povsem primerljiva z remšniško. Kristalno zgradbo je leta 1988 določil Effenberger. Revidiral je kemijsko formulo in jo iz prejšnje oblike popravil v $(Cu,Zn)_{15}(SO_4)_4(OH)_{22}\cdot 6(H_2O)$.

Ramsbeckit iz Janičkovega rova nastopa v pravilnih kristalih, velikih nekaj desetink mm, največ do 0,5 mm, ki so makroskopsko vidni le kot barvne prevleke (sl. 9). Pri povečani fotografiji so lokalno že prepoznavni nejasni, živo zeleni kristali (sl. 10). Pod binokularno lupo imajo zeleno barvo, vendar zaradi močne refleksije od kristalnih ploskev, fotografije niso bile uspešne. Za boljšo predstavo barve minerala je ustrezna fotografija ramsbeckita iz nahajališča Penrhiw na Walesu, prikazana na spletni strani (Internet 2 ali Internet 3), ki povsem odgovarja primerkom iz Remšnika. Kristali so prosojni in imajo nekoliko svileno steklast sijaj. Na vzorcu, ki je bil shranjen v suhem prostoru, so kristali nekoliko izgubili zeleno barvo, medtem ko je modrikasta niansa postala izrazitejša.

Ramsbeckit kristalizira v monoklinskem sistemu. Kristali so različnih oblik. Najizrazitejša je ploskev osnovnega pinakoida (001), po katerem je vidna nejasna razkolnost. Izraziti sta ploskvi (100) in (010). Ploskev (210) je praviloma manjša od ostalih (sl. 11), medtem ko se ploskvi (120) in (310) v večini primerov sploh nista razvili (sl. 12, v sredini). V nekaterih kristalih pa so razvite le ploskve (100), (001) in (010) (sl. 12, levo spodaj in desno zgoraj).

Skice idealiziranih oblik kristalov ramsbeckita, ki smo jih našli do sedaj, so prikazane na sliki 13. Na sliki 13 B so z indeksi označene kristalne ploskve oblik 1, 2 in 3 s slike 13 A. Kristalne ploskve, ki določajo morfologijo ramsbeckita so pinakoidi (001), (100), (010) in (210) ter prizma 3. reda (110) (slika 13, risbi 2A, 2B). Prizma (110) je lahko bolj, ali manj izrazita. Kristali ramsbeckita imajo lahko razvite samo kristalne ploskve pinakoidov (slika 13,

Sl. 9. Modrikasto zelene prevleke prevladujočih sulfatnih sekundarnih mineralov z ramsbeckitom iz Janičkovega rova. Opuščen rudnik Remšnik. Foto M. Trajanova.

Fig. 9. Bluish green coatings of predominant sulphate minerals with ramsbeckite from Janiček pit. Abandoned Remšnik mine. Photo M. Trajanova.

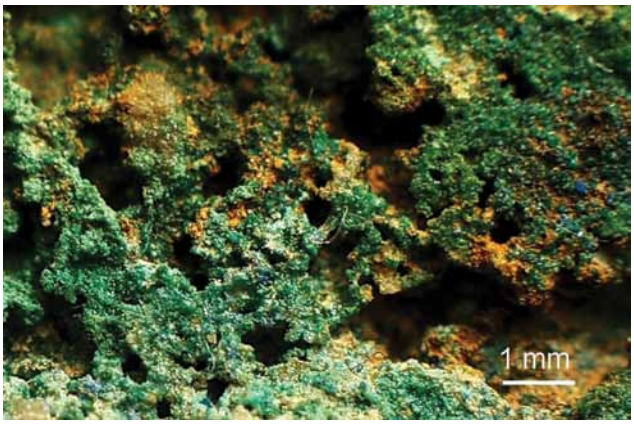

Sl. 10. Zeleni kristali ramsbeckita iz Janičkovega rova. Redka modra zrna so langit. Opuščen rudnik Remšnik. Foto M. Demšar.

Fig. 10. Bright green crystals of ramsbeckite from Janiček pit. Blue grains belong to langite. Abandoned Remšnik mine. Photo M. Demšar.

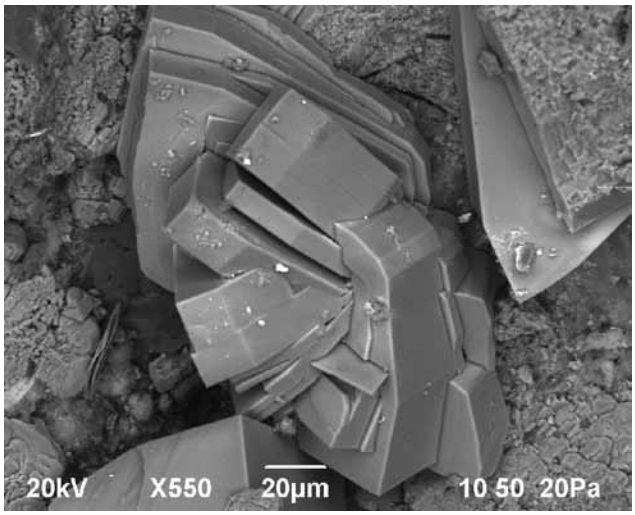

Sl. 11. Kristalni zraščenci ramsbeckita z lepo vidnimi ploskvami osnovnega pinakoida in prizem. SEM (BSE) posnetek.

Fig. 11. Intergrown ramsbeckite crystals with expressed plains of basal pinacoid and prisms. SEM (BSE) image.

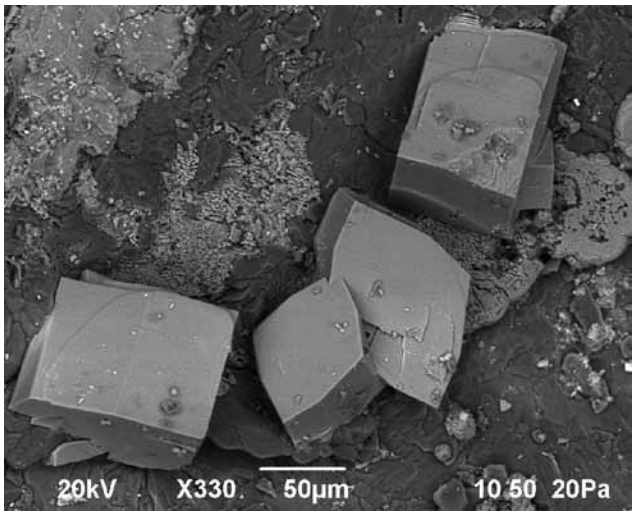

Sl. 12. Dve zrni ramsbeckita v sredini predstavljata najpogostejšo obliko s ploskvami (001), (100), (110), (010) in (210). Levo spodaj in desno zgoraj sta kristala z razvitimi pinakoidi. SEM posnetek.

Fig. 12. Two grains in the figure centre represent the most frequent form with planes (001), (100), (110), (010) and (210). Crystals with developed pinacoids can be seen at the bottom left and top right. SEM (BSE) image.

risba 1A, 1B). Najpogostejša je oblika 2, pri kateri je lahko ploskev (010) krajša, na račun podaljšane ploskve (210), kot je primer oblika 2 na sliki 13A. Najpestrejša in redkejša je oblika 3, ki ima razvitih največ kristalnih ploskev. V tem primeru je ploskev (110) lomljena, tako da se je razvila ploskev (120). Tudi ploskev (010) je lomljena in na njen račun je nastala ploskev (310) (sl. 13, oblika 3A, 3B). Primer te oblike vidimo na sliki 11 na spodnji desni polovici največjega kristala osrednjega zraščenca.

Peacor in sodelavci (1987) in Ohnishi in sodelavci (2004) omenjajo razkolnost ramsbeckita po osnovnem pinakoidu, ki je nakazana tudi v našem primeru (slika 11, na osrednjem zraščencu, zgoraj). Višji kristal 4 (sl. 13A) najverjetneje predstavlja dvojček. Kot zasledimo v Mineraloškem priročniku, verzija 1 (Bideaux & Nichols, 2004, ©

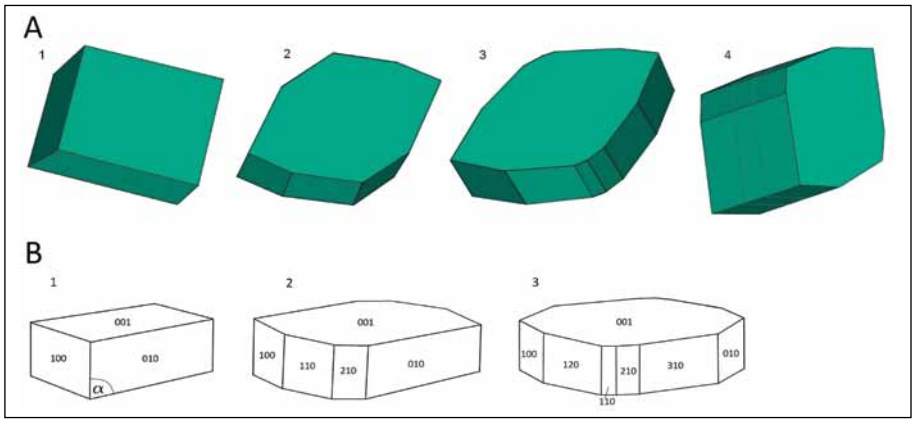

Sl. 13. Skica do sedaj najdenih kristalnih oblik ramsbeckita v opuščenem rudišču Remšnik. Glej razlago v tekstu.

Fig. 13. Sketch of the so far found ramsbeckite crystal forms in the abandoned Remšnik mine. See explanation in the text.

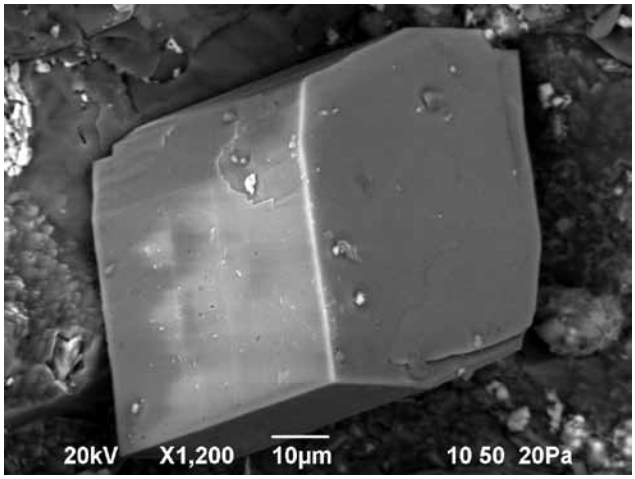

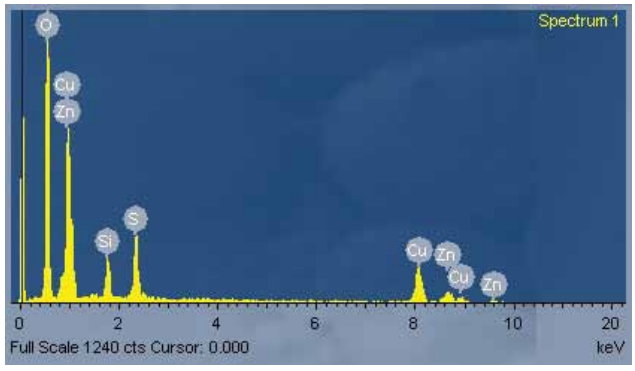

Sl. 14. EDS spekter ramsbeckita (leva točka na sliki levo).

Fig. 14. EDS spectrum of ramsbeckite (left spot in the left figure).

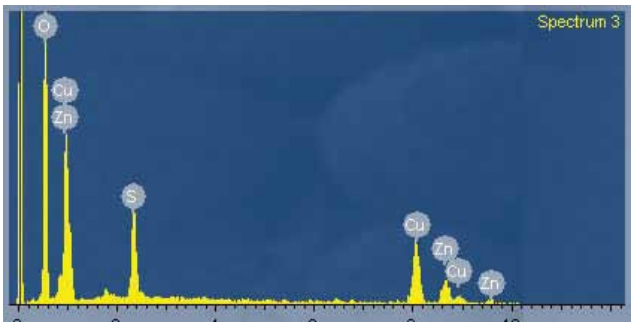

Sl. 15. EDS spekter čiste površine zrna ramsbeckita vidnega na desni strani na sliki 12.

Fig. 15. EDS spectrum of clear ramsbeckite grain surface seen at the right side of figure 12.

2004-2013), ima ramsbeckit ponavljajoče dvojčke, ki oblikujejo cilindrične skupke. Tak primer bi lahko predstavljal kristal na SEM posnetku (sl. 14 levo). Podobnost nekaterih oblik kristalov z remšniškimi (np. oblika 1 s slike 13A, 13B) vidimo na sliki 1 Ohnishi-ja in sodelavcev (2004) iz rudnika Hirao blizu Osake na Japonskem, kjer prevladujejo na videz romboedrski kristali.

Kvalitativna kemična sestava ramsbeckita je prikazana na EDS spektru (sl. 14 desno). Zaradi drobnih zrnc na površini kristala se pojavi neznaten pik Si. Za ploščati ramsbeckit nenavadno visok kristal verjetno predstavlja dvojček, ki je enak obliki 4 na sliki 13 A.

EDS spekter čistega ramsbeckita (sl. 15) je sneman na čisti, gladki površini spodnjega kristala ob zgornjem desnem robu slike 11. V sestavi zato ni primesi silicija, kot na EDS spektru na sliki 14.

Po kemični sestavi je ramsbeckitu sorodnih kar nekaj redkih mineralov sulfatov, kot na primer: langit, posnjakit, wroewolfeit, spangolit, ktenasit, pa tudi namuwit.

Na rentgenskem difraktometru smo poskusili snemati košček vzorca z mikrokristalnim oprhom, vendar analiza ni bila uspešna.

Namuwit

V sestavi modrikasto zelenih, na oko amorfnih oprhov, se v razpokah ob ramsbeckitu nahaja še en mikrokristalen sekundarni sulfatni mineral, ki smo ga zaenkrat določili kot namuwit.

Namuwit so prvič opisali Bevins in sodelavci leta 1982. Določen je bil v vzorcu iz rudišča Aberllyn, ki se nahaja v zbirki Narodnega muzeja na Walesu, po katerem je dobil ime (NAtional MUseum of Wales). Istega leta ga je potrdila IMA (Internet 4). Leta 1983 je bil na kratko prikazan tudi v reviji American mineralogists pod »New mineral names« (Fleischer & Pabst, 1983). Od tedaj dalje so ga našli na številnih mestih po svetu, tako v oksidacijskih conah bakrovo cinkovih rudišč, kot tudi na rudniških odvalih, največkrat v paragenezi z ramsbeckitom.

Kemijska formula namuwita je $(Cu, Zn)_4(SO_4)(OH)_6 \cdot 4(H_2O)$ (Bevins et al., 1982). Avtorji ga opisujejo kot svetlo morsko zelen mineral z bisernim sijajem. Ker je v začetnih raziskavah upoštevana le kemična sestava, določena na SEM EDS, smo ga prišteli k ramsbeckitu (Žorž & Trajanova, 2010). Zaradi oblike kristalov s šesterokotnimi preseki, podobnimi sljudam, je bila določitev dvomljiva, zato smo s SEM naredili dodatne raziskave. Skupaj z ramsbeckitom smo ga poskušali določiti tudi z rentgensko difrakcijo, vendar neuspešno. Z EDS dobljena kvalitativna kemična sestava je enaka kot za ramsbeckit. Semikavntitativna kemična sestava pa se nekoliko razlikuje, čeprav je zaradi uporabe nepoliranega vzorca in premajhnih zrnc nezanesljiva.

Po obliki rozet je namuwit zelo podoben še enemu sulfatu, posnjakitu, razlikuje pa se po barvi (posnjakit je moder, namuwit bledo zelen) in kemični sestavi, ker vsebuje poleg bakra tudi cink. Na osnovi tega in oblike kristalov sklepamo, da mineral najverjetneje pripada namuwitu. Značilni svetlo zeleni, submikroskopski cvetasti skupki namuwita (sl. 16) na skorjastih prevlekah sorodne kemične sesta-

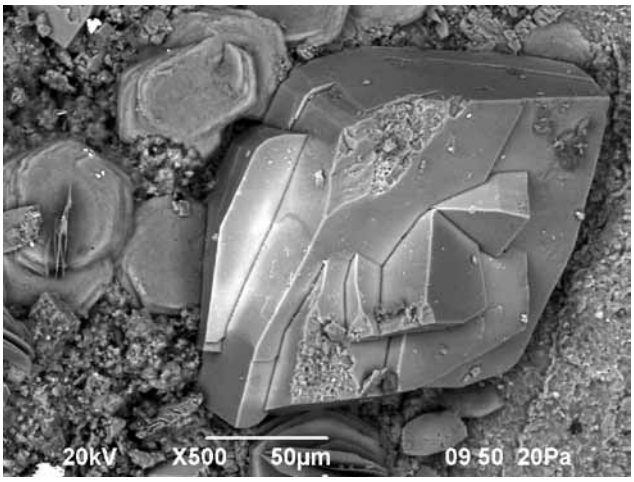

Sl. 16. Ob zraščencu ramsbeckita se nahajajo drobni kristalni skupki namuwita (?), ki kažejo šesterokotno simetrijo. SEM (BSE) posnetek.

Fig. 16. Tiny crystal clusters of namuwite (?), showing hexagonal symmetry, are seen beside ramsbeckite. SEM (BSE) image.

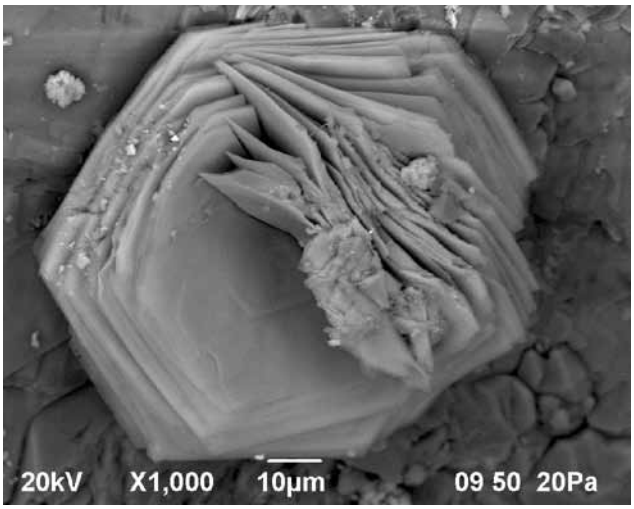

Sl. 17. Cvetasto preraščanje heksagonalnih ploščic namuwita. SEM (BSE) posnetek.

Fig. 17. Flowery intergrowing of hexagonal plates of namuwite. SEM (BSE) image.

ve ob ramsbeckitu so enaki oblikam, ki so jih opisali Bevins in sodelavci (1982) in Groat (1996). Po njihovih podatkih je namuwit izomorfen s sintetičnim cinkovim sulfatom ($Zn_4SO_4OH)_2 \cdot 4H_2O$).

Kristali rastejo iz pretežno amorfne podlage in redko presegajo velikosti 50 µm, izjemoma pa dosežejo tudi 80 µm. Imajo izrazito razkolnost po ploskvah osnovnega pinakoida (001). Pogosti so primeri prečnega preraščanja lističev, kot je vidno na slikah 16 (ob levem robu) in 17.

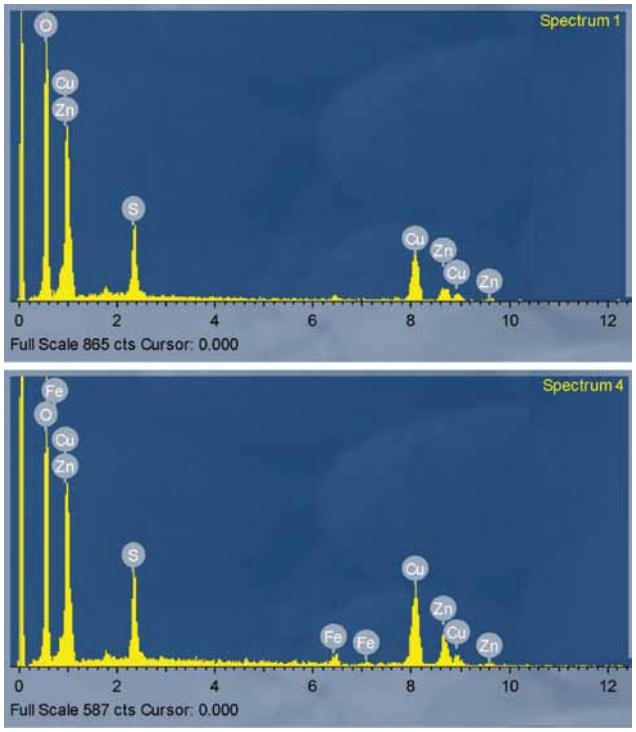

Sl. 18. EDS spektra namuwita s slike 17.
Fig. 18. EDS spectra of namuwite from figure 17.

Kvalitativna kemična sestava remšniškega namuwita s slike 17 je prikazan na sliki 18. Tako kot ramsbeckit, pripada bakrovemu cinkovemu vodnemu sulfatu z dodatnimi anioni. Zaradi neugodne lege kristalnih ploskev glede na lego detektorja, imajo piki spektra nesorazmerno velikost.

Kristalno strukturo namuwita je določil Groat (1996). Sestavljen je iz ponavljajočih slojev tetraeder-oktaeder-tetraeder (T-O-T), ki so z vodikovo vezjo povezani z medslojno H_2O. Isti avtor je ugotovil, da je namuwit podvržen procesom hidracije in dehidracije, odnosno prehodom iz tetrahidrata v pentahidrat in obratno, pri približno sobni temperaturi.

Zaključek

Polimetalno orudenje v Remšniku je nastalo vzdolž klivažnih razpok sovpadajočih s foliacijo, kar nakazuje njegovo terciarno starost in zelo verjetno povezanost s pohorskim magmatizmom. V procesu oksidacije in pripovršinskega preperevanja primarne sulfidne mineralizacije so v mlajših razpokah kristalizirali številni sekundarni minerali, med katerimi najdemo tudi zelo redke vrste. Pri nas sta to prvič opisana bakrovo cinkova sulfata ramsbeckit in namuwit. Določitev slednjega še ni enoznačna, zato upamo, da bo naslednja najdba količinsko bogatejša in bo omogočila uporabo analitskih tehnik, s katerimi bomo potrdili ali ovrgli sedanjo določitev.

Zahvala

Raziskave je finančno podprla Agencija za raziskovalno dejavnost Republike Slovenije v okviru raziskovalnega programa P1-0025, Sedimentologija in mineralne surovine. Zahvaljujeva se recenzentoma za koristne pripombe in popravke ter dr. Milošu Milerju za pomoč pri delu s SEM.

Abandoned Remšnik mine with ramsbeckite and namuwite(?)

Introduction

The investigations of the Austroalpine in Slovenia have been focused mostly on the area of Pohorje, while other areas have been included to a lesser extent. Detailed study of mineral deposits and mineralogy has usually been left aside. It is the enthusiasm of mineral collectors we have to thank that things are moving forward also in the area of mineral finds in Slovenia.

Though the Remšnik ore deposit has been known for a long time, the recognition of its mineral association is still not finished. Secondary minerals in the oxidation zones are frequently first indicators for tracing ores. Only insignificant quantities of these minerals are usually found, but they indicate what might occur in the surroundings. The find of ramsbeckite in the Remšnik ore deposit is therefore important from mineralogical point of view and also for tracing of cognate ore mineralization in other regions.

Remšnik is nowadays not of interest as an ore deposit; nevertheless, it represents the only insight into the third dimension in this region to structural geologists and particularly a "Mecca" for rare minerals collectors. The latter often like to joke that God punished them with a vast number of blue and green minerals. It is thus not surprising that also the presented ramsbeckite find belongs to green crystals. Despite the fact, they differ macroscopically and particularly under the hand lens from the so far known minerals in the Remšnik ore deposit. Their determination is the basis for the presented study.

Ramsbeckite has been already found in several mines around the world beside the parent occurrence near Ramsbeck in Germany, e.g.: in limonitic gangue in »La Venezia« mine for the first time in Italy (Orlandi & Perchiazzi, 1989), it is reported from Ecton mine in Pennsylvania (Peacor et al, 1987), from Penrhiw mine (Mason & Green, 1995)

and other locations in Great Britain, from Japan (Ohnishi et al., 2004) etc. As for known data, it was found on different locations in 11 countries up to now. In other localities, it is probably still waiting for a coincidental finder, as it is well hidden among numerous other greenish minerals and by its microscopic crystal size.

Geographic setting

Parallel with the Pohorje Mountains and north of the Drava valley, a hilly area extends in northern Slovenia. As it has no continuous mountain chain, several attempts were made in the past to name the area with one name. The name Kobansko appears in some topographic maps and in the others Kozjak. In the central part of this region, drained by the Brezniški, Štimpaški and Vaški brooks, the scattered village of Remšnik is situated. On the western slopes of the south-southeast trending Remshnik ridge, abandoned Remshnik mine (Janiček pit) occurs south of the village (Fig. 1).

Janiček pit marked in Figure 1 is the most accessible mining object. Its surrounding is densely vegetated and therefore not easy to be found.

Some data about the Remšnik ore deposit

The Remšnik ore deposit first attracted attention of researchers more than 250 years ago. We can read in documents stored in the Archive of Slovenia that count Michelangelo Zois opened the mine in 1763 and constructed a smelter in Brezno by the Drava River. This shows that the deposit had been discovered much earlier, though we could find no written sources to support this theory. A concession for the mine opening has been vested on the base of feudal letter dated June 14th 1850, under No. 1937. It was worded under the name »Drauwalder silberhältiger Blei, Kupfer und Zink Bergbau« (silver bearing lead, copper and zinc mine Drava forest). The first owners of the mine were Jakob Krušnik, Karl Kranz and Johan Baumgartner. Pits were named Maria and Franz, or the Zwilling Stollen (the twin pit). At that time, the produced ore had been melted in the village of Ožbalt by the Drava River. According to the data of the then Graz Chamber of Commerce 74.66 kg of silver was extracted in 1853 and only about 50 kg three years later. In October 1887, Karel Wehrkan from Litija became the owner of the mine and as soon as in 1888 he sold it to the Litija Mining Company. They stopped with exploitation of ore in Remšnik on December 22nd, 1891. In the meantime, they excavated a pit near the Dijak farm and named it Janiček pit and the mine itself »Fressen Bergbau«. Until the Second World War, the ownership of the mine had changed several times. It was nationalized in 1946 and afterwards only geologists and mineral collectors entered the pits.

In the Remšnik mine, gangue material was used to support the pit walls instead of wooden pillars. Walls of the pits and bigger excavated spaces have been underpinned by blocks of country rock, which is why the Janiček pit is still accessible today in the front part, though only 5 to 7 m below the surface. It is collapsed in the back part.

According to the available data, ore mineralization in the Remšnik mine occurs in the old Palaeozoic low metamorphic rocks of the Magdalensberg formation. The mineralized bodies form lenses in metatuffs, dolomitic marbles and phyllites (Drovenik et al. 1980). The oldest known publication about the mine is the one by Tornquist (1929), where he mentioned mining works below the Ulbing farm. He designated two mine pits in his Figure 1 (Janiček and Ulbing) below the thrust contact of old Palaeozoic rocks (altpaläozoische Sedimente) with retrogressed and mylonitized rocks (Mylonit-diaphtorite), shown in Figure 2. The manuscript geological map of the exploitation pit below the Dijak farm, kept at the Mežica mine Archive (Reports of the geological service, 1984-1989) contains no distinction between mylonites and phyllites. Consequently, it is still not clear, which formation (if it is only one) the mineralization is connected to. Only hanging wall rocks are pertained to Magdalensberg formation to which Mioč and Ramovš (1973) determined Lower Devonian age in the Remšnik area.

There are different opinions about the Remšnik ore deposit genesis. Some researchers connect the mineralization to the Miocene Pohorje magmatism (Tornquist, 1929; Duhovnik, 1956; Berce, 1963, Grafenauer, 1965), others to the Palaeozoic magmatism (Hegemann, 1960; Drovenik et al. 1980).

The Remšnik polymetallic ore deposit prides itself on variety of minerals. The mineral paragenesis consists of numerous ore and gangue minerals, together exceeding 55 types. The following ore minerals have been determined: galenite, sphalerite, pyrite and chalcopyrite as the prevailing types, and subordinately cuprite, tetrahedrite, boulangerite, bornite, chalcosine, covelline, freibergite, gersdorffite, acanthite and polybasite. Drovenik (1980) and Grafenauer (1966) did not found polybasite and acanthite yet; therefore Drovenik supposed that silver (and bismuth) is a component of the galenite and chalcopyrite structure. Indirectly, he made a hint that inadequate analytical method could be the reason for high content of silver in galenite.

The main gangue minerals in the ore are quartz, iron dolomite and subordinately calcite and aragonite. Particularly variegated are secondary minerals, which crystalized in the oxidizing zone of the Remšnik mine. Among numerous types only some are stated: cuprite, tenorite, hematite, goethite, manganese oxides and hydroxides, malachite, azurite, smithsonite, cerussite, hydrozincite, brianyoungite, rosasite, aurichalcite, barite, gypsum, linarite, langite, baverite,

posnjakite and carbonate cyanotrichite, aragonite, pyromorphite and chrysocolla.

Žorž and co-workers (2007) presented some more frequent minerals (particularly quartz crystals) of the Kobansko area.

Materials and methods of investigation

Presented results are based on field observations and laboratory investigations. Samples were taken near the vein with ore mineralization from the Janiček pit. Diversity of secondary minerals occurring in fractures can be seen under binocular lens, but they are too small for determination. The quantity of gathered samples was not suitable for making either thin sections and/or polished samples; thin coatings would be lost in preparation. A small piece of sample with microcrystallized coating was scanned by X-ray diffractometer. It was equally impossible to isolate thin crystals for chemical analysis. Finally, from the pallet of investigation methods, the only one that remained was scanning electron microscopy (SEM). The analyses were made with SEM JEOL JSM 6490LV at the acceleration energy of 20 kV and at working distance of 10 mm. The BSE mode in low vacuum was used, without coating. Basic semiquantitative chemical composition was determined by Oxford INCA EDS (compo mode) with the same acceleration energy.

Results and discussion

On the 1:100 000 scale Basic geological map of Slovenia, sheet Slovenj Gradec (Mioč & Žnidarčič, 1977) the Remšnik mine is marked between the Remšnik nappe composed of Magdalensberg formation rocks and the footwall Pohorje formation of retrograde schists of the Austroalpine basement. A thin belt of phyllites occurs between the two. Determination of phyllites in this area and further eastward is somewhat disputable. Due to multiple secondary alterations, it is not clear whether this layer belongs to real phyllite or to mylonite, originating retrogressively from dynamometamorphosed rocks of the Pohorje formation (named Kobansko series after Mioč, 1978). It is clear, however, that a part of the Magdalensberg formation rocks, trapped in the thrust zone, is comprised in the phyllite belt.

Macro- and microstructures of the rocks reveal several phases of tectonic activity, including twice reactivated subhorizontal shear movements, due to which dynamometamorphic imprint can be followed in all rocks. The first one is reflected as ductile deformations, yielding mylonitization and foliation. The second shear produced a slaty cleavage, which broadly follows foliation. The origin of these two structures is associated with upper Cretaceous nappe stacking and Tertiary Austroalpine eastward escape (e.g. Fodor et al. 1998, 2002, 2008). Structural parameters of the wider area suggest that Pohorje and Kobansko/Kozjak were still one common block at the time of the Pohorje granodiorite magma emplacement in Lower Miocene and were separated later.

The state of previous investigations does not allow strict definition of the Remšnik ore deposit genesis. Nevertheless, some important relations can be drawn, which neglect its Palaeozoic origin: sulphide mineralization and strong silicification, which obscured structural properties of the rocks, followed cleavage, which is of Tertiary (probably of Miocene) origin; the Kobansko block separated from the Pohorje block probably in middle Miocene and Kobansko was until then, closer to the impact area of the granodiorite intrusion; mineral composition and sulphur isotope composition of the Remšnik and Okoška gora (Pohorje) ore deposits are closely related (Drovenik et al. 1976, 1980). Consequently, there is a great probability that the Remšnik ore mineralization is connected to the Miocene Pohorje magmatism, as has already been proposed by Tornquist (1929), Duhovnik (1956), Berce (1963) and Grafenauer (1965). The question is, whether the mineralization could be related to remobilization of preexisting (Cretaceous/Palaeozoic?) ore minerals, as Drovenik and co-workers (1980) attribute Palaeozoic age to the Okoška gora ore deposit. They argue the age with blastic growth of ore minerals in the time of regional metamorphism, what to us is not a sufficient proof.

Younger oblique fractures, which cut foliation and slaty cleavage, developed as a consequence of renewed shearing. Secondary cleavage plains formed indicating dextral sense of shear (Fig. 3). These fractures are not silicified and contain no primary (sulphide) ore mineralization. All structures are cut by the youngest subvertical faults (Fig. 4) of prevailingly southwest-northeast trend, and subordinately transversely to this direction.

Conditions in the Janiček pit, in which the rocks of the Magdalensberg and Pohorje formations are comprised, show that mostly carbonate lenses and partly wider thrust zone contain ore mineralization. The primary ore mineralization and silicification followed fracture porosity of the older slaty cleavage, which macroscopically follows foliation, while only secondary mineralization can be found in two generations of transverse fractures and faults (Fig. 5). Silicified brecciated rocks appear massive.

Z. Žorž found most of rare secondary minerals in the Remšnik mine and determined them together with Moser (Žorž & Moser, 2002). Among them, particularly interesting is beaverite, the lead-copper-iron-aluminium sulphate. Upon attainable data, beaverite was known only as yellow coatings before the Z. Žorž find; here, caramel

brown, transparent to translucent crystals up to one millimetre in size occur as coatings on quartz (Fig. 6).

Among carbonates, the rosasite and aragonite at partly limonitized quartz base (Fig. 7) are particularly beautiful.

In the base of some secondary minerals, hemimorphite has been determined by SEM. It is nearly amorphous; therefore, also under SEM, just its colloidal texture is noticed. It can be seen near the ramsbeckite crystals at the left side of Figure 8. The main chemical components of hemimorphite Zn, Si and O are shown at the EDS spectrum (Fig. 8, right).

Rare minerals, determined in the Remšnik mine, occur in traces in microscopic to submicroscopic sizes; therefore, they have remained unnoticed until recent years. Among them are two especially beautiful forms of sulphates, found in Slovenia for the first time. They belong to secondary minerals formed in the process of near-surface weathering of copper and zinc ores, dumps and slags. The first one belongs to ramsbeckite, which was shortly introduced by Žorž and Trajanova (2010). It represents grassy green to bluish green microcrystal coatings in some fractures and fissures (Fig. 5, lower half).

Determination of the second mineral is still questionable. It occurs in so insignificant a quantity and as so tiny crystals that it is invisible under binocular lens and we did not manage to actually prove its type by SEM analysis. Semiquantitative chemical composition and crystal habit indicate that it most probably belongs to namuwite.

Ramsbeckite

Characteristic Remšnik mine ore veins are composed mostly of chalcopyrite, galenite and sphalerite in the matrix of quartz and carbonates, of which the most frequent is dolomite. In the abandoned pits, the veins reach an average thickness between 3 and 5 centimetres. Thicker veins usually consist of several layers separated by bands of quartz and iron dolomite. The latter looks like split wall rock and/or remobilized carbonate from it. Secondary mineralization is found in opened fractures and faults. Fractures of secondary cleavage cut the ore veins obliquely. Only coatings of secondary minerals characteristic for oxidation zone occur in the youngest steep fractures and faults.

A thicker ore vein with ramsbeckite was found in the lower (second) level, lying about 7 m below the surface. The vein consisted mostly of chalcopyrite, galenite and sphalerite. Between separate layers of the vein, pyrite crystallized as pentagon dodecahedrons up to 1 mm in size. Coatings of the copper and zinc secondary minerals occur in the fracture in the upper part of the vein. The fracture in the middle of the vein contained mostly linarite and langite. In the lower part of the vein, malachite and rosasite prevailed in association with some aurichalcite and hydrozincite.

Ramsbeckite is still considered as a rare sulphate despite increasing number of finds. In the Nickel-Strunz classification of minerals, it belongs to the group of sulphates with additional anions, with H_2O, and to the space group P 2_1/a 2/m**.** It is named after Ramsbeck in Germany (Bastenberg mine), where it was found for the first time in 1984 and approved by IMA in 1985 (Internet 2)**.** First description is of Hodenberg and co-workers (1985), who presented ramsbeckite stoichiometric chemical formula $(Cu, Zn)_7(SO_4)_2(OH)_{10}\cdot 5(H_2O)$ and determined mineral paragenesis, which is comparable with the one in Remšnik mine. Effenberger (1988) determined crystal structure of ramsbeckite. He revised chemical formula, and from previous form it was corrected to $(Cu,Zn)_{15}(SO_4)_4(OH)_{22}\cdot 6(H_2O)$.

Ramsbeckite from the Janiček pit occurs in euhedral crystals some tenth of mm in size, maximum up to 0.6 mm and is macroscopically seen only as coloured coatings (Fig. 9). At magnified photo unclear, bright green grains are seen locally (Fig. 10). They have green colour under binocular lense and strong reflection from crystal planes, which prevents us to make a successful photo. Therefore, the photo of ramsbeckite from Penrhiw mine in Wales (Internet 2 or 3) is suitable to better imagine the colour of the mineral, which is the same as the one in Remšnik. The crystals are transparent with silky glassy lustre.

The ramsbeckite crystals of the sample kept in a dry room become slightly less green and blue tint became stronger.

Ramsbeckite crystallize in the monoclinic system. The crystals have diverse habits. The most pronounced is the crystal face of basal pinacoid (001), along which indistinct cleavage can be seen. Distinctive are faces (100) and (010). The face (210) is usually smaller than the others (Fig. 11), while the faces (120) and (310) in most cases are not developed at all (Fig. 12 in the middle). In some crystals only faces (100), (001) and (010) developed (Fig. 12, bottom left and top right).

Sketch of idealized ramsbeckite crystals found so far in the Remšnik mine, is given in Fig. 13. Figure 13 B show indexed crystal faces of forms 1, 2 and 3 shown in figure 13A. Crystal faces defining ramsbeckite morphology are pinacoids (001), (100), (010) and (210) and prism of the 3rd order (110) (Fig. 13, forms 2A, 2B). The prism (110) can be more, or less pronounced. Some of the crystals developed only crystal faces of pinacoids (Fig. 13, sketch 1A, 1B). The most frequent is form 2,

which can have shorter (010) face on the account of longer (210) face, as can be seen in Fig. 13A, form 2. Faces richest, but infrequent is form 3. In this case, an additional face (120) developed on the account of the face (110). Seemingly, face (310) developed on the account of the face (010) (Fig. 13, forms 3A and 3B). An example of such form can be seen in figure 11 at the bottom right half of the biggest crystal in the central intergrown crystal cluster.

Peacor et al. (1987) and Ohnishi et al. (2004) determined ramsbeckite cleavage along basal pinacoid, which can be traced also in our case (Fig. 11, crystal at the top of the central intergrown crystals). High crystal of form 4 (Fig. 13A) most probably belongs to twins. As we can find in the Handbook of Mineralogy, version 1 (Bideaux & Nichols, 2004, © 2004-2013), ramsbeckite has repeated twinning, forming cylindrical aggregates. An example of such twin can be seen in SEM image (Fig. 14 left). Similarity of some crystal forms with the ones from Remšnik (e.g. form 1 in Fig. 13A and 13 B) can be seen in figure 1 of Ohnishi and co-workers (2004) from the Hirao mine, near Osaka in Japan, where rhombohedra-like crystals prevail.

Qualitative chemical composition of ramsbeckite is shown in EDS spectrum (Fig. 14 right). Indistinct Si peak occurs due to small grains on the crystal surface. Unusually high crystal form for tabular ramsbeckite is the same as form 4 in figure 13A.

An EDS spectrum of pure ramsbeckite (Fig. 15) is scanned on the clear smooth surface of the bottom crystal at the right edge of figure 11. Therefore, no admixtures of Si appear in the spectrum in comparison to Fig. 14.

Several rare sulphate minerals are related to ramsbeckite in chemical composition as for example: langite, posnjakite, wroewolfeite, spangolite, ktenasite, and also namuwite.

An attempt was made to scan a piece of sample with microcrystalline coating with X-ray diffractometer, but the analysis was not successful.

Namuwite

Beside ramsbeckite another microcrystalline secondary sulphate is present in the composition of macroscopically amorphous bluish green coatings. With a shade of doubt, it is determined as namuwite.

Namuwite was described for the first time by Bevins and co-workers in 1982. It was determined in a sample originating from the Aberllyn mine. It is kept in the National Museum of Wales, whereupon its name originates (NA-MU-W-ite). The same year, the mineral was approved by IMA (Internet 4). It was shortly presented in the American mineralogists periodical under the »New mineral names« (Fleischer & Pabst, 1983). From then on, the mineral was found in oxidation zones of Cu, Zn ore deposits, as well as in mine gouges in several places around the world.

Namuwite chemical formula is $(Cu, Zn)_4(SO_4)(OH)_6 \cdot 4(H_2O)$ (Bevins et al., 1982). The authors described it as a sea blue mineral with emerald luster. Because only chemical composition, determined by SEM EDS, had been considered in the initial investigations, it was ascribed to ramsbeckite (Žorž & Trajanova, 2010). Due to its hexagonal form the determination was dubious; therefore we made additional SEM analyses. The x-ray diffraction analysis was made together with ramsbeckite, but was unsuccessful. EDS qualitative chemical composition of namuwite is the same as the one of ramsbeckite. It differs semiquantitatively, but because of small grains and the use of unpolished sample the results were not reliable and are not applicable.

As for the form of rosettes namuwite is similar to another sulphate mineral, posnjakite. They can be differentiated according to the colour (posnjakite is blue, namuwite pale green) and chemical composition (Zn beside Cu in namuwite). Based on the mentioned facts and on crystal form, we concluded that the mineral most probably belongs to namuwite. Typical are light green submicroscopic flowery aggregates (Fig. 16) on crusty coatings of related chemical composition, occurring together with ramsbeckite. They are the same as the forms described by Bevins and co-workers (1982) and Groat (1996). According to their data namuwite is isomorphous with the synthetic zinc sulphate $(Zn_4SO_4OH)_2 \cdot 4H_2O$).

The namuwite crystals grow out of predominantly amorphous ground and rarely exceed 50 µm, exceptionally 80 µm in size. They have pronounced cleavage along basal pinacoid (001). Frequent transverse intergrowing of leaflets can be seen, like the ones in figures 16 (near the left edge) and 17.

Qualitative chemical composition of the Remšnik mine namuwite from figure 17 is shown in figure 18. Like ramsbeckite, it belongs to copper, zinc sulphate with additional anions and H_2O. The spectra peaks have disproportional heights due to the unfavourable orientation of the crystal surface according to the detector position.

Groat (1996) determined crystal structure of namuwite. It consists of repeated tetrahedral-octahedral-tetrahedral (T – O – T) layers held together by hydrogen bonds to interstitial H_2O molecules. The author found out that namuwite is subjected to hydration, dehydration processes, and to transitions from tetrahydrate to pentahydrate at about room temperature.

Conclusion

Polymetallic ore mineralization of the Remšnik mine developed along cleavage fractures coinciding with foliation, which indicates its Tertiary age and most probable connection with the Pohorje magmatism. Numerous secondary minerals crystallized in younger fractures in the process of oxidation and near-surface weathering. Among them some very rare types can be found, such as copper zinc sulphates ramsbeckite and namuwite (?) described for the first time in Slovenia. The namuwite determination is still not univocal; therefore, we hope that the next find will be of bigger quantity enabling thus the use of analytical techniques which will confirm or reject the present determination.

Acknowledgement

The investigations were financially supported by the Slovenian Research Agency within the frame of the research programme P1-0025, Sedimentology and mineral resources. We thank to reviewers for helpful comments and corrections and to Dr Miloš Miller for his assistance at the SEM.

Literatura - References

Arhiv RS, 1950: Rudarska knjiga A za okrožje Celje. Ljubljana: 185-204.

Arhiv RS, 1850a: Fevdna in koncesijska knjiga: Drauwalder Gesmbh Lehensbrief.

Berce, B. 1963: The formation of the ore-deposits in Slovenia. Rendiconti della Società Mineralogica Italiana, 19: 1-16.

Bevins, R.E., Turgoose, S. & Williams, P.A. 1982: Namuwite, $(Zn, Cu)_4SO_4(OH)_6 \cdot 4H_2O$, a new mineral from Wales. Mineralogical Magazine, 46: 51-54.

Bideaux, A. & Nichols, B. 2004: Handbook of mineralogy. Mineralogical Soc. of America. Mineral Data Publishing, version 1/ V: © 2004-2013, 791 p.

Drovenik, M., Duhovnik, J., & Pezdič, J. 1976: Izotopska sestava žvepla v sulfidnih rudnih nahajališčih v Sloveniji. Rud. met. zbornik, 2-3: 193-246.

Drovenik, M., Pleničar, M. & Drovenik, F. 1980: Nastanek rudišč v SR Sloveniji. Geologija, 23/1: 1-157.

Duhovnik, J. 1956: Über die metallogenetischen Epochen und Provinzen Jugoslawiens. Berg- und Hüttenmännische Monatshefte 101. Jahrgang 2: 30-32.

Effenberger, H. 1988: Ramsbeckite, $(Cu, Zn)_{15}(OH)_{22}(SO4)_4 \cdot 6H_2O$: revision of the chemical formula based on a structure determination. Neues Jahrbuch für Mineralogie, Monatshefte, 38–48.

Fleischer, M. & Pabst, A. 1983: New mineral names. American Mineralogist 68: 280-283.

Fodor, L., Gerdes, A., Dunkl, I., Koroknai, B., Pécskay, Z., Trajanova, M., Horváth, P., Vrabec, M., Jelen, B., Balogh, K. & Frisch, W. 2008: Miocene emplacement and rapid cooling of the Pohorje pluton at the Alpine-Pannonian-Dinaridic junction, Slovenia. Swiss J. Geosci., Birkhäuser Verlag, 255-271.

Fodor, L., Jelen, B., Márton, E., Rifelj, H., Kraljić, M., Kevrić, R., Márton, P., Koroknai, B. & Báldi-Beke, M. 2002: Miocene to Quaternary deformation, stratigraphy and paleogeography in Northeastern Slovenia and Southwestern Hungary. Geologija, 45/1: 103–114, Ljubljana; doi:10.5474/geologija.2002.009.

Fodor, L., Jelen, B., Márton, E., Skaberne, D., Čar, J. & Vrabec, M. 1998: Miocene - Pliocene tectonic evolution of the Slovenian Periadriatic fault: implications for Alpine - Carpathian extrusion models. Tectonics, 17: 690-709.

Geološka služba rudnika Mežica I. 1984-1989: Metalogenetska problematika kovinskih nahajališč v metamorfnih kameninah na Kobanskem in Pohorju, ECM Inštitut za gospodarski in socialni razvoj Ravne na Kor. Arhivska poročila o delu od 1984 do 1989.

Groat, L.A. 1996: The crystal structure of namuwite, a mineral with Zn in tetrahedral and octahedral coordination, and its relationship to the synthetic basic zinc sulfates. American mineralogist, 81/1-2: 238-243.

Grafenauer, S. 1965: Genetska razčlenitev svinčevih in cinkovih nahajališč v Sloveniji. Rud. Met. Zbornik, 2: 165-171.

Grafenauer, S. 1966: Metalogenija i mineraloške karakteristike bakrovih pojava u Sloveniji. Referati VI. savetovanja geologa SFRJ II, Ohrid, 377-396.

Hegemann, F. 1960: Über extrusiv-sedimentäre Erzlagerstätten der Ostalpen. II. Teil. Zeitschrift für Erzbergbau und Metallhüttenwesen, B.-A. XII: 122-127.

Hodenberg, R.V. Krause, W., Schnorrer-Köhler, G. & Täuber, H. 1985: Ramsbeckite, $(Cu, Zn)_7(SO4)_2(OH)_{10} \cdot 5H_2O$, a new mineral. Neues Jahrbuch für Mineralogie, Monatshefte: 550–556.

Mason, J.S. & Green, D. I. 1995: Supergene minerals including exceptional ramsbeckite from Penhriw mine, Ystumtuen, Dyfed. UK Journal of Mines and Minerals, 15: 21-27.

Mioč, P.& Ramovš A. 1973: Erster Nachweis des Unterdevons im Kozjak Gebirge (Posruck), westlich von Maribor (Zentralalpen). Bull. Sci. Cons., Acad. Sci. Yugosl. (A), 18/7-9: 135-136.

Mioč, P. 1978: Osnovna geološka karta SFRJ 1 : 100.000. Tolmač za list Slovenj Gradec. Zvezni geološki zavod, Beograd: 74 p.

Mioč, P. & Žnidarčič, M. 1977: Osnovna geološka karta SFRJ 1 : 100.000, list Slovenj Gradec. Zv. geol. zavod, Beograd.

Ohnishi, M., Kobayashi, S., Kusachi, I., Yamakawa, J. & Shirakami, M. 2004: Ramsbeckite from the Hirao mine at Minoo, Osaka, Japan. Journal of Mineral. and Petrol. Sci., 99: 19-24.

Orlandi, P. & Perchiazzi, N. 1989: Ramsbeckite, $(Cu, Zn)_{15}(OH)_{22}(SO4)_4 \cdot 6H_2O$, a first occurrence for Italy from "La Veneziana" mine, Valle dei Mercanti, Vicenza. Eur. Journ. Mineral., 1: 147–149.

Peacor, D.R., Dunn, P.J. & Sturman, B.D. 1987: Ramsbeckite: an American occurrence at the Ecton mine, Pennsylvania. Mineralog. Record, 18: 131–132.

Štrucl, I. 1984-1989: Metalogenetska problematika kovinskih nahajališč v metamorfnih
kameninah na Kobanskem in Pohorju, ECM Inštitut za gospodarski in socialni razvoj Ravne na Kor. Arhivska poročila o delu od 1984 do 1989.

Tornquist, A. 1929: Die perimagmatische Blei-Kupfer-Silber-Zinkerzlagerstätte von Offberg im Remschnigg. Akad. Wissenschaften, mat.-naturw. Kl. Abt. I, 138 /1-2: 47-68.

Žorž, Z. & Moser , B. 2002: Remšnik, zgodovina-geologija-minerali. Založba Voranc, Ravne na Koroškem.

Žorž, Z., Golob, F., Rečnik, A. & Hinterlechner-Ravnik, A. 2007: Mineralizirane alpske razpoke na Kobanskem in na severnem Pohorju. V: Rečnik, A. (ur.): Nahajališča mineralov v Sloveniji. Institut Jožef Stefan, Odsek za nanostrukt. materiale: 269-272.

Internetni viri dostopni / Internet resources available to 20.5.2013

Internet 1: http://www.mindat.org/min-3358.html

Internet 2: http://www.museumwales.ac.uk/en/800/?mineral=120

Internet 3: http://webmineral.com/specimens/picshow.php?id=966&target=Ramsbeckite

Internet 4: http://www.mindat.org/min-2837.html

GEOLOGIJA *56/1*, 073-086, Ljubljana 2013

doi:10.5474/geologija.2013.006

Ostanki rib iz miocenskih plasti Višnje vasi blizu Vojnika

Fish remains from Miocene beds of Višnja vas near Vojnik, Slovenia

Aleš ŠOSTER[1] & Vasja MIKUŽ[2]

[1]Dobrna 20, SI-3204 Dobrna, Slovenija; e-mail: geolog.baucig@mail.com

[2]Naravoslovnotehniška fakulteta, Oddelek za geologijo; Privoz 11, SI-1000 Ljubljana, Slovenija; e-mail: vasja.mikuz@ntf.uni-lj.si

Prejeto / Received 25. 3. 2013; Sprejeto / Accepted 15. 5. 2013

Ključne besede: ribe, morski psi (Elasmobranchii), špari (Sparidae), miocen, Centralna Paratetida, Višnja vas, Slovenija

Key words: fishes, sharks (Elasmobranchii), porgies (Sparidae), Miocene, Central Paratethys, Višnja vas, Slovenia

Izvleček

V prispevku so obravnavani ostanki zob morskih psov (Elasmobranchii, Neoselachii) in kostnic družine šparov (Teleostei, Sparidae) iz miocenskih glavkonitnih peščenjakov v Višnji vasi pri Vojniku. Ugotovljeni so ostanki zob, predvsem zobne krone hrustančnic rodov *Notorynchus*, *Carcharias*, *Carcharoides*, *Isurus* in *Cosmopolitodus* ter kostnice rodu *Pagrus*.

Abstract

This paper discusses fossil teeth of sharks (Elasmobranchii, Neoselachii) and porgies (Teleostei, Sparidae) from the Miocene glauconite sandstones of Višnja vas near Vojnik. The remains of fish teeth, mostly tooth crowns, belong to cartilaginous fishes of the genera *Notorynchus*, *Carcharias*, *Carcharoides*, *Isurus* and *Cosmopolitodus* and to a bony fish genus *Pagrus*.

Uvod

Naselje Višnja vas leži severno od Celja, natančneje vzhodno od Vojnika, ob glavni cesti Vojnik – Dobrna (sl. 1). Reka Hudinja, ki izvira v Rakovcu nad Vitanjem na Pohorju, je globoko erodirala podlago in razkrila izdanke miocenskih zelenih glavkonitnih peščenjakov, katerih izdanki so ob strugi potoka debeli tudi do treh metrov (sl. 2). Plasti v izdankih kažejo jasno plastnatost ter rahlo vpadajo proti jugozahodu. Omenjeni miocenski zeleni peščenjaki se raztezajo na območju v dolžini 11 km severozahodno do severno od Celja, kjer mejijo na anizijsko-ladinijske predornine pirešičkega vulkanizma in se stikajo s soteškimi plastmi; na njihovem južnem delu mejijo na miocenske govške plasti, skrajni vzhodni rob pa omejujejo ladinijski, delno metamorfozirani keratofirski tufi, ki se razprostirajo vzhodno, vse do Dramelj (Buser, 1979).

Peščenjaki so spodnjemiocenske starosti in jih stratigrafsko primerjamo z govškimi plastmi z znane lokacije Govce nad Laškim. Peščenjaki diskordantno ležijo na triasnih keratofirskih tufih.

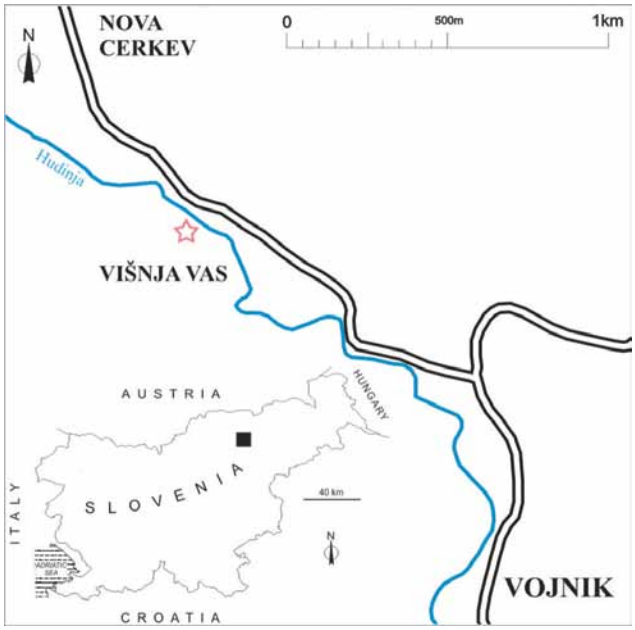

Sl. 1. Geografski položaj najdišča miocenskih rib pri Višnji vasi.

Fig. 1. Geographical position of site of Miocene fishes at Višnja vas.

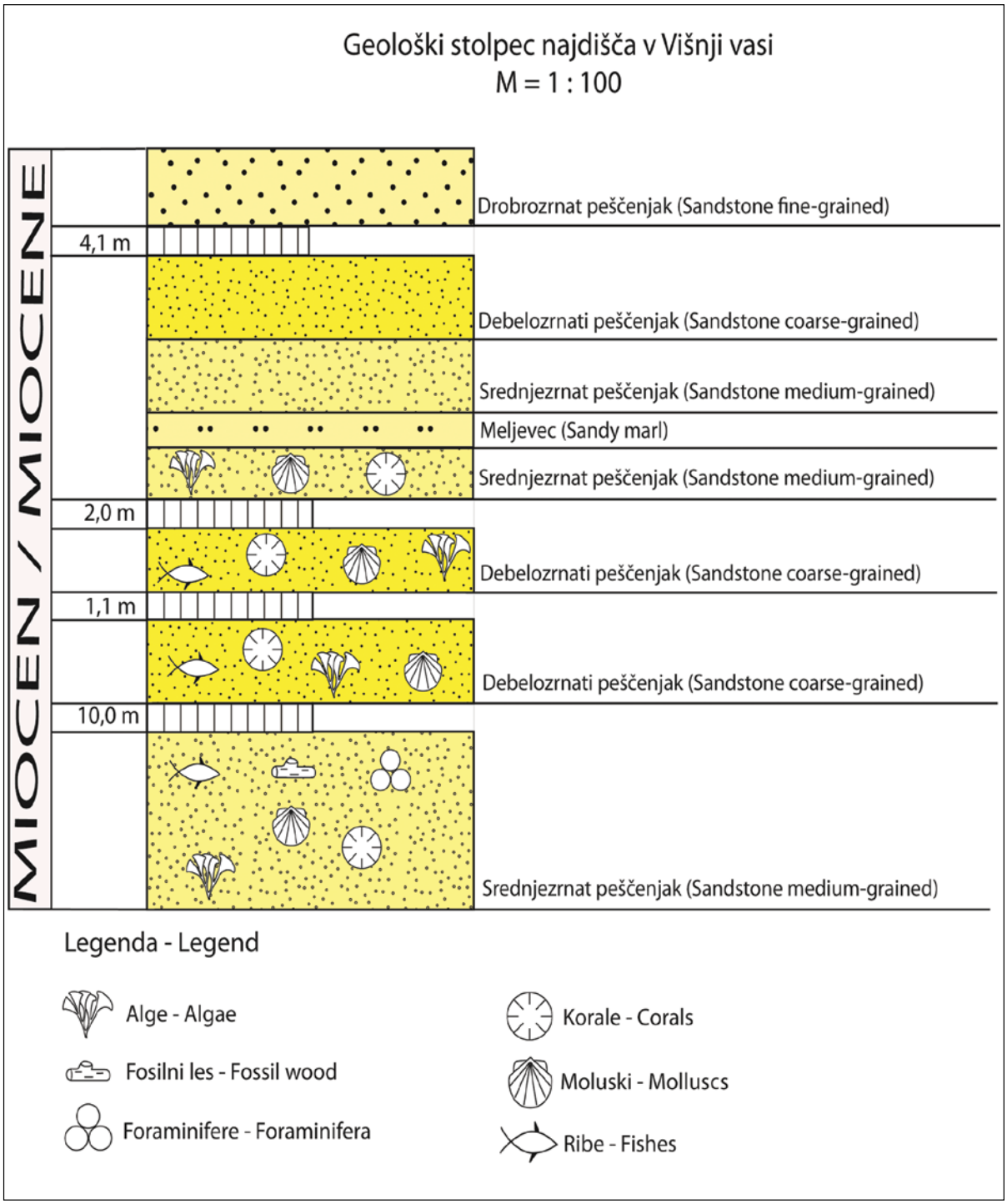

Sl. 2. Geološki stolpec najdišča Višnja vas
Fig. 2. Geological column of site Višnja vas

Večinoma gre za srednje do debelozrnate različke peščenjakov, ki ponekod v obliki zapolnitev paleoreliefa preidejo v konglomeratne bazalne tvorbe (Buser, 1979: 33). Peščenjaki so izrazito stratificirani v obliki bolj ali manj debelih plasti, med katerimi so tanke, do 2 mm debele lamine izredno drobnozrnatih sedimentov. Gre za postorogeni sediment ali molaso, ki je nastala, ko se je lokalno zaključil proces orogeneze.

Fosilna makrofavna je prisotna v spodnjem in srednjem delu izdanka, v debelo do srednjezrnatih peščenjakih, kjer so morski fosilni ostanki razmeroma pogosti. Sledijo še plasti meljevca in različno zrnatih peščenjakov, ki so brez vidnih fosilnih ostankov. V meljevcu in nad njim je fosilni zapis prekinjen (sl. 2). Očino je prišlo do okoljskih sprememb in najverjetneje je bila prekinjena komunikacija z morjem. Med fosili so makroskopsko opazni ostanki rib hrustančnic in kostnic, koral, alg, školjk (pekteni in ostrige) ter fosilnega lesa. Poleg navedenih fosilnih ostankov opazimo tudi foraminifere, ki so zaradi diagenetskih procesov povsem korodirane in zato nedoločljive.

Da bi ugotovili bolj zanesljivo starost kamnin pri Višnji vasi, smo dali v analizo tudi dva vzorca

na kalcitni nanoplankton. Žal v vzorcih, ki jih je pregledal dr. Miloš Bartol, ni bilo niti sledov kalcitnega nanoplanktona.

Dosedanje raziskave miocenskih rib v najdišču in na širšem območju

Z raziskavami miocenskih sedimentov se je v Sloveniji ukvarjalo več raziskovalcev, ki so med drugim navajali tudi najdbe fosilnih zob morskih psov, vendar so se le redki lotili tudi njihovega prepoznavanja in sistematske klasifikacije. Prve raziskave segajo v leto 1871, povezane so bile z odkrivanjem premogovih plasti znotraj soteških plasti. Izvajal jih je avstroogrski geolog Stur, ki v svojem poročilu omenja najdbe vretenčarjev in sesalcev v soteških plasteh. Ne navaja za kakšne najdbe gre, vendar lahko sklepamo, da gre za zobovje. Med letoma 1880 in 1882 je v okolici Mozirja raziskoval Kramberger, ki je poleg rastlinskih ostankov navedel tudi najdbe skeletov in zob rib kostnic, ostanke hrustančnic pa je našel le v fragmentarni obliki. Sklepal je, da gre za rodova *Hemipristis* in *Lamna*. Kasneje omenja najdbo vretenčarjev v svojem članku Hoernes (1883: 212), ki jih umešča v spodnjemiocenski del soteških plasti, ne zapiše pa, kakšni fosili so bili najdeni. Mikuž (1999) je pisal o velikozobem morskem psu vrste *Carcharocles megalodon* iz badenijskih plasti nad Trbovljami. Še posebej se je posvetil razlikam med rodovama *Carcharocles* in *Carcharodon*, ki so ju mnogi avtorji dotedaj zmotno zamenjevali. Majcen (2001: 26) navaja najdbo zoba morskega psa *Isurus oxyrhynchus hastalis* pri vasi Govce nad Laškim, v značilnih miocenskih govških peščenjakih. Brezigar (2007: 263) v svojem članku omenja najdbo zob morskih psov iz karpatijskih klanških plasti v okolici Dobrne, kjer med makrofavno navaja zobce morskih psov, fragmente ehinodermov, korale, mahovnjake in školjke. V članku pa se ni ukvarjal z razpoznavanjem in uvrščanjem zob. Križnar (2008: 28) v članku poroča o najdbah šestškržnega morskega psa *Notorynchus primigenius* iz srednjemiocenskih plasti kamnoloma Lipovica in spodnjemiocenskih plasti pri Moravčah. Križnar (2011: 40) predstavlja najdbe zob rib kostnic iz okolice Moravč, iz najdišč z območja med Zagorjem, Trbovljami in Hrastnikom ter pri Govcah, v tako imenovanih govških plasteh. Ribe naj bi pripadale družini Sparidae, ter rodovom *Sparus*, *Diplodus*, *Dentex* in en najden primerek rodu *Sphyraena*. Navaja še, da se tovrstno združbo rib našli na celotnem območju Centralne Paratetide in Mediterana.

Paleontološki del

Sistematika po: Cappetta 1987

Classis Chondrichthyes Huxley, 1880
Subclassis Elasmobranchii Bonaparte, 1838
Cohort Euselachii Hay, 1902
Subcohort Neoselachii Compagno, 1977
Superordo Squalomorphii Compagno, 1973
Ordo Hexanchiformes De Buen, 1926
Subordo Hexanchoidei German, 1913
Familia Hexanchidae Gray, 1851

Genus *Notorynchus* Ayres, 1855

Notorynchus primigenius (Agassiz, 1835)
Tab. 1, sl. 1-3

1833-43 *Notidanus primigenius* Agass. – Agassiz, 218, Tab. 27, Figs. 9, 13, 16-17
1855 *N. primigenius* – Giebel, 116, Taf. 47, Fig. 3
1858 *Notidanus primigenius* Ag. – Probst, 124-126, Figs. 7-10
1922 *Notidanus primigenius* Ag. – Vardabasso, Fig. 15, 15a-15b
1955 *Hexanchus (Notidanus) primigenius* Agassiz – Veiga Ferreira, 35, Est. 7, Fig. 52
1957 *Notidanus primigenius* Agassiz – Leriche, 22, Pl. 1, Figs. 1-6
1959 *Notidanus primigenius* Agassiz, 1843 – Kruckow, 85, Taf. 1, Figs. 1-2
1964b *Notidanus primigenius* Agassiz, 1843 – Glikman, 158, Tab. 6, Fig. 1-1a
1965 *Notidanus primigenius* Agassiz, 1843 – Radwański, Pl. 1, Figs. 1-2
1966 *Hexanchus primigenius* (Agg.) – Steininger, Taf. 3, Fig. 3
1968 *Hexanchus primigenius* (Agassiz, 1843) – Schultz, 68, Taf. 1, Figs. 1-7
1969 *Notidanus primigenius* Agassiz 1843 – Menesini, 9, Taf. 1, Figs. 1-6
1971 *Hexanchus primigenius* (L. Agassiz, 1843) – Brzobohatý & Schultz, 720, Taf. 1, Fig. 8a-8b
1971 *Hexanchus primigenius* (Agassiz, 1843) – Schultz, 315, Taf. 1, Figs. 1-3
1973 *Hexanchus primigenius* (Agassiz, 1843) – Brzobohatý & Schultz, 656, Taf. 1, Figs. 4-5
1978 *Hexanchus primigenius* (Ag.) – Brzobohatý & Schultz, 456, Taf. 1, Figs. 1-3
1987 *Notorhynchus primigenius* (Agassiz, 1843 B) – Cappetta, 48
1990 *Notorynchus primigenius* (Agassiz, 1843) – Kruckow & Thies, 26
1995 *Notorhynchus primigenius* (Agassiz, 1843) – Holec, Hornáček & Sýkora, 38, Pl. 8, Figs. 1-2
1996 *Notorhynchus primigenius* (Agassiz, 1843) – Hidden, 55, Taf. 2, Fig. 1
1998 *Notorhynchus primigenius* (Agassiz) – Schultz, 122-123, Taf. 55, Figs. 1-2, 3a-3b
2001 *Notorynchus primigenius* (Agassiz, 1843) – Reinecke, Stapf & Raisch, 7, Taf. 3, Figs. c, d
2005 *Notorynchus primigenius* (Agassiz, 1835) – Reinecke et al. 8,Taf. 2, Fig. 2
2007 *Notorynchus primigenius* (Agassiz, 1843) – Kocsis, 29, Figs. 3.1-3
2008 *Notorynchus primigenius*. – Križnar, 28, Sl. 1
2011 *Notorynchus primigenius* (Agassiz, 1835) – Reinecke et al., 9, Pl. 4, Fig. 8a-c
2012 *Notorynchus primigenius* (Agassiz, 1833) – Ávila, Ramalho & Vullo, 174, Figs. 3, 1-2

Material: Uporabljeni trije primerki zob v kamnini, od tega dva primerka z ohranjenim bazalnim delom.

Opis zoba: Apikalno asimetričen zob z nazobčano krono, ki ima gladek rezalni rob. Zobna krona sestoji iz primarne največje konice, distalno ima še več manjših konic, navspred sledi nekaj zelo drobnih in nizkih konic, ki se zaključijo blizu koreninskega dela. Koreninski del je masiven in asimetričen, distalno je nizek, proksimalno visok.

Opazna je rahla ukrivljenost v mezialni smeri. Sklenina je temno rjave barve.

Velikosti zob:

Primerki Specimens	Višina in širina zoba (Height and width of tooth) mm	Višina krone (Crown height) mm	Debelina krone (Crown thickness) mm	Širina krone (Crown width) mm
Tab. 1, Sl. 1	/	11	3	11
Tab. 1, Sl. 2	15x?	10	/	23
Tab. 1, Sl. 3	14x?	6	3	14

Stratigrafska in geografska razširjenost: Reinecke in sodelavci (2011: 11-12) pišejo, da ima vrsta *Notorynchus primigenius* (Agassiz, 1835) veliko vertikalno in horizontalno razširjenost. Razširjena je od srednjega oligocena do srednjega miocena in se najde v prav vseh evropskih bioprovincah, severnomorski, keltsko-luzitanski, mediteranski in paratetidini. V miocenu je poznana tudi iz vzhodne obale ZDA. Po podatkih Križnarja (2008) so zobje vrste *Notorynchus primigenius* v Sloveniji najdeni v srednjemiocenskih plasteh kamnoloma Lipovica.

Superordo Galeomorphii Compagno, 1973
Ordo Lamniformes Berg, 1958
Familia Odontaspididae Müller & Henle, 1839

Genus *Charcharias* Rafinesque, 1810

***Carcharias* sp.**
Tab. 1, sl. 4-9; tab. 2, sl. 10-14

Material: Uporabljenih je bilo enajst primerkov zob, od tega devet v kamnini in dva izolirana. Zobna korenina je ohranjena le izjemoma v posameznih fragmentih.

Opis zob: Na zobeh, ki so predstavljeni na slikah 5, 7, 9, 12 in 13, vidimo apikalno simetrično krono z gladkim rezalnim robom in brez stranskih konic. Mezialni in distalni rezalni rob sta gladka in se enakomerno ožita proti konici. Krona je inklinirana proč od centra zoba, z opazno lingvalno ukrivljenostjo konice. Sklenina je temno rjave barve. Bazalni del je slabo ohranjen ali pa ga ni. Pri zobeh, ki so na slikah 4, 6, 8, 10, 11 in 14 opzujemo apikalno asimetrično krono z gladkim rezalnim robom in brez stranskih konic. Mezialni rezalni rob je gladek in se položno zaključi v konici. Distalni rezalni rob je rahlo inkliniran od centra zoba v distalno smer. Na konici je opazna lingvalno-labialna rekurvatura. Sklenina je temno rjave barve. Bazalni del je slabo ohranjen. Ponekod je vidna globoka zareza.

Pripomba: Zaradi manjkajočih zobnih korenin, ki so pomemben taksonomski kriterij, ter zaradi široke speciacije, pri rodu *Carcharias* vrst nismo izdvajali. V preteklosti so vse takšne zobce zmotno pripisovali vrsti *Carcharias acutissimus*, čeprav poznamo v miocenskih skladih še vrste *Carcharias vorax*, *C. cuspidatus*, *C. taurus* in *C. gustrowensis*.

Velikosti zob:

Primerki Specimens	Višina in širina zoba (Height and width of tooth) mm	Višina krone (Crown height) mm	Debelina krone (Crown thickness) mm	Širina krone (Crown width) mm
Tab. 1, Sl. 4	/	11	/	3
Tab. 1, Sl. 5	/	16	/	4
Tab. 1, Sl. 6	/	11	/	4
Tab. 1, Sl. 7	/	17	4	6
Tab. 1, Sl. 8	/	14	2	4
Tab. 1, Sl. 9	19x?	14	/	4
Tab. 2, Sl. 10	/	13	/	5
Tab. 1, Sl. 11	/	8	1	3
Tab. 2, Sl. 12	/	11	1	3
Tab. 2, Sl. 13	/	11	/	3
Tab. 2, Sl. 14	17x?	14	2	6

Stratigrafska in geografska razširjenost: Predstavniki tega rodu so številni po celem svetu, od spodnjega oligocena do danes. So geografsko zelo razširjeni, vrhunec doživijo v obdobjih med srednjim oligocenom in srednjim miocenom. Ostanki zob rodu *Carcharias* so zelo pogostni tudi v miocenskih skladih celotne Centralne Paratetide.

Carcharias gustrowensis (Winkler, 1875)
Tab. 2, sl. 15

2005 *Carcharias gustrowensis* (Winkler, 1875) – Reinecke et al., 19,Taf. 14, Fig. 4a-b
2011 *Carcharias gustrowensis* (Winkler, 1875) – Reinecke et al., 21, Pl. 21, Fig. 12a-b

Material: Uporabljen je en sam, delno poškodovan primerek zoba, s še ohranjenim mezialnim dentiklom.

Opis zoba: Apikalno asimetričen zob z gladkim rezalnim robom. Ohranjena je ena stranska konica. Bazalni del se mezialno-distalno razdeli na dva koreninska kraka. Mezialni rezalni zob je gladek in se od stranske konice strmo zaključi v konici. Distalni rezalni rob je gladek, ter nagnjen navzad. Krona je inklinirana proč od centra zoba v distalno smer. Obrobnica je ovalne oblike. Sklenina je temnorjave barve.

Velikost zoba:

Primerek Specimen	Višina in širina zoba (Height and width of tooth) mm	Višina krone (Crown height) mm	Debelina krone (Crown thickness) mm	Širina krone (Crown width) mm
Tab. 2, Sl. 15	9x?	5	/	8

Stratigrafska in geografska razširjenost: Po podatkih Reinecke-ja in sodelavcev (2005; 2011) je vrsta *Carcharias gustrowensis* prvikrat dokazana v zgornjeoligocenskih skladih na severovzhodu Nemčije, njena prednica pa je vrsta *Carcharias acutissimus*. V kamninah Severnomorskega bazena prevladujejo zobje vrste *Carcharias gustrowensis* nad vsemi drugimi vrstami rodu *Carcharias*. Vrsta *Carcharias gustrowensis* je najverjetneje iz reinbekija oziroma srednjega miocena, v lagenfeldiju izgine. V Ameriki je ista vrsta opisana iz burdigalijskih skladov formacije Pogo River v Severni Karolini (ZDA). V Sloveniji ta vrsta morskega psa do sedaj še ni bila najdena.

Familia Lamnidae Müller & Henle, 1838

Genus *Carcharoides* Ameghino, 1901

Carcharoides catticus (Philippi, 1846)
Tab. 2, sl. 16

1851 *Otodus catticus* – Philippi, 24, Tab. 2, Figs. 5-7
1968 *Lamna cattica* (Philippi, 1846) – Schultz, 82, Taf. 4, Fig. 58
1971 *Lamna cattica* (Philippi, 1846) – Brzobohatý & Schultz, 729
1973 *Lamna cattica* (Philippi, 1846) – Brzobohaty & Schultz, 663, Taf. 3, Fig. 1
1974 *Lamna cattica* (Philippi), 1846 – Menesini, 135, Tav. 1, Figs. 19a-19c, 20a-20b
1987 *Carcharoides catticus* – Cappetta, 94, Figs. 83e-h
1990 *Lamna cattica* (Philippi, 1846) – Kruckow & Thies, 45
1995 *Charcharoides catticus* (Philippi, 1846) – Holec, Hornáček & Sýkora, 42, Pl. 12, Fig. 2a-b
2005 *Charcharoides catticus* (Philippi, 1846) – Reinecke et al., 28, Taf. 19, Fig. 4a-c
2007 *Charcharoides catticus* (Philippi, 1851) – Kocsis, 33, Fig. 5. 2a-b
2011 *Carcharoides catticus* (Philippi, 1846) – Reinecke et al., 31, Pl. 28, Fig. 5a-c

Material: Uporabljen en sam primerek zoba, brez ohranjene zobne baze.

Opis zoba: Apikalno asimetrična krona z gladkim rezalnim robom in brez ohranjene stranske konice. Mezialni rezalni rob je gladek in se pod ostrim kotom zaključi v konici. Distalni rezalni rob je subvertikalen. Krona je nagnjena proč od centra zoba, na konici pa je opazna labialna ukrivljenost. Obrobnica je na mezialno-distalnem delu rahlo izbočena. Sklenina je svetlo rjave barve.

Pripomba: Vrsta se je razširila v morja Centralne Paratetide, Mediterana in Severnega morja skozi srednji oligocen do srednjega miocena. Zelo pogost je v miocenu Amerike. Glikman (1964) je bil mnenja, da je genus *Lamna* vezan le na miocen.

Velikost zoba:

Primerek Specimen	Višina in širina zoba (Height and width of tooth) mm	Višina krone (Crown height) mm	Debelina krone (Crown thickness) mm	Širina krone (Crown width) mm
Tab. 2, Sl. 16	/	11	/	5

Stratigrafska in geografska razširjenost: Po podatkih Reinecke-ja in sodelavcev (2005; 2011) se vrsta C*archaroides catticus* prvikrat pojavi v rupeliju v Böhlenski formaciji pri Leipzigu. V Mediteranu je vrsta *Carcharoides catticus* (Philippi, 1846) registrirana od akvitanija do langhija, v Centralni Paratetidi od eggenburgija do badenija, v sarmatiju je ni več. Tudi v časovno vzporednem reinbeckiju in lagenfeldiju v bazenu Severnega morja se ne pojavlja več. V Sloveniji ta vrsta morskega psa dosedaj še ni bila najdena.

Genus *Isurus* Rafinesque, 1810

Isurus oxyrinchus Rafinesque, 1810
Tab. 3, sl. 17, 18

1810 *Sp. Isurus Oxyrinchus* – Rafinesque Schmaltz, 12
1977 *Isurus oxyrhinchus* Rafinesque 1810 – Landini, 110, Tav. 3, Figs. 2a-2c, 7a-7c
1990 *Isurus oxyrinchus* Rafinesque 1810 – Kruckow & Thies, 45
2005 *Isurus oxyrinchus* Rafinesque, 1810 – Reinecke et al., 31,Taf. 17, Fig. 1a-1b
2011 *Isurus oxyrinchus* Rafinesque, 1810 – Reinecke et al., 37, Pl. 38, Figs. 3a-c, 4a-c

Material: Uporabljena dva primerka zob v kamnini, oba brez ohranjenega koreninskega dela.

Opis zob: Prvi zob je apikalno asimetričen z gladkim rezalnim robom (tab. 3, sl. 17). Mezialna rezalna ploskev je gladka in polkrožno konveksna, distalna ploskev je polkrožno konkavna, obe se združita v zašiljeni konici. Krona je inklinirana proč od centra zoba, rekurvatura ni opazna. Bazalni del na primerku ni ohranjen.

Drugi zob (tab. 3, sl. 18) je apikalno asimetričen masiven zob z gladkim rezalnim robom in brez stranskih zobčkov. Mezialni rezalni rob je gladek in se v obliki loka povija proti konici. Distalni rezalni rob je subvertikalen in se zaključi v konici. Krona je inklinirana od centra zoba, z rahlo lingvalno ukrivljenostjo. Sklenina je temno rjave barve. Bazalni del ni ohranjen.

Velikost zoba:

Primerka Specimens	Višina in širina zoba (Height and width of tooth) mm	Višina krone (Crown height) mm	Debelina krone (Crown thickness) mm	Širina krone (Crown width) mm
Tab. 3, Sl. 17	/	12	3	8
Tab. 3, Sl. 18	/	20	4	9

Stratigrafska in geografska razširjenost: Vrsta *Isurus oxyrinchus* Rafinesque, 1810 se po podatkih Reinecke-ja in sodelavcev (2005; 2011) prvikrat pojavi v bazenu Severnega morja v oligocenu, v spodnjem chattiju skupaj z vrsto *Cosmopolitodus hastalis* (Agassiz, 1838). Obe vrsti sta se obdržali do hemmoorija, do meje med spodnjim in srednjim miocenom (glavkonitni peski) skupaj z vrsto *Isurus retroflexus* (Agassiz, 1838). V Centralni Paratetidi je vrsta *I. oxyrinchus* prisotna od eggenburgija do badenija, v Mediteranu pa od akvitanija do pliocena.

Genus *Cosmopolitodus* Glückman, 1964a, b

Cosmopolitodus hastalis (Agassiz, 1838)
Tab. 3, sl. 19, 20

1838 *Oxyrhina hastalis* Agass. – Agassiz, 277, Tab. 34, Figs. 1-2
1849 *Oxyrhina hastalis* Ag. – Sismonda, 40, Tav. 1, Figs. 41, 43-44
1850 *Oxyrhina hastalis*, Ag. – Costa, 196, Tav. 9, Fig. 10
1964a *Cosmopolitodus hastalis* Agassiz, 1843 – Glikman, 231
1964b *Cosmopolitodus hastalis* (Ag.) – Glikman, 154
1965 *Oxyrhina hastalis* Agassiz, 1843 – Radwański, 269, Pl. 1, Fig. 3a-3c
1966 *Oxyrhina hastalis* (Agg.) – Steininger, Taf. 4, Fig. 1
1968 *Oxyrhina hastalis* Agassiz, 1843 – Schultz, 77, Taf. 2, Figs. 27-34
1969 *Isurus hastalis* (Agassiz) 1843 – Menesini, 15, Tav. 2, Figs. 7a-7c, 8a-8c
1971 *Isurus hastalis hastalis* (L. Agassiz, 1843) – Brzobohatý & Schultz, 731, Taf. 2, Figs. 10a-10b, 11a-11b
1971 *Isurus hastalis hastalis* (Agassiz,1843) – Schultz, 21
1972 *Isurus hastalis hastalis* (Agassiz) – Schultz, 489
1973 *Isurus hastalis hastalis* (L. Agassiz, 1843) – Brzobohatý & Schultz, 666, Taf. 3, Fig. 15
1973 *Isurus oxyrhychus hastalis* (Agassiz), 1843 – Caretto, 42, Tav. 7, Fig. 2a-2c
1974 *Isurus hastalis* (Agassiz), 1843 – Menesini, 129, Tav. 2, Fig. 6a-6c
1977 *Isurus hastalis* Agassiz 1843 – Landini, 107, Tav. 5, Fig. 18a-18c
1978 *Isurus hastalis hastalis* (Ag.) – Brzobohatý & Schultz, 458, Taf. 2, Fig. 18
1987 *Isurus hastalis* (Agassiz, 1843B) – Cappetta, 96
1990 *Isurus hastalis* (Agassiz, 1843) – Kruckow & Thies, 44
1995 *Isurus hastalis* (Agassiz, 1843) – Holec, Hornáček & Sýkora, 42, Pl. 12, Fig. 4a-b
2007 *Isurus hastalis* (Agassiz, 1843) – Kocsis, 34, Fig. 5. 8
2010 *Cosmopolitodus hastalis* (Agassiz, 1843) – Schultz, Brzobohatý & Kroupa, 500-501, Pl. 1, Figs. 10a-10b, 11a-11b
2011 *Cosmopolitodus hastalis* (Agassiz, 1838) – Reinecke et al., 36, Pl. 29, Fig. 7a-d

Material: Uporabljena sta dva izolirana primerka zob. Obema manjka bazalni del.

Opis zob: Apikalno simetričen zob z gladkim rezalnim robom. Mezialni rezalni rob je gladek, in se v loku zaključi v konici. Distalni rezalni rob zoba je gladek in zelo malo inkliniran proč od centra v distalni smeri. Ukrivljenost konice ni opazna. Bazalni del ni ohranjen. Sklenina je temno rjave barve (tab. 3, sl. 19).

Drugi zob (tab. 3, sl. 20) je apikalno asimetričen z gladkim rezalnim robom. Mezialni rezalni rob je gladek in distalno rahlo zakrivljen. Distalni rezalni rob je subvertikalen, in se pred konico povije v distalni smeri. Oba rezalna robova sta sploščena in ostra. Krona je inklinirana proč od centra zoba in opazna je lingvalna ukrivljenost. Sklenina je temno rjave barve. Bazalni del ni ohranjen.

Pripomba: Glikman (1964) navaja, da je vrsta *hastalis* tipična za rod *Cosmopolitodus*, z opombo, da je vrsta srednjemiocenska; sicer jo moramo pripisati k rodu *Isurus*.

Velikost zob:

Primerka Specimens	Višina in širina zoba (Height and width of tooth mm	Višina krone (Crown height) mm	Debelina krone (Crown thickness) mm	Širina krone (Crown width) mm
Tab. 3, sl. 19	/	4	1	3
Tab. 3, sl. 20	/	17	4	10

Stratigrafska in geografska razširjenost: Reinecke in sodelavci (2011) pišejo, da je vrsta *Cosmopolitodus hastalis* (Agassiz, 1838) v Severnomorskem bazenu živela od katija do pliocena, v Centralni Paratetidi je prisotna v vseh morskih skladih, v Mediteranu in drugod je registrirana od spodnjega miocena do srednjega pliocena. Ta kosmopolitska vrsta je bila najbolj pogostna v miocenu. Po Glikman-u (1964b) je vrsta *Cosmopolitodus hastalis* karakteristična za cono *Odontaspis crassidens* (cona 12) v evropskem srednjem miocenu.

Classis Osteichthyes Huxley, 1880
Subclassis Actinopterygii Klein, 1885
Divisio Teleostei Müller, 1846
Ordo Perciformes Bleeker, 1859
Familia Sparidae Bonaparte, 1851

Genus *Pagrus* Cuvier, 1817

Pagrus cinctus (Agassiz, 1836)
Tab. 3, sl. 21-25

1849 *Sphaerodus cinctus* Ag. – Sismonda, 21, Tav. 1, Figs. 2-4
1850 *Sphaerodus cinctus*, Ag. – Costa, 197, Tav. 9, Fig. 24
1955 *Sparus cinctus* Agassiz – Veiga Ferreira, 37, Est. 6, Fig. 38
1969 *Sparus cinctus* (Agassiz) – Menesini, 41, Tav. 7, Figs. 8, 9a-9b, 10a-10c, 11a-11b
1973 *Sparus cinctus* (Agassiz) – Caretto, 65, Tav. 14, Fig. 5a-b
1974 *Sparus cinctus* (Agassiz), 1843 – Menesini, 156, Tav. 8, Figs. 21a-21b, 23a-23c
1998 *Pagrus cinctus* (Agassiz) – Schultz, 126-127, Taf. 57, Fig. 3
2010 *Pagrus cinctus* (Agassiz, 1836) – Schultz, Brzobohatý & Kroupa, 504-505, Pl. 3, Figs. 8-9
2011 *Pagrus cinctus* – Križnar, 40, Sl. 1a-1c, 2

Material: Uporabljenih je bilo pet primerkov zob, vsi so v kamnini.

Opis zob: Simetrični do asimetrični zobje, v prerezu okrogle do eliptične oblike. Krone so nizke in hlebčasto konveksne. Posamezni zobje so sestavni deli zobovja v zgornjih in spodnjih čeljustnicah pri šparidah oziroma pagarjih. Bazalni deli zob niso ohranjeni. Sklenina je temno do svetlo rjave barve.

Velikost zob:

Primerki Specimens	Tab. 3, sl. 21	Tab. 3, sl. 22	Tab. 3, sl. 23	Tab. 3, sl. 24	Tab. 3, sl. 25
Premer Diameter	3 mm	5 mm	3 mm	3 mm	7 mm

Stratigrafska in geografska razširjenost: Pagar vrste *Pagrus cinctus* (Agassiz, 1836) je pogosten v morskem miocenu celotne Centralne Paratetide in Mediterana. Križnar (2011: 40) navaja najdbe ostankov vrste *Pagrus cinctus* iz okolice Moravč, z območja Zasavja, zlasti iz okolice Zagorja, Trbovelj in Hrastnika. Omenja jih tudi iz miocenskih govških plasti, ki se raztezajo od Govc proti Laškem.

Zaključki

V profilu spodnjemiocenskih zelenih do sivih skladnatih glavkonitnih peščenjakov v Višnji vasi pri Vojniku smo iz nabranega fosilnega materiala določili več vrst morskih psov, *Notorynchus primigenius* (Agassiz, 1835), *Carcharias* sp., *Carcharias gustrowensis* (Winkler, 1875), *Carcharoides catticus* (Philippi, 1846), *Isurus oxyrinchus* Rafinesque, 1810, *Cosmopolitodus hastalis* (Agassiz, 1838) in kostnico vrste *Pagrus cinctus* (Agassiz, 1836). Ohranjene so samo krone njihovih zob, ki so večinoma brez koreninskega dela, ali pa je ta le delno ohranjen. Čeprav so zobje rodu *Carcharias* najštevilčnejši, smo določili samo eno obliko, ker so zobje za ta rod brez ključnih vrstnih taksonomskih značilnosti. Razen tega je rod *Carcharias* v miocenu doživel zelo široko speciacijo. V Višnji vasi je ugotovljena tipična spodnje, lahko tudi srednjemiocenska ribja združba, ki je najdena v Centralni Paratetidi in v drugih evropskih bioprovincah. Ribji zobje z območja Višnje vasi so prvikrat raziskovani, opisani in predstavljeni.

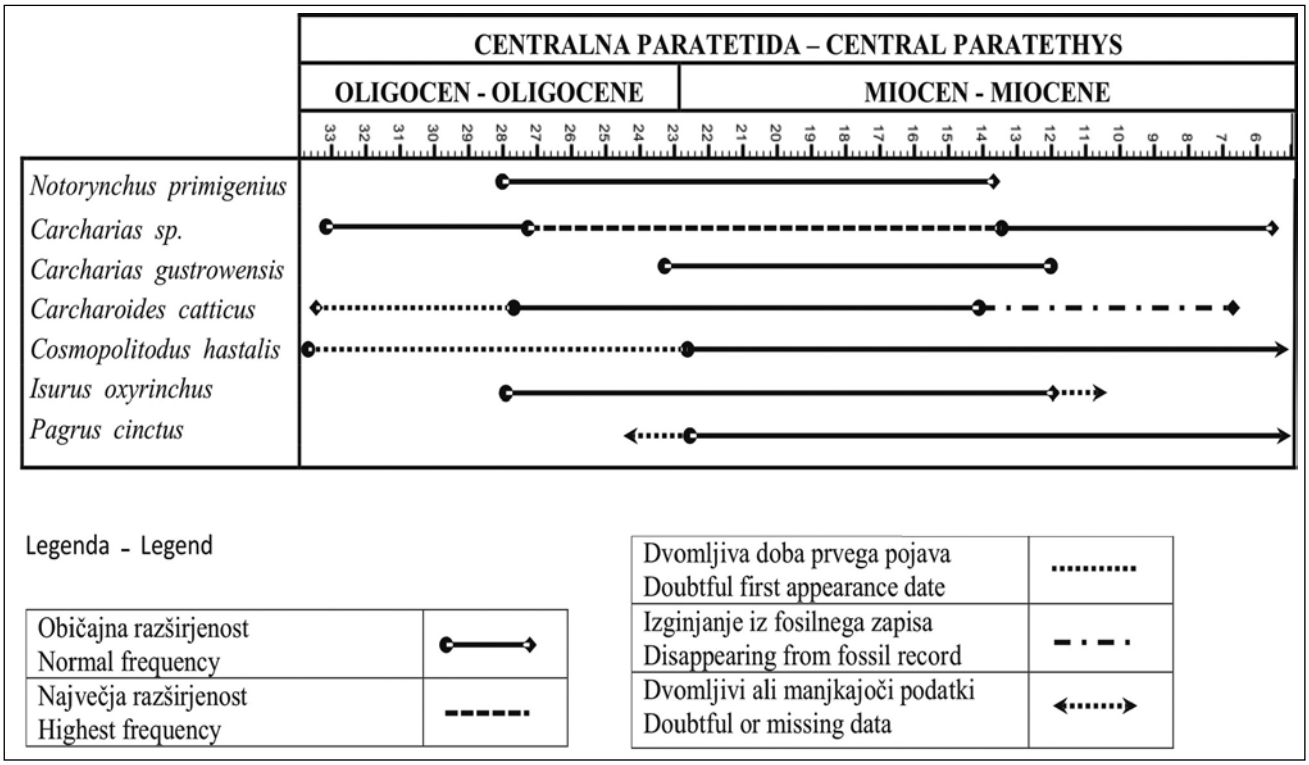

Sl. 3. Stratigrafska razširjenost vrst iz Višnje vasi.
Fig. 3. Stratigraphical distribution of species from Višnja vas.

Fish remains from Miocene beds of Višnja vas near Vojnik, Slovenia

Extended summary

In profile of Lower Miocene green to gray glauconite sandstones of Višnja vas near Vojnik we collected fossil material and determined several species of sharks: *Notorynchus primigenius* (Agassiz, 1835), *Carcharias* sp., *Carcharias gustrowensis* (Winkler, 1875), *Carcharoides catticus* (Philippi, 1846), *Isurus oxyrinchus* Rafinesque, 1810, *Cosmopolitodus hastalis* (Agassiz, 1838) and a bony fish species *Pagrus cinctus* (Agassiz, 1836). In most cases only teeth crowns were preserved with roots absent or partly preserved. The teeth belonging to the *Carcharias* genus were most abundant, however, only a single form was determined, as the fish teeth of this genus experienced significant evolutionary radiation during the Miocene. In the Višnja vas locality we determined a Lower to Middle Miocene fish assemblage typical of the Central Paratethys and other European bioprovinces. This paper presents the first study descriptions of fossil fish teeth from Višnja vas.

Zahvale

Za nasvete pri seznanjanju s potrebnimi predstavitvenimi tehnikami se zahvaljujeva tehničnemu sodelavcu Marijanu Grmu. Posebna zahvala gre Mihaelu Ravnjaku iz Zreč, stanujočemu na Cesti na Roglo 21, za posojene primerke in pomoč pri terenskem delu. Dr. Milošu Bartolu se zahvaljujeva za pregled dveh vzorcev na kalcitni nanoplankton in za prevode v angleščino.

Literatura – References

Agassiz, L. 1833-1843: Recherches sur les Poissons Fossiles. (Neuchatel, Suisse) 3: VIII, 1-390, Tab. 1-47, A-S.

Ávila, S. P., Ramalho, R. & R. Vullo, 2012: Systematics, palaeoecology and palaeobiogeography of the Neogene fossil sharks from the Azores (Northeast Atlantic). Annales Paléontologie, 98: 167-189.

Brezigar, A. 2007: Geološka pisna dediščina Šaleške doline in okolice. Geologija, 50/2: 233-245, doi:10.5474/geologija.2007.017.

Brzobohatý, R. & Schultz, O. 1971: Die Fischfauna der Eggenburger Schichtengruppe. In: J. Seneš (redaktor), Chronostratigraphie und Neostratotypen, Miozän der zentralen Paratethys, Bd. 2. M_1, Eggenburgien.Vydavatelstvo Slovenskey akadémie vied (Bratislava): 719-759, (Taf. 1-8).

Brzobohatý, R. & Schultz, O. 1973: Die Fischfauna der Innviertler Schichtengruppe und der Rzehakia Formation. In: Seneš, J. (redaktor): Chronostratigraphie und Neostratotypen, Mio-

---

TABLA 1 – PLATE 1

1 *Notorynchus primigenius* (Agassiz, 1835); spodnji zob; a) ustniča stran, b) jezična stran. Višnja vas pri Vojniku. Velikost: 9 mm x 5 mm.
Notorynchus primigenius (Agassiz, 1835); lower tooth; a) labial view, b) lingual view. Višnja vas near Vojnik. Size: 9 mm x 5 mm.

2 *Notorynchus primigenius* (Agassiz, 1835); spodnji desni antero-lateralni zob, jezična stran; Višnja vas pri Vojniku. Velikost: 14 mm x 25 mm.
Notorynchus primigenius (Agassiz, 1835); lower right antero-lateral tooth, lingual view; Višnja vas near Vojnik. Size: 14 mm x 25 mm.

3 *Notorynchus primigenius* (Agassiz, 1835); spodnji desni antero-lateralni zob, ustnična stran. Višnja vas pri Vojniku. Velikost: 15 mm x 12 mm.
Notorynchus primigenius (Agassiz, 1843); lower right antero-lateral tooth, labial view. Višnja vas near Vojnik. Size: 15 mm x 12 mm.

4 *Carcharias* sp.; zgornji zob, ustnična stran. Višnja vas pri Vojniku. Velikost: 11 mm x 3 mm.
Carcharias sp.; upper tooth, labial view. Višnja vas near Vojnik. Size: 11 mm x 3 mm.

5 *Carcharias* sp.; prvi sprednji zgornji zob, ustnična stran. Višnja vas pri Vojniku. Velikost: 16 mm x 4 mm.
Carcharias sp.; first anterior upper tooth, labial view.Višnja vas near Vojnik. Size: 16 mm x 4 mm.

6 *Carcharias* sp.; zgornji zob, ustnična stran. Višnja vas pri Vojniku. Velikost: 11 mm x 4 mm.
Carcharias sp.; upper tooth, labial view. Višnja vas near Vojnik. Size: 11 mm x 4 mm.

7 *Carcharias* sp.; zgornji zob, a) jezična stran b) s strani, c) ustnična stran. Višnja vas pri Vojniku. Velikost: 17 mm x 6 mm.
Carcharias sp.; upper tooth, a) lingual view, b) lateral view, c) labial view. Višnja vas near Vojnik. Size: 17 mm x 6 mm.

8 *Carcharias* sp.; zgornji zob, a) ustnična stran b) s strani c) jezična stran. Višnja vas pri Vojniku. Velikost: 14 mm x 4 mm.
Carcharias sp.; upper tooth, a) labial view, b) lateral view, c) lingual view. Višnja vas near Vojnik. Size: 14 mm x 4 mm.

9 *Carcharias* sp.; prvi sprednji zgornji zob, ustnična stran. Višnja vas pri Vojniku. Velikost: 18 mm x 4 mm.
Carcharias sp.; first anterior upper tooth, labial view. Višnja vas near Vojnik. Size: 18 mm x 4 mm.

TABLA 1 – PLATE 1

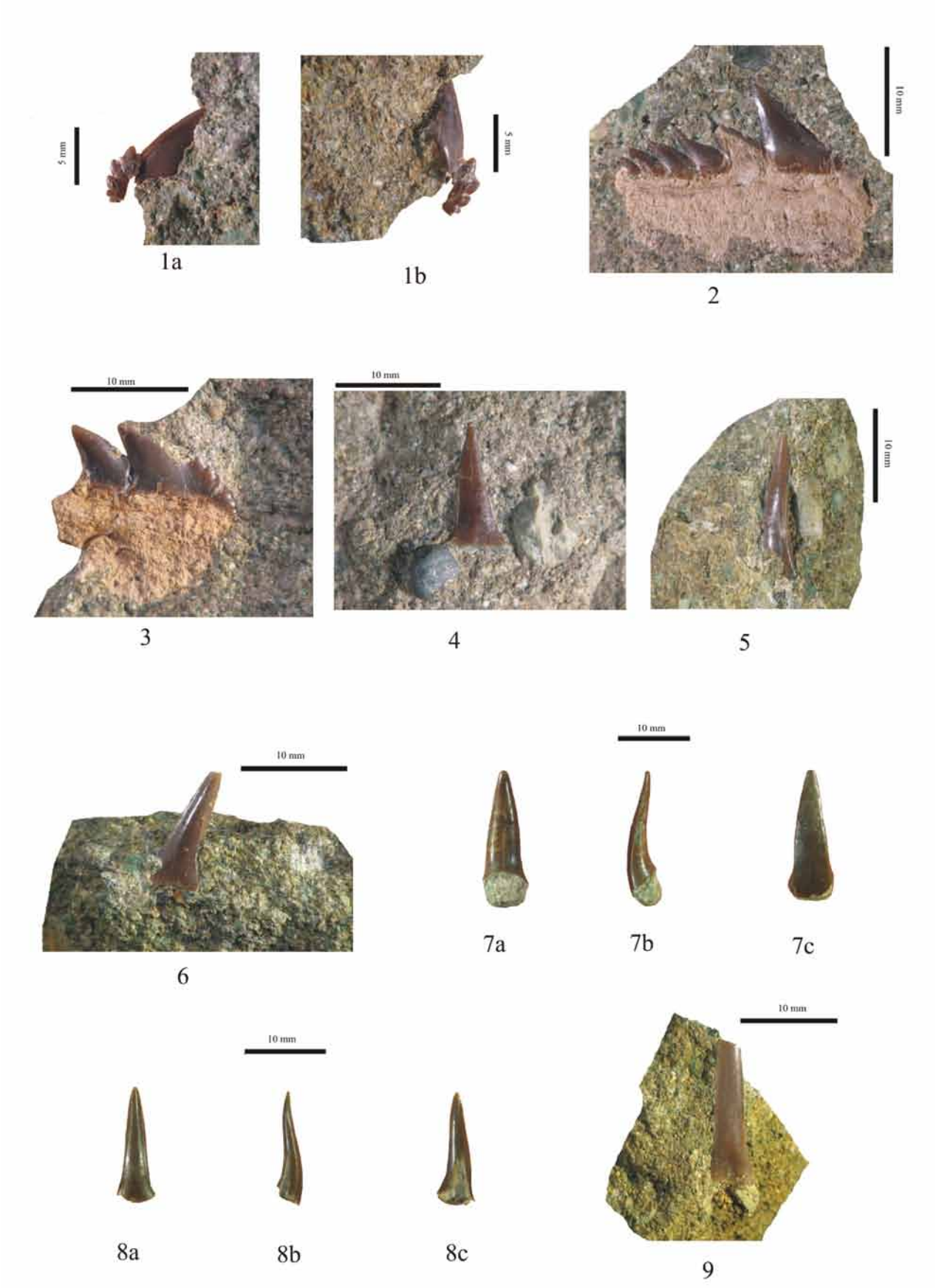

zän der zentralen Paratethys, Bd. 3. M_2, Ottnangien. Vydavatelstvo Slovenskey akadémie vied (Bratislava): 652-693, (Taf. 1-5).

Brzobohatý, R. & Schultz, O. 1978: Die Fischfauna des Badenien. In: Seneš, J. (redaktor): Chronostratigraphie und Neostratotypen, Miozän der Zentralen Paratethys, Bd. 6. M_4 Badenien (Moravien, Wielicien, Kosvien). Verlag der Slowakischen Akademie der Wiessenschaften (Bratislava): 441-464, (Taf. 1-5).

Buser, S. 1979: Tolmač lista Celje. Osnovna geološka karta SFRJ 1:100 000. Zvezni geološki zavod Beograd (Beograd): 1-72.

Cappetta, H. 1987: Chondrichthyes II. Mesozoic and Cenozoic Elasmobranchii. In: H.-P. Schultze, Handbook of Paleoichthyology, 3B. Gustav Fischer Verlag (Stuttgart, New York): 1-193, Figs. 1-148.

Caretto, P. G. 1973: Osservazioni tassonomiche su alcuni Galeodei del Miocene piemontese. Boll. Soc. Paleont. Italiana, (1972) 11/1:14-85, Tav. 3-14.

Costa, O. G. 1850: Paleontologia del regno di Napoli contenente la descrizione e figura di tutti gli avanzi organici fossili racchiusi nel suolo di questo regno. Parte 1. Stabilimento tipografico del Tramater (Napoli): 1-203, Tav. 1-15.

Giebel, C. G. 1855: Odontographie. Vergleichende darstellung des Zahnsystemes der lebenden und fossilen Wirbelthiere. Verlag von Ambrosius Abel (Leipzig): 1-129, Taf. 1-52.

Glikman, L. S. 1964a: Podklass Elasmobranchii. Akylovie. In: Orlov, J. A. (editor): Osnovi paleontologii. Spravočnik dlja paleontologov i geologov SSSR. Izdatelstvo »Nauka« (Moskva): 196-237.

Glikman, L. S. 1964b: Akuli paleogena i ih stratigrafičeskoe značnie. Izdatelstvo »Nauka« (Moskva-Leningrad): 1-227, Tab. 1-31.

Hiden, H. R. 1996: Elasmobranchier (Pisces, Chondrichthyes) aus dem Badenium (Mittleres Miozän) des Steirischen Beckens (Österreich). Mitt. Abt. Geol. Paläont. Landesmus. Joanneum 1994-95, 52/53: 41-109, (Taf. 1-10).

Hoernes, R. 1883: Ein Beitrag zur Kenntniss der miocänen Meeres-Ablagerungen der Steiermark. Mitt. Naturwiss. Vereines Steiermark. Jg. 1882, 19/20: 195-242, Taf. 1.

Holec, P., Hornáček, M. & Sýkora, M. 1995: Lower Miocene Shark (Chondrichthyes, Elasmobranchier) and Whale Faunas (Mammalia, Cetacea) near Mučín, Southern Slovakia. Geologické práce, 100: 37-52, Pl. 8-22.

Kocsis, L. 2007: Central Paratethyan shark fauna (Ipolytarnóc, Hungary). Geol. Carpathica, 58/1: 27-40.

Kramberger, D. 1880: Die fossilen Fische von Wurzenegg bei Prassberg in Steiermark. Jb. Geol.R.A, 30: 565-572.

Kramberger, D. 1882: Vorläufige Mittheilungen über die aquitanische Fischfauna der Steiermark. Ver. Geol. R.A.: 27-29.

Križnar, M. 2008: *Notorynchus primigenius* – zanimiv miocenski morski pes v Sloveniji. Društvene novice, 39: 28.

Križnar, M. 2011: Miocenski zobje rib kostnic iz Zasavja. Društvene novice, 44: 40-41.

Kruckow, T. 1959: Eine untermiozäne Haifisch--Fauna in Schleswig-Holstein. Meyniana, 8: 82-95, Taf. 1-2.

Kruckow, T. & Thies, D. 1990: Die Neoselachier der Paläokaribik (Pisces: Elasmobranchii). Cour. Forsch.-Inst Senckenberg., 119: 1-102.

Landini, W. 1977: Revisione degli »Ittiodontoliti pliocenici« della collezione Lawley. Paleontographia Italica, 70, n. ser. 40: 92-134, Tav. 12-16.

Leriche, M. 1957: Les Poissons néogènes de la Bretagne de L'Anjou et de la Touraine. Mém. Soc. Géol. France, (Nouv. Sér.) Mém., 81: 7-64, Pl. 1-4.

TABLA 2 – PLATE 2

10 Carcharias sp.; tretji sprednji zgornji zob, ustnična stran. Višnja vas pri Vojniku. Velikost: 13 mm x 5 mm.
Carcharias sp.; third anterior upper tooth, labial view. Višnja vas near Vojnik. Size: 13 mm x 5 mm.

11 Carcharias sp.; zgornji desni zob, jezična stran. Višnja vas pri Vojniku. Velikost: 8 mm x 3 mm.
Carcharias sp.; upper right tooth, lingual view. Višnja vas near Vojnik. Size: 8 mm x 3 mm.

12 Carcharias sp.; sprednji zgornji desni zob, ustnična stran. Višnja vas pri Vojniku. Velikost: 11 mm x 4 mm.
Carcharias sp.; anterior upper right tooth, labial view. Višnja vas near Vojnik. Size: 11 mm x 4 mm.

13 Carcharias sp.; ustnična stran. Višnja vas pri Vojniku. Velikost: 12 mm x 3 mm.
Carcharias sp.; labial view. Višnja vas near Vojnik. Size: 12 mm x 3 mm.

14 Carcharias sp.; sprednji zgornji tretji levi zob, jezična stran. Višnja vas pri Vojniku. Velikost: 17 mm x 6 mm.
Carcharias sp.; anterior upper third left tooth, lingual view. Višnja vas near Vojnik. Size: 17 mm x 6 mm.

15 Carcharias gustrowensis (Winkler, 1875); zgornji desni zob, jezična stran. Višnja vas pri Vojniku. Velikost: 9 mm x 9 mm.
Carcharias gustrowensis (Winkler, 1875); upper right tooth, lingual view. Višnja vas near Vojnik. Size: 9 mm x 9 mm.

16 Carcharoides catticus (Philippi, 1846); zgornji stranski desni zob, jezična stran. Višnja vas pri Vojniku. Velikost: 10 mm x 6 mm.
Carcharoides catticus (Philippi, 1846); upper lateral right tooth, lingual view. Višnja vas near Vojnik. Size: 10 mm x 6 mm.

TABLA 2 – PLATE 2

10

11

12

13

15

14

16

Majcen, T. 2011: Geološka učna pot na Govce. Že spet ali še vedno? Društvene novice, 44: 26-28.
Menesini, E. 1969: Ittiodontoliti miocenici di terra dž Otranto. Palaeontographia Italica 65, n. ser. 35: 1-61, Tav. 1-7.
Menesini, E. 1974: Ittiodontoliti delle formazioni terziarie dellž Arcipelago maltese. Palaeontographia Italica, 67 (1971) 37: 121-162, Tav. 54 (1)- 61(8).
Mikuž, V. 1999: Velikozobi morski pes *Carcharocles megalodon* (Agassiz) tudi v srednjemiocenskih-badenijskih plasteh nad Trbovljami. (The great-teeth shark *Carcharocles megalodon* (Agssiz) also from Middle Miocene-Badenian beds above Trbovlje, Slovenia). Geologija, 42: 141-150, (Tab. 1), doi:10.5474/geologija.1999.008.
Philippi, R. A. 1851: Ueber Tornatella abbreviata, Otodus mitis, Otodus catticus und Myliobatis Testae. Druck und verlag von Theodor Fischer. Palaeontographica – Beiträge Naturgeschichte Vorwelt, 1: 24-25, (Tab. 2).
Probst, J. 1858: Ueber das Gebiss des Notidanus primigenius Ag. Jh. Ver. Vaterl. Naturkde. Würtemberg, 14: 124-127.
Radwański, A. 1965: A contribution to the knowledge of Miocene Elasmobranchii from Pińczów (Poland). Acta Palaeontologica Polonica, 10/2: 267-276, Pl. 1-2.
Rafinesque Schmaltz, C. S. 1810: Caratteri di alcuni nuovi generi e nuove specie di animali e piante della Sicilia con varie osservazioni sopra i medesimi. Stampe di Sanfilippo: 3-105.
Reinecke, T., Louwye, S. Havekost, U. & Moths, H. 2011: The elasmobranch fauna of the late Burdigalian, Miocene, at Werder-Uesen, Lower Saxony, Germany, and its relationships with Early Miocene faunas in the North Atlantic, Central Paratethys and Mediterranean. Palaeontos, 20: 1-170, Pl. 1-101.
Reinecke, T., Moths, H., Grant, A. & Breitkreutz, H. 2005: Die Elasmobranchier des norddeutschen Chattimus, insbesondere des Sternberger Gesteins (Eochattium, Oberes Oligozän). Palaeontos, 8: 1-135, Taf. 1-60.
Reinecke, T., Stapf, H. & Raisch, M. 2001: Die Selachier und Chimären des Unteren Meeressandes und Schleichsandes im Mainzer Becken (Alzey--und Stadecken-Formation, Rupelium, Unteres Oligozän). Palaeontos, 1: 1-73, Taf. 1-63.
Schultz, O. 1968: Die Selachierfauna (Pisces, Elasmobranchii) aus den Phosphoritsanden (Unter-Miozän) von Plesching bei Linz, Oberösterreich. Naturkundl. Jb. Stadt Linz, 14: 61-102, Taf. 1-4.
Schultz, O. 1971: Die Selachier-Fauna (Pisces, Elasmobranchii) des Wiener Beckens und seiner Randgebiete im Badenien (Miozän). Ann. Naturhistor. Mus. Wien, 75: 311-341, Taf. 1-4.
Schultz, O. 1972: Eine Fischzahn-Brekzie aus dem Ottnangien (Miozän) Oberösterreichs. Ann. Naturhistor. Mus. Wien, 76: 485-490, Taf. 1.
Schultz, O. 1998: Tertiärfossilien Österreichs. Wirbellose, niedere Wirbeltiere und marine Säugetiere. Goldschneck-Verlag (Korb): 1-159, (Taf. 1-65).

TABLA 3 – PLATE 3

17 Isurus oxyrinchus Rafinesque, 1810; zgornji desni stranski zob, a) ustnična stran, b) s strani, c) jezična stran. Višnja vas pri Vojniku. Velikost: 12 mm x 9 mm.
Isuris oxyrinchus Rafinesque, 1810; upper right lateral tooth, a) labial view, b) lateral view, c) lingual view. Višnja vas near Vojnik. Size: 12 mm x 9 mm.

18 Isurus oxyrinchus Rafinesque, 1810; prvi zgornji sprednji zob, ustnična stran. Višnja vas pri Vojniku. Velikost: 21 mm x 8 mm.
Isuris oxyrinchus Rafinesque, 1810; first upper anterior tooth, labial view. Višnja vas near Vojnik. Size: 21 mm x 8 mm.

19 Cosmopolitodus hastalis (Agassiz, 1838); komisurin zob, jezična stran.Višnja vas pri Vojniku. Velikost: 5 mm x 3 mm.
Cosmopolitodus hastalis (Agassiz, 1838); commissural tooth, lingual view. Višnja vas near Vojnik. Size: 5 mm x 3 mm.

20 Cosmopolitodus hastalis (Agassiz, 1838); zgornji stranski zob, a) ustnična stran, b) s strani, c) jezična stran. Višnja vas pri Vojniku. Velikost: 11 mm x 8 mm.
Cosmopolitodus hastalis (Agassiz, 1838); upper lateral tooth, a) labial view, b) lateral view, c) lingual view. Višnja vas near Vojnik. Size: 11 mm x 8 mm.

21 Pagrus cinctus (Agassiz, 1836); zgornja stran. Višnja vas pri Vojniku. Premer: 3 mm.
Pagrus cinctus (Agassiz, 1836); occlusal view. Višnja vas near Vojnik. Diameter: 3 mm.

22 Pagrus cinctus (Agassiz, 1836); zgornja stran. Višnja vas pri Vojniku. Premer: 5 mm.
Pagrus cinctus (Agassiz, 1836); occlusal view. Višnja vas near Vojnik. Diameter: 5 mm.

23 Pagrus cinctus (Agassiz, 1836); zgornja stran. Višnja vas pri Vojniku. Premer: 3 mm.
Pagrus cinctus (Agassiz, 1836); occlusal view. Višnja vas near Vojnik. Diameter: 3 mm.

24 Pagrus cinctus (Agassiz, 1836); pogled s strani. Višnja vas pri Vojniku. Premer: 3 mm.
Pagrus cinctus (Agassiz, 1836); lateral view. Višnja vas near Vojnik. Diameter: 3 mm.

25 Pagrus cinctus (Agassiz, 1836); zgornja stran. Višnja vas pri Vojniku. Premer: 7 mm.
Pagrus cinctus (Agassiz, 1836); occlusal view. Višnja vas near Vojnik. Diameter: 7 mm.

Fotografije (Photos): Aleš Šoster

TABLA 3 – PLATE 3

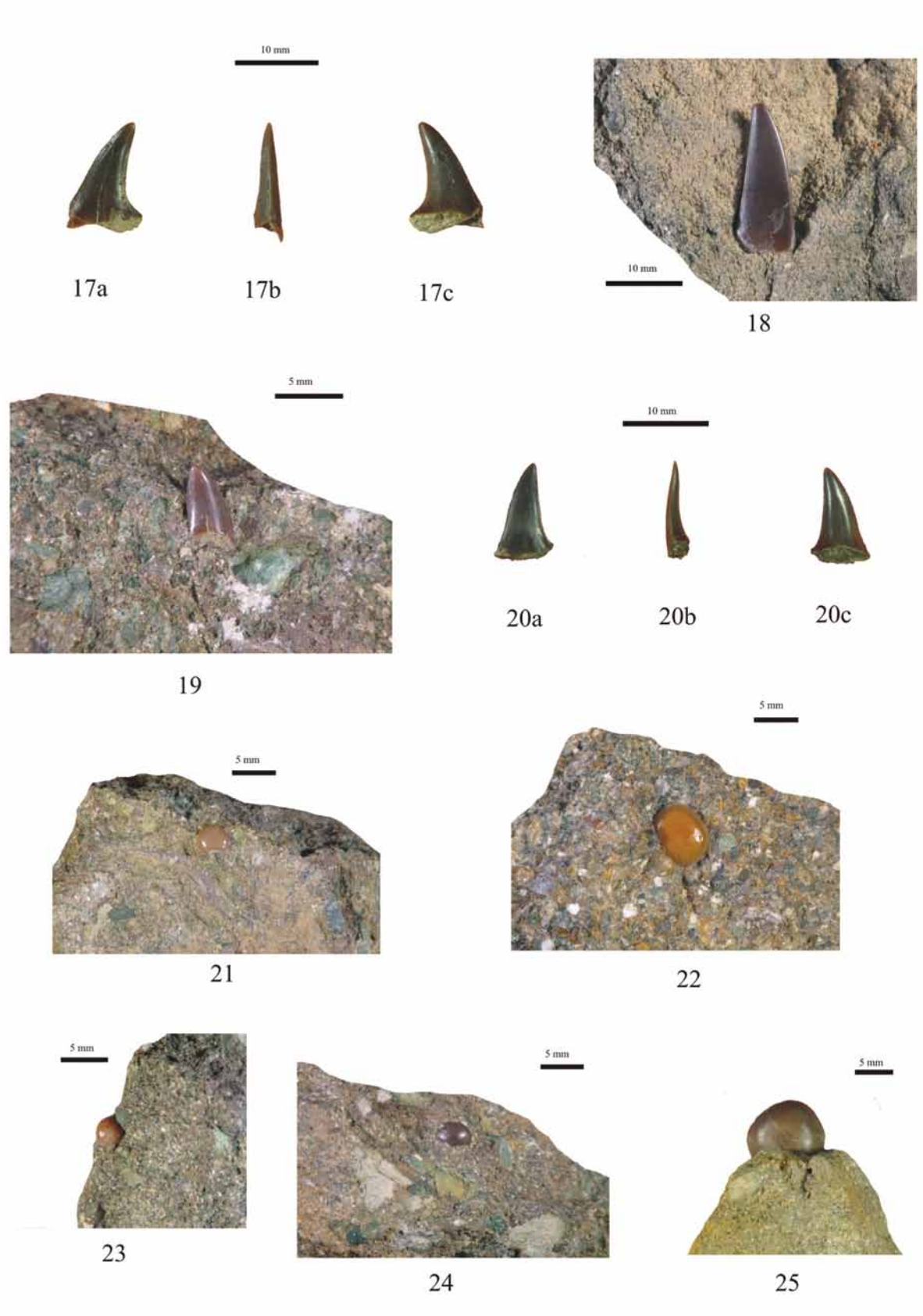

Schultz, O., Brzobohaty, R. & Kroupa, O. 2010: Fish teeth from the Middle Miocene of Kienberg at Mikulov, Czech Republic, Vienna Basin. Ann. Naturhistor. Mus. Wien, Serie A, 112: 489-506, (Pl. 1-3).

Sismonda, E. 1849: Descrizione dei pesci e dei crostacei fossili nel Piemonte. Mem. R. Accad. Sci. Torino, ser. 2, T.10: 1-88, Tav. 1-3.

Steininger, F. 1966: Über eine Fossiliensammlung aus dem Stadtbereich von Linz. Naturkdl. Jb. Stadt Linz, 12: 7-10, Taf. 1-4.

Stur, D. 1871: Geologie der Steiermark. Erläuterungen zur geologischen Uebersichtskarte des Herzogthumes Steiermark. Graz: XXXI, 1-654.

Vardabasso, S. 1922: Ittiofauna delle arenarie mioceniche di Belluno. Mem. Ist. Geol. Univ. Padova, 6: 1-23, Tav. 1-2.

Veiga Ferreira, O. 1955: A Fauna Miocénica da Ilha de Santa Maria (Açores). Comun. Serv. Geol. Portugal, 36: 9-40, Est. 1-11.

GEOLOGIJA *56/1*, 087–096, Ljubljana 2013

doi:10.5474/geologija.2013.007

Organic compounds in the urban dusts in Celje area

Organske spojine v urbanih prahovih na območju Celja

Gorazd ŽIBRET

Geological survey of Slovenia, Dimičeva ulica 14, SI – 1000 Ljubljana, Slovenia;
e-mail:gorazd.zibret@geo-zs.si

Prejeto / Received 18. 4. 2013; Sprejeto / Accepted 18. 6. 2013

Key words: attic dust, household dust, street sediment, organic pollutants, Celje, Slovenia
Ključne besede: podstrešni prah, hišni prah, cestni sediment, organske spojine, Celje, Slovenija

Abstract

This paper presents the results of the analysis of organic chemicals in different urban dusts. The aim of the research is preliminary evaluation of the presence of organic contaminants in household dust, attic dust and street sediment. Celje area has been chosen as a pilot study site due to availability of sampling materials from previous sampling campaigns. Samples have been tested to the presence of 120 organic compounds. Attic dust contains 98 different organic compounds or 82 % of all measured. Terpenoids, alkylbenzenes and different Polycyclic Aromatic Hydrocarbons (PAH's), as well as plasticizers, halogenated compounds (among them also PCB's) and pesticides (DDT and degradation products) can be found there. It also contains all of the in this study analysed US-EPA priority pollutants. Street dust contained 70 different organic chemicals (58 %), among them 14 priority pollutants. Traces of aliphatic organic compounds, PAH's, aldehydes and ketones, esters, and plasticizers are found there. House dust contains lowest number of organic compounds. Among 45 detected (38 % of total measured), 8 are priority pollutants. Aliphatic compounds, alkylbenzenes, aldehides, ketones, acids and PAH's can be found there. Current number of analysed samples, as well as only qualitative evaluations were made does not allow making any solid interpretation of obtained results in regarding to the potential sources of chemicals or potential environmental hazards. This study can thus be used only as a guideline for future studies of organic chemicals in urban dusts.

Izvleček

Na območju Celja je bilo do sedaj opravljenih veliko raziskav onesnaženja s strupenimi kovinami. Vendar pa je bilo opravljenih premalo raziskav v povezavi s tematiko onesnaženja z organskimi spojinami na tem območju. Zato je namen te raziskave preliminarno ugotoviti, katere organske spojine so prisotne v prahovih na tem območju. Zaradi bremen iz preteklosti lahko pričakujemo tudi obremenjenost okolja na področju onesnaženja z organskimi spojinami. Vzrokov je več, izpostavimo pa lahko poleg rastlinstva in mikrobnega delovanja, ki je naravni vir organskih spojin, potencialne antropogene vire, ki so: izhlapevanje spojin iz deponij katrana na območju stare Cinkarne (zaradi proizvodnje tehničnega plina iz premoga v preteklosti), delovanje današnje kemične, papirne in lesno-predelovalne industrije, promet in drugo izgorevanje fosilnih goriv, izhlapevanje spojin iz asfaltiranih površin in gradbenih materialov ter druge vire. V gospodinjstvih pa lahko k prej naštetim virom dodamo tudi uporabo kemikalij (barvila, laki, topila ipd.) in proizvodov, ki vsebujejo kemikalije (pohištvo, gradbeni materiali, tekstil, plastični izdelki ipd.), kajenje, kuhanje na plinu in ostale vire. V tej raziskavi smo analizirali vzorec podstrešnega prahu, ki kaže na „zgodovinsko" onesnaženje zraka, vzorec cestnega prahu, ki kaže na današnje stanje zraka in vzorec hišnega prahu, ki kaže na morebitno izpostavljenost ljudi. Analiziranih je bilo 120 različnih organskih spojin po metodi plinske kromatografije in masne spektroskopije, od tega jih 17 spojin spada pod t.i. prioritetna onesnažila, ki so na seznamu ameriške agencije za okolje. Podstrešni prah vsebuje največ različnih spojin (82 % od vseh analiziranih), od katerih so zastopane skoraj vse skupine (tabeli 1 in 2) organskih spojin. Najbolj značilne skupine so: terpenoidi, alkilbenzeni in policiklični aromatski ogljikovodiki in produkti delnega razpada le-teh. Zanimivo je tudi, da podstrešni prah vsebuje sledi DDT-ja (uporaba v kmetijstvu) in PCB-ja (industrija), ki sta oba že več kot 40 let prepovedana, a njihove ostanke še vedno lahko najdemo v njem. Cestni prah vsebuje 58 % vseh analiziranih spojin, od katerih so značilne skupine: policiklični aromatski ogljikovodiki, aldehidi in ketoni, etri, amini in plastifikatorji. Hišni prah vsebuje najmanj različnih spojin (38 % vseh analiziranih). V njem najdemo terpenoide, alkilbenzene, policiklične aromatske ogljikovodike, aldehide in ketone ter organske kisline. Od 17-ih analiziranih US-EPA prioritetnih polutantov, v podstrešnem prahu najdemo sledi prav vseh, v cestnem prahu 14 in v hišnem prahu 8 različnih. Ker v tej raziskavi ne razpolagamo s koncentracijami, ampak le s prisotnostjo snovi, prav tako pa je vzorcev malo, pa še ti so bili odvzeti zgolj na območju, kjer pričakujemo najvišjo stopnjo onesnaženja, ne moremo delati prav nobenih ocen, kakšni so morebitni viri spojin in ali predstavljajo prisotnosti rakotvornih spojin tveganje za okolje in zdravje ljudi. Analiz organskih spojin je draga metoda, zato je dodana vrednost te raziskave v tem, da lahko sedaj bolje načrtujemo morebitne nove raziskave organskih onesnažil v prahovih in okolju in ne „zapravljamo" denarja za analize spojin, katerih ne najdemo. S tem lahko zmanjšamo morebitne stroške. Avtor se zahvaljuje Radim Lána, ki je opravil analize, in Evi Franců (oba iz Češkega geološkega zavoda, izpostava Brno), ki je kot vodja laboratorija omogočila kemijsko analizo.

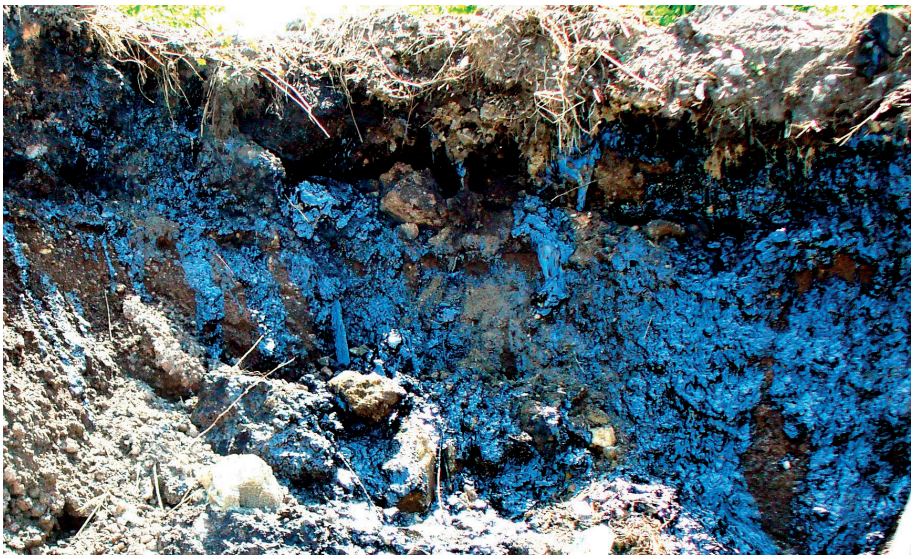

Fig. 1. Pyrometallurgical waste deposit and tar creosote around past Zn smelting furnaces in Celje.

Introduction

Celje area is well known for its environmental contamination. In the past studies main focus has been put on the evaluation of toxic metals contamination in soil due to past smelting and ironworking activities (Frančiškovič-Bilinski et al., 2006; Leštan et al., 2003; Lobnik et al., 1989; Šajn, 2005; Zupan et al., 2000; Žibret, 2002, 2008; Žibret & Šajn, 2008). But few researches have been done regarding the evaluation of organic pollutant contamination in the area, and even existing studies are focused mainly on the presence of very limited list of organic pollutants in drinking water.

This article presents the results of the chemical analyses of urban dusts in the Celje area by the means of gas chromatography / mass spectrometry. The focus has been put on the detection of the presence of 120 different organic substances. Description of the research area gives the main reason why the Celje area needs such pilot study. Materials and methods chapter describes the sampled materials, samples preparation, samples handling and chemical analyses. In the Results chapter results are presented and evaluated in the Discussion chapter. Main conclusions are presented in the Summary chapter.

Description of the research area

Celje, the third biggest town in Slovenia with the inhabitants around 50.000, lies in Celje basin in central Slovenia. It is surrounded with the Sava folds hills on the south (up to 1200 m above sea level) and with the Periadriatic lineament hill range on the north (1100 m above sea level). On the east side there is Voglajna River valley and on the west side the open space of Savinja River valley dominates.

Mayor pollution from the past was caused by zinc smelting by Cinkarna Celje plant. In its 100-year history of operation (between 1870 and 1970) approximately 500.000 tons of raw zinc has been produced (Žibret, 2008). On the peak of the production there has been 12 pyrometalurgical furnaces operating. This resulted in high rate of environmental pollution, caused by airborne particle sedimentation on the wider area of Celje basin. The Zn smelting process required highly caloric burning material, which was produced by coal gasification process. Formation of brownfield, containing highly toxic pyrometallurgical waste and coal tar creosote (Fig. 1) around past furnaces is a direct follow-up of zinc production. There were also other possible sources of organic chemicals, like Štore ironworks, traffic, small furnaces for heating of houses, chemical, paper and wood processing industry, metal manufacturing, domestic use of chemicals and products containing chemicals. Taking into account organic pollutants in Celje area several possible sources can thus be identified:

- Evaporation of volatile organic compounds from tar creosote in Celje brownfield area;
- Emissions from traffic;
- Past and present coal and other fossil fuel combustion for heating of houses and other purposes, including cooking with natural gas;
- Intensive hop and other crops farming west from Celje area and substantial use of phytopharmaceuticals;
- Emissions from Celje industry, including chemical industry, as well as wood processing, paper industry and others;
- Vaporisation of compounds from asphalt (tarred) surfaces and other construction materials;
- Domestic indoor and outdoor uses of chemical products or products containing chemicals.

Since atmospheric dust particles can travel distances of several hundred km from their source to their deposition, regional influences to the composition of the urban dusts might also be mentioned here. Two coal-powered power stations exist in the vicinity of Celje. The first one is Šoštanj power station, located 21 km NW and the other one is Trbovlje-Hrastnik power station,

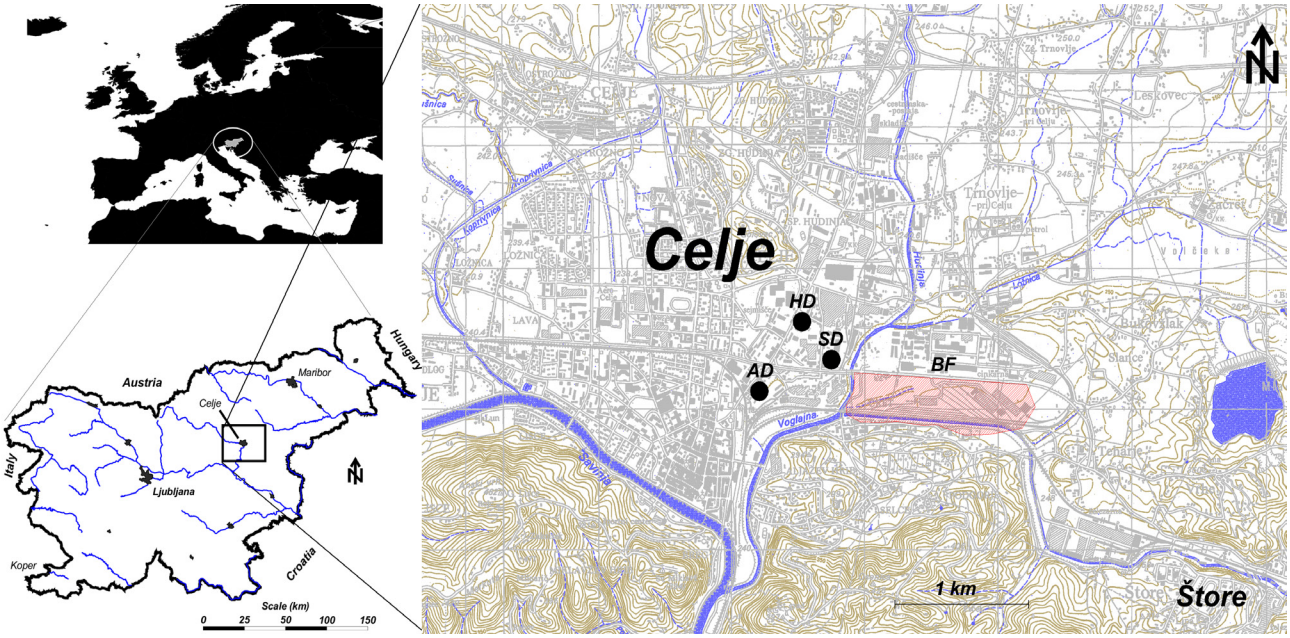

Fig. 2. The map of Celje area indicating the position of sampling points. HD - house dust sampling point; AD - attic dust sampling point; SD - street dust sampling point; BF - approximate area of pyrometallurgical slag and coal creosote deposit.

located 20 km SW. Cement factory is also located next to the aforementioned power plant. Mayor wind direction is SW wind. During the winter period, temperature inversion with fog is an important factor which influences the transportation of atmospheric particles.

Materials and methods

Three sampling materials have been chosen: attic dust, household dust and street sediment because of their availability from past studies (Žibret, 2002; Žibret & Rokavec, 2010). Positions of the samples are shown on Figure 2.

Attic dust has been sampled in the attics of old house in the vicinity of past Cinkarna Celje smelting plant and Celje brownfield where the highest Zn-Cd-Pb contamination has been detected (Šajn, 2005) and there is clear influence of Cinkarna Celje to the chemical composition of soil and attic dust detected. This sampling point also lies next to the busiest road in Celje (Mariborska Street). Attic dust is formed by the deposition of airborne particles. Being situated under the roof it is preserved from rain, heavy winds or sun's radiation, so it contains the record of past atmospheric pollution from the time the house was build. Its composition is not influenced by everyday activities of the inhabitants of the house (Balbanova et al., 2011; Bačeva et al., 2011; Šajn, 2006 and others). Sample was taken from the wooden roof bearing trams using plastic brush. Special attention was put not to sample possible roof tiling dust, sand from walls or possible plant remains. Sample in this study was collected in September 2001 in a building constructed in the beginning of 20 century, as a part of the other project, which aim was to evaluate the extent of toxic metal contamination in Celje area (Žibret, 2002; Šajn, 2005).

Street dust is regarded as a sink of atmospheric dust in urban environments (AYRAULT et al., 2013). It shows the contamination with particulate matter in the period of past 6 - 12 months. The reason for this is that storm events remove only a minority of the particles, deposited on the road surface (Chiew et al., 1997; Malmquist, 1978) and during rain events its composition is changed in the sense that larger particles are washed up so smaller particles prevail (Vaze & Chiew, 2002). Such dust cannot be removed by street sweeping, since street sweeper machines efficiently remove only particles larger than 0.25 mm, but they do not affect much of the particles below that size (Bender & Tarstreip, 1984). Therefore atmospheric deposit and pollutants build-up occurs on dry days and electrostatically bound to the pores in the asphalt or concrete in the form of street dust. Sample of street dust was brushed from the road surface with the hard plastic brush (Fig. 3) prior sweeping the road with the soft broom to remove sand particles. Approximately of 2 m^2 of road has to be brushed to collect enough atmospheric deposit. Road was brushed on 10-15 places in the radius of 20 m around sampling point to eliminate possible small-scale sample composition fluctuations. Importance of studying the street dust lies in the fact, that re-mobilised street dust by traffic is a dominant source of inhalable particles in urban environments (Amato et al. 2009; Piña et al. 2000; Sutherland, 2003).

Household dust reflects ambient air pollution and pollution from other sources, indoor and outdoor (ABT et al., 2000; TONG, 1998). The importance of studying house dust lies in the fact that this is the material we are exposed daily. Its latency is between 1 to 3 months. Its composition depends on the size of the house, dwelling habits of the inhabit-

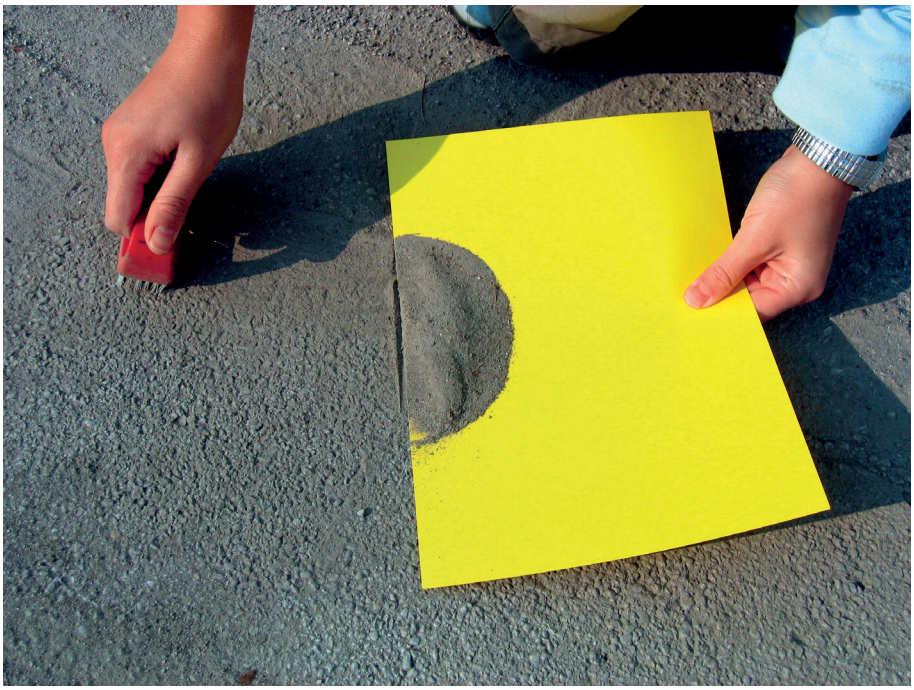

Fig. 3. Sampling of street dust sediment. After sweeping the surface with the soft broom to remove coarse particles, fine-grained dust were extracted from pores with the hard plastic brush.

ants, pet presence etc. Household dust sample was represented by three full vacuum cleaner bags from dwellings next to the sampling point. We sampled only bags, which were used for cleaning the interior of the houses or apartments. Bags, used for vacuuming of any construction works, paint jobs, pet droppings, cars or workshops were avoided. Conversation with the owner of the house helped to identify good samples. Samples of household dust and street sediment were taken in dry weather condition in the early spring 2009, as a part of the study of Žibret & Rokavec (2010).

Laboratory preparation of the samples included drying on 303K until no weight loss is observed, and sieving. When particles coagulated into clods due to the presence of humidity, the aggregates were softly crushed in the ceramic mortar. Fraction under 0.125 mm represented material for chemical analysis. Special procedure was applied to household dust sample preparation to remove as much fibres as possible. The contest of the vacuum cleaner bag (coagulates of hair, dirt, fibres etc...) was rubbed on the 1 mm sieve to extract finer particles (Fig. 4). Hair and other fibres and coarse particles were discarded. The remains were sieved with quick and strong hand shaking on 0.5 mm sieve, and after that the procedure was repeated with the 0.125 mm sieve. During this procedure majority of fibres were removed and only dry air deposit and possible soil particles remained.

Samples were stored in the dark and dry place in the air-sealed plastic containers prior chemical analyses, which were done in the Czech Geological survey, using gas chromatography and mass spectrometry. Only qualitative measurements were made for screening purposes for 120 different organic compounds. Extraction, fractionation and analysis were done according to Czech geological survey procedures (Franců et al., 2010). The presence of certain chemicals was evaluated according to the presence of the peak on the chromatogram. However, no evaluation of the peak significance was made.

Fig. 4. Household dust preparation. Material was rubbed on the 1 mm sieve. Fibres (right) were discarded, remains (left) were sieved several times on 0.5 and 0.125 mm sieves to remove as much smaller fibres as possible.

Results

Table 1 shows the aggregated results - presence of chemicals among different groups of organic compounds. The presence of the peak on chromatograph, representing a specific substance, is indicated in table 2. Unfortunately, chromatography data system for the identification of the substances, as well as identification of their sources, was unavailable to the author of this article. This is why extensive literature search was performed in order to try to interpret results. Special emphasis was put on the identification of possible origin of a certain substance, and to determine possible industrial or domestic use of it. We did not provide data sources for each of the chemicals separately, because table 2 would be too large and would loose its clarity. Therefore we provide a list of data sources for uses and occurrence for chemicals in table 2, which are:

1. Scientific books, chemical atlases and articles (Bryant et al., 2007; CCME, 2008; Harvey et al., 1991; Kavouras et al., 1998; Kingsbury et al., 1979; Melber, 2004; Tsapakis et al., 2002; U.S. EPA, 2006; US Public Health Service, 1995; Weschler & Nazaroff, 2008);
2. Chemical safety information factsheets (Internet 1 and 2),
3. Data from search engines of suppliers of chemicals (Internet 3 and 4)
4. Information from on-line chemical databases (Internet 5 and 6) and for fragrance and food additives (Internet 7);
5. If aforementioned information sources did not provided enough information for specific chemical, a search at google.com and duckduckgo.com search engines were performed.

Since there is not much scientific information about many of the analyzed organic chemicals in world literature, and even that is scattered in a vast amount of publications, also non-scientific sources of information were used to search for the specific chemical. Therefore provided information about the occurrence and use of chemicals can be incorrect or incomplete and this information must be therefore taken into account by knowing aforementioned fact.

A special emphasis was put on US-EPA priority pollutants list (Internet 8), which are regarded as high threat to the humans and environment. However, some studies revealed that also other chemicals can also be a similar environmental threat as US-EPA priority pollutants. When such study was found during literature search it is noted in the table 2, despite not indicated as being a priority pollutant.

Table 1 shows that attic dust is the most diverse "cocktail" of organic substances, containing 98 organic substances out of 120 analysed (82 %). It also contains all of the analysed priority pollutants and representatives of almost all of the analysed groups of organic chemicals. Among them the most abundant are terpenoids, alkylbenzenes and polycyclic aromatic hydrocarbons (PAH's). Street dust contains 70 of different organic compounds out of 120 analysed (58 %). PAH, aldehydes, ketones, ethers, amines and plasticizers are the most characteristic. Among 17 analysed priority pollutants, 14 were detected in street dust. House dust contains the fewest different organic compounds among three types of dusts - 45 compounds out of 120 analysed, which means 28 % of all analyzed. Terpenoids, alkylbenzenes, PAH's, aldehides and ketones, organic acids and other compounds can be found there. 8 out of 17 analysed priority pollutants were detected in house dust.

Table 1. Analysed groups of organic compounds. Table shows total number of different compounds analysed in a specific group (TOT) and detected in attic dust (AD), household dust (HD) and street dust (SD).

groups of chemicals	TOT. ANAL.	AD	HD	SD
Aliphatic compounds	5	3	3	3
Terpenoids and degradation products	17	16	6	5
Alkylbenzenes	8	8	4	2
Polycyclic aromatic hydrocarbons (PAH)s	51	49	21	38
Sulphur containing PAHs	7	5	3	2
Oxygen containing PAHs	4	4	1	3
Nitrogen containing PAHs	2	2	0	1
Oxygenated aromatic compounds	3	1	0	2
Alcohols and phenols	2	0	1	1
Aldehydes and ketones	3	1	2	3
Ethers	1	0	0	1
Amines	1	0	0	1
Acids	2	0	2	0
Esters	2	0	0	2
Plasticizers	5	3	1	4
Fragrances	3	1	1	1
Halogenated compounds	2	2	0	1
Pesticides and degradation products	1	1	0	0
Other compounds	1	1	0	0
TOTAL	120	98	45	70
%		82	38	58
PRORITY POLLUTANTS ANALYSED	**17**	**17**	**8**	**14**

Discussion

With only few data available, the interpretation of the results certainly contains the speculations, at some extent. From the number of different chemicals present in dusts it can be concluded, that diversity of organic molecules is decreasing in the following order: attic dust > street dust > house dust. The same order is also when we take into account priority pollutants. Lower number of different chemicals found in street dust in comparison with attic dust can be attributed to the fact that street dust is exposed in comparison to attic dust is exposed to

Table 2. Organic compounds identified in environmental samples from Celje (Slovenia). AD – attic dust; HD – household dust; SS - street dust. US-EPA priority pollutants are indicated with italic underline letters.

	occurrence & use	AD	HD	SS
Aliphatic compounds				
Homologues series of n-alkanes (C10 to C30)[a]		+	+	+
Series of various methylated n-alkanes[b]		+	+	+
n-alkylcyclohexanes with side chains[b]	intermediate in industrial processes, unstable	+		
n-alkylcyclohexenes[b,c]	intermediate in industrial processes, unstable		+	
Misc. alkyl cycloalkanes[b,c]	naturally occurring molecules; chrysanthemic acid, prostoglandins, steroids			+
Terpenoids and degradation products				
D-Limonene[b]	citrus, detergents, cosmetics, orange juice	+	+	+
Cymenes[b,c]	cosmetic, food, medicine	+	+	+
3-Methoxy-p-cymene[b]	wood industry, plant gradient, cumin, thyme	+		
(+)-4-Carene[b]	wood turpentine; paints, solvent, volatile oil	+	+	
Octahydro-4b,8-dimethyl-2-isopropylphenanthrene[b]	cigarette smoke, coal burning	+		
Cadalene[b]	essential oil of high plants	+		
Calamenene[b]	essential oil	+		+
a-Cedrene[b]	cedar oil, spices	+	+	
a-Muurolene	essential oil, perfumes, medicines		+	
Longicyclene[b]	essential oil (*Orchidacaea, Asparagales*)	+		
Junipene[b]	essential oil (*Abies cilicica*)	+		+
Ferruginol[b]	essential oil (*Sequoia sempervirens*), anti-tumour, anti-bacterial activity	+		
Squalene[b]	lipid, produced by plants, animals, incl. humans, olive oil, cosmetics, vaccines	+	+	+
Selinane[b]	enzymes, found in algae, plants and insects	+		
Isophyllocladene[b]	essential oil of *Araucaria excelsa*	+		
Aromadendran ('2')	flavonoid (Pinus sibirica)	+		
ß-Patchoulane	terpene, extracted from *Pogostemon cablin*	+		
Alkylbenzenes				
5-Ethyl-m-xylene[b]	wood, petrochemical, coke fuel, additive in gasoline	+		
Trimethylbenzenes[b,c]	coal tar, petroleum, mineral oils, gasoline additive, dyes, perfumes, scintilators	+	+	+
Tetramethylbenzenes[b,c]	toxic, curing agents, plastics, cross-linking agents, alkyd resins	+	+	+
Dimethylstyrenes[b,c]	flavour and fragrance agent; orchids Catasetum.	+		
Linear alkylbenzenes (Cx-benzenes)[b,c]	surfactants, detergents	+	+	
1-Methyl-4(1-methylpropyl)benzene[b]	-	+		
2,4-diphenyl-4-methyl-2(E)-pentene	-	+		
4,4'-Diacetyldiphenylmethane[b]	polyurethane foams	+	+	
Polycyclic aromatic hydrocarbons, PAH				
Naphtalene[a]	coal tar, heavy petroleum fractions, petroleum based fuels, coal, burning of wood and tobacco, indoor air pollutant	+	+	+
Ethylnaphthalene[b]	coal tar, heavy petroleum fractions (oil spills)			+
1-Methylnaphtalene[b]	coal tar, heavy petroleum fractions (oil spills)	+	+	+
2-Methylnaphtalene[b]	coal tar, heavy petroleum fractions (oil spills)	+	+	+
C2-Naphthalenes[b,c]	coal tar, heavy petroleum fractions (oil spills)	+	+	+
C3-Naphthalenes	coal tar, heavy petroleum fractions (oil spills)	+	+	+
C4-Naphthalenes	coal tar, heavy petroleum fractions (oil spills)	+		+
2-Phenylnaphthalene[b]	occurrence with PAH in sediments, decomposition of plastics, coal	+		+
Phenylmethylnephtalenes[b,c]	-	+		+
2,6-Diisopropylnaphthalene[b]	pesticides, natural plant growth regulator	+	+	+
Biphenyl[b]	organic compounds, plastics, coal tar, oil, natural gas, preservative (E230)	+	+	+
3- and 4-methylbiphenyl[b]	naturally occurrence in cocoa, spicy odour, flavouring agent	+		+
C2-Biphenyls[b,c]	organic compounds, plastics, emulsifiers, naturally occurrence in coal, crude oil and natural gas	+	+	+
1-Phenyl-1,3,3-trimethylindan	fragrance agent	+		+
Acenaphthylene[a]	coal tar	+		+
Acenaphtene[a]	coal tar	+		+
Fluorene[a]	coal tar	+	+	+
Methylfluorenes[b,c]	coal liquefaction by-product	+		+
Dimethylfluorene[b]	organic electroluminescent elements			+
1- and 2-phenylnaphthalenes[b,c]	plant lignans, found in organic sediments	+		+
Phenanthrene[a]	combustion by-product, cigarette smoke, coal burning	+	+	+
Anthracene[a]	coal tar, dyes, plastics, incomplete combustion of coal, gas or garbage	+		
2-Ethylanthracene	toxic to aquatic organisms	+		+
9-Phenylanthracene	component in crude oil, final stage of oil generation	+		
Methylphenanthrenes[b,c]	natural oil, coal-derived liquids, tar, traffic	+	+	+
Methylanthracenes[b,c]	diesel engines exhaust, crude oil component	+	+	+
Dimethylphenanthrenes[b,c]	wood combustion, motor vehicle exhaust, tars, coal-derived liquids, oxidation of resins	+	+	+

C3-Phenanthrenes[b,c]	cigarette smoke, coal burning, dyes, plastics, pesticides, garbage incineration, oil, oil marker	+	+	+
4H-Cyclopenta(def)phenanthrene[b]	pyrolysis product of catechol (precursor chemical of pesticides, flavours and fragrances), fuel component	+		
Retene[b]	coal tar fraction, resinous wood distillation	+		
Fluoranthene[a]	low-temperature combustion by-product, carcinogen	+	+	+
Pyrene[a]	incomplete combustion of organic compounds, coal tar	+	+	+
Methylfluoranthenes/-pyrenes[b,c]	?	+		+
o,p,m-Terphenyls[b,c]	fungus and mould growth prevention, sunscreen lotion component, pharmaceuticals, intermediate for many other chemicals	+		+
Benzo(ghi)fluoranthene[b]	tobacco smoke, fuel combustion	+		+
Chrysenea/Triphenylene[b]	coal tar, electronic and optic cables, wood preservative, stable	+	+	+
Benzo(a)anthracene[a]	coal tar, roasted coffee, smoked foods, automobile exhaust, intermediate for other chemicals, carcinogen	+		+
Methylbenz(a)anthracenes[b,c]	?	+		
Cyclopenta(cd)pyrene[b]	gasoline engine exhaust	+		
Methylchrysenes[b,c]	tobacco smoke, diesel engine emissions, carcinogen	+		+
1,2'- and 2,2'-Binaphthyl[b]	?	+		
Benzo(x)fluoranthene (x=j,b,k)[b,c]	tobacco smoke, incomplete combustion of fossil fuel, carcinogen	+	+	+
Benzo(a)pyrene[a]	coal tar, diesel engine exhaust, wood combustion, highly carcinogenic	+	+	+
Perylene[b]	tobacco smoke, Rylene dyes, in-situ biogenic origin from organic matter	+		
Indeno(1,2,3-cd)pyrene[a]	coal slurry, coal tar, tobacco smoke, gasoline engine exhaust	+	+	+
Dibenzo(a,h)anthracene[a]	automobile exhaust, cigarette smoke, carcinogenic	+		
Benzo(g,h,i)perylene[a]	incomplete combustion or pyrolysis of organic matter, fossil fuels combustion, cigarette smoke	+	+	+
Benzo(b)chrysene[b]	coal tar, airborne pollution (traffic)	+		
Coronene[b]	hydrothermal mineral carpathite, gasoline exhaust	+		
Dibenzopyrenes[b,c]	coal tar, forest fires, cigarette smoke	+		
Indeno(1,2,3-fg)naphthacene	tobacco smoke	+		
Oxygenated aromatic compounds				
Benzanthrone[b]	dyes, pyrotechnics industry-green and yellow colour smokes	+		
Sulphur containing PAHs				
Dibenzothiophene[b]	heavier fractions of petroleum	+	+	
Methyldibenzothiophene(s)	component of crude oil, occurrence in sedimentary rocks	+	+	
Dimethylbenzothiophene[b]	component of crude oil, occurrence in sedimentary rocks, coal-derived liquids		+	
C2-Dibenzothiophenes[b,c]	component of crude oil	+		
Benzo(b)naphtho(1,2 or 2,1-d) thiophene[b]	product of crude-oil microbial degradation	+		+
Mono- and dimethylbenzonaphthothiophenes[b,c]	product of crude-oil microbial degradation			+
Benzothieno(4,5-b)benzothiophene	?	+		
Oxygen containing PAHs				
Dibenzofuran[b]	coal tar, oil, insecticide, production of PVC, industrial bleaching and incineration	+	+	+
Methylbenzofuranes[b,c]	occurrence in coffee, flavouring agent	+		+
Benzonaphthofuran[b,c]	burning of residential waste, coal tar	+		+
Benzobisbenzofuranes[b,c]	oled diodes	+		
Nitrogen containing PAHs				
Carbazole[b]	coal tar; intermediate in synthesis of pharmaceuticals, agrochemicals, dyes, pigments, optoelectronics...	+		
Methylcarbazoles[b,c]	coal tar, crude oil;	+		+
Oxygenated aromatic compounds				
9-Fluorenol[b]	substance in coal	+		
Ditertbutylquinone	oxidant, polymerization catalyst			+
Benzanthrone[b]	dyes, pyrotechnics			+
Alcohols and phenols				
Butylated hydroxytoluene (BHT)[b]	antioxidant (=E321), fuel additive, hydraulic fluid, jet fuel, rubber		+	
Di-tert-butylphenol	antioxidant in petrochemicals and plastics, aviation fuel			+
Aldehydes and ketones				
Misc. n-aldehydes[b,c]	polyurethane and other construction materials production, plastics, essential oils	+	+	+
Misc. x-alkanones[b,c]	solvent, polymer precursor, pharmaceuticals, natural molecules		+	+
Diisobutyl ketone[b]	solvent (leather, cleaning, paint, lack...)			+
Ethers				
Dioctyl ether	lubricant , anti-static agent, electrical insulator, water repellent			+
Amines				
Diphenylamine[b]	food			+
Acids				
Misc. n-alkanoic acids[b,c]	soap, food, drugs, rubber, dyes, perfumes		+	
Benzoic acid	food preservative (E210), pharmaceutics, sunscreen, body wash...		+	
Esters				
Isopropyl myristate[b]	cosmetics			+
Methylpalmitate	detergents, resins, plastics, lubricants, food			+

Plasticizers				
Diethylphthalate[b]	cosmetics, detergents, sprays	+		+
Dibutyl phthalate (DBP)[b]	solvent, additive to pesticides, repellents, adhesive, ink	+		+
Di-iso-butylphthalate[b]	PVC, PVC copolymers, footwear, jackets			+
Bis(2-ethylhexyl)phthalate (DEHP)[b]	PVC, capacitors, hydraulic fluid	+		+
Phthalic anhydride	plastics, paints, urethane polyester, insect repellent		+	
Fragrances				
?-, ?-Muurolene[b]	herbs, spices, wood	+		
Geranylacetone[b]	perfumery, food (chocolate, marzipan)		+	
Hexahydrofarnesyl acetone	long-lasting fresh jasmine, celery odour			+
Halogenated compounds				
Mixture of di- to hexachlorinated biphenyls (PCB's)[a,b]	heat-transfer fluids, dielectric fluid, persistent pollutant, carcinogenic	+		
Tetrachloro-m-xylene[b]	pesticides & metabolites	+		+
Pesticides and degradation products				
o,p- and p,p-DDT	phytopharmaceutical, pollutant	+		
Other compounds				
Octasulfur	yellow sulphur powder	+		

[a] Identified by comparison of GC and MS data with those of reference compounds
[b] Identified by comparison of MS data with those of MS data bases (NIST98)
[c] Mixtures of isomers/homologues

the ultraviolet light from sun produce photo degradation and oxidation of many of the compounds. Also other weather influences might change the composition of street dust. As the retention time of the street dust is estimated to be between 6 to 12 months, certain chemicals, which are banned today, are no longer found there, but they are preserved in attic dust (such as DDT and PCB for example). Lowest number of compounds in house dust can be explained that certain chemicals can be effectively removed by regular cleaning of homes in contaminated environments.

First group of organic chemicals of interest are terpenoids, which are dominantly the compounds, found in plants. Their origin is from wood remains, pollen and other plant remains. Majority of terpenoids are of natural origin. They are most abundant in attic dust, most probably because attic dust contains a lot of pollen or similar windblown organic material. Alkylbenzenes are also abundant in all types of dusts. Since alkylbenzenes are usually biodegradable, we assume that their presence in dusts do not pose increased long-term environmental or health risk.

But the focus of future studies might be on PAH's and other aromatic compounds, since the occurrence of this group of chemicals has the major potential to pose a health or environmental risk. Some of them are regarded also as priority pollutants. Literature search points out the source of PAH's are dominantly coal tar and by-products of incomplete combustion of all types of burning materials. From current dataset it is impossible to determine the source of PAH's in Celje. Traffic and burning of fossil fuels can be suspected to be responsible for their presence. But it can be speculated that vaporisation from tar at the Celje brownfield can also be an important source of PAH's in the attic and street dust, and to some extent also in house dust. It is interesting, that also short-lived PAH's are present in attic dust. Thus it can be suspected that a continuous source of such compounds exists in Celje. Regarding the the occurrence of PAH's indoors, it must be denoted that beside outdoor sources also smoking, grilling of food, wood burning for heating (like fireplace indoors), vaporisation of petroleum products and burning of natural gas can all be possible indoor sources.

Aldehides and ketones, ethers, amines, organic acids, esters and fragrances are abundant natural molecules and usually do not pose increased risk at exposure to small quantities, so their occurrence will not be discussed here.

Another group which contains priority pollutants are plasticizers, and this group of chemicals might also be a focus of future studies. Street dust contains 4 among 5 chemicals from this group, attic dust 3 and house dust 1 representative. It can be speculated, that additives to construction materials can be a reason for plasticizer occurrences in urban atmosphere. House dust, contrary, contains no priority pollutant plasticizers. Among environmentally dangerous and carcinogenic pollutants, PCB's were found in attic dust, but not in street and house dust, which might indicate that PCB's are no longer emitted in Celje any more, but they were used at some point in the past. Last priority pollutant chemical is pesticide DDT and its degradation products. As at PCB case, they can be found only in attic dust, but not in street or house dust. This can be explained by the possible use of DDT containing insecticides for the hop and other crops production in the Celje area in the past, thus proving that attic dust is really a museum for atmospheric contamination in the area of interest, as being expressed by Davis & Gulson (2005). Our results also points out that no sources of DDT exist in Celje area today.

Conclusions

Attic dust, house dust and street dust samples from Celje area were analysed for the presence of 120 different organic substances using gas chromatography and mass spectrometry. Attic dust contains 82 % of organic substances, among them all of the US-EPA priority pollutants. Terpenoids,

alkylbenzenes and PAH's are the most abundant. Street dust contains 58% of analysed organic chemicals. Most abundant groups of compounds are PAH's, aldehydes, ketones, ethers, amines and plasticizers. House dust contains the least different organic compounds – 38 % of all analysed. Terpenoids, alkylbenzenes, PAH's, aldehides, ketones and organic acids can be found there. Among 17 analysed priority pollutants, all were detected in attic dust, 14 of them in street dust and 8 of them in house dust. Evaporation of organic compounds from Cinkarna brownfield, traffic and other types of fossil fuel combustion, use of certain chemical and natural products, construction, evaporation from tarred road surfaces, wood-processing and chemical industry, wood burning, as well as natural gas burning for cooking, smoking or food grilling can be suspected anthropogenical sources of detected organic chemicals.

Since no quantitative evaluation was made, this study must be used only as a guideline for possible further studies. Its main added value is that certain groups of chemicals are evaluated in street, attic and house dust, thus the results can point to the direction of future interests. Since analyses of organic compounds are expensive, this study can be very useful for reducing possible costs of future studies of organic pollutants. Moreover, an analysis of groundwater in the area around industrial waste deposit might be useful. Author recommendation is, that the most interesting groups of organic chemicals for the future studies of ambient dusts in Celje, as well as also in the other places, might be PAH's and plasticizers. Measuring actual concentrations of such organic compounds in different natural and anthropogenical materials in Celje area might be an useful follow-up of this study.

Acknowledgments

This study was made within the scope of programme group "Mineral resources" (P1-0025), funded by the Slovenian Research Agency. Author would like to kindly acknowledge the gratitude to the Radim Lána for chemical analyses, who was at the time when the chemical analysis were done employed at the Czech Geological Survey in Brno, and to Eva Franců, who kindly allowed to conduct the analyses in the laboratory she was in charge for.

References

Abt, E., Suh, H.H., Allen, G. & Koutrakis, P. 2000: Characterization of Indoor Particle Sources: A Study Conducted in the Metropolitan Boston Area. Environ. Health Persp. 108/1:35-44.

Amato, F., Pandolfi, M., Viana, M., Querol, X., Alastuey, A. & Moreno, T. 2009: Spatial and chemical patterns of PM_{10} in road dust deposited in urban environment. Atmos. Environ., 43:1650–1659.

Bačeva, K., Stafilov, T., Šajn, R., Tănăselina, C. & Ilić Popov, S. 2011: Distribution of chemical elements in attic dust in the vicinity of a ferronickel smelter plant. Fresenius environ. bull., 20/9:2306-2314.

Balabanova, B., Stafilov, T., Šajn, R., Bačeva, K. 2011: Distribution of chemical elements in attic dust as reflection of their geogenic and anthropogenic sources in the vicinity of the copper mine and flotation plant. Arch. environ. contam. toxicol., 61/2:173-184, doi:10.1007/s00244-010-9603-5.

Bender, G.M. & Terstriep, M.L. 1984: Effectiveness of street sweeping in urban runoff pollution-control. Sci. Total Environ., 33: 185-192.

Bryant, W.L., Goodbred, S.L., Leiker, T.L., Inouye, Laura & Johnson, B.T. 2007: Use of chemical analysis and assays of semipermeable membrane devices extracts to assess the response of bioavailable organic pollutants in streams to urbanization in six metropolitan areas of the United States; U.S. Geological Survey Scientific Investigations Report 2007–5113. US Geological Survey, 46 p.

CCME 2008: Canadian Soil Quality Guidelines for Carcinogenic and Other Polycyclic Aromatic Hydrocarbons (Environmental and Human Health Effects). Scientific Supporting Document. Canadian Council of Ministers of the Environment, Gatineau: 218 p.

Chiew, F.H.S., Duncan H.P. & Smith W. 1997: Modelling pollutant buildup and washoff: keep it simple. In Proceedings of the 24th International and Water Resources Symposium (131–136). New Zealand Hydrological Society, Auckland: 131-136.

Davis, J.J. & Gulson, B.L. 2005: Ceiling (attic) dust: a "museum" of contamination and potential hazard. Environ. Res., 99/2: 177-94.

Frančišković-Bilinski, S., Bilinski, H., Tibljaš, D. & Hanžel, D. 2006: Sediments from Savinja, Voglajna and Hudinja rivers (Slovenia), reflecting anomalies in an old metallurgic area. Fresen. Environ. Bull., 15/3: 220-228.

Franců, E., Schwarzbauer, J., Lána, R., Nývlt, D. & Nehyba, S. 2010: Historical Changes in Levels of Organic Pollutants in Sediment Cores from Brno Reservoir, Czech Republic. Water Air Soil Pollut., 209:81–91, doi:10.1007/s11270-009-0182-x.

Harvey, R.G. 1991: Polycyclic aromatic hydrocarbons: chemistry and carcinogenicity. University Press, Cambridge: 405 p.

Kavouras, I., Stratigakis, N. & Stephanou, E.G. 1998: Iso- and Anteiso-Alkanes: Specific Tracers of Environmental Tobacco Smoke in Indoor and Outdoor Particle-Size Distributed Urban Aerosols. Environ. Sci. Technol., 32: 1369-1377.

Kingsbury, G.L., Sims, R.C. & White, J.B. 1979: Multimedia Environmental Goals for Environmental Assessment; Volume IV. MEG Charts and Background Information Summaries (Categories 13-26). US EPA, Washington, DC: 401 p.

Leštan, D., Grčman, H. & Zupan, M. 2003: Relationship of soil properties to fractionation of Pb and Zn in soil and their uptake into Plantago lanceolata. Soil Sediment contam., 12/4: 507-522.

Lobnik, F., Medved, M., Lapajne, S., Brumen, S., Žerjav, E., Vončina, E., Štajnbaher, D. & Lobovič, A. 1989: Tematska karta onesnaženosti zemljišč celjske občine. Biotehniška fakulteta, oddelek za agronomijo, Ljubljana: 159 p.

Malmquist, P.A. 1978: Atmospheric Fallout and Street Cleaning - Effects on Urban Stream Water and Snow. Prog. Wat Tech., 10/5-6: 495-505.

Melber, C., Kielhorn, J. & Mangelsdorf, I. 2004: Concise International Chemical Assessment Document 62 – Coal Tar Creosote. World Health Organisation, Geneva: 140 p.

Piña, A.A., Torres, G.V., Monroy, M.F., Luszczewski, A.K. & Leyva, R.R. 2000: Scanning electron microscope and statistical analysis of suspended heavy metal particles in San Luis Potosi, Mexico. Atmos. Environ., 34: 4103–4112.

Sutherland, R.A. 2003: Lead in grain size fractions of road-deposited sediment. Environ. Pollut., 121:229–237.

Šajn, R. 2005: Using attic dust and soil for the separation of anthropogenic and geogenic elemental distributions in an old metallurgic area (Celje, Slovenia). Geochem., explor. environ. anal., 5/1:59-67.

Šajn, R. 2006: Factor analysis of soil and attic-dust to separate mining and metallurgy influence, Meža Valley, Slovenia. Math. geol., 38/6:735-747, doi:10.1007/s11004-006-9039-7.

Tong, S.T.Y. 1998: Indoor and Outdoor household dust contamination in Cincinnati, Ohio, USA. Environ. Geochem. Hlth., 20:123-133.

Tsapakis, M., Lagoudaki, E., Stephanou, E.G., Kavouras, I.G., Koutrakis, P., Oyola, P. & Von Baerd, D. 2002: The composition and sources of PM2.5 organic aerosol in two urban areas of Chile. Atmos. Environ., 36: 3851–3863.

U.S. EPA 2006: An inventory of sources and environmental releases of dioxin-like compounds in the United States for the years 1987, 1995, and 2000. US Environmental Protection Agency, National Center for Environmental Assessment, Washington, DC: 677 p.

US Public Health Service 1995: Toxicological profile for Polycyclic Aromatic Hydrocarbons. US department of health and human services, Atlanta: 458 p.

Vaze, J. & Chiew, F.H.S. 2002: Experimental study of pollutant accumulation on an urban road surface. Urban Water, 4:379–389.

Weschler, S.J. & Nazaroff, W.W. 2008: Semivolatile organic compounds in indoor environments. Atm. Environ., 42: 9018–9040.

Zupan, M., Einax, J.W. & Kraft, J. 2000: Chemometric characterization of soil and plant pollution: Part 1: Multivariate data analysis and geostatistical determination of relationship and spatial structure of inorganic contaminants in soil. Environ. sci. pollut. r., 7/2: 89-96.

Žibret, G. & Šajn, R. 2008: Modelling of atmospheric dispersion of heavy metals in the Celje area, Slovenia. J. Geochem. Explor., 97/1:29-41, doi:10.1016/j.gexplo.2007.08.001

Žibret, G. 2002: Geokemične lastnosti tal in podstrešnega prahu na območju Celja (diplomsko delo). Univerza v Ljubljani, Naravoslovnotehniška fakulteta, Ljubljana: 78 p.

Žibret, G. & Rokavec, D. 2010: Household dust and street sediment as an indicator of recent heavy metals in atmospheric emissions: a case study on a previously heavily contaminated area. Environ. earth sci., 61/3:443-453, doi: 10.1007/s12665-009-0356-2.

Žibret, G. 2008: Determination of historical emission of heavy metals into the atmosphere: Celje case study. Environ. geol., 56/1:189-196.

Internet resources available to 18. 6. 2013

Internet 1: http://www.inchem.org/

Internet 2: http://web.doh.state.nj.us/rtkhsfs/rtkhsl.aspx

Internet 3: http://www.lookchem.com/

Internet 4: http://www.chemindustry.com/

Internet 5: http://www.chemspider.com/

Internet 6: http://www.wikigenes.org/

Internet 7: http://www.thegoodscentscompany.com/

Internet 8: http://water.epa.gov/scitech/methods/cwa/pollutants.cfm

GEOLOGIJA *56/1*, 097-106, Ljubljana 2013

doi:10.5474/geologija.2013.008

Risk assesment of an urban aquifer based on environmental tracers

Ocena ranljivosti urbanega vodonosnika na osnovi okoljskih sledil

Branka TRČEK[1], Primož AUERSPERGER[2], Albrecht LEIS[3] & Jürgen SÜLTENFUSS[4]

[1]Faculty of Civil Engineering, University of Maribor, SI 2000 Maribor, Slovenia; e-mail: branka.trcek@um.si
[2] Water Supply Company Vodovod-Kanalizacija, Vodovodna 90, SI - 1000 Ljubljana Slovenia; e-mail: primoz.auersperger@vo-ka.si
[3] Laboratory Centre for Isotope Hydrology and Environmental Analytics, Joanneum Research, Elisabethstrasse 18/II, A 8010 Graz, Austria, e-mail: albrecht.leis@joanneum.at
[4]Institute of Environmental Physics, Department of Oceanography, University of Bremen, Bremen, Germany; e-mail: suelten@uni-bremen.de

Prejeto / Received 15. 4. 2013; Sprejeto / Accepted 11. 6. 2013

Key words: urban area, intergranular aquifer, contamination risk, environmental tracers
Ključne besede: urbano območje, medzrnski vodonosnik, tveganje onesnaženja, okoljska sledila

Abstract

Groundwater from a Pleistocene sandy-gravel aquifer is a drinking water resource for the Union brewery, located near the centre of Ljubljana (Slovenia). A large part of the aquifer recharge area is highly urbanized, which represents a great risk for the groundwater quality assurance. The groundwater dating techniques were used to study the contamination risk of this drinking-water resource. The application of chlorofluorocarbons (CFCs), sulphur hexafluoride (SF_6) and tritium-helium-3 (^3H-^3He) age indicator was tested, as they haven't been used in Slovene urban areas so far. The results reflect that the ^3H-^3He dating technique is the most suitable for a groundwater age determination in the study urban aquifer, since SF_6 and particularly CFCs concentrations could be affected by the local contaminations. They indicated that average groundwater residence times range from 10 to 30 years. Boreholes that are more distant from the Šišenski hrib hill are more vulnerable to contamination due to flow of young groundwater from a direction of the main aquifer, which is exposed to the urban pollution. The presented results were supplemented with chemical investigations of groundwater organic pollutants. An unknown trace organic pollutant with a base ion mass-to-charge ratio 147 was put into focus. Its identification based on chromatographic separation and a mass spectrometric detection with GC-MS, LC-MS and LC-TOF MS techniques. The newly detected trace organic pollutant in sampled groundwater represents together with the ^3H and ^3He data a new technique to study the flow paths and contaminant transport in the urban aquifer in both, the lateral and vertical directions.

Izvleček

Podzemna voda pleistocenskega peščeno-prodnega vodonosnika je vir pitne vode Pivovarne Union, v neposredni bližini centra Ljubljane. Velik del napajalnega območja vodonosnika je urbaniziran, kar lahko ogroža kvaliteto pitne vode. Tveganje onesnaženja obravnavanega vira pitne vode se je proučevalo s pomočjo tehnik za določanje starosti podzemne vode. V ta namen se je prvič v v slovenskih urbanih območjih testirala uporaba sledila ^3H-^3He, CFCs in SF_6. Razultati so pokazali, da je za določanje starosti podzemne vode v proučevanem urbanem vodonosniku najbolj uporabna ^3H-^3He tehnika, saj na koncentracije SF_6, zlasti pa CFC, vpliva lokalno onesnaženje. S pomočjo omenjene tehnike je ugotovljeno, da je povprečna starost podzemne vode raziskovanega območja med 10 in 30 let. Bolj ko so vrtine oddaljene od Šišenskega hriba, bolj so ranljive na onesnaženje, ker so pod vplivom dotoka mlade vode s centralnega območja vodonosnika, ki je izpostavljeno urbanemu onesnaženju. Kemijske raziskave organskih onesnaževal v podzemni vodi dopolnjujejo predstavljene rezultate. Le te slonijo na nepoznanem slednem organskem onesnaževalu z osnovnim ionom, v katerem je razmerje med maso in električnim nabojem 147. Omenjena spojina se je odkrila s pomočjo kromatografske separacije in različnimi sklopljenimi tehnikami – plinsko kromatografijio z masno spektrometrijo (GC-MS), tekočinsko kromatografijo z masno spektrometrijo (LC-MS) in tekočinsko kromatografijo z masno spektrometrijo na čas preleta ionov (LC-TOF MS). Odkrito sledno organsko onesnaževalo predstavlja, skupaj s ^3H in ^3He podatki, novo tehniko za proučevanje toka podzemne vode in prenosa onesnaženja v urbanem vodonosniku, tako v lateralni kot v vertikalni smeri.

Introduction

Groundwater from a Pleistocene sandy-gravel aquifer is an invaluable water resource for the Union brewery, which is located within an industrialized area near the centre of Ljubljana (Slovenia) and supplies quality groundwater from four production wells. A large part of the aquifer recharge area is highly urbanized, which represents a great risk for the groundwater quality assurance. The

quality groundwater is exploited from the lower gravel aquifer that is bounded by an impermeable barrier from the upper gravel aquifer that is contaminated.

The managers of the brewery were aware that sustainable groundwater resources management should be assessed and improved. Hence, an extensive study of groundwater flow and solute/contaminant transport began in 2006 in the catchment area of the brewery groundwater resources with the intention of assessing and predicting the directions of groundwater flow and contaminants transport through the Pleistocene sandy-gravel aquifer and of analysing the contamination risk of drinking-water resources in the lower Pleistocene aquifer. Knowledge of groundwater residence time is of great importance for understanding the key issues in the water quality evolution. For that purpose the groundwater dating techniques based on chlorofluorocarbons (CFCs), sulphur hexafluoride (SF_6) and tritium-helium-3 (^3H-^3He) age indicator were tested in the study urban aquifer, as they haven't been used in Slovenia so far.

^3H, ^3He, CFC and SF_6 are environmental tracers. Their concentrations in groundwater could be affected by numerous physical and chemical processes (Plummer & Busemberg, 2006), therefore a multi-tracer approach was essential to resolve estimates of sampled water ages in the study urban area.

Large-scale production of CFC-12 began in the early 1940s, followed by CFC-11 in the 1950s and by CFC-113 in the 1960s (Plummer & Busenberg, 2006). Inevitably they leaked into the environment, with atmospheric concentrations rising until the 1990s, when production was cut back to protect the ozone layer.

SF_6 has been detectable in the atmosphere since 1953 and is still rising strongly in concentration. It is a stable gas for which no chemical reactions are known to occur in shallow groundwater conditions, and it has a well-known input function (Busenberg & Plummer, 2000). The dating range of water with SF_6 is from 1970 to modern. The SF_6 data are particularly useful for dating post–1993 groundwater and yield excellent results in urban areas that are often contaminated with CFCs and other VOCs (Busenberg & Plummer, 2000).

The application of ^3H for groundwater age determination depends on knowledge of the ^3H input precipitation concentration, which may be poorly known or vary with time. Studying the relation between ^3H and its stable daughter product ^3He in water samples offers the possibility of determining groundwater ages without knowing the ^3H input function. The original ^3H input concentration could be reconstructed from the amount of tritiogenic ^3He in solution due to ^3H decay when no helium has been lost from the solution (Solomon et al., 1993). However, for this dating technique the recharge temperature, excess air and other sources and sinks which result from possible gains and losses of ^3He other than tritiogenic should be identified and corrected.

Tritium is considered to be a conservative tracer for most hydrologic studies. Its natural abundance drastically increased due to anthropogenic sources produced during nuclear weapons testing in the late 1950s and early 1960s. The present ^3H concentration is several magnitudes lower than during the period of the weapons testing and it continues to decrease. Groundwaters are typically in the 5–10 TU range today (Criss et al., 2007; Rose, 2007). ^3H derived tritiogenic ^3He is built up in the groundwater as the contained tritium decays. Therefore, the ^3H-^3He ratio decreases with age. The ^3H-^3He technique can be used to date groundwater that is not more than few years old, which is an advantage in comparison with a CFC dating (Han et al., 2006).

The results of groundwater dating were supplemented with chemical investigations of groundwater organic pollutants. A newly detected unknown trace organic pollutant was put into focus in order to study its source and application for risk assessment of the study urban aquifer.

Study area

The Union brewery is located in the Ljubljana city at an altitude of 300.3 m asl. The Ljubljana area is a large tectonic depression, surrounded by hills and mountains (up to 1300 m asl). It was formed in Plio–Quaternary by the sequential subsiding. Its northern part is named Ljubljana Field – Ljubljansko polje, while its southern part is named Ljubljana Moor –Ljubljansko barje (Fig. 1). The former is characterized by the Ljubljanica River with a karstic catchment and the latter by the Sava River with an alpine catchment. The recharge area of the brewery groundwater resources is situated close to the boundary line of the Ljubljana Moor –Ljubljansko barje and Ljubljana Field – Ljubljansko polje, while the Dravlje Valley borders its western part. This valley has a dolomite catchment area.

The geological composition of the study area is presented in Fig. 1. The Quaternary fluvial and lacustrine deposits fill the Ljubljana depression. The fluvial sediments form an urban intergranular aquifer that is opened in the NE part (t-wQ1 and š-a sediments in Fig. 1). The depth of sandy-gravel sediments increases in the Ljubljana Field – Ljubljansko polje from NW to S and SE where it exceeds 80 m. It varies between 30 and 90 m in the central part of the Ljubljana Field – Ljubljansko polje, where the Union brewery is located. Fig. 2 illustrates that the aquifer is approximately 90 m deep in the brewery area.

In other parts of the Ljubljana depression the impermeable or low permeable clay and sandy-clay layers (šg-a, p-mQ2, j-mQ2 sediments in Fig. 1) cover the aquifer. Locally lenses of mentioned sediments divide the aquifer into two parts - the upper and lower aquifer, as it is a case in the Union brewery area (Fig. 2).

Two isolated hills – the Šišenski hrib hill and the Ljubljana castle hill (Fig. 1) have an important role in groundwater dynamics. They consist of impermeable Carboniferous-Permian sediments

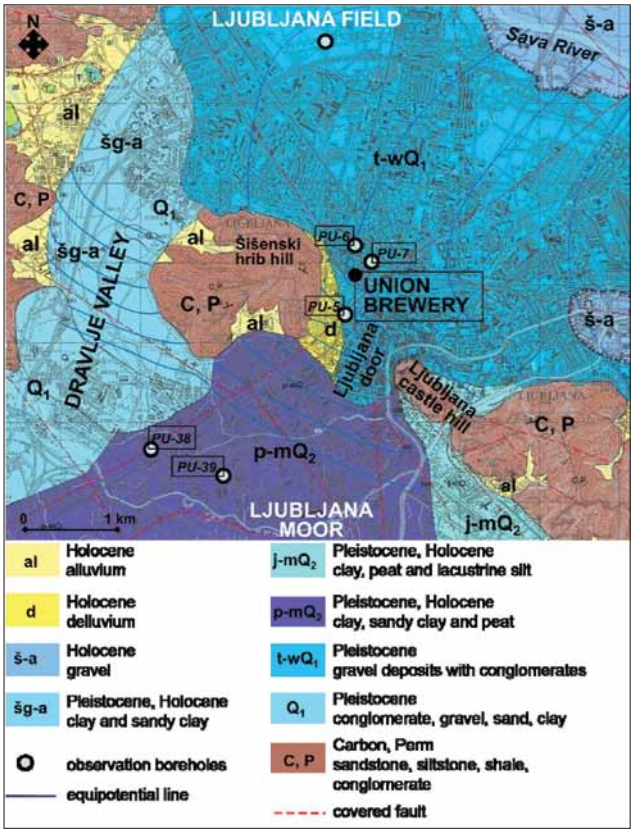

Fig. 1. Geological map of the Union brewery catchment area (Petauer & Juren, 2006 a)

Sl. 1. Geološka karta vplivnega območja Pivovarne Union (Petauer & Juren, 2006 a)

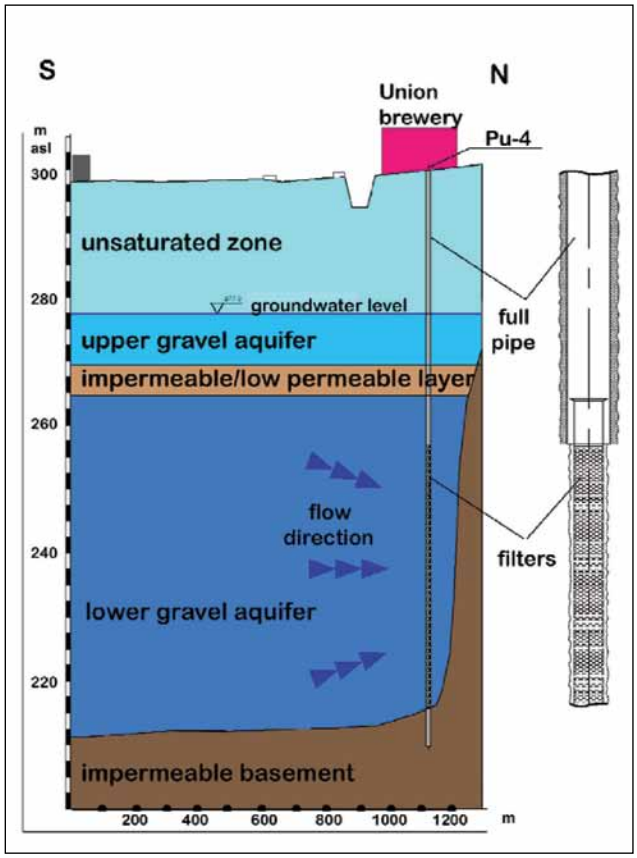

Fig. 2. Schematic aquifer cross-section in the Union brewery area, N-S direction (Petauer & Juren, 2006 b)

Sl. 2. Shematski prerez vodonosnika na območju Pivovarne Union, smer S-J (Petauer & Juren, 2006 b)

(Fig. 1), thus they are characterised by a prevalent runoff. The area between the hills is called the Ljubljana Door (Fig. 1).

The Pleistocene sandy–gravel aquifer of the Ljubljana Field – Ljubljansko polje is recharged by precipitation and inflows from the Sava and Ljubljanica Rivers. The groundwater flow from the Ljubljana Moor –Ljubljansko barje direction is additionally recharging the discussed aquifer through sediments of the Dravlje valley and the Ljubljana Door (Juren et al., 2008). Surface and subsurface run-off from the Šišenski hrib hill represent an additional recharge of the aquifer in the catchment area of the Union brewery groundwater resources. In this area groundwater table is 18–22 m below the surface under law water conditions (Juren et al., 2008).

Research methodology

The so–called quantity and quality monitoring was performed in the catchment area of the Union brewery groundwater resources in the period 2006-2009. The Pleistocene sandy-gravel aquifer was monitored in 13 observation boreholes, located in the Union brewery area and its catchment (Figs. 2 and 3). The observation boreholes capture groundwater of the lower aquifer, groundwater of the upper aquifer or both of them (Fig. 4).

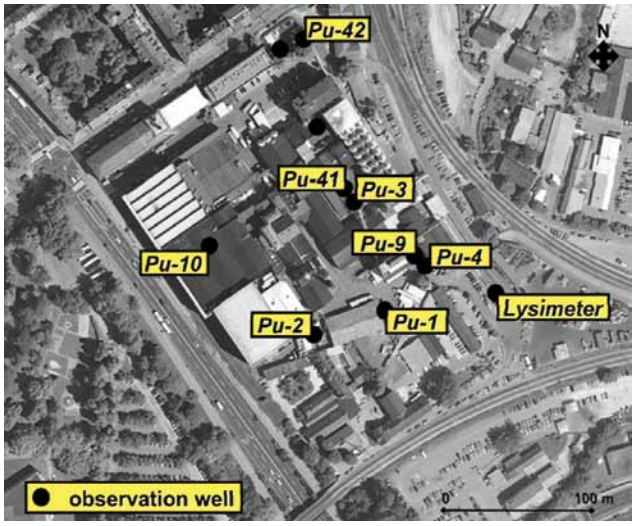

Fig. 3. Observation boreholes in the Union brewery area (Internet)

Sl. 3. Opazovalne vrtine na območju Pivovarne Union (Internet)

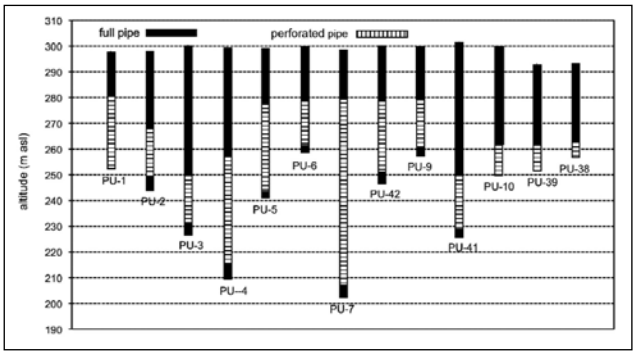

Fig. 4. Profiles of observation boreholes in the study area

Sl. 4. Profili opazovalnih vrtin na raziskovalnem območju

The discussed monitoring included continuous measurements of groundwater table and physico–chemical water parameters (T and SEC) and groundwater sampling for isotope, trace gas, noble gas and herbicide analysis. Groundwater table and physico–chemical water parameters were measured hourly by DMS (Data Merilni Sistemi d.o.o) data loggers.

On the basis of CFCs, $^{3}H/^{3}He$ and SF_6 data the groundwater ages were estimated. Groundwater sampling for CFCs and SF_6 analyses was performed on June 5, 2009 and for ^{3}H and ^{3}He measurements on September 1, 2009. Water samples for tritium analysis were collected in 100 mL HDPE bottles and 1L PE bottles, respectively. CFCs and SF_6 samples were collected unfiltered and without atmospheric contact in glass bottles contained within metal cans by the displacement method of Oster et al. (1996). This method ensures that the sample is protected from possible atmospheric contamination by a jacket of the same water. Water for noble gas analysis was pumped with a submersible pump (Grundfos MP1) through a transparent hose into a copper tube (volume 40 mL, outer diameter 1 cm). A transparent hose with a regulator clamp was attached to the outlet of the copper tube. The clamp was used to squeeze the hose to increase pressure in order to suppress potential degassing and the transparent hose was constantly checked for bubbles. Pumping proceeded until steady state conditions with regard to temperature and conductivity were reached. The copper tubes were subsequently pinched off with stainless steel clamps to maintain highly vacuum tight sealing.

An important distinction can be made between dating based on CFCs and SF_6 and dating by a $^{3}H/^{3}He$ technique. In the case of ^{3}H-^{3}He dating, the initial ^{3}H content of the water sample is reconstructed from measurements of both the parent isotope (^{3}H) and tritiogenic ^{3}He, while dating with CFCs and SF_6 requires prior knowledge of the initial condition (Han et al., 2006). The ^{3}H-^{3}He technique can be used to date groundwater that is not more than few years old, which is an advantage in comparison with a CFC dating (Han et al., 2006). For this dating technique the recharge temperature, excess air and other sources and sinks which result from possible gains and losses of ^{3}He other than tritiogenic were estimated on the bases of Ne and ^{4}He isotope analyses (Cook & Solomon, 1997).

Groundwater dating with CFCs and SF_6 refers to the process of estimating the historical date at which a parcel of water was recharged to a groundwater system. These techniques may provide reliable dating information only if physical and chemical processes affecting trace gas concentrations in groundwater are accounted for. For this purpose additional measurements were made – measurements of dissolved oxygen concentration for determination of potential for microbial degradation and noble gas measurements for defining recharge temperature and excess air (Plummer et al., 2006).

The CFCs and SF_6 measurements were performed at Spurenstofflabor, Wachenheim, Germany by gas chromatography using an electron capture detector (GC ECD) after pre-concentration using a purge-and-trap technique (Busenberg & Plummer, 2000). The detection limit of this method was 0.01 pmol/l for CFCs and 0.1 fmol/l for SF_6.

The ^{3}H and ^{3}He measurements were carried out with the ^{3}He-ingrowth method (Sültenfuss et al., 2006) at the Institute of Environmental Physics, University of Bremen, Germany. ^{3}H is expressed in tritium units – TU, which represents 1 ^{3}H atom in 10^{18} atoms of ^{1}H or an activity of 0.118 Bq/kg in water. The uncertainty is typically less than 3 % for samples of >1 TU and 0.01 TU for very low concentrations.

Isotopic analysis of He and Ne were performed at the Institute of Environmental Physics, University of Bremen, Germany. ^{4}He, ^{20}Ne and ^{22}Ne were measured with a quadrupole mass spectrometer Balzers QMG112A. Helium isotopes were analyzed with a high-resolution sector field mass spectrometer MAP 215–50 (Sültenfuss et al., 2006). The system was calibrated with atmospheric air and controlled for stable conditions for the He and Ne concentrations and the $^{3}He/^{4}He$ ratio. The precision of the He and Ne concentrations is better than 1 % and better than 0.5 % for the $^{3}He/^{4}He$ ratio.

During the monitoring period the herbicides were analysed in groundwater samples seasonally at the laboratory of JP Vodovod-kanalizacija d.o.o., alternately qualitatively and quantitatively (Auersperger et al., 2005 and 2009). The qualitative analyses detected the unknown trace organic pollutant with the source in the borehole PU-9. Therefore, the passive inox samplers with granular active carbon were installed into the borehole in order to identify this compound. The organic compounds were absorbed in the passive sampler for approximately 3 months and then analysed at the laboratory of JP Vodovod-kanalizacija d.o.o. and at the Jožef Stefan Institute, Department of environmental sciences (Auersperger et al., 2011). The identification of the unknown trace organic pollutant based on a pre-concentration by liquid-liquid extraction, solid-phase extraction, a chromatographic separation and a mass spectrometric detection with gas chromatography–mass spectrometry (GC-MS), liquid chromatography–mass spectrometry (LC-MS) and liquid chromatography–time of flight mass spectrometry (LC-TOF MS).

Results and Discussion

In the period 2006–2009 the groundwater table varied between 276 and 280 m asl in the study area. The annual parameter range was more than 2 m in 2009, while it was 1–1.5 m in other years.

The groundwater temperature ranged from 11 to 17 °C. The increased temperature values were measured in the brewery area in boreholes PU-41, PU-9 and PU-42 (Figs. 3 and 4), which could re-

sult from technological processes or a wastewater leakage.

Data of groundwater ages were essential for assessing the groundwater vulnerability to contamination. Trace gas, noble gas and tritium investigations provided valuable information on recharge temperatures and average residence times of sampled groundwater.

The use of CFCs and SF6 as indicators of residence time is based on the known rise of their atmospheric concentrations over the past 60 years, the observation that they are well-mixed in the atmosphere (unlike ^{3}H), and the assumption that they dissolve in water according to their Henry's Law solubility at the temperature of recharge (Plummer & Busenberg, 1999).

Concentrations of CFCs in groundwater samples are presented in Table 1. All concentrations, except CFC-113 of PU-39, were above the equilibrium values, suggesting some anthropogenic addition of CFC. Such CFC excess values are typical for densely populated urban areas. In such cases the age dating based on CFCs isn't possible. Nevertheless, the site–specific excess values give information about the groundwater flow direction and mixing processes. It is remarkable that all three CFC species are simultaneously in excess. The excess is observed more often for CFC-12/CFC-11 or CFC-113, respectively. This structure results from different use patterns of these substances in former times.

Table 1 presents also concentrations of SF_6 in groundwater samples. All samples had values near or below the recent equilibrium value with the atmosphere, except samples PU-9 and PU-4. This indicates that groundwater samples contain post–1970's water (Kipfer et al., 2002). Under the assumption of the piston flow in the study aquifer groundwater ages were derived from the SF_6 data. A piston-flow model is a very common and frequently used approach in groundwater hydrology. Several researchers used it for age determination in alluvial aquifers (Hunt et al., 2005). However, the piston-flow model is a simplification showing a mean groundwater age, which is identical to an advective age in the case if dispersion and diffusion are zero.

Ages of groundwater in the study area, derived from the SF_6 concentrations are listed in Table 2. The groundwater average residence time based on the SF_6 measurements is in the range between 10 and 16 years. In the brewery area the youngest groundwater is captured from the upper sandy-gravel aquifer that is the most distant from the Šišenski hrib hill (PU-6, Figs.1-4). On the other hand, groundwater captured from boreholes close to the Šišenski hrib hill has the longest residence time (PU-5 and PU-10, Figs.1-4).

Sampling point	Model ages (years)
PU-1	≈12
PU-4	
PU-5	≈15
PU-6	≈10
PU-9	
PU-10	≈16
PU-38	≈11
PU-39	≈14

Table 2. Ages of groundwater in the study area, derived from the SF6 concentrations under the assumption of the piston flow model

Tabela 2. Starost podzemne vode na raziskovalnem območju, izračunana na podlagi koncentracij SF6 ob upoštevanju modela batnega toka

The ^{3}H/^{3}He ratio in groundwater samples was used to reconstruct the initial ^{3}H concentration in sampled groundwater during the infiltration period and to provide an independent check of dating results obtained from CFC and SF_6 data. Namely, the common effects that affect the CFC and SF_6 based ages, such as local contaminant sources, chemical processes and mixing fractions do not have an impact on the ^{3}H/^{3}He based ages (Han et al., 2006). Ages were determined from the following relationship:

$$\textit{Groundwater Age (years)} = -17.8 \times \ln\left(1 + {}^3He_{trit}/{}^3H\right) \quad (1)$$

The longtime data series of annual weighted values of ^{3}H in Vienna precipitation (Fig. 6) were used to calculate the ^{3}H input function.

The results of ^{3}H and ^{3}He measurements in groundwater samples are given in Table 3. The ^{3}H-^{3}He dating technique required corrections, related to excess air and non–tritiogenic sources of ^{3}He that based on Ne and ^{4}He data (Tab. 3). All groundwater samples show significant concentration of ^{4}He from radiogenic sources (Fig. 5). The solubility equilibrium concentrations of all

Sampling point	Sampling date	CFCs [pmol/l]			SF_6 [fmol/l]
		CFC-12	CFC-11	CFC-113	
PU-1	05.06.2009	7,1 ±0,8	83 ±25	24 ±5	1,9 ±0,2
PU-4	05.06.2009	7,1 ±0,8	22 ±5	8 ±2	3,5 ±0,4
PU-5	05.06.2009	8,0 ±0,8	13 ±3	2,1 ±0,3	1,5 ±0,2
PU-6	05.06.2009	3,3 ±0,2	58 ±18	11 ±3	2,1 ±0,3
PU-9	05.06.2009	4,5 ±0,5	37 ±8	15 ±3	3,8 ±0,4
PU-10	05.06.2009	5,8 ±0,3	cca 490	ca. 75	1,4 ±0,2
PU-38	05.06.2009	4,8 ±0,3	15 ±3	1,5 ±0,2	2,0 ±0,2
PU-39	05.06.2009	3,5 ±0,2	7,8 ±0,8	0,49 ±0,05	1,6 ±0,2

Table 1. CFCs and SF6 concentrations in groundwater samples

Tabela 1. Koncentracije CFC in SF6 v vzorcih podzemne vode

groundwater samples were calculated assuming the mean annual temperature of 10°C for the period of infiltration. The portion of the He excess is typical, namely in the order of 15–30% of the equilibrium value.

Average ages of sampled groundwater determined with the ^{3}H-^{3}He dating technique are presented in Table 3. As in the case of groundwater dating with the SF_6 technique the piston flow conditions were assumption in the study aquifer. Groundwater ages vary between 4 and 33 years. Groundwater of the upper sandy-gravel aquifer, captured in the borehole PU-9 is the youngest, while the oldest groundwater recharges the borehole PU-10 with a perforated pipe in the lower aquifer (Figs. 1-3).

Sampling point	Tritium [TU] (1.9.2009)	Ne excess [%]	^{4}He radiogenic [ccSTP/kg]	^{3}He tritiogenic [TU]	Age [y] normalized to (1.9.2009)
PU-1	5.35 ±0.1	21	5.25 E-5	9	18±1
PU-4	5.3 ±0.2	16	4.6 E-5	4.5	11±1
PU-9	5.7 ±0.2	20	4.2 E-6	1.5	4±1
PU-10	4.4 ±0.1	30	3.5 E-5	25	33±2
			error: 1E-6	error: 0.5 TU	error: 1 year

Table 3. Tritium and noble gases values in groundwater samples and groundwater ages, derived from 3H--3He dating

Tabela 3. Vrednosti tricija in žlahtnih plinov v vzorcih podzemne vode ter starost podzemne vode, določena na osnovi 3H in 3He

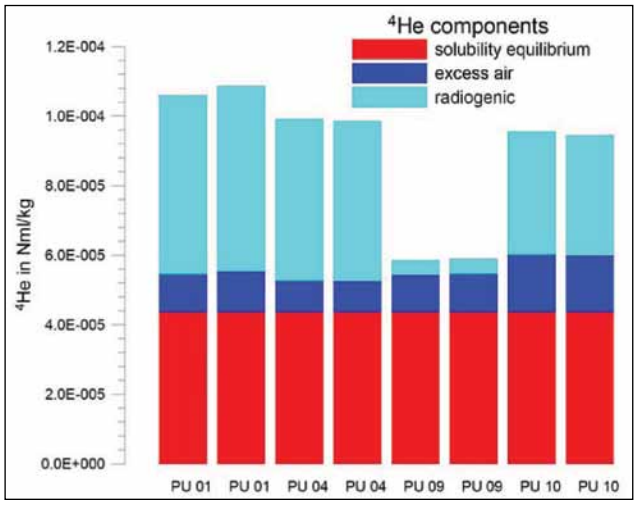

Fig. 5. Separation of 4He concentration by origin (double measurement included)

Sl. 5. Delitev koncentracije 4He glede na izvor (vključene so dvojne meritve)

Except for the PU-10 groundwater sample the concentrations of ^{3}H and tritiogenic ^{3}He match the ^{3}H concentration in precipitation quite well (Fig. 6). Hence, average residence times of sampled groundwater were determined quite well with the ^{3}H-^{3}He dating technique. PU-1, PU-4 and PU-9 groundwater samples do not contain any tritium-free water, while the PU-10 groundwater sample falls a little below the precipitation line (Fig. 6). This indicates that the PU-10 groundwater sample contains a portion of tritium–free water infiltrated into the aquifer before 1955. The tritium–free portion could be in the order of 20–50 %.

The concentration of radiogenic ^{4}He can be used as an indicator for older waters (Han et al., 2006). A concentration in the order of the equilibrium value marks hundreds to 1000 years old groundwater in sandy aquifers. A quite intensive source of radiogenic ^{4}He is assumed in the study area, because the ^{3}H-^{3}He data reflects that groundwater samples do not contain any water from before 1955, except PU-10 groundwater sample (Fig. 6). Even the youngest groundwater of the borehole PU-9 shows a significant concentration of radiogenic ^{4}He. It is assumed that radiogenic ^{4}He is accumulated in stagnant water close to the aquifer contact with the Šišenski hrib hill (Figs. 1-3). In this area groundwater could be trapped since the subsidence process and physical heterogeneities of the aquifer. Radiogenic ^{4}He could be accumulated in large amounts in this stagnant water and the petro-physical heterogeneities of the aquifer give rise to the coexistence of slow-velocity older waters residing in stagnant zones and fast-velocity younger waters of high-permeability zones (Pinti & Marty, 1998).

The differences in age estimates of sampled groundwater with different dating techniques are noticeable (Tabs. 2 and 3), which is not surprising, since all dating techniques have certain advantages and limitations in the application to specific hydrological problems. Numerous processes in the groundwater environment can affect tracer concentrations and consequently the groundwater age determination. A multi-tracer approach generally yields more information and helps to resolve conflicting results. Hence, the CFCs, SF_6 and ^{3}H-^{3}He techniques were used to compare the timescales derived from different tracers. The researches point out that the CFCs and SF_6 data could be influenced by the aquifer local contaminations and can yield wrong age estimates of groundwater in urban areas. Natural conditions are only reflected by the ^{3}H-^{3}He technique in the study area. Nevertheless, results of both – the SF_6 and ^{3}H-^{3}He dating techniques indicate that in the brewery area the oldest groundwater is stored in the aquifer part that is the most close to the Šišenski hrib hill.

On the basis of the ^{3}H-^{3}He dating the mixing of old and young groundwater was evidenced in the sandy-gravel aquifer due to the aquifer petrophysical heterogeneities. It is assumed that the old groundwater is stored in stagnant zones close to the aquifer contact with impermeable sediments of the Šišenski hrib hill (Figs. 1-3). Under the influence of the surface and subsurface run-off from the hill this water flows with a slow velocity towards high-permeability zones of the upper and

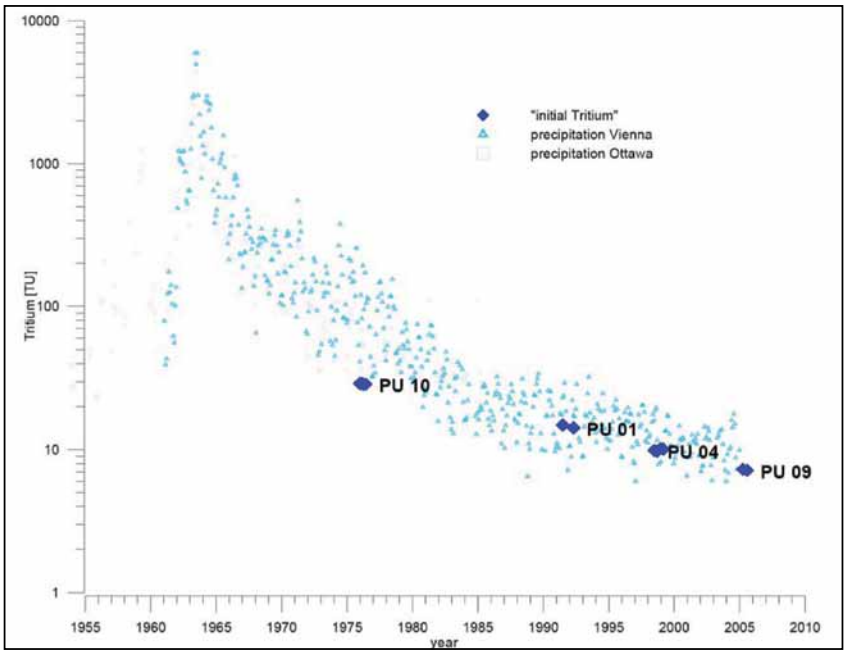

Fig. 6. Initial 3H concentrations in sampled groundwater during the infiltration period, calculated from the 3H and 3He measurements in groundwater samples and 3H concentrations in Vienna and Ottawa precipitation (symbols represent multiple measurements of the same sample)

Sl. 6. Začetne koncentracija 3H v vzorčeni vodi v obdobju infiltracije, izračunane na podlagi 3H in 3He meritev v vzorcih podzemne vode ter koncentracije 3H v padavinah na Dunaju in v Otavi (simboli predstavljajo večkratne meritve istega vzorca)

lower sand-gravel aquifer. Hence, the youngest groundwater with the mean age of 4 years was determined in the borehole PU-9, which is the most distant from the hill and capture only the upper aquifer (Figs. 1-4). This water reflects fast flow velocities, typical for the main Ljubljana urban aquifer (Juren et al, 2008).

The borehole PU-4 is only 2 m distant from the borehole PU-9, but it captures deeper groundwater of the lower sandy-gravel aquifer (Figs. 2-4). The mean age of its groundwater is 11 years, which reflects the lateral and vertical components of the groundwater flow in the study aquifer.

The borehole PU-1 captures groundwater from the upper and lower aquifer. It is located between boreholes PU-10 and PU-4. Although it is shallower from the borehole PU-4 its groundwater is older for approximately 7 years (Tab. 3, Figs. 2-4). This indicates that the discussed borehole is not influence a lot with young groundwater flow from a direction of the main aquifer, which is exposed to an urban pollution.

The results of groundwater dating were supplemented with chemical investigations based on data of specific electroconductivity (SEC) and the unknown trace organic pollutant in sampled groundwater to study the possibility of contamination spread through the upper gravel aquifer and its breakthrough into the lower sandy-gravel aquifer.

The values of specific electroconductivity (SEC) oscillated in observed boreholes between 200 and 1100 mS·cm^{-1}/25 °C (Fig. 7). The lowest SEC values, 200–300 mS·cm^{-1}/25 °C refer to boreholes PU-41 and PU-10 that are influenced by run-off from the Šišenski hrib hill (Fig. 1). The SEC values between 400 and 500 mS·cm^{-1}/25 °C were recorded in boreholes PU-1, PU-2, PU-3 and PU-4, which indicates a little contamination load. They are mostly recharged from the lower gravel aquifer (Figs. 2 and 4). High values, 700–1100 mS·cm^{-1}/25 °C were measured in boreholes PU-7, PU-9 and PU-42 that capture groundwater of the upper aquifer, which is locally contaminated (Trček & Juren, 2006 a). The borehole PU-7 is located in the brewery vicinity and other two boreholes inside the brewery (Figs. 1-4). The discussed boreholes have also the highest SEC

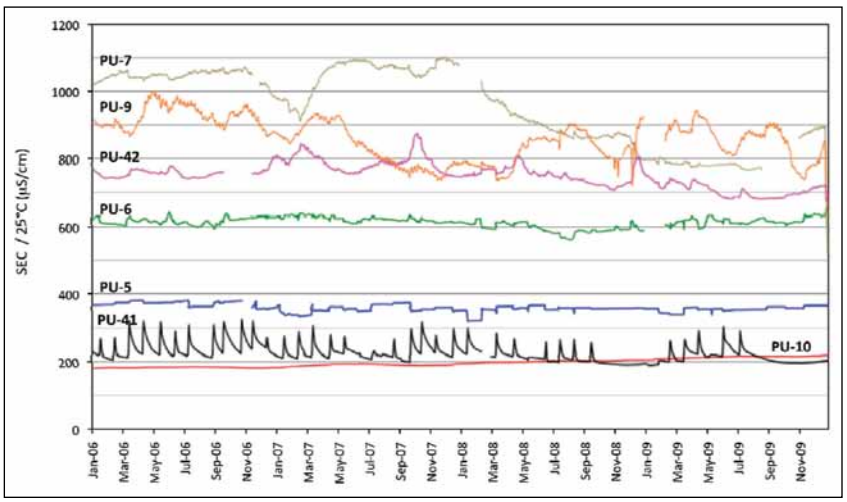

Fig. 7. Oscillation of groundwater specific electroconductivity in the study area in the period 2006-2009

Sl. 7. Nihanje specifične elektroprevodnosti podzemne vode na raziskovalnem območju v obdobju 2006-2009

ranges, which reflect the intensive groundwater dynamics and contaminant transport (oscillation in PU-10 resulted from the pumping for groundwater sampling).

The presented results confirm those based on groundwater dating techniques. The boreholes that are most distance from the Šišenski hrib hill and capture groundwater of the upper aquifer are contaminated, while those that are located closer to the hill are naturally protected from contaminated young groundwater that flows from a direction of the main aquifer.

The borehole PU-9 that captures the upper sandy-gravel aquifer should be exposed due to a high contamination load. A pollution sign was confirmed also by the unknown trace organic pollutant with a base ion mass-to-charge ratio (m/z) 147 (Fig. 8) that has been detected in this borehole with a GC-MS technique and additionally confirmed with LC-MS and LC-TOF MS techniques after pre-concentration by passive sampling on the active carbon.

The NIST05 library of GC-MS mass spectra search gave more than 100 possible results for the unknown compound, containing a bicyclical hetero aromatic rings with N and/or O (Fig. 8). One group indicated a chemical class of benzimidazoles with a widespread use – mostly as fungicides, lubricants, metal corrosion inhibitors and pharmaceuticals. The other compounds in same water samples could be: 5-methylbenzotriazole (CAS 136-85-6; metal corrosion inhibitors and antioxidants), 2-methyl-2H-benzotriazole (CAS 16584-00-2; pesticide formulations and antimicrobial agents) and 5.6-dimetilbenzotriazol (CAS 4184-79-6; lubricants, metal corrosion inhibitors and heat transfer fluids). A narrowing of the candidate list was conducted by the LC-MS techniques to confirm that the discussed compound is not a product of thermal degradation of a parent compound in the GC injector.

In the mean time a semi–quantitative monitoring of the unknown trace organic pollutant was established. The respond for the unknown compound was reporting relative to the internal standard calibration by a linear regression. M/z 147 of the unknown, m/z 161 of the 3,4-dichloroaniline and m/z 165 of the 3,4-dichloroaniline-D2 were used for the target ion, while m/z 104, 77 for the unknown and m/z 163, 128 for the 3,4-dichloroaniline and its deuterated analogue were used to confirm the discussed ions. A simple Electrospray (ESI) LC-MS method indicated that the unknown compound is not a high volatile compound and that m/z 147 belongs to a molecular ion. Concentration estimates for the study compound in borehole PU-9 were on a 0,1 μgL^{-1} level or higher.

Investigations with high resolution LC-TOF MS resulted in determination of a molecular formula of the unknown trace organic pollutant. Several chromatographic peaks identified that the study compound could be (a) MH+ m/z 148 (most probable $C_8H_{10}N_3$, less probable $C_9H_{10}NO$), (b) MH+ m/z 134 (most probable $C_7H_8N_3$, less probable C_8H_8NO) and (c) MH+ m/z 120 (most probable $C_6H_6N_3$, less probable C_7H_6NO) and that the most probable molecular formula of the unknown chemical tracer is $C_8H_9N_3$. Its pollution sources could be a lubricant containing alkyl–substituted benzotriazoles, a metal corrosion inhibitor or a degraded fungicide.

The unknown trace organic pollutant could be 2,4-dimethyl-2H-benzotriazole with traces of 2-methyl-2H-benzotriazole. Its origin is still not well explained. Lack of commercial available source for mentioned compounds could be explained by degradation and/or transformation of parent compounds containing triazoles. Nevertheless, the main characteristics of the discussed tracer are known, as well as the monitoring methods. This is very important, because the newly detected trace organic pollutant with the source in the upper sandy-gravel aquifer, in borehole PU-9 resents a valuable tool to study the flow paths and contaminant transport in the study aquifer in both, the lateral and vertical directions. As it has been already mentioned, the borehole PU-4 is only 2 m distant from PU-9 and captures the lower sandy-gravel aquifer (Figs. 2-4). Therefore, the two boreholes are an ideal polygon to study the risk of contamination

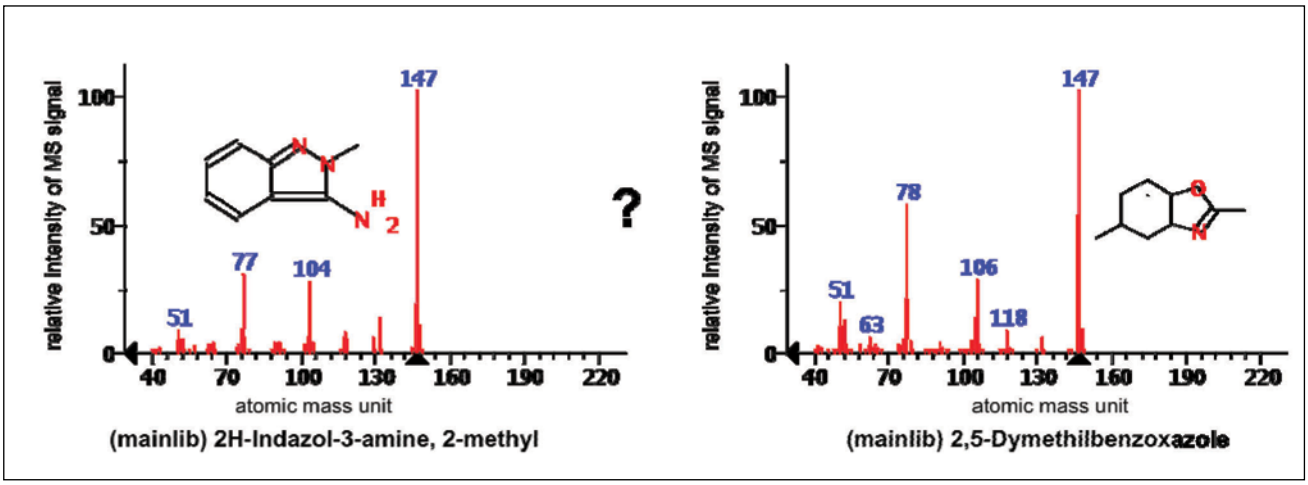

Fig. 8. GC-MS mass spectra of the unknown compound, detected in the study area

Sl. 8. GC-MS masni spekter neznane spojine, ki je bila odkrita na raziskovalnem območju

breakthrough from the upper into the lower aquifer, which was detected in this location with previous investigations (Trček, 2006; Juren et al, 2008).

Conclusions

The researches point out that the ^{3}H-^{3}He dating technique is the most suitable for groundwater age determination in the study urban aquifer, since SF_6 and particularly CFCs concentrations could be affected by the aquifer local contaminations. Its results, supported with SEC measurements provided an insight into groundwater age structure in the observed aquifer and hence into the aquifer hydraulic behaviour. The comparison of parameter presence at and between different sampling points gave important information on recharge conditions, groundwater residence times and mixing processes and with that on hydrodynamic connections and solute transport in the urban aquifer.

The results reflect that boreholes of the brewery area that are more distant from the Šišenski hrib hill are more vulnerable to contamination due to flow of young groundwater from a direction of the main aquifer, which is exposed to the urban pollution. On the other hand the boreholes located closer to the hill are naturally protected from contamination as they capture old groundwater, which flows towards central high-permeability zones of the upper and lower sand-gravel aquifer. The presented information is closely connected with flow velocities in the study aquifer, which decreases towards the Šišenski hrib hill.

The newly detected trace organic pollutant in sampled groundwater with a base ion mass-to-charge ratio (m/z) 147 represents together with the ^{3}H and ^{3}He data a new technique to study the flow paths and contaminant transport in the study urban aquifer in both, the lateral and vertical directions. It could be used for calibration of the hydraulic mathematical model of the Ljubljana Moor, Dravlje valley and Ljubljana Field aquifer (Juren et al., 2008) and for reconstruction of the contaminant load to the aquifer. For this purpose the transport of trace organic pollutant should be simulated and groundwater age data compared with travel times computed with the mention model.

The described approach needs further investigations. The monitoring of the unknown trace organic pollutant should continue in the unsaturated and saturated zone of the observed aquifer to obtain information of its distribution and concentrations.

Acknowledgement

The authors would like to acknowledge the Union brewery and K_{net}Water for the financial support of researches. Moreover the authors acknowledge dr. Harald Oster (Spurenstofflabor Wachenheim, Germany) for the CFC and SF_6 analysis and dr. Dušan Žigon (Jožef Stefan Institute) for analysis with for analysis with LC-TOF MS and LC-MS.

References

Auersperger, P., Lah, K., Kus, J. & Marsel, J. 2005: High precision procedure for determination of selected herbicides and their degradation products in drinking water by solid-phase extraction and gas chromatography-mass spectrometry. J. chromatogr., A, 1088/1-2: 234-241.

Auersperger, P., Lah, K., Jamnik, B. & Nartnik, M. 2009: Določitev racionalnega nabora organskih onesnaževal v podzemni vodi. In: Geološki zbornik. Ljubljana: 12-15.

Auersperger, P., Lah, K., Kramarič Zidar, V. & Mali, N. 2011: Kvalitativni monitoring organskih onesnaževal v podzemni vodi z uporabo pasivnega vzorčenja in plinske kromatografije z masno spektrometrijo = Qualitative monitoring of organic pollutants in groundwater by passive sampling and gas chromatography mass spectrometry. In: Kravanja, Z., Brodnjak-Vončina, D. & Bogataj, M. (eds.): Slovenski kemijski dnevi 2011, Portorož, 14-16 september 2011. FKKT, Maribor: 1-10.

Busemberg, E. & Plummer, L.N. 2000: Dating young groundwater with sulfur hexafluoride: Natural and anthropogenic sources of sulfur hexafluoride. Water Resources Research, 36/10: 3011–3030.

Cook, P.G. & Solomon, D.K. 1997: Recent advances in dating young groundwater: chlorofluorocarbons, $^{3}H/^{3}He$ and ^{85}Kr. J. Hydrol., 191: 245-265.

Criss, R.E., Davisson, M.L., Surbeck, H. & Winston, W.E. 2007: Isotopic Techniques. In: Goldscheider, N. & Drew, D. (eds.): Methods in karst hydrogeology. International contribution to hydrogeology 26, Taylor and Francis, London: 123–145.

Han, L.F., Gröning, M., Plummer, L.N. & Solomon, D.K. 2006: Comparison of the CFC technique with other techniques (^{3}H, $^{3}H/^{3}He$, ^{85}Kr). In: Use of Chlorofluorocarbons in Hydrology: A Guidebook, STI/PUB/1238. IAEA, Vienna: 191-198.

Hunt, R.J., Tyler B., Coplen, T.B., Haas, N.L., Saad, D.A. & Borchardt, M.A. 2005: Investigating surface water–well interaction using stable isotope ratios of water. Journal of Hydrology, 302: 154–172.

Juren, A., Trček, B., Harum, T., Leis, A. & Petauer, D. 2008: Project A.1.4, Water for beverage industry applying best management practices, final report, Phasing out. Kompetenznetzwerk Wasserresourcen GmbH, Graz: 38 p.

Kipfer, R., Aeschbach-Hertig, W., Peeters, F. & Stute, M. 2002: Noble gases in lakes and ground waters. In: Porcelli, D., Ballentine, C. & Wieler, R. (eds.): Noble gases in geochemistry and cosmochemistry. Rev. Mineral. Geochem., 47: 615-700.

Oster, H., Sonntag, C. & Münnich, C.O. 1996: Groundwater age dating with chlorofluorocarbons. Water Resources Research, 32/10: 2989–3001.

Petauer, D. & Juren, A. 2006a: Geological Map of the Union Brewery Groundwater Catchment Area in Scale 1: 25 000. GeoSI, Ljubljana: a CD-Rom.

Petauer, D. & Juren, A. 2006b: Hydrogeological Map of the Union Brewery Groundwater Catchment Area in scale 1: 25 000. GeoSI, Ljubljana: a CD-Rom.

Pinti, D. & Marty, B. 1998: The origin of helium in deep sedimentary aquifers and the problem of dating very old groundwaters. In: Parnell, J. (ed.): Dating and Duration of Fluid Flow and Fluid Rock Interaction. Geological society, Special Publications 144, London: 53-68.

Plummer, L.N. & Busenberg, E. 1999: Chlorofluorocarbons. In: Cook, P. & Herczeg, A. (eds.): Environmental tracers in subsurface hydrology. Kluwer Academic Publishers Boston: 441-478.

Plummer, L.N. & Busemberg, E. 2006: Chlorofluorocarbons in aquatic environments. In: Use of Chlorofluorocarbons in Hydrology: A Guidebook, STI/PUB/1238. IAEA, Vienna: 1-8.

Plummer, L.N., Busemberg, E. & Cook, P.G. 2006: Principles of chlorofluorocarbons dating. In: Use of Chlorofluorocarbons in Hydrology: A Guidebook, STI/PUB/1238. IAEA, Vienna: 17-30.

Rose, S. 2007: Utilization of decadal tritium variation for assessing the residence time of base flow. Ground Water, 45/3: 309–317, doi:10.1111/j.1745-6584.2006.00295.x.

Solomon, D.K., Schiff, S.L., Poreda, R.J. & Clarke, W.B. 1993: A validation of the $^{3}H/^{3}He$ method for determining groundwater recharge. Water Resources Research, 29/9: 2951–2962, doi:10.1029/93WR00968.

Sültenfuss, J., Roether, W. & Rhein M. 2006: The Bremen mass spectrometric facility for the measurement of helium isotopes, neon, and tritium in water. In: Proceedings of the IAEA International Symposium on Quality Assurance for Analytical Methods in Isotope Hydrology, CN-119. IAEA, Vienna.

Trček, B. 2006: Isotopic investigations in the Union brewery water body. Geologija, 49/1: 103-112.

Trček, B. & Juren, A. 2006a: Vulnerability study of the Union Brewery water body. In: Proceedings of the IAH Symposium, Dijon, France.

Trček, B. & Juren, A. 2006b: Protection of drinking-water resources in the Union Brewery water body (Ljubljana, Slovenia). In: 34th Congress of International Association of Hydrogeologists, Beijing, China, October 9-13, 2006. Proceedings of the 34th IAH Congress, Beijing, China.

Trček, B. & Juren, A. 2006c: Best management practices - Pivovarna Union d.d. (BMP-PU). In: Trauner, L. & Vovk Korže, A. (eds.): Water resources management. Faculty of Arts, K-net Subcenter, Maribor: 58-63.

Internet: https://maps.google.si/maps?hl=sl&q=Google+Image+Terra+Matrices&ie=UTF-8 (15.12. 2008).

GEOLOGIJA *56/1*, 107–128, Ljubljana 2013

doi:10.5474/geologija.2013.009

Mineral chemistry and genesis of Zr, Th, U, Nb, Pb, P, Ce and F enriched peralkaline granites of El-Sibai shear zone, Central Eastern Desert, Egypt

Mohamed A. ALI

Nuclear Materials Authority P. O. Box: 530 El-Maadi, Cairo, Egypt; e-mail: dr_mohamed1966@yahoo.com

Prejeto / Received 3. 8. 2011; Sprejeto / Accepted 20. 5. 2013

Key words: Thorite, zircon, zirconolite, cerite-(Ce), El-Sibai peralkaline granite, electron probe microanalyses, hydrothermal fluids, Central Eastern Desert, Egypt.

Abstract

El-Sibai mineralized shear zone trending NNE-SSW is located at the northern segment of Gabal El-Sibai (500 m in length and 0.5 to 1.5 m in width). Rocks along the shear zone show different types of alterations such as hematization, kaolinitization, fluoritization, and silicification. These alterations are good traps for rare metals of thorite, ferrocolumbite, pyroclore, plumbopyroclore, fluorite, cerite-(Ce), zircon, Th-rich zircon, zirconolite (mixture of zircon & columbite), fluorapatite, titanite, and monazite minerals.

The detailed mineralogical study of the El-Sibai shear zone revealed its enrichment in Th, Zr, Nb, Pb, U, F, P, LREE (Ce), especially concerning the hematization processes. The close correlation of ferruginated (hematitized) samples with high radioactivity is related to the high ability of iron oxides for adsorption of radioactive elements from their solutions. The rare-metal minerals found in altered peralkaline granites (shear zone) are associated with hematitization, albititization, chloritization, fluoritization, and pyritization. Electron probe microanalysis (EPMA) provides an indication of a range of solid solution between thorite and zircon, in which intermediate phases, such as Th-rich zircon were formed. These phases have higher sum of all cations per formula (2.0 to 2.09 atoms per formula unit, for 4 oxygen atoms) than that of ideal thorite and zircon. This is attributed to the presence of substantial amount of interstitial cations such as U, Y, Ca, and Al in these phases. Altered zircon enriched in Th and U (Th-rich zircon) preferentially involves coupled substitution $Ca^{2+} + (Th,U)^{4+} \leftrightarrow 2Zr^{4+} + 2Si^{4+}$, implying that significant amount of U and Th may enter the Zr and Si position in zircon.

Thorite and Th-rich zircon are related to hydrothermal fluid. Also the genesis of the studied zircon is related to metasomatic hydrothermal zircon (MHZ). The abundantly detected zircon, Th-rich zircon, Th-bearing minerals and fluorite of demonstrably hydrothermal origin can be attributed to the role of fluorine-rich fluids. Although Zr and Th are generally considered as highly immobile elements, yet the occurrence of zircon indicates that their significant concentrations can be transported under specified F-rich fluids. The hydrothermal origin could be accepted for the thorite, huttonite monazite, zircon, Th-rich zircon, ferrocolumbite, pyroclore, plumbopyrochlore, zirconolite, fluorite, cerite-(Ce), fluorapatite within the El-Sibai altered peralkaline granites (shear zone).

Introduction

Egyptian granitic rocks of Pan-African age occupy about 40 % of the exposed Precambrian of the Eastern Desert and Sinai. They are subdivided into two distinct major groups, namely the Older and the Younger granites. The Older granites have been referred to in the Egyptian literature as Grey granites (Hume, 1935; El-Ramly & Akaad, 1960), syn- to late-orogenic plutonites (El-Shazly, 1964), synorogenic granites (El-Gaby, 1975) and G1-granites (Hussein et al., 1982). They were emplaced around 930-850 Ma ago, and possibly extend to 711 Ma (El-Manharawy, 1977; Stern & Hedge, 1985; Hassan & Hashad, 1990). On the other hand, the younger granites (about 30 %) were previously mapped as Gattarian granites (Hume, 1935), red and pink granites (El-Ramly & Akaad, 1960), late- to post-orogenic granites (El-Gaby, 1975) and G-II to G-III granites (Hussein et al., 1982). They were emplaced around 622-430 Ma ago (El-Manharawy, 1977; Stern & Hedge, 1985; Hassan & Hashad, 1990; Moghazi et al., 2004; Moussa et al., 2008, Ali & Lentz, 2011).

Shear zones are known to represent important mechanical weaknesses that affect the geology of the continental lithosphere as a kinematic response to deformation (Butler et al., 1995). Stern (1985) and Sultan et al. (1988) suggested through their compilation of Landsat thematic mapper scenes of the Arabian-Nubian Shield (ANS) that the Najd system extends into the Egyptian Eastern Desert and dominates the structural pattern within its central part. Greiling et al. (1993) believed that shear zones in the Pan African basement of the Eastern Desert may be related to compressional as well as extensional stresses; however, both types of deformation led to formation of antiformal structures on a regional scale.

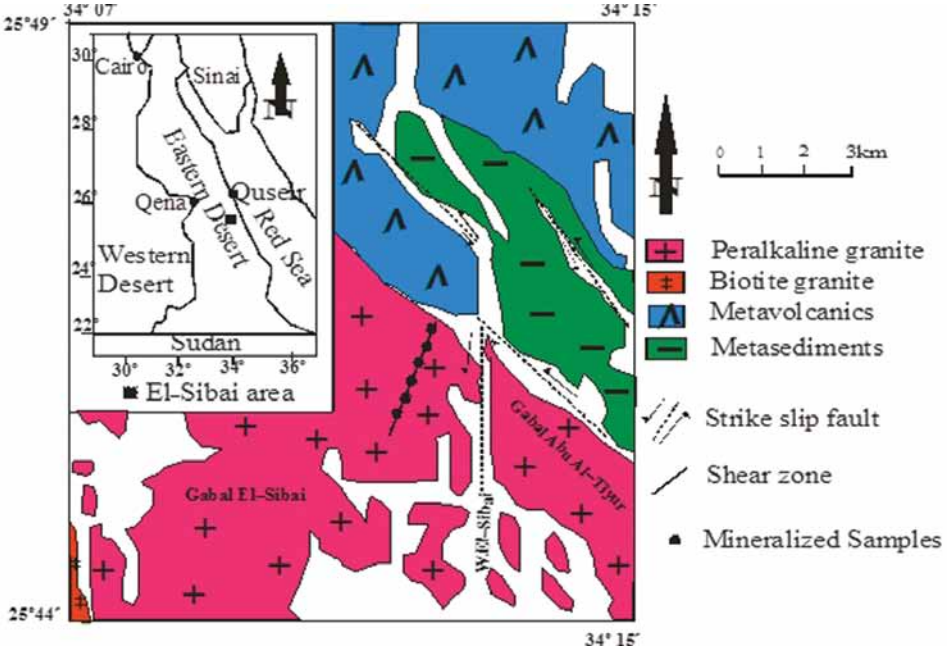

Fig. 1. Geological map of Gabal El-Sibai peralkaline granite (shear zone), Central Eastern Desert, Egypt (modified after Ali, 2001).

Kamal El-Din (1991) described Gabal El-Sibai swell as a doubly plunging anticline trending NW-SE, where the core is occupied by Pre-Pan-African gneisses intercalated in the upper parts by amphibolites. Recently, Ali (2001) delineated a NNE-SSW shear zone at Gabal El-Sibai peralkaline granite (Fig. 1). Abdel-Fattah et al. (2001) studied the anorogenic magmatism; chemical evolution of the Mount El-Sibai A-Type complex (Egypt) and implications for the origin of within-plate felsic magmas. Moussa (2001) studied Gabal El-Sebai alkali feldspar granite and its potentiality to host U-Th mineralization. Earlier geochronological studies indicate that El-Sibai complex is dated at 455 Ma (whole rock K-Ar method) and at 525 Ma (mica K-Ar method): both ages were determined by El-Ramly (1962).

Geochemical studies of the El-Sibai area, including the mineralized shear zone were carried out by Abdel Kader et al. (2001), who concluded that the younger granites are classified into the following types: a) biotite granites and b) alkali-feldspar granites. The biotite granites are classified as monzo-to syenogranites, weakly to mildly alkaline, peraluminous of differentiated I-types, of post orogenic volcanics arc tectonic setting. While the alkali-feldspar granites (El-Sibai granites) are strongly alkaline to peralkaline, A_1-type is rift-related anorogenic (within plate granites or WPG).

Ibrahim et al. (2003) studied the mineralogical and spectrometric characteristics of El-Sibai shear zone and found that the studied shear zone was affected by different types of hydrothermal solutions. Their average eU contents are 38, 29 and 21 ppm, whereas eTh averages 339, 156 and 115 ppm in ferruginated, kaolinized and silicified parts, respectively. Mineralogically, the high level of radioactivity in the shear zone is attributed to the presence of some radioactive minerals, in example plumbobetafite and uranophane as U-bearing minerals, thorite and uranothorite as Th-bearing minerals, zircon, fluorite, galena, magnetite and ilmenite as accessory minerals. In this paper we briefly report on the new mineralogical data obtained with the scanning electron microscope (SEM) and mineral chemistry with EPMA of mineralizations of the El-Sibai altered granites (shear zone).

Analytical methods

Six mineralized samples of the El-Sibai altered peralkaline granites (shear zone) were investigated in details regarding mineralogy and mineral chemistry. Polished thin sections were investigated in reflected and transmitted light in order to determine mineral association and parageneses. Backscattered electron images (BSE) were obtained with the scanning electron microscope (JEOL JSM 6400 SEM), equipped with energy dispersive X-ray spectrometry (EDS) at the Microscopy and Microanalyses Facility, University of New Brunswick (UNB), Fredericton, New Brunswick, Canada. Mineral compositions were determined on the JEOL JXA-733 Superprobe (EPMA); operating conditions were 15 kV, with a beam current of 50 nA and the spectra acquisition time was 30 s. As mineral standards jadeite, kaersutite, quartz, and apatite (for Na, Al, Si, P, and Ca, respectively), $SrTiO_3$ (for Ti), CaF_2 (for F), Fe, Nb, Hf, Ta, Sn, Th, and U metals (for Fe, Nb, Hf, Ta, Sn, Th, and U, respectively), YAG (for Y), cubic zirconia (for Zr), La, Ce, Nd, Sm, Pr, Er, Gd, Eu, Tb, Dy, and Yb; Al, Si glass (for La, Ce, Nd, Sm, Pr, Er, Gd, Eu, Tb, Dy, and Yb), and crocoite (for Pb) were used.

Geological setting

Field geology

Metavolcanics and metasediments are the oldest rock units in the El-Sibai area of granitic rocks. These rocks are intruded by a granitic intrusion of

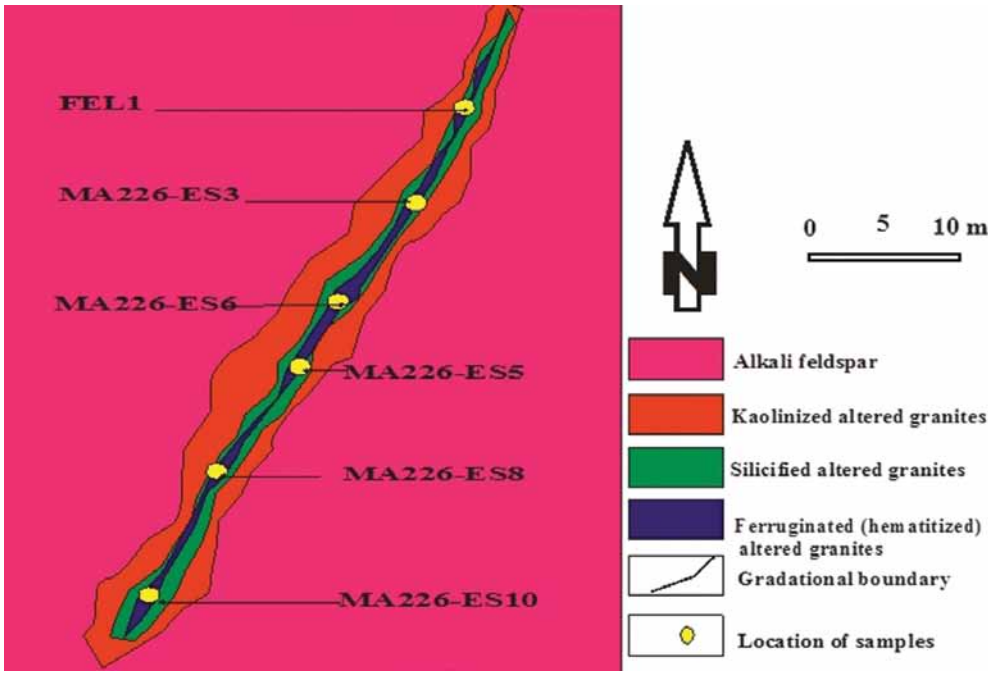

Fig. 2. Sketch of the different types of altered granites in El-Sibai shear zone, Central Eastern Desert, Egypt.

Gabal El-Sibai and Gabal Abu El-Tiyur. Younger granites of El-Sibai and Abu-Tiyur plutons are intruded in the metasediments, metavolcanics and several xenoliths from these older rocks of different sizes and shapes. They are pink in color and characterized by exfoliation and cavernous weathering. These granites are characterized by the presence of pegmatite pockets composed of feldspars, quartz and mica. All rock units are dissected by numerous mafic (basalt and dolerite) and alkaline bostonite dykes, which mainly follow the NW-SE direction. A NNE-SSW and N-S sets of faults cut the granitic pluton. These faults are mainly of strike-slip type (sinistral) and vary in length from 1.5 to 4 km.

A shear zone trending NNE-SSW dissects the northern segment of Gabal El-Sibai (1484 m.a.s.l) and extends for 3 km. The granite becomes mylonitized and cataclased within the shear zone. The identification of this shear zone was based on landsat images and field observations. The intensely exposed mineralized part of the shear zone varies in width from 0.5 to 3 m and in length from 300 to 500 m and is encountered at the alkali feldspar granite (Fig. 2).

Ferrugination, silicification and kaolinitization with few dark patches of manganese dendrites are the main wall rock alteration features observed within the investigated shear zone. These alterations are more pronounced in the granitic rocks on both sides of the shear zone (Fig. 3a). Deep reddish brown color mostly characterizes the strongly ferruginated rocks, while the lighter creamy and brownish yellow tones could be attributed to the weathering of feldspars by kaolinitization process. The silicified granite is characterized by its hardness and lighter rosy tones. Sheared and altered zones are suitable for circulating hydrothermal solutions and present favourable sites for the rare-metal mineralizations.

Petrography

Fresh surfaces of El-Sibai peralkaline granites are medium-to coarse-grained and consist essentially of perthites, quartz, oligoclase, microcline, biotite, minor amount of alkali amphiboles and alkali pyroxenes. Zircon, fluorite, apatite, monazite, allanite and hematite are the main accessory minerals. They are usually of hypidiomorphic granular texture. The microcline perthites may dominate strongly over orthoclase perthites. Quartz occurs as anhedral crystals. A graphic texture has been observed in few samples, i.e quartz intergrowth with K-feldspar. Plagioclase occurs as albite and is less abundant than perthites. It occurs as small interstitial crystals between quartz, perthites and riebeckite. Alkali pyroxene occurs as aegirin and is characterized by the presence of zircon, fluorite, apatite, allanite and monazite, which appear as inclusions. Alkali amphiboles occur as riebeckite and arfvedsonite, showing weak pleochroism from blue to deep blue.

All constituents of altered granites from the shear zone show cataclastic effects and have corroded edges. Quartz (30-45 %) sometimes shows clear signs of mylonitization and annealing. Brecciation took place prior to and/or is contemporaneous with the hydrothermal solutions. K-feldspars are represented by string type perthite with subordinate microcline. They are penetrated by relatively fine-grained veinlets of quartz and are kaolinized along the cleavage planes and fractures (Fig. 3 b, c). The cracks are filled with iron oxides which are originated from the hydrothermal solutions (Fig. 3 d). Cataclased albite (10 %) is commonly altered to sericite and its abundance increases in the mineralized samples. Cataclasis produced microfaults in the crystals and bending of the twin lamellae. Iron oxides are observed within all investigated thin sections either as a primary phase or as a secondary phase resulting

from the alteration of other primary minerals, which are completely replaced by hematite (Fig. 3 e, f). Sometimes the original composition of the granites is obscured and becomes difficult to be determined due to the high intensity of ferrugination.

Thorite appears in two forms; in euhedral to subhedral crystals, and as long acicular radiating aggregates associated with iron oxide and zircon (Fig. 3 d), displaying bright yellow and blue interference colours. Accessory minerals are mainly metamictic zircon, monazite, rutile, fluorite, xenotime and opaque minerals. Zircon is in an optical microscope light gray and surrounded by hematite (Fig. 4 a, b), while the thorite occurs as lighter gray long acicular

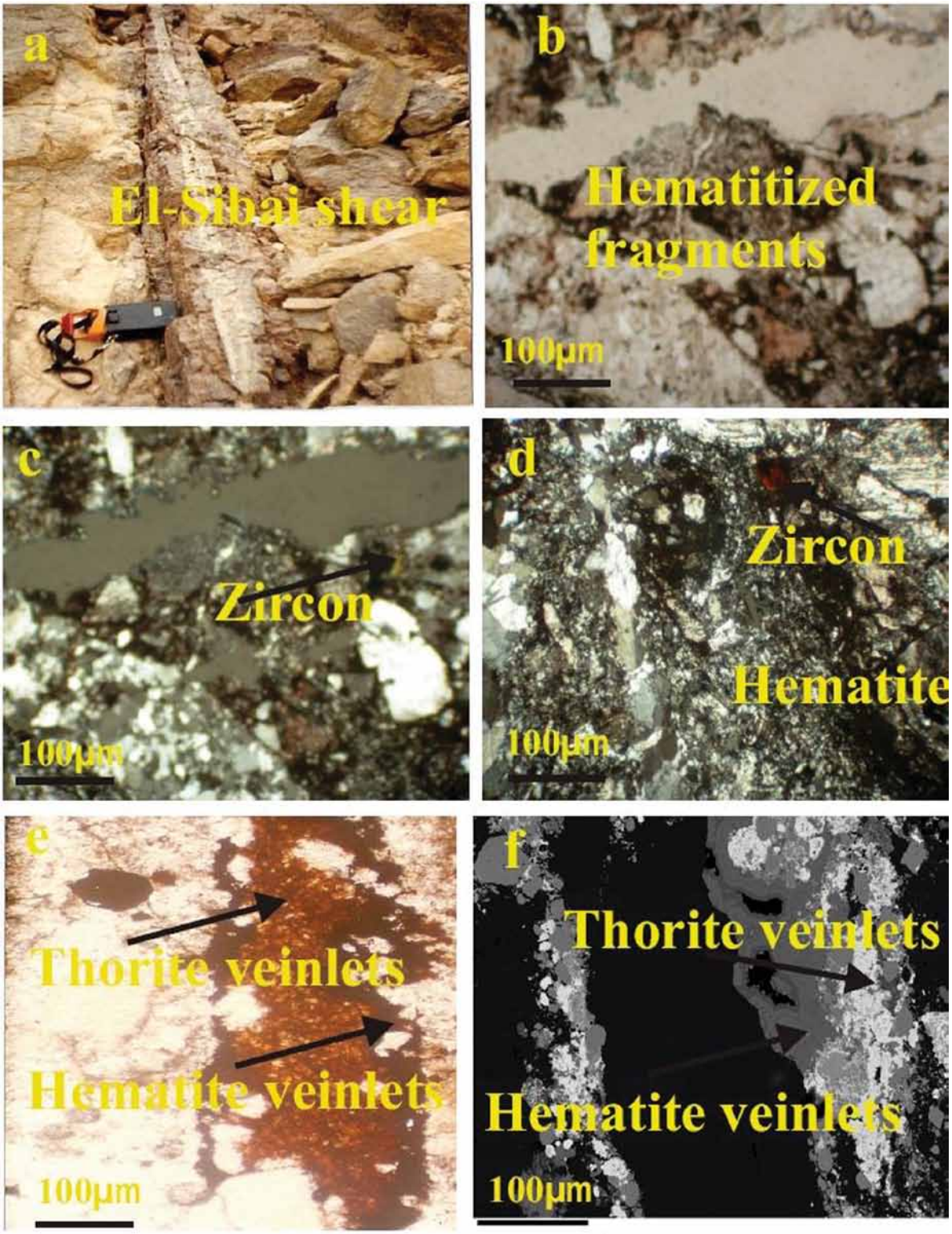

Fig. 3. a) NNE trending of peralkaline granite in El-Sibai shear zone, b) Average mineral composition of cataclastic and mylonite rocks within the El-Sibai shear zone, parallel nicoles and c) crossed nicols, d) Photomicrograph of large crystals of zircon associated with irone oxides (hematite) within the El-Sibai shear zone, e) Photomicrograph of mineralized veinlets of thorite associated with hematite, and f) its corresponding BSE image.

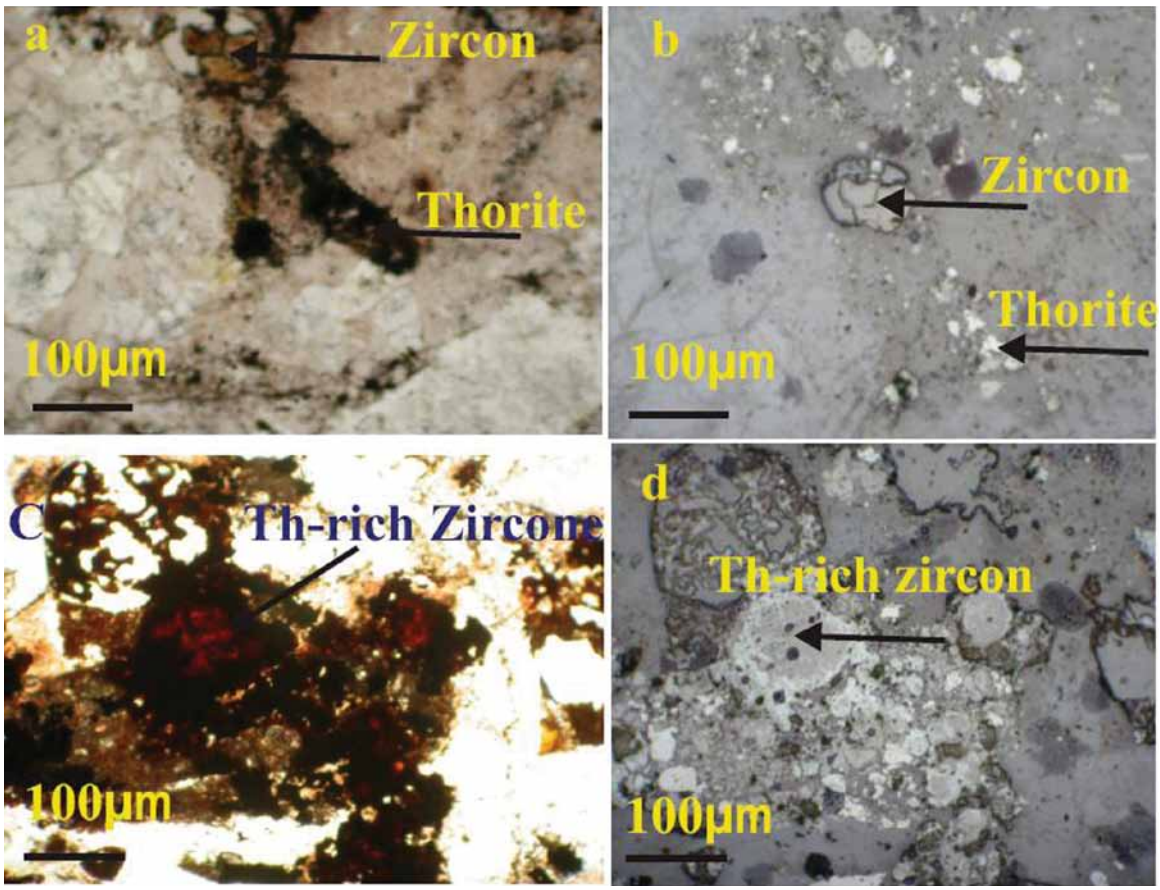

Fig. 4. a) Photomicrograph of zircon and thorite, polarized light b) The same as previous photograph under crossed nicols, c) Photomicrograph of large zircon crystals surrounded by thorite minerals in parallel nicols, and d) under crossed nicols.

radiating aggregates associated with hematite and display reddish brown, yellowish brown and dark brown interference colours (Fig. 4 c, d).

Mineralogy

Detailed mineralogical investigated of columbite–tantalite, Th- and U-Nb, zircon and Th-rich zircon minerals in the mineralized peralkaline granites of El-Sibai shear zone, revealed the presence of primary Th (thorite, huttonite monazite and Th-rich zircon), and U-Nb (plumbopyrochlore), zirconolite (Nb-Zr), zircon (Hf), monazite, fluorite, and fluorapatite. Optical microscopy, SEM, and EPMA were used to characterize ferrocolumbite, pyrochlore and plumbopyrochlore, primary Th (thorite, and huttonite), zirconolite (mixture of zircon and columbite), zircon (Hf), Th-rich zircon, monazite, fluorite, fluorapatite, and cerite-(Ce). A brief description of accessory heavy minerals in this study of rare-metal peralkaline granites are as follows:

Columbite group AB_2O_6

The Columbite group of minerals comprises a large number of structurally related orthorhombic AB_2O_6 coumpounds. The Columbite subgroup is Nb-dominant, and the Ta- subgroup Ta dominant. Most commonly occurring as accessory minerals in granite pegmatites (Gaines et al., 1997), columbite-group minerals contain U (and Th) in various amounts and are commonly metamict, but there is no description with U as an essential constituent. The relatively small octahedral A site is commonly occupied by Mg^{2+} (magnesiocolumbite) and transition-metal cations, such as Fe^{2+} (ferrocolumbite) and Mn^{2+} (manganocolumbite), U and Th substitutions are relatively rare.

Nb and Ta form mostly complex oxides or hydroxides, they appear rarely as silicates in different rock types. This series represents solid solution between columbite $(Fe, Mn)(Nb,Ta)_2O_6$ and tantalite $(Fe, Mn)(Ta,Nb)_2O_6$. In fact, similarity between Nb and Ta elements, both being pentavalent, preferring octahedral coordination in oxide compounds with similar ionic radii=0.72 Å (Whittaker & Muntus, 1970), cause extensive mutual substitution between them. The columbite-tantalite series are the most abundant in granites and pegmatites, particularly those containing albite and Li silicates associated with albite, microcline, lepidolite, and muscovite. Columbite is frequently considered to be a carrier of U-Th and REE. In many cases, its radioactivity is related to minute inclusions of radioactive minerals, surrounded by conspicuous radioactive halos.

A large number of complex Nb, Ta, and Ti oxides are known to contain U in various amounts. These minerals mostly occur as accessory minerals in granitic rocks and granitic pegmatites. There are several important Nb and Ta ore minerals, which may be mined for REEs. A few of them

contain U as an essential constituent, which is usually oxidied to a certain degree (Smith, 1984). Nearly all contain some U and Th in solid solution, and are therefore important actinide hosts in granitic rocks, as well as important source for dissolved U in the hydrothermal and meteoric waters with which they interact. Many of these minerals are commonly metamict; due to their abilities to incorporate radioactive elements, they can also be strongly altered.

Metamict minerals offer a special challenge to mineralogists trying to obtain structural information about their crystalline precursors. Redox conditions during annealing may change oxidation states of some elements (e.g. Fe or U). Due to possible post-formation alteration, it is not al-

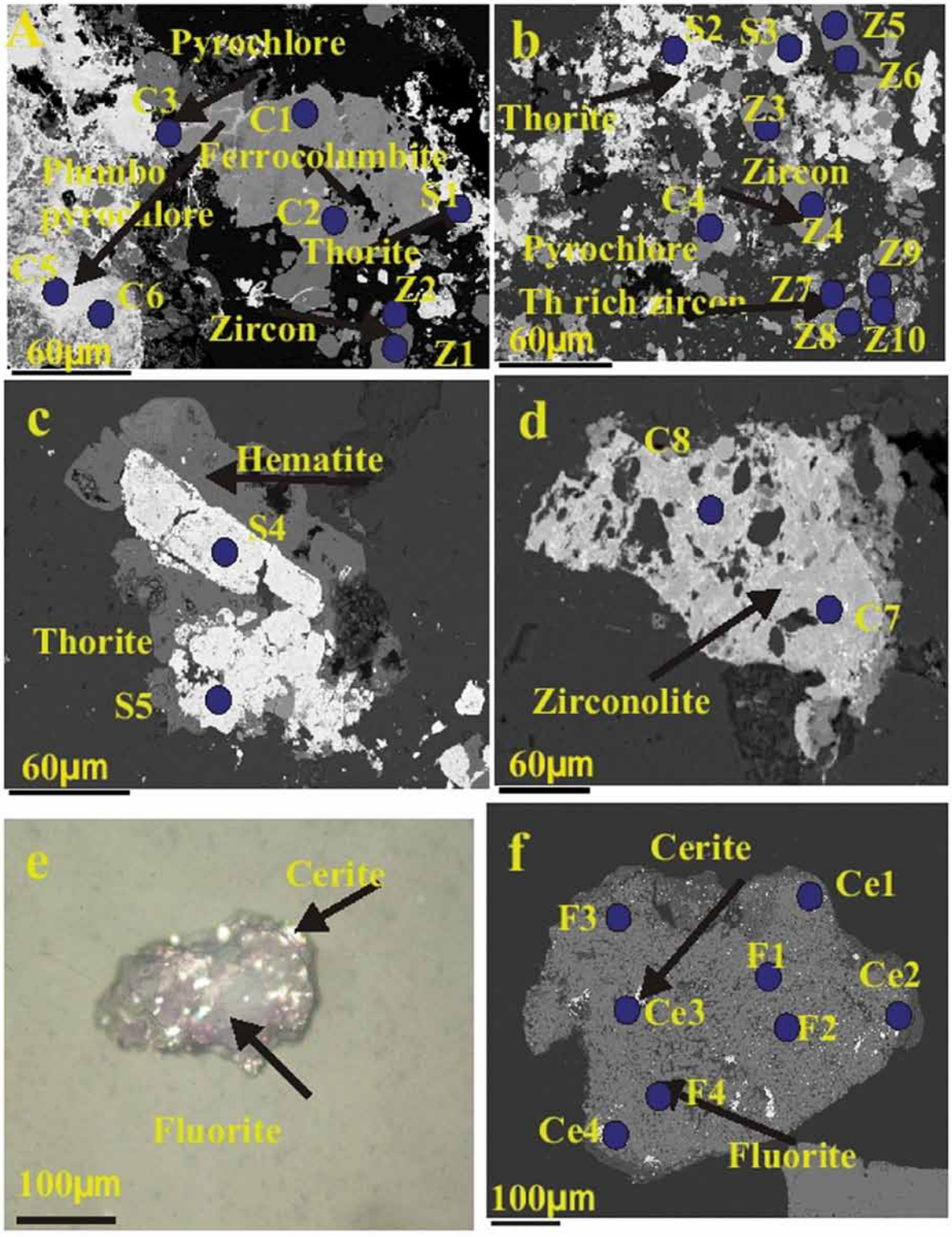

Fig. 5. a) pyrochlore and plumbopyrochlore associated with thorite and zircon in the El-Sibai shear zone, BSE image b) Thorite associated with euhedral crystals of zircon, BSE image c) large euhedral thorite with hematite, BSE image d) large crystal of zirconolite, and BSE image e) photomicrograph of violet fluorite with cerite inclusions, polarized light and f) its corresponding BSE image for the same crystal.

ways clear what was the oxidation state of some elements at the time of crystallization (Warner & Ewing, 1993). According to their structure these minerals are divided into ixiolite, samarskite (wolframite) and columbite groups. They consist of approximately hexagonal close packed O atoms. The A and B sites are octahedrally coordinated. Octahedra share edges to form chains along [001] and layers parallel to [100] (notation after Warner & Ewing, 1993). All three groups have structures that derivates of the α-PbO_2 structure (Warner & Ewing, 1993). The structures of pyrochlore and zirconolite share some basic features with those of fergusonite and aeschynite, namely octahedral chains and large A sites; however, the pyrochlore structure is a derivative of the CaF_2 structure (Chakoumakos, 1984) and zirconolite is a derivative of the pyrochlore structure (Bayliss et al., 1989). The most important U-bearing Nb-Ta-Ti oxides are discussed further below.

Ferrocolumbite [(Fe, Mn)$(Nb,Ta)_2O_6$] crystals that occur in the El-Sibai shear zone are generally dark grey to black when observed in the microscope. They are present in the form of subhedral to anhedral crystals and range in size from 30 to 100 μm (Fig. 5a, b). The EPMA of the minerals revealed that the major elements in ferrocolumbite at A sites are FeO (16.52 wt%) and MnO (4.57 wt%), and at B sites Nb_2O_5 (74.68 wt%), and Ta_2O_5 (2.61 wt%). Also, minor amounts of Ti, Th, U, Y and LREE were reported as substitutions in ferrocolumbite (Fig. 5a, Table 1).

Pyrochlore group [$A_{1-2}B_2O_6(O,OH,F)$]

This group is particularly important group with Nb-Ta-Ti oxides that contain substantial U. The structure of ideal pyrochlore group, is a derivative of the fluorite structure (Chakoumakos, 1984, 1986). The structure with Ta, Nd, and Ti, and which can also contain Fe, Sn, W, and Sb (Mandarino, 1999); Sb^{5+} can even dominate at the B site, as in the case of roméite (Brugger et al., 1997). The A site is eight coordinated (distorted cube) and may contain alkalis, alkaline earths, REE and actinides. In pyrochlore charge balance is maintained through cation substitutions at either A or B sites as well as throught anionic substitutions. Three pyrochlore subgroups are distinguished in accordance with the predominant cation in the B sites. Niobium prevail over Ta in the pyrochlore subgroup, whereas Ta exceeds Nb in the microlite subgroup. Both pyrochlore and microlite subgroups have (Ta+Nb)>2Ti, whereas the betafite subgroup is characterized by 2Ti>(Ta+Nb). U substitutions at the A sites and metamict pyrochlore are common. Although virtually all these minerals contains some U, only uranmicrolite and uranopyrochlore of pyrochlore group contain U as an essential constituent (Lumpkin & Ewing, 1995).

Pyrochlore [(Fe, Mn)(Nb, Ta, Ti)$_2O_6$(O,OH,F] occurs as subhedral to anhedral crystals in the El-Sibai altered peralkaine granites, and range in size from 5 to 10 μm (Fig. 5a, b). Its radioactivity is related to minute inclusions of radioactive minerals. The EPMA of the crystals showed that the major elements in pyrochlore are FeO (15.89 wt%) and MnO (4.57 wt%) at A sites, and Nb_2O_5 (65.94 wt%), Ta_2O_5 (3.2 wt%) and TiO_2 at B sites. Also minor amounts of U, Th, Y, and LREE were reported as substitutions in pyrochlore (Fig. 5a,b, Table 1).

Plumbopyrochlore [$(Pb,U,Ca)_{2-x}Nb_2O_6(OH)$] was found only in the El-Sibai shear zone as an alteration phase, containing potential concentrations of the high-field-strength elements (HFSE), such as Ti, Nb, and Ta, besides U. The EPMA of the sample MA226ES10-C5 revealed that the major elements in plumbopyrochlore are at A sites PbO (30.57 wt%), UO_2 (7.26 wt%), FeO (11.93 wt%), CaO (1.7 wt%) and MnO (0.26 wt%), and at B sites Nb_2O_5 (31.65 wt%), TiO_2 (5.81 %) and Ta_2O_5 (2.50 wt%), (Fig. 5 a, b; Table 1).

Zirconolite group ($A_2B_2O_7$)

The structure of zirconolite [(Ca,Fe)(Zr,U)Ti_2O_7] can be described as a derivative of the pyrochlore structure, with octahedrally coordinated B sites and A sites in distorted cubes. Zirconolite is monoclinic and has two distinct A sites, designated as A (Ca) and A' (Zr). Zirconolite is Ti dominant at the B site, Nb- dominant zirconolite minerals were identified from carbonatite in Kovdor (Williams & Gieré, 1996); however, no Ta- dominant zirconolite-group minerals are known. As for most other Ta-Nb-Ti oxides, U substitutes at the large cation sites primarily for Ca at the A site in zirconolite; no U dominant zirconolite-group minerals are known. Nevertheless, U and Th substitutions in zirconolite can induce substantial structural change, consequently the metamict zirconolite are not rare. As an important accessory mineral in large variety of rocks, zirconolite has also been studied as a potential actinide-bearing nuclear waste form (Lumpkin et al., 1994). It is as an alteration phase between columbite and zircon with size range from 20 to 50 μm (Fig. 5d). The EPMA of the sample MA226E8-C8 reflect the major elements in zirconolite are at A sites ZrO_2 (26.25 wt%), SiO_2 (18.97 wt%), FeO (13.21 wt%), and CaO (1.01 wt%), and at B sites Nb_2O_5 (10.99 wt%), TiO_2 (3.94 wt%), UO_2 (1.1 wt%), ThO_2 (8.79 wt%), Y_2O_3 (6.48 wt%), and Ta_2O_5 (0.2 wt%). Also small amounts of LREE (1.2 wt%) were reported as substitutions at B sites of zirconolite (Fig. 5d, Table 1).

Thorium mineralizations

In the El-Sibai altered granites (shear zone) two mineral species of Th-minerals, namely thorite and huttonite monazite are found. Under reducing conditions, U transport is likely to be measured in fractions of a centimeter, although F and Cl complexes can stabilize U (IV) within the solution (Keppler & Wyllie, 1990). If there is sufficient concentration of oxygen to stabilize the uranyl ion, UO^{2+} and its complexes, U can migrate many kilometers from its source to precipitate U-bearing minerals (plumbopyrochlore and zirconolite).

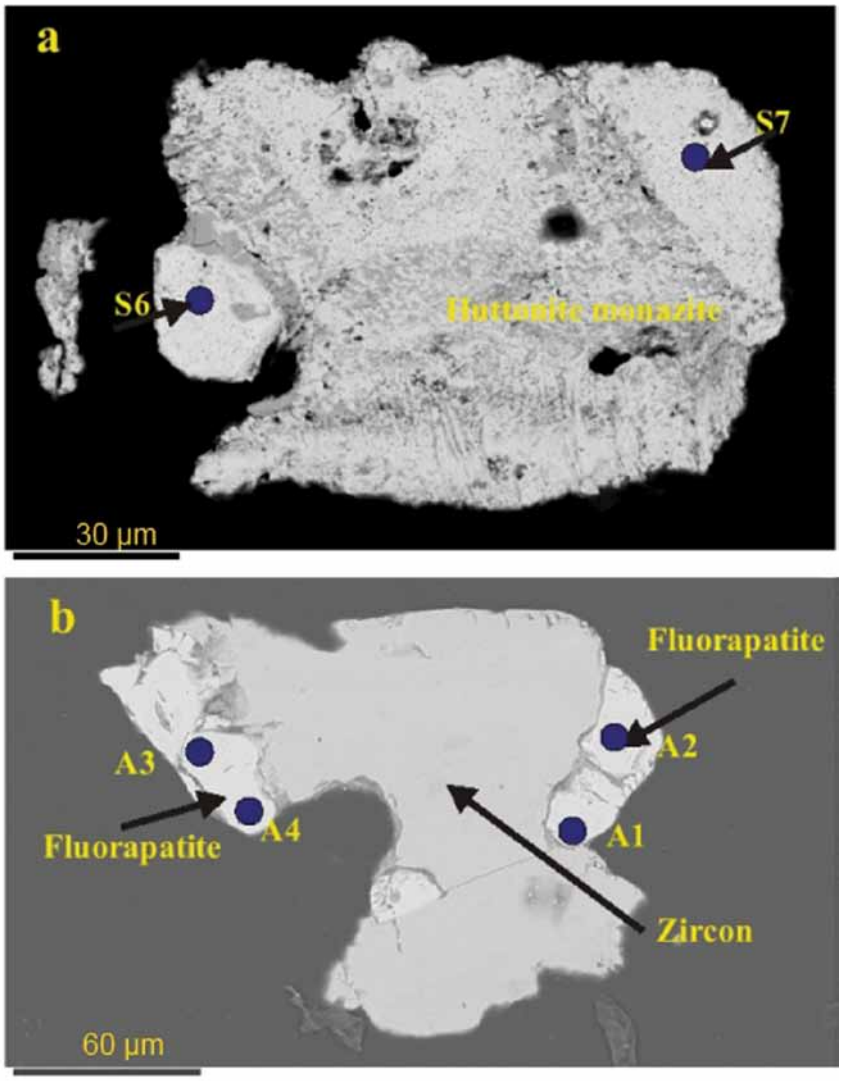

Fig. 6. SEM-BSE images a) huttonite after monazite, and b) fluorapatite cystals associated with zircon and titanite.

Thorite [Th,U(SiO_4)] exihibits euhedral to subhedral crystals in the El-Sibai altered peralkaline granites of the investigated area. Thorite is black to brown and shows varying degrees of alteration. It somewhat resembles zircon, occurring as small, square prismatic crystals with pyramidal points and has been found around the zircon crystals as yellowish brown phases (Fig. 5b, c). The chemical composition of thorite is given in Table 2. ThO_2 ranges from 68.13 to 78.64 wt% (mean 73.48 wt%), UO_2 ranges from 0.838 to 1.54 wt% (mean 1.07 wt%), SiO_2 ranges from 12.97 to 14.38 wt% (mean 13.71 wt%), Y_2O_3 (3.45 wt%), and FeO (3.22 wt%). Small amounts of Ca, P and LREE were reported as substitutions in thorite (Fig. 5b, c; Table 2).

Huttonite monazite [(Th,U,LREE)PO_4] occurs as as an alteration phase between thorite and monazite, and range in size from 30 to 100 µm (Fig. 5d). The EMPA of these crystals reflect the huttonite composition (Table 2). These results indicate that the mean values of major elements in huttonite monazite are ThO_2 (61.06 wt%), P_2O_5 (12.90 wt%), Al_2O_3 (1.11 wt%), CaO (4.75 wt%), Ce_2O_3 (11.80 wt%), Y_2O_3 (1.29 wt%), and U (0.7 wt%). Very small amounts of Si and LREE were reported as substitutions in huttonite (Fig. 6a, Table 2). According to Frondel and Cuttito (1955) huttonite and thorite are formed at hydrothermal conditions over a temperature range 300 °C to 700 °C. The formation of huttonite is favoured by alkaline conditions and thorite by acid conditions.

Accessory minerals

Accessory minerals include zircon, fluorite, monazite, and cerite-(Ce); among sulfides and hydroxides pyrite and hematite prevail.

Zircon ($ZrSiO_4$) is a common accessory mineral in plutonic igneous rocks. It is generally found as small inclusions in minerals, however in granites and pegmatites it can form large well developed crystals (Deer et al., 1966). Hussein (1978) and Abadalla et al. (2008) stated that the radioactive zircons are usually zoned and are characterized by metamictization. The explanation for the origin of the "metamict state" is that the internal order of the originally crystalline form has been destroyed by ∝-particles bombardment from radionuclides within the structure. It is partially or completely modified giving amorphous zircon a more isotropic character; i.e, metamict zircon. Zircon crystals

in the studied mineralized granites are mainly characterized by considerable metamictization due to thorium and uranium inclusions.

Zircon occurs as pale to deep brown euhedral prismatic grains and is generally sub-translucent to opaque with dull luster. The most common habit is the bipyramidal form with various pyramidal faces (Fig. 4a, b). However, some zircon crystals are characterized by extremely short prisms and are more or less equidimensional, exhibiting square cross section. Zircon occurs as euhedral to subhedral prismatic (six-or eight-sided), 20 to 150 μm zoned crystals, which contain clusters of inclusions of radioactive minerals. The core of zircon in the El-Sibai shear zone contains high Hf contents, in contract to the rim with low Hf contents (Table 3). Both varieties of zircon, unaltered and altered zircon (Th-rich zircon), have been recognized in the El-Sibai altered granites (shear zone). The chemical composition of zircon is presented in Table 3. Th-rich zircon has higher ThO_2 and UO_2, and lower ZrO_2 and SiO_2, in comparison to unaltered zircon. Generally, domains of altered zircon (Th-rich zircon) are characterized by greater enrichment in CaO, FeO, P_2O_5, HfO_2 and Al_2O_3 than unaltered domains (Fig. 5b, Table 4). Similar results were observed by Förster (2000, 2006) and Abd El-Naby (2009), who reported on

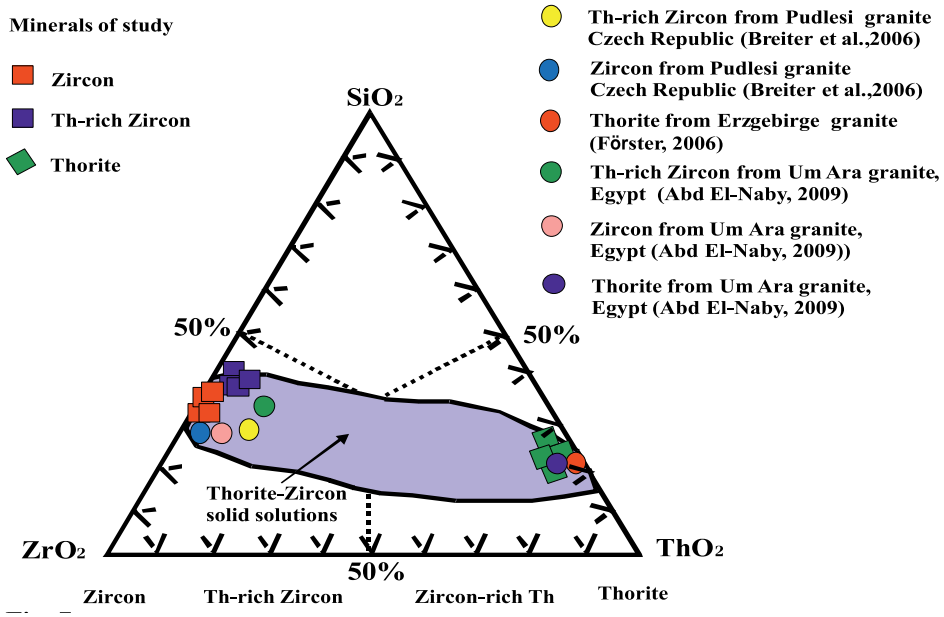

Fig. 7. Composition of thorite and zircon plotted on the basis of SiO_2–ThO_2–ZrO_2. The shaded field encloses the composition of thorite–zircon solid solution. See also Breiter et al. 2006, Fröster et al., 2006, and Abd El-Naby, 2009.

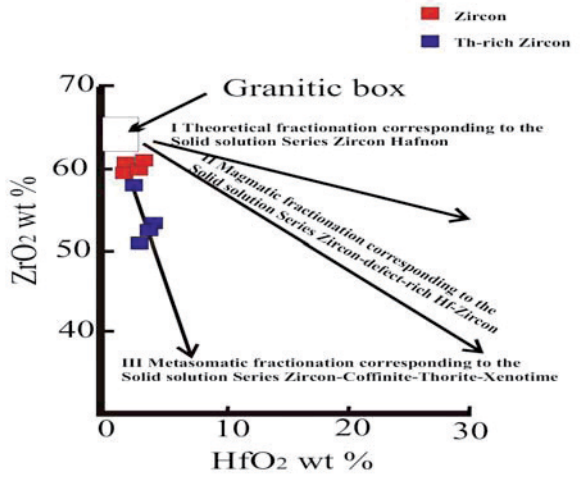

Fig. 8. ZrO2 versus HfO_2 diagram of zircons from rare metal granitoids, Eastern Desert, Egypt. The shown trends are modified from Kempe et al. (1997) and Abadalla et al. (2008). The granite box, comprising Zr-Hf ranges in granites from Wedepohl (1978).

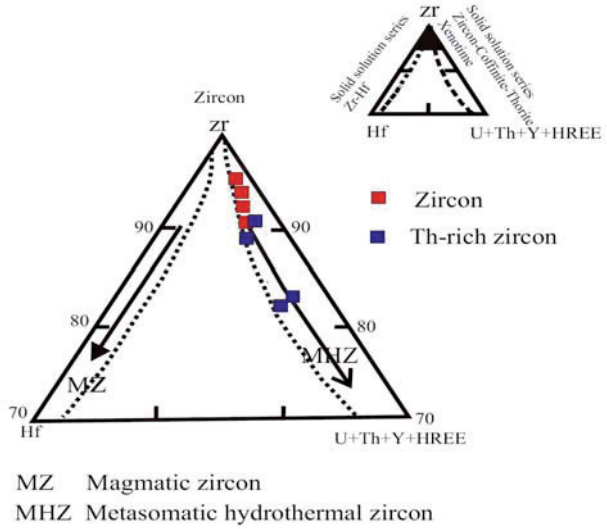

Fig. 9. Zr-Hf-(Y+ U+ Th +HREE) ternary diagram for zircon compositions in rare metal granitoids, Eastern Desert, Egypt, the dashed line represents an interpretative boundary that limits the compositional gap between the two zircon series. The shown trends of magmatic zircon (MZ) and metasomatic hydrothermal zircon (MHZ) are drawn by Abadalla et al. (2008).

Table 1. Mineral chemistry of selected some minerals from El-Sibai shear zone, the minerals obtained by EMPA, the major oxides by (wt%).

Rock	El-Sibai	El-Sibai	El-Sibai	El-Sibai	El-Sibai	El-Sibai	El-Sibai	El-Sibai
Sample	MA226 ES10-C1	MA226 ES10-C2	MA226 ES10-C3	MA226 ES6-C4	MA226 ES10-C5	MA226 ES10-C6	MA226 ES10-C7	MA226 ES8-C8
Mineral name	Ferro-columbite	Ferro-columbite	Pyrochlore	Pyrochlore	Plumbo-pyrochlore	Plumbo-pyrochlore	Zirconolite	Zirconolite
SiO_2	0.110	0.109	1.119	1.190	3.15	4.65	18.13	18.97
Na_2O	0.033	0.033	0.143	0.152	1.333	1.228	0.090	0.104
K_2O	0.000	0.000	0.000	0.000	0.033	0.030	0.000	0.000
ZrO_2	0.000	0.000	0.245	0.286	0.216	0.198	25.28	26.25
HfO_2	0.041	0.041	0.000	0.000	0.003	0.000	1.198	1.385
P_2O_5	0.032	0.031	0.030	0.032	0.086	0.079	0.281	0.325
CaO	0.047	0.046	2.106	2.240	1.705	1.570	0.047	1.013
FeO	16.52	16.38	14.91	15.89	11.93	10.98	12.28	13.21
TiO_2	1.511	1.498	5.95	6.34	5.81	5.35	3.41	3.94
MnO	4.57	4.53	1.093	1.165	0.289	0.266	0.104	0.120
Y_2O_3	0.329	0.326	0.852	0.908	0.287	0.264	5.60	6.48
Ce_2O_3	0.000	0.000	0.099	0.106	0.756	0.696	0.760	0.879
La_2O_3	0.004	0.004	0.000	0.000	0.219	0.201	0.137	0.159
Pr_2O_3	0.000	0.000	0.000	0.000	0.036	0.033	0.093	0.108
Nd_2O_3	0.074	0.073	0.000	0.000	0.042	0.038	0.069	0.079
Gd_2O_3	0.000	0.000	0.060	0.064	0.190	0.175	0.000	0.000
SnO_2	0.114	0.113	0.245	0.261	0.028	0.026	0.000	0.000
Nb_2O_5	74.68	74.03	61.87	65.94	31.65	29.14	9.50	10.99
Ta_2O_5	2.613	2.591	2.999	3.20	2.503	2.384	0.172	0.199
PbO	0.000	0.000	0.000	0.000	30.57	28.14	0.000	0.000
ThO_2	0.085	0.084	1.399	1.480	1.027	0.946	7.60	8.79
UO_2	0.111	0.110	0.688	0.733	7.26	6.68	0.868	1.104
Total	100.87	99.96	93.81	99.98	99.11	93.07	86.45	94.10
Structural formula for 4 oxygen atoms								
Si	0.003	0.003	0.035	0.037	0.158	0.145	0.567	0.655
Na	0.001	0.001	0.005	0.005	0.042	0.038	0.003	0.003
K	0.000	0.000	0.000	0.000	0.001	0.001	0.000	0.000
Zr	0.000	0.000	0.008	0.009	0.007	0.006	0.790	0.914
Hf	0.001	0.001	0.000	0.000	0.000	0.000	0.016	0.019
P	0.001	0.001	0.001	0.001	0.002	0.002	0.007	0.008
Ca	0.001	0.001	0.059	0.062	0.047	0.044	0.001	0.028
Fe	0.516	0.512	0.466	0.497	0.373	0.343	0.384	0.444
Ti	0.047	0.047	0.186	0.198	0.182	0.167	0.107	0.123
Mn	0.143	0.142	0.034	0.036	0.009	0.008	0.003	0.004
Y	0.007	0.007	0.018	0.019	0.006	0.006	0.117	0.135
Ce	0.000	0.000	0.002	0.002	0.016	0.015	0.016	0.018
La	0.000	0.000	0.000	0.000	0.005	0.004	0.003	0.003
Pr	0.000	0.000	0.000	0.000	0.001	0.001	0.002	0.002
Nd	0.002	0.002	0.000	0.000	0.001	0.001	0.001	0.002
Sn	0.001	0.001	0.003	0.003	0.001	0.001	0.000	0.000
Nb	1.167	1.157	0.967	1.030	0.495	0.455	0.148	0.172
Ta	0.025	0.025	0.029	0.031	0.014	0.013	0.002	0.002
Th	0.003	0.028	0.046	0.049	0.034	0.031	0.249	0.288
U	0.004	0.003	0.022	0.035	0.227	0.209	0.027	0.035
Nb / Ta	28.58	28.58	20.66	20.61	21.10	21.06	55.10	55.12
Th / U	0.76	0.76	2.03	1.34	0.14	0.14	8.76	7.96

chemical analyses of zircon, thorite, and Th-rich zircon (Fig. 7). Despite the incorporation of some oxides (e.g. CaO, FeO, P_2O_5, HfO_2 and Al_2O_3) and a hydrous component, the majority of domains of both zircon varieties maintain a constant SiO_2/ZrO_2 ratio (Table 4).

The EMPA for these crystals reflect the zircon composition (Table 3). This indicates that the major elements in zircon are ZrO_2 (60.44 wt%), SiO_2 (31.94 wt%), HfO_2 (2.94 %), and Yb_2O_3 (0.5 wt%) with significant amounts of ThO_2 (0.36 wt%), UO_2 (0.16 wt%), FeO (0.82 wt%), and Y_2O_3 (0.4 wt%). In contrast, the EPMA of the Th-rich zircon showed in average mainly ZrO_2 (53.47 wt%), SiO_2 (29.55 wt%), HfO_2 (3.34 wt%), and Yb_2O_3 (0.56 wt%) with significant amounts of ThO_2 (5.46 wt%), UO_2 (0.55 wt%), FeO (0.85 wt%), and Y_2O_3 (2.16 wt%) composed of Th-rich zircon (Table 4).

Petrogenesis of zircon

Kempe et al. (1997) and Abadalla et al. (2008) considered that both magmatic and metasomatic mechanisms or their combination were responsible for yielding extreme Zr/Hf fractionation and hence the formation of Hf-rich zircon. The aforementioned petrographical and geochemical characterization of metasomatically and magmatically specialized rare metal granitoids, has greatly contributed to clear discrimination of Zr/Hf fractionation in the two main associations (i.e. magmatic & metasomatic).

The zircon of the investigated rare metal El-Sibai altered granite frequently contains hafnium in amounts ranging between 2.14 and 4.23 wt%, therefore the nomenclature scheme of Correia Neves et al. (1974) for the isomorphous zircon ($ZrSiO_4$)–Hafnon ($HfSiO_4$) series has been used to designate it. The term #Hf denotes the hafnon end-member ($HfSiO_4$) mole% or more precisely, the atomic ratio: 100*Hf/(Zr + Hf) (Table 3). Zircon has #Hf = 0–10; hafnian zircon #Hf = 10–50; zirconian hafnon #Hf = 50–90 and Hafnon #Hf = 90–100.

However, in the present study zircon with enhanced Hf content (i.e. #Hf = 3–10) was designated as Hf-rich zircon in order to distinguish it from zircon with very low #Hf. Zircon of El-Sibai peralkaline granite is characterized by a primitive composition with respect to the content of Hf, Y, U, Th, and HREE (Figs. 8, 9; Table 3). Its ranging between 3.54 and 6.44 and thus, it can be designated as a normal zircon according to the scheme

Table 2. Mineral chemistry of selected some minerals from El-Sibai shear zone, the minerals obtained by EMPA, the major oxides by (wt%).

Rocks	El-Sibai	El-Sibai	El-Sibai	El-Sibai	El-Sibai	El-Sibai	El-Sibai	El-Sibai	El-Sibai
Sample	MA226 ES10-S1	MA226 ES10-S2	MA226 ES5-S3	MA226 ES6-S4	MA226 ES3-S5	Average N=5	MA226 ES3-S6	MA226 ES3-S7	Average N=2
Minerals	Thorite	Thorite	Thorite	Thorite	Thorite		Huttonite monazite	Huttonite monazite	
Al_2O_3	0.000	0.000	0.000	0.000	0.000	0.000	1.116	1.103	1.11
SiO_2	14.38	14.06	13.86	13.29	12.97	13.71	0.357	0.365	0.361
Na_2O	0.101	0.084	0.016	0.079	0.015	0.059	0.000	0.000	0.000
K_2O	0.113	0.048	0.000	0.045	0.000	0.069	0.000	0.000	0.000
ZrO_2	0.567	1.178	0.206	1.114	0.193	0.652	0.077	0.079	0.078
HfO_2	0.032	0.083	0.000	0.078	0.000	0.064	0.169	0.173	0.171
P_2O_5	0.201	0.269	0.254	0.254	0.238	0.243	12.74	13.05	12.90
CaO	0.328	0.260	0.742	0.245	0.694	0.454	4.69	4.80	4.75
FeO	1.062	0.350	7.43	0.330	6.95	3.22	1.01	0.985	0.998
MnO	0.077	0.026	0.009	0.024	0.009	0.029	0.000	0.000	0.000
Y_2O_3	3.38	3.63	3.51	3.43	3.29	3.45	1.289	1.296	1.293
Ce_2O_3	0.036	0.000	0.000	0.000	0.000	0.036	11.10	12.5	11.80
Pr_2O_3	0.145	0.000	0.000	0.000	0.000	0.145	0.000	0.000	0.000
La_2O_3	0.033	0.000	0.000	0.000	0.000	0.033	0.000	0.000	0.000
Nd_2O_3	0.066	0.000	0.000	0.000	0.000	0.066	1.595	1.634	1.615
Eu_2O	0.000	0.000	0.000	0.000	0.000	0.000	0.231	0.236	0.234
Gd_2O_3	.1500	0.075	0.000	0.071	0.000	0.076	0.907	0.929	0.918
Dy_2O_3	0.000	0.000	0.000	0.000	0.000	0.000	0.24	0.246	0.245
HO_2O_3	0.000	0.000	0.000	0.000	0.000	0.000	0.133	0.137	0.135
Er_2O_3	0.000	0.000	0.000	0.000	0.000	0.000	0.250	0.240	0.245
Yb_2O_3	0.000	0.000	0.000	0.000	0.000	0.000	0.022	0.023	0.023
Nb_2O_5	0.346	0.405	0.069	0.383	0.064	0.253	0.000	0.000	0.000
Ta_2O_5	0.043	0.000	0.000	0.000	0.000	0.043	0.000	0.000	0.000

Table 2. (continued)

PbO	0.000	0.000	0.000	0.000	0.000	0.000	0.111	0.114	0.112
ThO_2	73.49	78.64	72.81	74.32	68.13	73.48	60.69	61.43	61.06
UO_2	1.543	0.886	1.086	0.838	1.016	1.074	0.693	0.710	0.702
Total	96.09	99.98	100.01	94.51	93.57	96.83	98.60	99.95	99.28
Structural formula on basis of 4 oxygen atoms									
Al	0.000	0.000	0.000	0.000	0.000	0.000	0.023	0.023	0.023
Si	0.444	0.434	0.428	0.410	0.400	0.420	0.011	0.011	0.011
Na	0.003	0.003	0.001	0.003	0.001	0.002	0.000	0.000	0.000
K	0.003	0.001	0.000	0.001	0.000	0.002	0.000	0.000	0.000
Zr	0.018	0.037	0.006	0.035	0.006	0.020	0.001	0.001	0.001
Hf	0.001	0.001	0.000	0.001	0.000	0.001	0.002	0.002	0.002
P	0.005	0.007	0.006	0.006	0.006	0.006	0.319	0.326	0.323
Ca	0.009	0.007	0.021	0.007	0.012	0.013	0.130	0.133	0.131
Fe	0.030	0.010	0.206	0.009	0.193	0.090	0.032	0.031	0.032
Mn	0.002	0.001	0.001	0.001	0.000	0.002	0.000	0.000	0.000
Y	0.099	0.106	0.103	0.101	0.096	0.101	0.027	0.027	0.027
Ce	0.001	0.000	0.000	0.000	0.000	0.001	0.232	0.260	0246
Pr	0.004	0.000	0.000	0.000	0.000	0.004	0.000	0.000	0.000
La	0.001	0.000	0.000	0.000	0.000	0.001	0.000	0.000	0.000
Nd	0.002	0.000	0.000	0.000	0.000	0.002	0.033	0.034	0.034
Eu	0.000	0.000	0.000	0.000	0.000	0.000	0.005	0.005	0.005
Gd	0.005	0.001	0.000	0.002	0.000	0.003	0.019	0.019	0.019
Dy	0.000	0.000	0.000	0.000	0.000	0.000	0.005	0.005	0.005
Ho	0.000	0.000	0.000	0.000	0.000	0.000	0.003	0.003	0.003
Er	0.000	0.000	0.000	0.000	0.000	0.000	0.005	0.005	0.005
Yb	0.000	0.000	0.000	0.000	0.000	0.000	0.001	0.001	0.001
Nb	0.005	0.006	0.001	0.006	0.001	0.004	0.000	0.000	0.000
Pb	0.000	0.000	0.000	0.000	0.000	0.000	0.001	0.001	0.001
Th	1.341	1.435	1.329	1.356	1.243	1.34	1.108	1.121	1.115
U	0.026	0.015	0.019	0.014	0.017	0.018	0.012	0.12	0.012
Th / U	47.62	88.72	67.05	88.71	67.05	71.83	92.33	93.42	92.88
∑A+B	2.0	2.07	2.11	1.96	1.98	2.02	1.98	2.01	2.00

N= number of samples

of Correia Neves et al. (1974). Zircon of the studied altered peralkaline granite zone is characterized by UO_2 and ThO_2 occur in high quantities in HREE (Figs. 8, 9; Table 3). Meanwhile Th-rich zircons of the hematitized and albitized granites are characterized by complex chemistry which is reflected in high to enhanced contents of Hf, U, Th, Y, HREE (Figs. 8, 9; Table 3) and therefore this zircon can be designated as Hf-rich zircon. The zoning terminology used here is based on the geochemical criteria given by Černý et al. (1985) for fractionated rare metal granitoids and pegmatites.

Fluorite CaF_2

Fluorite showed large blue to violet euhedral to subhedral crystals with a size range of 10-40 μm (Fig. 5e, f). The EPMA indicate that the major elements in fluorite are CaO (68.75 wt%) and F (45.83 wt%), with significant amounts of Ce_2O_3 (0.7 wt%), Y_2O_3 (2.7 wt%), UO_2 (0.02 wt%), ThO_2 (0.2 wt%) and REE (2 wt%) are reported as substitutions in fluorite (Table 5). Yttrium partially substitutes Ca. El-Kammar et al. (1997) concluded that the change in colour of fluorite is mainly controlled by the Y content. The presence of fluorite accompanying the mineralization indicates that the hydrothermal alteration processes were involved during shearing.

Cerite-(Ce) $[Ce_9(Th, Ca)(Fe^{3+}, Mg)(SiO_4)_6[SiO_3(OH)](OH)_3]$

The nomenclature of the REE minerals is unique, because names of simple end-members no longer exist. Since 1966 each mineral name consists of a structural formula name and the symbol of the dominant lanthanide element (Fleischer, 1987, 1989; Bayliss & Levinson, 1988). The crystal structures of many REE minerals are poorly-

Table 3. Mineral chemistry of selected some minerals from El-Sibai shear zone, the minerals obtained by EMPA, the major oxides by (wt%).

Rock	El Sibai	El Sibai	El Sibai	El Sibai	El Sibai	El Sibai	El Sibai
Sample	Zircon Core MA226-E10 Z1	Zircon Rim MA226-E10 Z2	Zircon Core MA226-ES3 Z3	Zircon rim MA226-ES3 Z4	Zircon core FEL-2E4 Z5	Zircon rim FEL-2E4 Z6	Average N=6
Al_2O_3	0.000	0.026	0.000	0.000	0.000	0.000	0.056
SiO_2	32.74	33.05	32.82	32.62	30.42	30.00	31.94
ZrO_2	61.34	61.05	61.45	61.59	59.15	58.05	60.44
HfO_2	4.24	3.42	4.23	3.14	2.476	2.135	2.94
P_2O_5	0.128	0.009	0.040	0.087	0.694	0.569	0.254
CaO	0.007	0.000	0.016	0.011	0.069	0.178	0.056
FeO	0.187	0.430	0.878	1.366	0.172	1.891	0.821
MnO	0.000	0.021	0.000	0.000	0.000	0.066	0.044
Y_2O_3	0.120	0.000	0.000	0.011	0.639	0.835	0.40
Ce_2O_3	0.027	0.089	0.000	0.028	0.000	0.000	0.048
Yb_2O_3	0.205	0.139	0.037	0.160	1.297	1.157	0.499
PbO	0.016	0.047	0.000	0.048	0.000	0.069	0.045
ThO_2	0.400	0.165	0.127	0.076	0.934	0.444	0.358
UO_2	0.187	0.000	0.057	0.117	0.149	0.172	0.155
Total	99.60	98.47	99.66	99.25	96.01	95.65	98.11
Structural formula for 4 oxygen atoms							
Al	0.000	0.001	0.000	0.000	0.000	0.002	0.001
Si	1.011	1.020	1.013	1.007	0.939	0.926	0.986
Zr	0.921	0.917	0.923	0.925	0.924	0.907	0.920
Hf	0.032	0.040	0.040	0.030	0.034	0.029	0.034
P	0.003	0.001	0.001	0.002	0.017	0.014	0.006
Ca	0.000	0.000	0.001	0.001	0.002	0.005	0.002
Fe	0.005	0.011	0.022	0.034	0.005	0.059	0.023
Mn	0.000	0.001	0.000	0.000	0.000	0.002	0.002
Y	0.003	0.000	0.000	0.001	0.013	0.017	0.011
Ce	0.001	0.002	0.000	0.001	0.000	0.000	0.001
Yb	0.004	0.003	0.001	0.003	0.027	0.024	0.010
Pb	0.001	0.001	0.000	0.001	0.000	0.001	0.001
Th	0.013	0.005	0.004	0.003	0.017	0.008	0.008
U	0.002	0.000	0.001	0.001	0.003	0.003	0.002
∑A+B	2.0	2.0	2.05	2.01	1.98	1.98	2.0
Hf / Zr	17.94	14.40	14.53	19.61	23.89	27.19	19.59
U / Th	2.14	0.00	2.23	0.65	6.27	2.58	2.77
#Hf	5.28	3.54	6.44	4.85	4.02	3.56	4.62

#Hf = 100*Hf/(Zr+Hf)

N= number of samples

known; because the phases in nature are metamict (Th and U commonly substitute for REE in minerals, as mentioned above). The smaller or Y-group (heavy) REE exhibit irregular coordination numbers with coordination number from 6 to 9, most commonly 8, whereas the larger or Ce-group (light) REE exhibit larger coordination numbers from 7 to 12, most commonly 9 (Miyawaki & Nakai, 1987).

The trivalent Ce-group REE are structurally very similar to the Ca^{2+}, therefore they commonly substitute Ca in rock-forming minerals. Substitution of a trivalent REE cation for divalent Ca requires a charge compensating mechanism, i.e., a coupled substitution can be represented by the operators EuCa-1(for Eu^{2+}; add one Eu, remove one Ca or exchange Eu for a Ca), YCe_{-1}, and $CeTh_{-1}$ (for Ce^{4+}). The light rare earths (called cerium-group or LREE) have relatively large ionic radii similar to that of Ca^{2+} and Th^{4+}, in contrast to the heavy rare earths (plus Y and Mn^{2+}). All of the REE commonly substitute each other in minerals. LREE tend to be concentrated in highly fractionated basic rocks such as carbonatites (Förster,

Table 4. Mineral chemistry of selected some minerals from El-Sibai shear zone, the minerals obtained by EMPA, the major oxides by (wt%).

Rock	El Sibai	El Sibai	El Sibai	El Sibai	El Sibai
Sample	Th-rich zircon Core MA226-E10 Z7	Th-rich zircon Rim MA226-E10 Z8	Th-rich zircon Core MA226-ES6 Z9	Th-rich zircon Rim MA226-ES6 Z10	Average N=4
Al_2O_3	0.462	0.807	0.477	0.849	0.649
SiO_2	30.03	28.85	29.98	29.33	29.55
ZrO_2	58.07	51.60	52.91	51.20	53.47
HfO_2	3.18	2.63	4.28	2.77	3.34
P_2O_5	0.131	0.158	0.136	0.166	0.148
CaO	0.188	0.567	0.194	0.596	0.386
FeO	0.589	1.058	0.618	1.113	0.845
MnO	0.000	0.138	0.000	0.146	0.142
TiO_2	0.000	0.030	0.000	0.032	0.031
Y_2O_3	1.070	2.662	2.114	2,799	2.16
Ce_2O_3	0.099	0.228	0.102	0.240	0.167
Yb_2O_3	0.429	0.672	0.442	0.706	0.562
PbO	0.021	0.015	0.028	0.026	0.023
ThO_2	2.30	4.97	6.37	8.20	5.46
UO_2	0.362	0.710	0.374	0.746	0.548
Total	96.93	95.10	98.03	98.92	97.25
Structural formula for 4 oxygen atoms					
Al	0.010	0.017	0.015	0.027	0.017
Si	0.927	0.890	0.925	0.905	0.912
Zr	0.872	0.775	0.827	0.800	0.819
Hf	0.030	0.025	0.059	0.058	0.048
P	0.003	0.004	0.003	0.004	0.004
Ca	0.005	0.016	0.005	0.017	0.011
Fe	0.015	0.027	0.019	0.035	0.024
Mn	0.000	0.003	0.000	0.005	0.004
Ti	0.000	0.001	0.000	0.001	0.001
Y	0.022	0.056	0.044	0.058	0.045
Ce	0.002	0.005	0.002	0.005	0.004
Yb	0.009	0.014	0.009	0.015	0.012
Pb	0.001	0.001	0.001	0.001	0.001
Th	0.075	0.163	0.116	0.150	0.126
U	0.004	0.007	0.006	0.013	0.008
∑A+B	2.0	2.0	2.03	2.09	2.03
Hf /Zr	18.26	19.60	12.36	18.48	17.18
U /Th	6.35	7.00	17.61	10.94	10.48
#Hf	5.98	4.85	7.48	5.13	5.86

#Hf = 100*Hf/(Zr+Hf)

N= number of samples

2000), whereas HREE and especially Y tend to be concentrated in fractionated acid rocks in example alkaline granites and pegmatites. The EMPA for these crystals reflect the cerite composition. The EPMA indicate that the mean values of major elements in cerite are Ce_2O_3 (65.48 wt%), SiO_2 (7.16 wt%), ThO_2 (9.92 wt%), CaO (2.31 wt%), Y (2.13 wt%), Yb_2O_3 (1.31 wt%), Al_2O_3 (4.55 wt%), FeO (0.23 wt%), MgO (0.2 wt%), UO_2 (0.38 wt%) and F (2.46 wt%) with significant amounts of Sr, HREE, and Hf (Fig. 5f, Table 5).

Fluorapatite $Ca_5(PO_4)_3F$

Under binocular microscope, apatite grains are mainly massive with well rounded to subrounded

Table 5. Mineral chemistry of selected some minerals from El-Sibai shear zone, the minerals obtained by EMPA, the major oxides by (wt%).

Rocks	**El-Sibai**	**El-Sibai**	**El-Sibai**	**El-Sibai**		**El-Sibai**	**El-Sibai**	**El-Sibai**	**El-Sibai**	
Sample	**MA226 ES10**	**MA226 ES10**	**MA226 ES5**	**MA226 ES6**	**Average N=4**	**MA226 ES3**	**MA226 ES3**	**MA226 ES3**	**MA226 ES3**	**Average N=4**
Mineral name	**Flourite F1**	**Flourite F2**	**Flourite F3**	**Flourite F4**		**Cerite Ce1**	**Cerite Ce2**	**Cerite Ce3**	**Cerite Ce4**	
Al_2O_3	1.118	0.461	1.103	0.455	0.786	5.45	4.23	4.70	3.82	4.55
SiO_2	0.825	0.469	0.813	0.462	0.545	9.08	6.17	7.83	5.57	7.16
Na2O	0.941	0.472	0.928	0.466	0.702	0.000	0.000	0.000	0.000	0.000
F	45.21	47.06	44.60	46.43	45.83	2.979	2.300	2.569	2.008	2.464
CaO	67.64	70.80	66.72	69.85	68.75	2.383	2.528	2.055	2.283	2.31
P_2O_5	0.061	0.081	0.060	0.080	0.068	0.133	0.156	0.115	0.141	0.136
MgO	0.000	0.011	0.015	0.010	0.012	0.215	0.223	0.124	0.255	0.2
FeO	0.010	0.012	0.000	0.012	0.012	0.258	0.225	0.222	0.203	0.227
SrO	0.000	0.012	0.000	0.010	0.011	0.009	0.015	0.012	0.018	0.014
Y_2O_3	2.661	1.207	2.625	1.190	0.920	2.711	1.813	2.339	1.637	2.125
Ce_2O_3	0.730	0.000	0.720	0.138	0.435	67.02	66.60	67.81	60.16	65.48
La_2O_3	0.059	0.140	0.058	0.000	0.086	0.120	0.074	0.104	0.067	0.091
Pr_2O_3	0.028	0.071	0.028	0.000	0.042	0.000	0.000	0.000	0.000	0.000
Nd_2O_3	0.124	0.000	0.122	0.070	0.105	0.661	0.573	0.570	0.587	0.580
Eu_2O_3	0.010	0.000	0.000	0.000	0.011	0.000	0.348	0.000	0.314	0.331
Gd_2O_3	0.100	0.000	0.099	0.000	0.099	0.000	0.000	0.000	0.000	0.10
Dy_2O_3	0.117	0.126	0.115	0.124	0.121	0.508	0.280	0.438	0.253	0.37
Er_2O_3	0.244	0.011	0.241	0.011	0.090	0.778	0.244	0.471	0.220	0.478
Yb_2O_3	0.350	0.000	0.346	0.000	0.348	1.663	1.126	1.434	1.017	1.310
HfO_2	0.000	0.120	0.000	0.119	0.120	0.000	0.021	0.000	0.019	0.07
PbO	0.000	0.049	0.000	0.048	0.048	0.000	0.000	0.000	0.000	0.000
ThO_2	0.197	0.073	0.194	0.072	0.159	7.13	13.86	6.12	12.52	9.92
UO_2	0.021	0.026	0.000	0.026	0.068	0.382	0.421	0.329	0.380	0.375
Total	101.51	101.36	99.99	100.01	100.72	99.98	100.0	96.24	90.33	96.64
Structural formula on basis of 4 oxygen atoms										
Si	0.026	0.025	0.025	0.014	0.017	0.284	0.193	0.244	0.172	0.223
Na	0.023	0.015	0.024	0.015	0.020	0.000	0.000	0.000	0.000	0.000
Al	0.029	0.010	0.023	0.010	0.018	0.114	0.088	0.098	0.080	0.095
F	------	-----	-------	-------	------	------	------	------	------	-------
Hf	0.000	0.002	0.000	0.004	0.002	0.000	0.002	0.000	0.001	0.001
P	0.002	0.002	0.002	0.002	0.002	0.003	0.004	0.003	0.004	0.004
Ca	1.88	1.97	1.853	1.940	1.91	0.070	0.070	0.057	0.063	0.033
Mg	0.001	0.001	0.001	0.001	0.001	0.007	0.007	0.004	0.008	0.006
Fe	0.000	0.004	0.000	0.001	0.002	0.008	0.007	0.006	0.006	0.007
Sr	0.000	0.001	0.000	0.001	0.001	0.001	0.001	0.001	0.001	0.001
Y	0.055	0.025	0.077	0.035	0.048	0.057	0.038	0.069	0.048	0.051
Ce	0.015	0.004	0.021	0.004	0.011	1.40	1.39	1.986	1.762	1.63
La	0.001	0.003	0.002	0.000	0.007	0.003	0.002	0.003	0.002	0.003
Pr	0.001	0.001	0.001	0.000	0.001	0.001	0.000	0.000	0.000	0.001
Dy	0.002	0.003	0.004	0.003	0.003	0.011	0.006	0.020	0.007	0.009
Nd	0.003	0.000	0.004	0.002	0.003	0.014	0.012	0.017	0.015	0.015
Eu	0.001	0.000	0.000	0.000	0.001	0.000	0.000	0.000	0.009	0.008
Gd	0.002	0.000	0.003	0.000	0.002	0.000	0.000	0.000	0.000	0.000
Er	0.005	0.001	0.007	0.004	0.004	0.016	0.005	0.020	0.007	0.012

Table 5. (continued)

Yb	0.007	0.000	0.010	0.000	0.009	0.035	0.023	0.042	0.030	0.032
Pb	0.000	0.001	0.000	0.002	0.001	0.000	0.000	0.000	0.000	0.000
Th	0.004	0.003	0.006	0.002	0.004	0.130	0.253	0.112	0.228	0.181
U	0.001	0.001	0.000	0.001	0.001	0.006	0.007	0.006	0.006	0.007
Th/U	9.38	2.81	0.000	2.81	5.00	18.66	32.92	18.66	32.90	25.86

-----not calculated

N= number of samples

shapes. The color of apatite grains generally varies from pale yellow to dark brown. The EPMA (Fig. 6a, b) reflects the chemical composition of apatite associated with minor amount of uranium (1.63 wt%) and manganese. Uranium usually substitutes for Ca in fluorapatite. According to Deer et al. (1966, 1992) the intensity of the color in fluor-apatite increases with increasing Mn content. The EMPA for these crystals reflect the zircon composition (Fig. 6b, Table 6). The EPMA indicate that the major elements in zircon are CaO (55.21 wt%), P_2O_5 (42.08 wt%), and F (2.7 wt%). Significant amounts of Th, Fe, Y and LREE were reported as substitutions in fluorapatite (Table 6).

Other minerals

Monazite [LREE,Th(PO_4)] is the most common accessory mineral in many magmatic and metamorphic rocks, especially rocks characterized by mildly to strongly peraluminous compositions. Monazite crystals appear mainly as euhedral to subhedral inclusions in the zircon and columbite minerals (Fig. 6a).

Pyrite (FeS_2) is the main sulfide encountered and it is disseminated in the shear zones. Generally, pyrite of the El-Sibai shear zones is partially or entirely oxidized to oxyhydroxides such as hematite and goethite. This process can be classified as pseudomorphic desulfidization under oxidizing conditions. Desulfidization of pyrite precursor creates voids that can be refilled by secondary minerals enriched in Th, REE, U and Ti. Pyrite occurs as well developed cubic octahedron crystals with pale-brass yellow colour and metallic luster. This confirms the reducing conditions during the late stages of columbite crystallization, which is also responsible for the formation of pyrite. This may explain the metasomatic processes that took place under alkaline medium.

Titanite $CaTi(SiO_4)(O,OH,F)$ is an important constituent of ijolitic and nepheline syenitic alkaline rocks. Amounts of trace elements, particularly the LREE, Nb, Ta and Zr, titanite and other accessory phases such as apatite and perovskite are important in the study of the genesis and geochemical evolution of alkaline igneous rocks. Titanite is an important factor controlling the REE distribution in a wide variety of rock compositions and geochemical processes because it is one of the most common and pervasive accessory phases and it has the ability to incorporate large quantities

Table 6. Mineral chemistry of selected some minerals from El-Sibai shear zone, the minerals obtained by EMPA, the major oxides by (wt%).

Rocks	**El-Sibai**	**El-Sibai**	**El-Sibai**	**El-Sibai**	**El-Sibai**
Sample	**ZS6-1**	**ZS6-1**	**ZS6-1**	**ZS6-1**	
Mineral name	**Fluorapatite Core-A1**	**Fluorapatite Rim-A2**	**Fluorapatite Core-A3**	**Fluorapatite Rim-A4**	**Average N=4**
F	2.154	2.156	2.744	2.242	2.324
SiO_2	0.086	0.140	0.211	0.327	0.191
MgO	0.016	0.019	0.014	0.020	0.018
CaO	54.75	55.19	54.40	56.48	55.21
P_2O_5	41.51	42.16	41.43	43.20	42.08
Cl	0.147	0.144	0.222	0.285	0.2
FeO	0.088	0.297	0.278	2.36	0.756
SrO	0.000	0.014	0.033	0.047	0.031
Y_2O_3	0.000	0.009	0.000	0.011	0.011
La_2O_3	0.096	0.032	0.020	0.043	0.048
Ce_2O_3	0.043	0.000	0.062	0.097	0.067
Pr_2O_3	0.110	0.000	0.022	0.044	0.059
Nd_2O_3	0.080	0.000	0.150	0.341	0.19
Sm_2O_3	0.029	0.000	0.000	0.000	0.029

Table 6. (continued)

Gd_2O_3	0.113	0.000	0.000	0.000	0.113
PbO	0.091	0.056	0.000	0.000	0.088
ThO_2	0.020	0.000	0.041	0.081	0.047
UO_2	0.000	0.000	0.000	0.000	0.000
Total	98.38	99.27	98.40	104.0	100.01
Structural formula on basis of 4 oxygen atoms					
F	------	-------	-------	--------	------
Mg	0.001	0.001	0.001	0.001	0.001
Si	0.003	0.004	0.006	0.010	0.006
P	1.038	1.054	1.036	1.080	1.05
Cl	-------	-------	-------	-------	------
Ca	0.978	0.986	0.971	1.008	0.986
Fe	0.003	0.009	0.009	0.074	0.024
Sr	0.000	0.001	0.001	0.002	0.001
Y	0.000	0.001	0.000	0.001	0.001
La	0.001	0.000	0.002	0.003	0.001
Ce	0.003	0.001	0.001	0.001	0.002
Pr	0.003	0.000	0.001	0.001	0.002
Nd	0.002	0.000	0.000	0.000	0.005
Sm	0.001	0.000	0.000	0.000	0.001
Gd	0.003	0.000	0.000	0.000	0.003
Pb	0.002	0.001	0.000	0.000	0.002
Th	0.001	0.000	0.001	0.000	0.001
U	0.000	0.000	0.000	0.000	0.000

-----no calculation

N= number of samples

of LREE in its crystal structure (Henderson, 1980; Seifert & Kramer, 2003).

Hematite (Fe_2O_3) appears most commonly in igneous rocks, especially in the mineralized granites. It is also very important in sedimentary rocks and their more metamorphosed equivalents (Deer et al., 1966). In the mineralized shear zone of El-Sibai peralkaline granites, hematite occurs as a secondary phase of magnetite crystals in the form of aggregates with thorite and zircon minerals.

Disscussion

Accessory minerals that have crystallized from magma display different stabilities during fluid-induced, pervasive late-magmatic to hydrothermal alteration that normally affect granites. Intergrowths of thorite and zircon are abundant in the alkali-feldspar granites (Figs. 3a, 7). Zircon and thorite crystallize in space group I41/amd (Taylor & Ewing, 1978; Hazen & Finger, 1979). Their structures consist of chains of alternating edge-sharing SiO_4 tetrahedra and MeO_8 (Me=Zr or Th) triangular dodecahedra extending parallel to **[**001**]** and linked by edge-sharing MeO_8 polyhedra. The structural modifications also affect the behavior of zircon and thorite during high- and low-T alterations. Solid-solution ranges between thorite and zircon were identified in the present study (Fig. 8). These ranges (from Th-rich zircon to zircon) could be connected to the high-T fluid-induced alteration of precursor minerals. Some thorite and zircon crystals have compositions close to ideal stoichiometry, on the contrary others show varying degrees of alteration. Based on 4 oxygen atoms, the calculated formula of zircon is $^{A}(Zr_{0.92}\ Hf_{0.034}Th_{0.008}U_{0.002}Ca_{0.002}Fe_{0.023}Pb_{0.001})\ ^{T}{}_{\Sigma\ 0.99}\ ^{B}(Si_{0.99}P_{0.006}\ Al_{0.056})_{\Sigma\ 1.01}O_4$, where Th, Si and Zr represent the principle elements with considerable amounts of Ca, U, Fe, and trace Pb. The calculated formula of Th-rich zircon is $^{A}(Zr_{0.82}Hf_{0.05}Th_{0.126}U_{0.008}Ca_{0.011}Fe_{0.024})\ ^{T}{}_{\Sigma 0.91}\ ^{B}(Si_{0.91}P_{0.004}\ Al_{0.017})_{\Sigma 0.93}O_4$.

Zircon and Th-rich zircon have higher sum of all cations per formula (2.06 and 2.05 apfu, respectively) than that of ideal thorite and zircon (2 apfu, for 4 oxygen atoms). This is in agreement with Hoskin et al. (2000), Finch & Hanchar (2003) and Förster (2006), who noted that the sum of all cations per formula unit in thorite and zirconmay be N2, when these phases contain substantial amount of interstitial cations such as Ca, U and Al. Enrichment in the latter elements, in addition to F, is believed to have been introduced into the zircon–thorite system during solid state alteration, rather than during primary igneous crystallization. Solubility andmobility of Zr and Th fromthese phases require a pH between 5 and 6, at which they form $Zr(OH)_4$ complexes. At more basic pH the obtained complex changes to $Zr(OH)_5$ and the solubility increases strongly. The elevated alkalinity in the hydrothermal solutions plays an

important role. The hydrothermal solution could be of magmatic origin representing residual fluids expelled from F-rich melts. This conclusion is supported by the widespread fluorite mineralization associated with Fe-oxides and dendritic Mn-oxides along joint planes. Uranium bonding within the crystal structure of thorite and zircon is not expected to be easily dissolved by the mobilizing low-T solutions (Murakami et al., 1991). It is thus likely that these minerals underwent some changes by a metamictization process. During this process U could be released from the crystal lattices. Metamictization was largely caused by nucleic recoil of U and Th during alpha decay. The bombardment of the crystal lattice by large nuclei progressively distorts and eventually destroys the crystal lattice (Murakami et al., 1991).

Zircon enriched in Hf in peralkaline granite was connected to post-magmatic metasomatic activity rather than to magmatic fractionation (Wang et al., 2000). This may be confirmed by the fact that normal fractionation during evolution of the peralkaline melt does not result in separation of Zr and Hf and hence the Zr/Hf ratio is retained at a constantly high value (e.g. approx. 20 in El-Sibai peralkaline granite). Thus, Hf-enrichment in the El-Sibai altered granite association and hence in the associated hafnian zircon is controlled by other factors. Very important is F in the evolution of such highly fractionated melts that tend to be enriched in Na and Al with decreasing silica. Fractionation includes a combination of crystal settling and flow accumulation of progressively evolved, more F-rich, lower-temperature, less dense, less viscous melts towards the upper and inner parts of the magma chamber. This leads to an increase in diffusion rates of HFSE, thus permitting late liquid–liquid fractionation of granitic melt (Hannah & Stein, 1990). The #Hf ratios (Table 3), ranging between 3.54 and 6.44 with average 4.62 in the investigated zircon of metasomatized peralkaline granites, is not so high, which manifests that an alkaline and relatively high temperature >425 °C (Abdalla et al. 1994) environment could be suitable for their deposition, in which the Hf-complexes are thermally unstable (Portnov, 1965).

Zircon of the El-Sibai altered peralkaline granites is closely concordant with the trends III and MHZ (Figs. 8, 9) that presumably represent a preserved metasomatic hydrothermal trend. This trend deviates from the theoretical trend exhibited by the zircon-hafnon solid solution series (i.e. trend I, Fig. 8). This discrepancy can be attributed to a significant deficit of Zr and Hf relative to Si content (i.e. high concentration of vacancies on the Zr lattice position (Kempe et al., 1997; Abdalla et al., 2008).

The trends III and MHZ (Figs. 8, 9) exhibited by zircons from metasomatized hydrothermal environment are in accordance with the trend defined by the substitution scheme Zr^{4+}, $(Si^{4+}) \leftrightarrow Hf^{4+} + HREE^{3+} + U^{4+} + Th^{4+} + Y^{3+} + (P^{5+})$. According to Speer (1982) and Belousova et al. (1998) zircon is unusual composition occurring along such a trend. These zircons were interpreted by Pointer et al. (1988) as metastable solid solution, in the series zircon-xenotime (YPO_4), thorite ($ThSiO_4$), coffinite ($USiO_4$). Minerals of this series are isostructural and can show limited substitution range with zircon even at higher temperature (Mumpton & Roy, 1961). Because the HREE are geochemically close to Y, they also tend to be involved in this isomorphic substitution series. This zircon is formed from fluids that transported Th, U, Y, P, and HREE. Zircon is highly soluble in alkalic and F-rich magmas (Keppler, 1991), therefore Zr is progressively enriched in differentiating magmas. Over a range of 0-6 wt% F, solubility of zircon increases with the square of the F content, and the solubility of other refractory minerals, including rutile and thorite also increases (Keppler, 1991). Zircon crystallization removes most Zr from the magma. Zircon is extremely stable, even during most hydrothermal alterations, which inhibit subsequent mobilization. In contrast, sodic pyroxenes and amphiboles are more easily broken down and there Zr would be easily released to hydrothermal fluids (Rubin et al., 1993). Susceptibility of zircon to alteration can be enhanced by metamictization or mechanical fracturing during deformation.

Ferrugination (hematitization) process is mainly related to strongly alkaline hydrothermal solutions at pH value of more than 10 with temperatures varying between 350 °C and 450 °C (Sweewald & Sayfried, 1990), while kaolinitization and silicification processes are essentially associated with strongly acidic solutions at pH from 1 to 3 with temperatures varying between 150 °C and 400 °C (Bucanan, 1982). Accordingly, the temperatures of the solution ranged between 150 °C and 450 °C. It is believed that the mineralizing hydrothermal solutions never reached more than 500 °C due to destruction of Al_2O_3 above this temperature (Frantz & Weisbrod, 1974). Ferrugination along the shear zone was accompanied by higher intensity of radioactivity compared to the silicification and kaolinitization processes (Fig. 3). This is due to the high ability of iron oxides to adsorb radioactive elements from its solutions. The reported ferrugination process may be due to the mobilization of ferric ions released from the ferromagnesian minerals during the alteration processes. Hematite may be precipitated according to the oxidation- reduction reaction.

$$4\ Fe_3O_4\ \textit{(Magnetite)} + O_2 \rightarrow 6\ Fe_2O_3\ \textit{(Hematite)}$$

Silicification process in a shear zone is also well developed and most commonly represented by quartz veinlets varying in thickness from a few mm to less than 20 cm, extending for variable distances, not exceeding 80 m. The silicification process results in an increase of SiO_2 at the expense of the other major oxides. Pier (1992) attributed the development of SiO_2 to the hydration of feldspars as follows:

$$75Na_2CaAl_4Si_8O_{24} + 2H^+ + K^+\ \textit{(Plagioclase)} \rightarrow KAl_3Si_3O_{10}(OH)_2 + 1.5Na^+ + 0.75Ca^{+2} + 3SiO_2\ \textit{(Muscovite)}$$

$1.5KAlSi_3O_8 + H^+$ *(Potassium feldspar)* $\rightarrow 0.5$ $KAl_3Si_3O_{10}(OH)_2 + K^+ + 3SiO_2$ *(Muscovite)*

Kaolinitization accompanies, but to a less extent, the ferrugination and silicification alterations in the shear zone. The kaolinitization process causes an increase in the amount of Fe_2O_3, CaO and MnO at the expense of the other major oxides. The intensity of kaolinite alteration increases near the edge of the shear zone. Rice (1973) pointed out that kaolinite may be formed in granite due to hydrolysis of albite. In this reaction silica precipitates as an amorphous phase.

$4NaAlSi_3O_6 + 4H_2CO_3 + 18H_2O$ (*Albite*) $\leftrightarrow 4Na^+ + 8H_4SiO_4 + 4HCO_3 + Al_4Si_4O_{10}(OH)_8$ *(Kaolinite)*

Crystallization of fluorite, galena and pyrite in the mineralized shear zone reflects the important role of F and S. Zr, Hf, Th and Ti are typical HFSE, which are generally considered immobile during hydrothermal water-rock interactions. Experimental and natural evidences, however, have demonstrated that Zr, Ti and Th may become mobile especially in high-temperature (magmatic or hydrothermal) environments containing strong complexing agents such as fluorine, sulfur and others (Keppler, 1993). The mobility of the REE and Th was attributed to high F contents in the hydrothermal fluids (Poitrasson, 2002) as F-rich fluids are capable of transporting Th (Keppler & Wyllie, 1990). The critical role of F complexing in REE transport in hydrothermal fluids is also indicated by Y, Ho fractionation (Bau & Dulski, 1995). The fact that F may play a prominent role in the hydrothermal mobilization of HFSE has been indicated for Zr, Th and REE (Moine & Selvi, 1999). Harris & Marin (1980) reported on the important role of mobile fluoride complexes such as $[Na(REE)F_4]$ and $[(ZrF)(REEF_4)_3]$ in determining the distribution of REE and other trace elements such as Zr during hydrothermal conditions. Moreover, Taylor et al. (1981) added carbonate complexes in the alkali-enriched fluid as an important factor responsible for Zr and HREE transportation. The abundantly detected zircon and Th-bearing minerals, of demonstrably hydrothermal origin, can be attributed to the role of F-rich fluids. Zr and Th are generally considered as highly immobile elements, yet the occurrence of zircon indicates that their significant concentrations can be transported via specified F-rich fluids.

Pichavant (1983) showed that the F-rich fluid phase equilibrated with alkali feldspars, is strongly enriched in Na in comparison to the Cl-rich fluid. Thus any process leading to reduction of F-rich fluid (such as volatile loss or stabilizing F into F-bearing minerals, e.g. fluorite, and fluorapatite), will result in the albitization of the granite. Consequently, an increased pH of the exsolved fluids from the crystallizing peralkaline granite will lead to the destabilization of rare element complexes including those of Zr and Hf in these fluids and promote their deposition. Zircon and xenotime are isostructural and exhibits the general formula ABO_4, where A refers to the larger Zr and Y atoms and B to the smaller P and Si atoms. Xenotime-substituted zircon is formed as the result of the coupled substitution:

$Zr^{4+} + Si^{4+} \rightarrow Y(HREE)^{3+} + P^{5+}$ (Romans et al., 1975).

Conclusion

Mineralized shear zone trending NNE-SSW is located at the northern segment of Gabal El-Sibai peralkaline granites (500 m in length and 0.5 to 1.5 m in width). Ferrugination, kaolinitization, and silicification are the main wall-rock alteration features developed within the shear zone. There the rare-metal minerals are associated with ferrugination (hematitization) zone. These alterations are good traps for rare metals of thorite, ferrocolumbite, pyroclore, plumbopyroclore, fluorite, cerite-(Ce), zircon, Th-rich zircon, zirconolite (mixture of zircon and columbite), fluorapatite, titanite, and monazite minerals. Cerite-(Ce), zirconolite and plumbopyroclore minerals are represented the first time in the rare-metals peralkaline granites in the Eastern Desert of Egypt.

Electron probe microanalysis (EPMA) provides an indication of a range of solid solutions between thorite and zircon, in which intermediate phases, i.e. Th-rich zircon, were formed. These phases have higher sum of all cations per formula (2.0 to 2.09 apfu, for 4 oxygen atoms) than that of ideal thorite and zircon. This is attributed to the presence of substantial amount of interstitial cations such as U, Y, Ca, and Al in these phases. Enrichment of Th and U in an altered zircon (Th-rich zircon) preferentially involves coupled substitution $Ca^{2+} + (Th,U)^{4+} \leftrightarrow 2Zr^{4+} + 2Si^{4+}$, implying that significant amount of U and Th may enter the Zr and Si position in zircon. Although Zr, Hf, and HREE are considered as highly immobile elements, yet the occurrence of the formed Zircon enriched Hf-, U-, Th-, Y- and HREE of hydrothermal origin indicates the mobilization of these elements via specified (K^+, Na^+, H^+, CO^{3-}, O_2 and F^-)-rich fluids.

This study shows zircon and Th-rich zircon related to metasomatic hydrothermal zircon (MHZ). Zircon and fluorite of demonstrably hydrothermal origin can be attributed to the role of fluorine-rich fluids. Fluoride complexes such as $[Na(REE)F_4]$ and $[(ZrF)(REEF_4)_3]$ are important to determine the distribution of REE and other trace elements, such as Zr during hydrothermal conditions. Zr and Th are generally considered as highly immobile elements, yet the occurrence of zircon indicates that significant concentrations of Zr and Th can be transported under specified F-rich fluids. The zircon of El-Sibai altered peralkaline granite is interpreted as a metastable solid solution, in the series zircon–thorite ($ThSiO_4$). The Hf-concentrating mechanism is assumed due to solid-state action (subsolidus reaction) of exsolved fluids rich in K^+, Na^+, F^- and subsequently H^+.

The shear zone was affected by different types of hydrothermal solutions with temperatures varying between 150 °C and 450 °C. The produced al-

terations acted as good traps for Th- and U-bearing minerals with rare metals in the El-Sibai peralkaline granites (shear zone). The detailed mineralogical investigations of these zone revealed its enrichment in Th, Zr, Nb, Pb, U, F, P, LREE (Ce), especially concerning the hematization processes. The close correlation of ferruginated samples with high radioactivity is related to the high ability of iron oxides to adsorb radioactive elements from their solutions.

The shear zone facilitates the circulation of hydrothermal fluids, leading to mobilization and redistribution of radioactive elements. Also the presence of galena and deep violet fluorite are very good evidences for the presence of hydrothermal fluids. Therefore, it is clear that alteration processes have resulted from ascending (hypogene) hydrothermal solutions rather than descending (supergene) meteoric water. So, the hydrothermal origin could be accepted for mineralizations within the shear zone.

From the study of El-Sibai altered granites (shear zone), we concluded that the studied area contains high concentrations of Th, Zr, Nb, U, Pb, P, Ce, F and REE, especially in the ferruginated parts of the area. Accordingly, the El-Sibai shear zone could represent a favorable source for rare metals (Th, Zr, Nb, U, Pb, P, Ce, F, and REE).

References

Abadalla, H. M., Helba, H. & Matsueda, H. 2008: Chemistry of zircon in rare metal granitoids and associated rocks, Eastern Desert, Egypt, Resource Geology, 59/1: 51-68, doi:10.1111/j.1751-3928.2008.00079.x.

Abdalla, H.M., Matsueda, H., Ishihara, S. & Miura, H. 1994: Mineral chemistry of albite-enriched granitoids at Um Ara, Southeastern Desert, Egypt. Int. Geol. Re., 36/11: 1067-1077, doi:10.1080/00206819409465505.

Abdel-Fattah, M., Abdel-Rahman, A.M. & El-Kibbi, M.M. 2001: Anorogenic magmatism: chemical evolution of the Mount El-Sibai A-Type complex (Egypt), and implications for the origin of within-plate felsic magmas, Geological Magazine, 138: 67-85.

Abdel Kader, Z.M., Bakhit, F.S. & Ali, M.A. 2001: Geochemistry of the younger granites in El Sibai area, Central Eastern Desert, Egypt, The Mineralogical Society of Egypt. The Fourteenth Annual Meeting, Abstract: 16 p

Abd El-Naby, H. H. 2009: High and low temperature alteration of uranium and thorium minerals, Um Ara granites, South Eastern Desert, Egypt, Ore Geology Reviews, 35: 436-446.

Ali, M.A. 2001: Geology, petrology and radioactivity of Gabal El-Sibai area, Central Eastern Desert, Egypt, Ph. D. Thesis, Cairo University: 300 p.

Ali, M.A. & Lentz, D. R. 2001: Mineralogy, geochemistry and age dating of shear zones hosted Nb-,Ta-, Zr-Hf-, Th-, U-bearing granitic rocks at Ghadir and El-Sella areas, South Eastern Desert, Egypt, Chin. J. Geochem., 30/4: 453–478, doi:10.1007/s11631-011-0531-5.

Bayliss, P., Mazzi, F., Munno, R. & White, T. J. 1989: Mineral nomenclature: Zirconolite. Mineral Mag., 53: 565-569.

Bayliss, P. & Levinson, A. A. 1988: A system of nomenclature for rare-earth mineral species: Revision and extension. Am. Mineral., 73: 422-423.

Bau, M. & Dulski, P. 1995: Comparative study of yttrium and rareearth element behaviours in fluorine-rich hydrothermal fluids. Contrib. Mineral. Petrol., 119: 213–223.

Belousova, E. A., Griffin, W. L. & Pearson, N. J. 1998: Trace element composition and cathodoluminescence properties of Southern African kimberlitic zircon. Mineral Mag., 62: 355–366.

Brugger, J., Gieere, R., Graeser, S. & Meisser, N. 1997: The crystal chemistry of roméite. Contrib. Mineral. Petrol., 127: 136-146.

Butler, C. A., Holdsworth, R. E & Stachan, R. A. 1995: Evidence for Caledonian sinistral strike-slip motion and associated fault zone weakening, Outer Hebrides fault zone, NW Scotland. Journal of Geological Society, London, 152: 743-746.

Bucanan, M. S. 1982: The geochemistry of some igneous rock series. Geochimica et Cosmochimica Acta, 9: 101-137.

Breiter, K., Förster, H. J. & Škoda, R. 2006: Extreme P-, Bi-, Nb-, Sc-, U- and F-rich zircon from fractionated perphosphorous granites: the peraluminous Podlesí granite system, Czech Republic. Lithos, 88: 15–34.

Chakoumakos, B. C. 1984: Systematics of the pyrochlore structure type, ideal. J., Sol. State, Chem, 53: 120-129.

Chakoumakos, B. C. 1986: Pyrochlore. In McGraw-Hill Yearbook of Science and Technology 1987. Parker, S. P. (ed.): McGraw-Hill, New York: 393-395.

Correia Neves, J.M., Nunes, J.E. & Sahama, T.G. 1974: High hafnium members of the zircon-hafnon series from the granite pegmatites of Zambezia, Mozambique, Contrib. Mineral. Petrol., 67: 73-80.

Černý, P., Meintzer, R. E. & Anderson, A. J. 1985: Extreme fractionation in rare-element granitic pegmatites: Selected examples of data and mechanisms. Candian Mineralogist, 23: 381–421.

Deer, W. A., Howie, R. A. & Zussman, J. 1966: An introduction to rock forming minerals. Longmans, London: 517 p.

Deer, W. A., Howie, R. A. & Zussman, J. 1992: Rock forming minerals, 5. Non silicates, John Wiley & Sons, New York: 371 p.

El-Gaby, S. 1975: Petrochemistry and geochemistry of some granites from Egypt. Neu. Jb. Miner. Abh., 124: 147-189.

El-Ramly, M. F. 1962: The absolute ages of some basement rocks in the Eastern and Southwestern Deserts of Egypt. Geological Survey of Egypt paper, 15: 12 p.

El-Ramly, M.F. & Akaad, M.K. 1960: The basement complex in the Central Eastern Desert of

Egypt between lat. 24° 30' and 25° 40' N. Geological. Survey, Egypt. P., 8: 35 p.

El-Shazly, E. M. 1964: On the classification of the Precambrian and other rocks of magmatic affiliation in Egypt. XXII Inter. XXII Inter. Geol. Congr. Proc. Sect. 10, India, 88-101.

El-Kammar, A. M., EL-Hazik, N. S., Mahdi, M. & Ali, N. 1997: Geochemistry of accessory minerals associated with radioactive mineralization in the Central Eastern Desert, Egypt. Journal of African Earth Sciences, 25/2: 237-252.

El-Manharawy, M. S. 1977: Geochronological investigation of some basement rocks in Central Eastern Desert, Egypt between lats. 25° 00 and 26° 00 N. Ph. D. Thesis, Fac. Sci., Cairo University: 238 p.

Finch, R. J. & Hanchar, J. M. 2003: Structure and chemistry of zircon and zircon group minerals. In: Hanchar, J.M. & Hoskin, P.W.O. (eds.): Zircon. Reviews in Mineralogy and Geochemistry, Mineralogical Society of America, Geochemical Society, Washington, DC 53: 26 p.

Förster, H. J. 2006: Composition and origin of intermediate solid solutions in the system thorite–xenotime–zircon–coffinite. Lithos, 88: 35–55.

Förster, H. J. 2000: Cerite-(Ce) and thorian synchysite-(Ce) from Niederbobritzsch (Erzgebirge, Germany): implications for the differential mobility of Th and the LREE during granite alteration. Canadian Mineralogist, 38: 67–79.

Fleischer, M. 1987: Glossary of Mineral Species, 5th Edition. Mineral. Rec, Inc., 227, Tucson, AZ.

Fleischer, M. 1989: Additions and corrections to the Glossary of Mineral Species, 5th Edition. Mineral. Rec., 20 (1987): 289-298.

Frantz, J. D. & Weisbord, A. 1974: Infiltration metasomatism in the system K_2O-SiO_2-Al_2O_3-H_2O-HCl. In: Geochemical transport and kinetics, 634: 261-271.

Frondel, J. W. & Cuttito, A. 1955: Glossary of uranium and thorium-bearing minerals. Geological Survey Bulletin, 5: 1009.

Gaines, R. V., Skinner, H. C. W., Foord, E. E., Mason, B., Rosenzweig, A., King, V.T. & Dowty, E.1997: Dana's New Mineralogy. 8th ed. Wiley and Sons, New York: 1819 p.

Greiling, R.O., El-Ramly, M.F., Rashwan, A.A. & Kamal El-Din, G.M. 1993: Towards a comprehensive structural synthesis of the (Proterozoic) Arabian Nubian Shield in E. Egypt. In: U-Thorweihe & H. Schandelmeie (eds.); Geoscientist Res. Northeast Africa. Balkema, Rotterdam, 15-19.

Hannah, J.L. & Stein H.J. 1990: Magmatic and hydrothermal processes in ore-bearing systems. In: Stein, H. & Hannah, J. (eds.): Ore-bearing granite systems: Petrogenesis and mineralizing processes. Geol. Soc. Am. Spec. Paper, 1-11.

Hassan, M. A. & Hashad, A. H. 1990: Precambrian of Egypt. "The anorogenic alkalic rocks, South Eastern Desert, Egypt". Annal Geological Survey of Egypt, 9: 81-101.

Hazen, R. M. & Finger, L.W.1979: Crystal structure and compressibility of zircon at high pressure. Am. Mineral., 64: 157–161.

Hoskin, P. W. P. O., Kinny, P. D., Wyborn, D. & Chappell, B.W. 2000: Identifying accessory mineral saturation during differentiation in granitoid magmas: an integrated approach. Journal of Petrology, 41: 1365–1396.

Henderson, P.1980: Rare earth element partitioning between sphene, apatite and other coexisting minerals of the Kangerdlugssuaq intrusion, E. Greenland. Contrib. Mineral. Petrol., 72: 81–85.

Hussein, H. A. 1978: Lecture course in nuclear geology: 101 p.

Hussein, A. A., Ali, M. M. & El-Ramly, M. F. 1982: A proposed new classification of the granites of Egypt. Journal Volcanic Geoth., Re., 14: 187-198.

Hume, W.F.1935: Geology of Egypt. Vol II, Part II. The later plutonic and intrusive rocks, Geological Survery Egypt, Government press, Cairo, 301-688

Ibrahim, I.H., Ali, M.A. & Abdel Wahed, A.A. 2003: Mineralogical and spectrometric studies of El-Sibai shear zone, Central Eastern Desert, Egypt. 6th Intern. Conf. on Geochemistry. Alex. Univ., Egypt, I-A: 25-43.

Kamal El-Din, G.M.1991: Geochemistry and tectonic significance of the Pan-African El-Sibai window, Central Eastern Desert, Egypt. Ph.D. Thesis, Heidelberg University:114 p.

Keppler, H. 1991: Influence on the solubility of high field strength trace elements in granitic melts. Eos Trans. Am. Geophys. Union, abstract 72: 532-533.

Keppler, H. 1993: Influence of fluorite on the enrichment of high field strength trace elements in granitic rocks. Contrib. Mineral. Petrol., 114: 479-788.

Keppler, H. &.Wyllie, P. J. 1990: Role of fluids in transport and fractionation of uranium and thorium in magmatic processes. Nature 348:531-533, doi:10.1038/348531a0.

Kempe, U., Gruner, T., Renno, A.D. & Wolf, D. 1997: Hf- rich zircons in rare-metal bearing granites: Magmatic or metasomatic origin. In: Papunen, H. (ed.): Mineral deposits: Research and exploration where do they meet? A.A. Balkema, Rotterdam, 643-646.

Lumpkin, G.R., Hart, K.P., McMlinn, P.J., Payne, TE., Gieré, R. & Williams, C.T. 1994: Retention of actinides in natural pyrochlores and zirconolite. Radiochim. Acta, 66/67: 469-474.

Lumpkin, G.R. & Ewing, R.C. 1995: Geochemical alteration of pyrochlore group minerals: Pyrochlore subgroup. Am. Mineral., 80: 732-743.

Mandarino, J.1999: Fleischer's Glossary of Mineral Species. Mineralogical Recored, Tucson, Arizona.

Miyawaki, R. & Nakai, I. 1987: Crystal structures of rare-earth minerals. Rare Earths (Kidorui), 11:1-133.

Moghazi, A.M., Hassanen, M.A., Mohamed, F.H. & Ali, S. 2004: Late Neoproterozoic strongly peraluminous leucogranites, South Eastern Desert, Egypt-petrogenesis and geodynamic significance. Mineralogy and petrology, 81: 19-41.

Moine, B. & Salvi, S. 1999: Role of fluorine-rich fluids in the hydrothermal transport of "immobile" elements (Th, Zr, REE, Zl). Bull. De liaison de la Societe Francaise de Mineralogie et de Cristallographie (S. F. M. C.), 11: 90-92.

Moussa, E.M. 2001: Petrographical and geochemical characteristics of Gabal El-Sibai and Abu Garadi alkali feldspar granite phase and their potentialities to host uranium-thorium mineralization. Egyptian Mineralogist, 13: 101-124.

Moussa, E. M., Stern, R. J., Manton, W. I & Ali, K. A. 2008: SHRIMP zircon dating and Sm/Nd isotopic investigations of Neoproterozoic granitoids, Eastern Desert, Egypt. Precambrian Research, 160: 341–356.

Murakami, T., Chakoumakos, B. C., Ewing, R. C., Lumpkin, G. R. & Weber, W. J. 1991: Alphadecay event damage in zircon. Am. Mineral., 76: 1510–1532.

Pier, C.A 1992: Geochemistry of granites and trachytes from the Summit region of Mt. Kenya. Contrib. Mineral. Petrol., 89: 394-409.

Pichavant, M. 1983: (Na, K) exchange between alkali feldspars and aqueous solutions containing borate and fluoride anions, experimental results at p=1 kbar. 3rd. NATO Adv. Stud. Inst. Feldspars and feldspathoids, Rennes. XXX: 102 p.

Pointer, C.M., Ashworth, J.R. & Ixer, R.A. 1988: The zircon thorite mineral group in metasomatized granite, Ririwai, Nigeria. 1: Geochemistry and metastable solid solution of thorite and coffinite. Mineral. Petrol., 38: 245–262.

Poitrasson, F.2002: In situ investigations of allanite hydrothermal alteration: examples from calc-alkaline and anorogenic granite of Corsica (southeast France).Contri. Mineral. Petrol., 142: 485-500.

Portnov, A.M. 1965: The zirconium: hafnium ratio in minerals of the Burpala massif. Geochem Int., 2: 238–241.

Rice, C.M.1973: Chemical weathering on the Carnmenellis granite. Mineralogical Magazine, 39: 429-447.

Romans, P. A., Brown, L. & White, J. C. 1975: An electron microprobe study of yttrium, rare earth and phosphorous dis tribution in zoned and ordinary zircon. Am. Mineral., 60: 475–480.

Rubin, J. N., Henry, C. D. & Price, J. G. 1993: The mobility of zirconium and other "immobile" elements during hydrothermal alteration. Chemical Geology, 110: 29-47.

Seifert, W. & Kramer, W. 2003: Accessory titanite: an important carrier of Zr in lamprophyres. Lithos, 7: 81–98.

Smith, D. K. J. 1984: Uranium mineralogy. In: DeVivo, B., Ippolito, F., Capaldi, G. & Simpson, P.R. (eds.): Uranium geochemistry, Mineralogy, Geology, Exploration and Resources, Institute of Mining and Metalluragy, London, 43-88.

Speer, J. A. 1982: The actinide orthosilicates. In: Ribbe, P. H. (ed.): Reviews in Mineralogy, Mineralogical Society of America, 5, 2nd Edition, 113-135.

Stern, R. J. & Hedge C. E.1985: Gechronologic and isotopic contraints on Late Precambrain crustal evolution in the Eastern Desert in Egypt. Am. Journal Science, 258: 97-127.

Sultan, M., Arvidson, R.E., Duncan, I. J., Stern, R.J. & El-Kalioubi, B. 1988: Extension of the Najd shear system from Saudi Arabia to the central Eastern Desert of Egypt based on integrated field and landsat observations. Tectonics, 7/6: 1291-1306.

Sweewald, J. S. & Sayfried, J. W. 1990: The effect of temperature on metal mobility in subsea floor hydrothermal systems: constraints from basalt alteration experiments. Earth Planet Science, 101: 388-403.

Taylor, M. & Ewing, R. C. 1978: The crystal structure of $ThSiO_4$ polymorphs: huttonite and thorite. Acta Crystallographica B 34, 1074–1079.

Taylor, R. P., Strong, D. F. & Fryer B. J. 1981: Volatile control of contrasting trace element distributions in peralkaline granitic and volcanic rocks. Contrib. Mineral., Petrol., 77: 267–271.

Wang, R. C., Zhao, G. T., Lu, J. J., Chen, X. M., Xu, S. J. & Wang, D. Z. 2000: Chemistry of Hf-rich zircons from the Laoshan I- and A-type granites, Eastern China. Mineralogical Magazine, 64: 867 – 877.

Warner, J. K. & Ewing, E. R.1993: Crystal chemistry of samarskite. Am. Mineral., 78: 419-424.

Wedepohl, K. H. 1978: Handbook of geochemistry. Springer Verlag, Berlin: 478 p.

Whittaker, E. J. & Muntus, R. 1970: Ionic radii for use in geochemistry. Geochimica et Cosmochimica Acta, 34: 945.

Williams, J. k. & Gieré, R.1996: Zirconolite a review of localities worldwide, and a compilation of its chemical compositions. Bull. Nat. Hist. Museum Geol. Ser., 52: 1-24

Woodhead, J. A., Rossman, G. R. & Thomas, A. P. 1991: Hydrous species in zircon. Am. Mineral., 76: 1533-1546.

GEOLOGIJA *56/1*, 129-130, Ljubljana 2013

Nova knjiga

Miloš BAVEC, 2013: Zgodbe iz podzemlja – Geologija za vse otroke.
Študentska založba in Geološki zavod Slovenije, 58 str.

Na pogovoru o tem, kako predstaviti geologijo otrokom, je neki geolog vprašal, kako je mogoče, da so skoraj vsi otroci tako navdušeni nad dinozavri in vedo vse o njih, pozneje pa se jih tako malo odloči za študij geologije. Odgovor ene od osnovnošolskih učiteljic je bil: »Večina otrok odraste«.

Zgodbe iz podzemlja s podnaslovom *Geologija za vse otroke* je napisal dr. Miloš Bavec, eden tistih, »ki se potikajo po grmovju, s kladivi razbijajo kamne in si jih potem ogledujejo s povečevalnimi stekli, zbirajo fosile, z velikimi stroji vrtajo luknje v tla … in ob vsem tem početju stikajo glave in modrujejo, kot da gre za nekaj popolnoma resnega«, kakor je sam opisal geologe.

Knjižica je namenjena vsem otrokom. Tudi tistim iz zgornje anekdote z neke internetne strani, ki so odrastli, a so vendar v sebi ohranili toliko pristne otroške radovednosti, da jih svet okrog njih, predvsem pa pod njimi, še vedno zanima in navdušuje.

Knjižic in slikanic, ki otrokom ponujajo prvi vpogled v to zanimivo vedo, je v tujih jezikih veliko, v slovenskem pa so žal zelo redke. Tudi v šolah v tujini se o geologiji učijo veliko, pri nas pa bolj malo. Samo kdor geološke vsebine resnično razume, jih lahko predstavi tako, da so razumljive, zanimive, poučne in privlačne. In na tak način, obogaten s prav takimi barvnimi ilustracijami Tine Žen, avtor *Zgodb iz podzemlja* predstavlja osnove geologije.

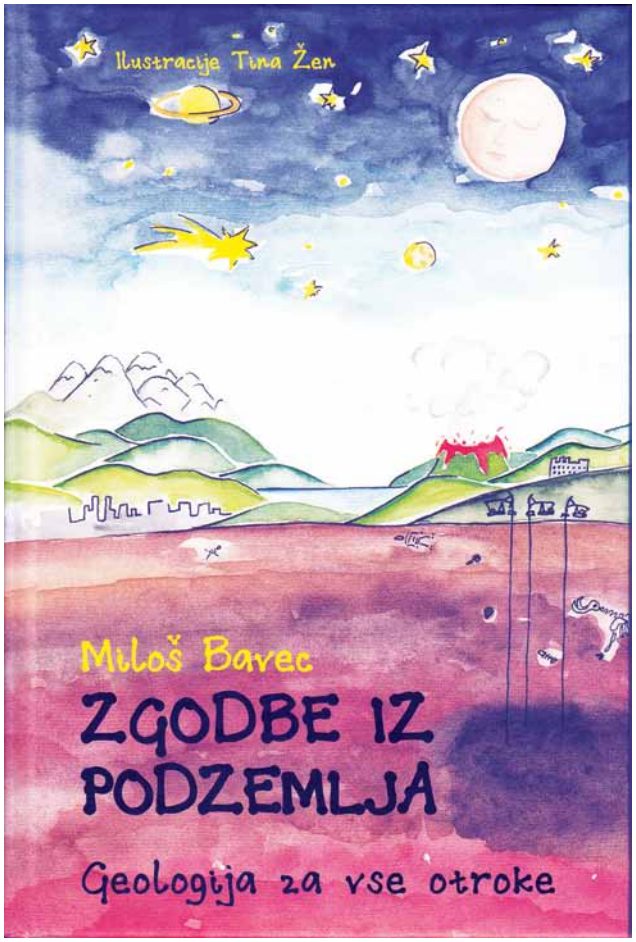

Lansko leto smo zabeležili 100. obletnico Wegenerjeve teorije o potovanju celin. S to teorijo, po mnenju mnogih eno najpomembnejših, je geologija doživela izrazit napredek in se iz vede, ki je večinoma opisovala pojave in strukture na ali v Zemljini skorji brez prave medsebojne povezave, razvila v vedo, ki zna najbolj celovito razložiti vzroke in posledice naravnih procesov ter povezave med njimi. Odnosi med procesi pod Zemljinim površjem in naravnimi pojavi ter oblikami na površju, posledično pa z življenjem na Zemlji, razvojem človeka, podnebjem itn., so se s teorijo o tektoniki litosferskih plošč zlili v čudovito zgodbo. Zaradi načina, kako so v *Zgodbah iz podzemlja* opisani »glavni igralci« te čudovite zgodbe in njihovi »poklici«, bo knjižica nedvomno navdušila otroke vseh starosti.

Geologija za vse otroke? Res? – *Zgodbam iz podzemlja* ob rob

Zgodbe iz podzemlja zapolnjujejo majhen del ogromne vrzeli, ki je nastala v Sloveniji zaradi sistematičnega izbrisa geologije kot samostojnega predmeta iz vseh učnih programov, tako osnovnošolskih kot srednješolskih. Geološke vsebine so zdaj do neprepoznavnosti razpršene po učbenikih različnih predmetov in predstavljene na način, ki učencem ne omogoča povezovanja naravnih pojavov in življenja na Zemlji v razumljive in zaključene celote. Suhoparno učenje imen fosilov in dolgih kemijskih formul mineralov večinoma odvrne od geologije še tiste najbolj navdušene nad dinozavri. S tem, nekoliko karikiranim primerom želim opozoriti na resnično stanje, ki je posledica dolgoletne odsotnosti resnega poučevanja geologije, za katero smo imeli nekoč celo samostojen štirileten srednješolski program. Danes pa je to v rokah učiteljev drugih predmetov in pri mnogih, ki so se primorani spopadati z geološko snovjo, je zaznati nekakšen strah in negotovost pri podajanju le-te, saj se tudi sami zavedajo pomanjkljivega znanja na tem področju.

Kljub temu je malo verjetno, da se bo v kratkem spremenil odnos snovalcev izobraževalnih programov do geologije kot temeljne vede, podlage za vse druge naravoslovne predmete. Težko je razumeti, da 99,997 odstotka naše daljne zgodovine, o kateri učenci ne izvejo skoraj nič, ni vrednih samostojnega šolskega predmeta. Če je znano, da je preteklost ključ do razumevanja sedanjosti in

prihodnosti, koliko vrat jim bo odprlo 0,003 odstotka preteklosti? Ali se upravičeno čudimo stotinam neukih butljev, ki verjamejo vsaki ponovni napovedi konca sveta? S povsem življenjskega in materialnega stališča je še težje doumeti, da malokoga zanima, od kod izvira kar 1.340 ton mineralov, kovin in goriva, kolikor jih povprečen Evropejec rabi v svojem življenju, ali zakaj mu je voda poplavila klet ali zemeljski plaz odnesel hišo na položnem pobočju, sosedova na strmem bregu pa še vedno stoji. Tako imenovani »zgodovinski spomin« na naravne katastrofe (mimogrede, geologi jim pravimo naravni procesi), ki je že sicer zelo kratek, ne pomaga preprečiti nove materialne škode ali celo človeških žrtev, če ne poznamo vzrokov za naravne pojave in ne razumemo njihovega obnašanja.

Na razsežnosti geološke neizobraženosti nas geologe vsak dan opominja že zaskrbljujoče nepoznavanje najbolj osnovnega geološkega izrazoslovja in pojavov. Marsikateri visoko izobražen človek je za konglomerat, torej ime ene najpogostejših kamnin ob rečnih strugah in pod našimi domovanji, slišal samo v besedni zvezi »finančni konglomerat«. Ko te nekdo vpraša, katera je ta kamnina ob poti, in mu pojasniš, da gre za apnenec, torej najpogostejšo kamnino v Sloveniji, pa te velikokrat doleti nejeveren pogled in začudeno vprašanje: »Kaj? Apnenec je lahko tudi črn?« Geolog mora zbrati veliko volje in poguma, da se loti pisanja poljudnega besedila ob zavedanju, da bo moral pojasniti vsak »čuden« geološki izraz.

Problem ima še drugo plat. Zaradi zanemarjanja geoloških vsebin v šolah strokovnjaki ne čutimo velike potrebe po razvijanju slovenskega geološkega izrazoslovja. Slednje je danes prežeto s tujkami in le še redko kdo se jih sploh trudi posloveniti, še redkeje pa se kakšen od takih poskusov prime. In dokler bo tudi vrednotenje po merilih znanstvene in strokovne uspešnosti ARRS raziskovalcem, ki jim ta merila odmerjajo dnevni kruh, jasno sporočalo, da take knjižice in tudi znanstvene monografije v slovenskem jeziku za slovenske bralce niso vredne počenega groša, se nam piše samo še slabše. V takih primerih se pokaže, da lahko njihovo tolmačenje uspešnosti upravičeno nekoliko parafraziramo in zapišemo, da je za objavljanje pri tujih založbah dovolj dobra tudi angleščina. Vendar, kot že nekdo pred nami ni preklinjal, ampak je molil za svoje krvnike, odpustimo jim, saj ne vedo, kaj delajo. Ker so sami žrtve taistega problema. Resno pa nas mora skrbeti, ali pri takem stanju geološke ozaveščenosti v širši javnosti sploh še kdo izmed tistih, ki o tem odločajo, zna ovrednotiti pomembnost uvajanja geologije v šole. Ker, ko se enkrat sprijaznimo s tem, da se o njej pač bolj malo vé, ne vidimo nobenega razloga, da bi moral kdo prav izstopati.

Od vseh naštetih posledic slabe geološke izobrazbe se marsikateremu geologu zdi še najbolj »tragična« ta, da toliko ljudi prikrajša za tisoč zanimivosti, ki jih (ne) vidi na nedeljskem izletu. Kakor je napisal Marcel Proust, pravo raziskovalno popotovanje ni iskanje novih dežel, temveč gledanje z drugačnimi očmi.

Matevž Novak

GEOLOGIJA *56/1*, 131-133, Ljubljana 2013

Poročila

Predstavitev Slovenskega geološkega društva in letno poročilo za leto 2012

Timotej VERBOVŠEK

Oddelek za geologijo, NTF, UL, Aškerčeva 12, SI-1000 Ljubljana; e-mail: timotej.verbovšek@geo.ntf.uni-lj.si

Slovensko geološko društvo (Aškerčeva 12, 1000 Ljubljana) je strokovno združenje slovenskih geologov. Ustanovljeno je bilo leta 1951 in povezuje raziskovalce, učitelje, druge poklicne geologe in ljubitelje stroke. Njegov cilj je napredek znanosti in prakse na področju vseh vej geologije. Društvo zato prireja javna predavanja, strokovne ekskurzije, razstave in znanstvene sestanke, skrbi za popularizacijo geologije in za vključevanje geoloških ved v osnovnošolske in srednješolske učne programe. Sodeluje pri prizadevanjih za varstvo okolja in pri izdelavi zakonskih aktov in normativov s področja geologije. Sodeluje tudi z drugimi strokovnimi društvi v Sloveniji in tujini in je vključeno v mednarodne organizacije: Mednarodno združenje za geološke znanosti (IUGS), Evropsko zvezo geologov (EFG), Mednarodno mineraloško zvezo (IMA), ProGeo. V okviru društva deluje pet sekcij; *sekcija za geokemijo* (predsednica Mateja Gosar), *sekcija za sedimentarno geologijo* (predsednik Bojan Otoničar), *sekcija za mineralogijo* (predsednica Meta Dobnikar), *sekcija za geološko dediščino* (predsednica Martina Stupar) in *študentska sekcija* (predsednik Klemen Černič). Društvo sestavlja ožji izvršni odbor (predsednik Timotej Verbovšek, podpredsednica Nadja Zupan Hajna, tajnica Mirijam Vrabec, blagajničarka Bernarda Bole, Boštjan Rožič, Vladimir Vukadin, Suzana Fajmut Štrucelj, Bojan Režun, Matevž Novak), razširjeni izvršni odbor (predsedniki sekcij), nadzorni odbor (Špela Goričan, Franci Čadež, Bojan Ogorelec) in častno razsodišče (Katica Drobne, Dragica Turnšek, Pavle Florjančič).

Slovensko geološko društvo za uresničitev svojega cilja opravlja naslednje aktivnosti:

- povezovanje raziskovalnega, strokovnega in vzgojno-izobraževalnega dela na področju vseh vej geoloških ved in sorodnih strok,
- popularizacijo geoloških ved s pomočjo poljudnih člankov, z organizacijo ekskurzij, poletnih taborov, izdajanjem razglednic in brošur z geološko vsebino,
- sodelovanje z upravnimi službami in organi pri izdelavi zakonskih aktov ter pravnih in tehničnih normativov in pri drugih strokovnih vprašanjih z navedenih področij,
- sodelovanje z univerzami, raziskovalnimi organizacijami, javnimi ustanovami in zavodi, s podjetji in z osebami, katerih dejavnost sega na strokovno področje različnih vej geoloških ved,
- sodelovanje z drugimi strokovnimi društvi v Sloveniji in v tujini, ki delujejo na področju različnih vej geoloških ved,
- sodelovanje z mednarodnimi organizacijami; predvsem z Mednarodno zvezo geoloških društev (IUGS), EFG, Zvezo evropskih geoloških društev (AEGS), IUGS pridruženimi specializiranimi mednarodnimi strokovnimi zvezami in z drugimi sorodnimi nacionalnimi ali mednarodnimi strokovnimi organizacijami in društvi
- sodelovanje pri prizadevanjih za varstvo okolja,
- obveščanje članov in širše javnosti v okviru možnosti z:
  - informacijami o najnovejših dosežkih znanosti in stroke,
  - organizacijo strokovnih seminarjev, simpozijev, kongresov in drugih znanstvenih sestankov, s področja delovanja društva,
  - organizacijo javnih predavanj, s področja delovanja društva,
  - organizacijo strokovnih ekskurzij,
  - publiciranjem v sredstvih javnega obveščanja, o perečih strokovnih in organizacijskih vprašanjih,
  - izdajanjem tiskanih Obvestil društva in drugih izdaj nekomercialnega značaja.

Redni član društva lahko postane vsak, ki se poklicno ali kako drugače ukvarja z vsaj eno od vej geoloških ved in s svojim raziskovalnim, strokovnim, pedagoškim ali ljubiteljskim delom in ki z drugimi aktivnostmi prispeva k razvoju geoloških ved in z njimi povezanih strok. Častni člani lahko postanejo posamezniki, ki so pomembno prispevali k razvoju geoloških ved v Sloveniji in v mednarodnem prostoru. Častni člani ne plačujejo članarine. Pridruženi člani so fizične osebe, ki se ljubiteljsko ukvarjajo z zbiranjem mineralov in fosilov ali se drugače zanimajo za geologijo. Podporni člani so fizične in pravne osebe, ki finančno podpirajo delovanje društva, lahko sodelujejo na sejah skupščine, vendar nimajo pravice odločanja. Za **včlanjenje v društvo** je treba predložiti pisno pristopnico (dostopna na spletni strani), s katero se posameznik zaveže, da bo deloval v skladu s statutom in plačeval članarino. Članarina za leto 2013 za člane znaša 15 EUR, za študente 5 EUR. Izpolnjeno pristopnico s potrdilom o plačilu pošljite na naslov društva (Aškerčeva 12, 1000 Ljubljana). Več informacij o društvu je dostopnih na spletni strani http://www.geoloskodrustvo.si/.

V preteklih letih je društvo delovalo v skladu z določili društva in programom dela, ki je bil sprejet na IO društva v vsakem koledarskem letu. Del zastavljenega programa iz prejšnjega leta je bil realiziran, nekaj nalog (predavanje in dve ekskurziji) pa nam ni uspelo izvesti, zato so bile prestavljene na naslednje leto.

Slovensko geološko društvo (SGD) si je kot nevladna in neprofitna organizacija prostovoljno združenih strokovnjakov in ljubiteljev geologije zadalo za temeljni cilj napredek znanosti in pra-

kse na področju vseh vej geologije, ki je zapisan tudi v njegovem statutu.

V okviru društva delujejo naslednje sekcije: Sekcija za sedimentarno geologijo, Sekcija za geokemijo, Sekcija za mineralogijo, Sekcija za geološko dediščino in Študentska sekcija.

Strokovna predavanja

Namen predavanj na SGD je, da se slovenski geologi srečamo, predstavimo svoje strokovno delo na zelo različnih področjih geologije (sedimentologija, stratigrafija, paleontologija, mineralogija, petrologija, geokemija, hidrogeologija, inženirska geologija, GIS) in razpravljamo o novih idejah ter o naši vpetosti v svetovne geološke tokove. V letu 2012 so bila izvedena naslednja predavanja in okrogle mize:

1. Sreda, 25. 1. 2012: **Mikroramanska spektroskopija pri preiskavah mineralnih materialov v kulturni dediščini,** dr. Sabina Kramar (Restavratorski center Zavoda za varstvo kulturne dediščine Slovenije), v Ljubljani na Oddelku za geologijo NTF, Privoz 11 (na Prulah), v predavalnici P-02 v kleti.
2. Četrtek, 15. 3. 2012: **Geoparki Slovenije**, dr. Bojan Režun (Rudnik živega srebra Idrija), mag. Suzana Fajmut Štrucl (**Družba Podzemlje Pece, d.o.o.),** ga. Katja Fedrigo (občina Sežana) in dr. Martina Stupar (Zavod RS za varstvo narave), v Ljubljani na Oddelku za geologijo NTF, Privoz 11 (na Prulah), v predavalnici P-02 v kleti.
3. Četrtek, 5. 4. 2012: **Uporaba prenosnega XRF analizatorja za določitev elementne sestave različnih materialov,** dr. Nastja Rogan Šmuc in doc. dr. Matej Dolenec (UL NTF OG), v Ljubljani na Oddelku za geologijo NTF, Privoz 11 (na Prulah), v predavalnici P-02 v kleti.
4. V četrtek, 15. 3. 2012, je bila v sklopu predavanj izvedena okrogla miza z naslovom **Geoparki Slovenije**, ki jo je vodila predsednica Sekcije za geološko dediščino Martina Stupar zaposlena na Zavodu RS za varstvo narave, OE Nova Gorica. Izpostavljeno je bilo predvsem vključevanje geološke stroke, Univerze - Oddelka za geologijo NTF, Inštitutov v okviru ZRC SAZU, Zavoda RS za varstvo narave, Geološkega zavoda Slovenije, Slovenskega geološkega društva in druge geološke javnosti v aktivnosti geoparkov.

Strokovna ekskurzija

Strokovna ekskurzija je bila izvedena 2. 6. 2012 pod vodstvom dr. Ladislava Placerja, na fosilni plaz pri Ilirski Bistrici. Poleg članov društva so se je udeležili tudi zunanji udeleženci.

Vključitev v domače in mednarodne zveze

Včlanjeni smo v Evropsko federacijo geologov (EFG), IMA (Mednarodno združenje mineralogov) in EMU (European Mineralogical Union) ter slovensko inženirsko zvezo (SIZ). Ustanovili smo Nacionalni komite (National Vetting Committee) Slovenskega geološkega društva v Evropski federaciji geologov (EFG), v sestavi komisije Barbara Čenčur Curk, Mirka Trajanova in Slavko Šolar, ki bodo pregledovali vloge za pridobitev naziva Evrogeolog (EurGeol).

Ostali dogodki

V časopisu Delo smo se oktobra 2012 z osmrtnico poklonili preminulemu članu in nekdanjemu predsedniku društva dr. Dušanu Kuščerju.

V skladu s sklepom sestanka razširjenega izvršnega komiteja društva v 2011 se letna poročila SGD izdajajo kot prispevki v reviji Geologija ter v letnem biltenu Geološkega zavoda Slovenije.

Za leto 2013 so načrtovane naslednje aktivnosti društva:

Predvidena so strokovna predavanja doc. dr. Mirijam Vrabec (od lani) z naslovom »Sveže novice s pohorske golice« o rezultatih geoloških raziskav v zadnjih 6 letih na področju Pohorja v četrtek 19. 9. 2013, doc. dr. Boštjana Rožiča z naslovom »Kobla kot druga Meka slovenske geologije« na temo Slovenskega bazena v četrtek 20. 6. 2013 in v sodelovanju z Geomorfološkim društvom Slovenije predavanje prof. Hansa Grüningerja iz Kanade v sredini maja 2013. Od strokovnih ekskurzij sta v planu neizvedeni ekskurziji v Medvednico in Potočko Zijalko z Olševo (slednja v izvedbi prof. dr. Vide Pohar), ekskurzija na Pohorje predvidoma v soboto, 21.9.2013, ki sledi predavanju Mirijam Vrabec, ekskurzija na Koblo v soboto, 22.6.2013, ki sledi predavanju Boštjana Rožiča ter pogojno še ekskurzija v Karnijske Alpe pod vodstvom dr. Matevža Novaka.

Poleg teh aktivnosti je predvidena tudi včlanitev v zvezo INQUA (International Union for Quaternary Research), aktivnosti pri izvajanju varstva geoloških naravnih vrednot in ohranjanje nahajališč, popularizaciji geologije ter ponovna vzpostavitev dejavnosti pri PROGEO, sodelovanje z EFG in Hrvaškim geološkim društvom ter zaščita izdankov ultravisokotlačnih metamorfnih kamnin na Pohorju.

Ker jedro društva tvorijo njegovi člani, pozivam vse izmed njih k večji aktivnosti, izvedbi predavanj in ekskurzij ter seveda k spodbujanju debat in reševanju odprtih problemov slovenske geologije.

Letna skupščina Slovenskega združenja za geodezijo in geofiziko

Polona VREČA

Institut "Jožef Stefan", Odsek za znanosti o okolju, Jamova cesta 39, 1000 Ljubljana, Slovenia

V Ljubljani je 29. januarja 2013, na Fakulteti za gradbeništvo in geodezijo potekala redna letna skupščina Slovenskega združenja za geodezijo in geofiziko (SZGG), v okviru katere je bilo organizirano tudi 18. strokovno srečanje z naslovom: »Raziskave s področja geodezije in geofizike – 2012«. Srečanja se je udeležilo približno 40 članov SZGG.

Letošnjo skupščino smo pričeli s spominom na geofizika in seizmologa dr. J. K. Lapajneta, ki je preminil leta 2012. J. K. Lapajne je bil pobudnik ustanovitve SZGG in njen prvi predsednik. Sledilo je kratko poročilo predsednika združenja J. Rakovca, poročilo tajnika združenja M. Kuharja in obravnava predlogov spremembe pravilnika SZGG. V okviru teh sprememb je bil obravnavan tudi predlog o ustanovitvi Sekcije za kriosfero, ki smo ga v letu 2012 pripravili kolegi iz Geodetskega inštituta Slovenije, Geografskega inštituta Antona Melika in Instituta »Jožef Stefan«. Glavni namen nove sekcije je povezati ljudi in znanje na področju raziskav snega in ledu v Sloveniji in se aktivno vključiti v delovanje Mednarodnega združenja za znanosti o kriosferi (International Association of Cryospheric Sciences – IACS), povezovanje z drugimi sekcijami v okviru SZGG (predvsem s Sekcijo za meteorologijo in atmosferske znanosti, Sekcijo za geodezijo in Sekcijo za hidrologijo) ter povezovanje z raziskovalci v tujini, ki delujejo na področju raziskav kriosfere. Vse predlagane spremembe pravilnika so bile sprejete in ustanovljena je bila nova Sekcija za kriosfero.

V okviru združenja je do leta 2012 delovalo sedem sekcij, ki jih vodijo M. Kobold (Sekcija za hidrologijo), A. Gosar (Sekcija za seizmologijo in fiziko notranjosti Zemlje), P. Kralj (Sekcija za vulkanologijo in kemijo Zemlje), V. Malačič (Sekcija za oceanografijo), N. Žagar (Sekcija za meteorologijo), B. Stopar (Sekcija za geodezijo) in R. Čop (Sekcija za geomagnetizem). Vodje posameznih sekcij so podali kratka poročila o delu v preteklem letu. V okviru skupščine smo pripravili predstavitev o delu v letu 2012 tudi člani novo-ustanovljene Sekcije za kriosfero v sodelovanju z raziskovalci, ki so na tem področju aktivni. Od leta 2013 ima tako SZGG osem sekcij in formalnega predstavnika Slovenije v IACS.

Sledilo je strokovno srečanje, na katerem je dvanajst predavateljev predstavilo rezultate svojega raziskovalnega dela. M. Brenčič je predstavil bilanco vode na Zemlji, P. Vreča s sodelavci pa prve rezultate raziskav izotopske sestave padavin in snega na območju Julijskih Alp in Karavank. Sledilo je predavanje M. Z. Božnar s sodelavci o modeliranju možnih nezgodnih izpustov iz NE Krško z Lagrangeevim modelom delcev in G. Dolška, ki je predstavil izdelavo Huffovih krivulj in njihovo analizo za izbrane padavinske postaje v Sloveniji. Nadalje je N. Bezak s sodelavci predstavil izbiro metod pri verjetnostni analizi visokovodnih konic, G. Skok s sodelavci pa analizo toče v Sloveniji z uporabo radarskih podatkov. S. Šebela nam je predstavila značilnosti temperature zraka v Predjamskem sistemu, J. Kogovšek pa nas je seznanila z vplivi sušnih razmer na kakovost vodnih virov na območju izvira Malenščica. Sledili sta predstavitvi rezultatov raziskav M. Triglav Čekada s sodelavci, ki sta jih zaradi odsotnosti predstavila D. Radovan in K. Oven. D. Radovan je predstavil rezultate proučevanja poplav novembra 2012 na podlagi nemerskih posnetkov z vključevanjem javnosti, K. Oven pa je predstavila zračno lasersko skeniranje zasneženega površja. K. Bajec s sodelavci je predstavila spremljanje ionosferskih motenj nad Slovenijo s pomočjo omrežja stalnih GNSS-postaj SIGNAL. Strokovno srečanje se je zaključilo s predavanjem R. Čopa s sodelavci o vplivu neviht na geomagnetne meritve na Gori nad Ajdovščino.

SZGG je združenje, ki povezujejo zelo različne profile strokovnjakov, ki se ukvarjajo z raziskavami Zemlje in omogoča zanimivo izmenjavo različnih znanj. O pestrosti delovanja združenja se lahko prepričate ob prebiranju poročil predstavnikov sekcij in predavanjih, ki so dostopna na http://www.fgg.uni-lj.si/sugg/ . Na navedenem naslovu najdete tudi več informacij o združenju in njegovem delovanju.

Dipl. ing. Marjanu Dolencu v slovo

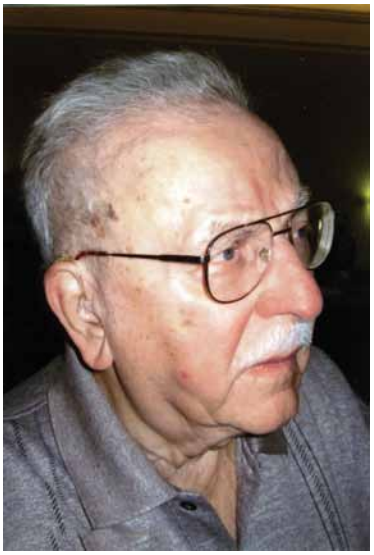

6. marca 2013 smo se v deževnem vremenu na kranjskem Mestnem pokopališču poslovili od gospoda Marjana Dolenca, dipl. inženirja rudarstva, ki je bil s svojimi 94 leti starosta slovenskih montanistov.

Rodil se je v znani trgovski družini v Kranju, kjer je tudi preživljal svojo mladost in obiskoval gimnazijo. Po maturi se je vpisal na Rudarski oddelek Tehniške fakultete v Ljubljani. Z željo, da bi do neke mere spoznal problematiko pridobivanja premoga, je študentski praksi opravljal v premogovnikih Kakanj in Mostar. Na površini plasti v premogovniku Mostar je našel lepe in velike kristale žvepla, ki jih je prinesel v Ljubljano, kjer sta jih z njegovim profesorjem V. Nikitinom, svetovno znanim mineralogom, skrbno pregledala in na enem od njih ugotovila preko 140 ploskev – tako je zapisal g. Dolenc v svojih spominih. Ker ga je mineralogija in parageneza metalnih rud čedalje bolj zanimala, se je v diplomski nalogi opredelil za študij nastanka bakrove rude v rudišču Bor. Za to izvrstno študijo je v letu 1941 prejel Svetosavsko nagrado. S tem delom pa se je, kot je sam rekel, dokončno opredelil za svoje bodoče strokovno življenje. Po diplomi je bil kratek čas asistent pri profesorju Duhovniku v Ljubljani.

V vojnem času je bil interniran v Italijo, nato pa premeščen v nemške rudnike – najprej v rudišče Bleiberg pri Beljaku, kjer se je srečal tudi s svojima študentskima kolegoma Danilom Jelencem in Slavkom Paplerjem, nato pa v severno Nemčijo v rudnik bakra Rammelsfeld.

Kmalu po osvoboditvi, v začetku leta 1946, je dobil dekret Zveznega ministrstva za rudarstvo, da mora v Makedonijo. Sprva je šel v rudnik mangana Cer pri Kičevu, kamor je v zimskih razmerah potoval cel teden. Zaradi precejšnje izčrpanosti rudnika je dobil od Generalnega direktorata za rudarstvo pooblastilo za obsežne nove geološke raziskava manganove in predvsem železove rude. To je bilo obdobje napornega dela, saj je bilo vse raziskave potrebno opraviti peš ali s konji, ob pomanjkanju strokovne opreme. Leta 1949 je vodil terenske raziskave, ko so v masivu Bistre planine pri Tajmištu odkrili bogato sideritno-šamozitno nahajališče, ki je bilo kasneje osnova za izgradnjo železarne v Skopju. To odkritje železove rude, ocenjeno na preko sto milijonov ton rezerv, je bilo eno njegovih največjih strokovnih dosežkov. Raziskave je nadaljeval na celotnem ozemlju Makedonije. Ker v Tajmištu ni bilo predvidenih dodatnih geoloških raziskav, je leta 1958 postal glavni geolog in nato direktor Geološkega zavoda v Skopju. Že v tistem obdobju je v okviru štipendije OZN nekaj mesecev raziskoval manganova rudišča v Maroku (1953), z Elektrosondo krajši čas limonit in kromit v Libanonu in Siriji (1958), nekoliko kasneje (1960) pa železovo rudo v priobalnem delu Nubijske puščave v Sudanu.

Leta 1961, po 15 letnem bivanju v Makedoniji, je g. Dolenc prišel na Geološki zavod v Ljubljano. Kot je pripovedoval, mu je ta selitev rešila življenje, saj je bilo stanovanje, v katerem je stanoval z družino, v skopskem potresu leta 1963 popolnoma porušeno.

Po prihodu v Ljubljano se je sprva kot višji svetovalec in namestnik sektorja za inozemska dela intenzivno vključil v delo ekonomskih geologov – predvsem na raziskavah urana, bakra in boksitov, kasneje pa tudi v ostale veje geologije in postal direktor Geološkega sektorja znotraj takratnega Geološkega zavoda Ljubljana.

To je bilo obdobje, v katerem so se v okviru novonastalih neuvrščenih držav odpirala za geologe in rudarje številna raziskovalna dela, predvsem v Afriki in na Bližnjem vzhodu. Tako je Geološki zavod v okviru Rudisa izvajal tovrstne raziskave v Egiptu (monacitni peski v Nilovi delti, stari faraonski rudniki zlata), Somaliji (študija izkoriščanja sadre za cement in mavec), Tanzaniji (karbonatiti in tanzanit, zlato, itaberit, premog, redke zemlje, magnetit, nefelin). V Gvineji je pridobil vrtalna dela na nahajališčih železove rude v Nimbi ter raziskoval ležišča diamantov, v Keniji pa je izvedel ocene nahajališč sadre in črnih peskov z monacitom, v Zambiji pa nahajališč dragih mineralov – zelenega grosularja, rubina in rodolita. Študijsko je obiskal tudi Bolivijo (zaloge cinka) in otok Lesbos v Grčiji (perliti).

Posebno intenzivno, več kot 10 let pa je bil povezan z Alžirijo, za katero je izdelal program za oživitev rudarske dejavnosti rudišč cinka, svinca in železa. V sklopu tega programa so več let potekale tudi regionalne geološke raziskava na več območjih Atlasa. Vloga g. Dolenca pri vseh teh delih je bila neprecenljiva. Razen za ekonomsko geologijo pa je znotraj Geološkega zavoda skrbel za razvoj tudi ostalih področij geologije. Posebno pomembni so bili stiki z Univerzama v Berlinu in Heidelbergu, ki so privedla do dolgoletnega sodelovanja na področju okoljske geologije.

Po upokojitvi leta 1989, tisto leto je bila tudi njegova zadnja afriška misija na kromite v Egipt, se je s soprogo preselil na Črni vrh nad Polhovim Gradcem, kjer je užival v neokrnjeni naravi in kmetovanju. Tu je ostal do ženine smrti, nato pa se je vrnil v Ljubljano, kjer je živel z drugo ženo Vido. A kruta usoda je zopet posegla v njegovo življenje, ko sta mu umrla sin in soproga. V tem času se je v večji meri posvetil svoji bogati mineraloški zbirki, ki šteje preko 2000 vzorcev in mineraloškemu slovarju. Uredil je tudi zbirko mineralov in rudnin na Geološkem zavodu. V zadnjih letih je živel v domu starejših občanov v Trzinu, kjer ga je z vso pozornostjo spremljala njegova snaha ga. Miljana.

Za svoje delo je dobil več priznanj in odlikovanj, leta 2007 pa je bil imenovan za častnega člana Geološkega zavoda Slovenije.

Gospoda Dolenca bomo njegovi stanovski kolegi ohranili v spominu kot izrednega strokovnjaka, poštenega, skromnega, natančnega in delovnega človeka ter iskrenega prijatelja.

Bojan Ogorelec, Danilo Ravnik

GEOLOGIJA *56/1*, 135-141, Ljubljana 2013

Izpela je pesem ptica trnovka.
Ni več bolečine, zastal je njen čas.
Je veter ponesel njen glas med doline,
čez alpske apnene vrhove v naročje valov.
Zadrži korak in prisluhni – ga sliši'?

V spomin prof. dr. Bojanu Ogorelcu

V torek 2. 7. 2013 je med nas kot grom udarila vest, da nas je v svojem 69. letu starosti zapustil prijatelj, sodelavec in učitelj, profesor dr. Bojan Ogorelec. Kar pet let se je boril z zahrbtno boleznijo. Ni pokazal slabosti, ni se zaprl vase in vedrina njegovega nasmeha je vsem, ki smo mu bili blizu, potihoma dajala upanje, da jo bo premagal. Bila je premočna. Klonil je še poln načrtov za življenje in delo. Pred nami je zazijala vrzel, ki je ni mogoče na hitro zapolniti; sčasoma jo bomo morali. Zapolnila jo bodo njegova dela in spomini, polni, kot je bilo njegovo življenje.

Bojan se je rodil v Celovcu, 5. marca 1945-ega leta. Naključje negativne ocene iz geologije v srednji šoli in zagnanost, da jo popravi, je Bojana navdušila za študij geologije na takratni Fakulteti za naravoslovje in tehnologijo na Univerzi v Ljubljani. Že med študijem je odšel na prakso v Skandinavijo, kjer se je spoznaval z najstarejšimi kamninami v Evropi, predvsem pa se je zavedel majhnosti nacionalnega ozemlja, kadar govorimo o geoloških procesih in dejstva, da se geologija ne konča na političnih mejah. Bil je odličen učenec prof. Dušana Kuščerja, utemeljitelja niza smeri sodobne geologije na slovenskih tleh, kar je močno vplivalo na njegovo poznejšo raziskovalno miselnost. Pokazal je veliko zanimanje za sedimentne kamnine in procese njihovega nastanka. To je potrjevala tema njegove diplomske naloge – Flišne plasti Gornjega Posočja, s katero je leta 1970 zaključil svoj dodiplomski študij. Leta 1971 se je zaposlil na takratnem Geološkem zavodu Ljubljana, kateremu je ostal zvest celih 38 let, vse do upokojitve 15. aprila 2009.

Že takoj po vključitvi v kolektiv Geološkega zavoda Ljubljana se je za eno leto pridružil skupini regionalnih geologov na misiji v Alžiriji. Dobil je bogate delovne izkušnje, na osnovi katerih si je začel utirati strokovno pot. Ko se je vrnil domov, je bil vključen v enega najkompleksnejših geoloških projektov, v izdelavo Osnovne geološke karte Jugoslavije v merilu 1 : 100.000. Kartiranje, kjer je potrebno množico podatkov združiti in postaviti v prostor, je v njem še dodatno spodbudilo željo po spoznavanju tako razvejane vede, kot je geologija. Ni torej naključje, da ga je pot prav kmalu zanesla na univerzo v Heidelbergu, kjer se je izpopolnjeval v študijskem letu 1973/74. Navdušil ga je pogled v mikro-dimenzije kamnin, njihova živopisna mineralna sestava in nenavadnost fosilnega gradiva, ki je pripovedovalo o času v katerem so organizmi živeli.

Po vrnitvi iz Heidelberga se je Bojan priključil takratnemu Oddelku za laboratorijske raziskave na Geološkem zavodu Ljubljana. Dodobra je izkoristil svoje znanje in uvedel sodoben način raziskav karbonatnih kamnin ter poglede nanje z okoljskega in dogodkovnega zornega kota, ki so bili takrat novi za večino njegovih kolegov. Na tem področju se je uveljavil kot utemeljitelj sodobne sedimentologije karbonatnih kamnin v Sloveniji. Del novih spoznanj je že vtkal v timsko delo pri izdelavi Osnovne geološke karte 1 : 100 000 in v raziskave na področju mineralnih surovin. V tem pogledu pa imata posebno mesto tolmač za Formacijsko geološko karto južnega dela Tržaško-komenske planote 1 : 50.000: kredne in paleogenske karbonatne kamnine, in avtorska Geološka karta Kozjanskega v merilu 1 : 50.000. Zanjo je praktično v celoti napisal tolmač, vendar je njegov izid preprečila neusmiljena bolezen.

Leta 1983 je prevzel vodenje Oddelka za paleontologijo in petrologijo, ki ga je vodil vse do upokojitve.

Sredi osemdesetih let je bil imenovan za koordinatorja pomembnega raziskovalnega projekta »Plan in program raziskav ležišč nafte in plina v SR Sloveniji za obdobje 1986 – 1990«, katerega cilj je bil ponovno ovrednotenje starih in prognoza potencialnih območij za nova ležišča energentov na območju Slovenije, predvsem v njenem severovzhodnem delu. Spoznaval je klastične sedimentne kamnine, ki jih je bilo potrebno opredeliti tako stratigrafsko, mineraloško in strukturno, kot tudi z vidika potencialnosti zadrževanja ogljikovodikov.

Glavna nit njegovega znanstveno-raziskovalnega dela in njegova ljubezen pa so ostale karbonatne kamnine. Proučeval jih je na terenu in nadaljeval v tistem segmentu, kamor ne seže človeško oko. To so bili mikrofaciesi mezozojskih karbonatnih kamnin Slovenije, na osnovi katerih je lahko določal sedimentacijska okolja širšega alpskega in dinarskega prostora. Neposreden vpogled v sedimentacijske procese so mu pri tem nudile raziskave recentnih sedimentov. Tako je sodeloval v raziskavah sedimentov Blejskega in Bohinjskega jezera, kot tudi Koprskega zaliva in Sečoveljskih solin, katerih začetek je imel okoljevarstven vidik, vendar je izsledke nadgradil s spoznavanjem dogodkov, ki so pripeljali do njihovega nastanka. Sodeloval je tudi pri raziskavah krednih plasti Primorske.

Leta 1988 je svoje dolgoletno sodelovanje s heidelberško univerzo kronal z doktoratom na temo mikrofaciesa, geokemičnih lastnosti in diageneze dachsteinskega apnenca in glavnega dolomita v jugozahodni Sloveniji, ki ga je uspešno zagovarjal v nemškem jeziku pred tamkajšnjo komisijo. S številnimi novimi ugotovitvami je bilo njegovo delo za tisti čas v mnogočem pionirsko.

Posledica njegove visoke strokovnosti in nepristranskosti je bilo njegovo imenovanje za nacionalnega koordinatorja za področje geologije pri takratnem Ministrstvu za znanost in tehnologijo, ki ga je opravljal več let. Do upokojitve je vodil raziskovalno programsko skupino »Sedimentologija, mineralogija in petrologija«. V svojem vodenju raziskovalne dejavnosti v slovenskem in mednarodnem okviru je bil Bojan dosleden pristaš pravičnega razdeljevanja sredstev in spodbude raziskovalcem iz raznih geoloških okolij. Zaradi natančnega očesa in raziskovalnega ugleda je bil 1995 imenovan v uredniški odbor domače znanstvene revije Geologija in že leta 1998 je postal njen glavni in odgovorni urednik. To delo je nadvse zavzeto opravljal do leta 2010. Sprejel je povabilo v uredniška odbora dveh tujih znanstvenih revij, Rudarsko-geološko-naftnega zbornika in Geologia-e Croatica-e. Poleg rednega urednikovanja pa je imel tudi vodilno vlogo pri nastanku obsežne knjige Geologija Slovenije, kjer je na preko 600-tih straneh dvojezično predstavljena pestra geološka zgradba našega nacionalnega ozemlja. Brez njegove zagnanosti in predanosti, bi je verjetno še danes ne imeli. V dveh mandatih, od 1991 do 2010, je bil tajnik Slovenskega odbora IGCP UNESCO. Zavzemal se je za slovensko zastopanost v najodličnejših mednarodnih raziskovalnih projektih, predvsem mladih raziskovalcev, ki jim je bil to pogosto prvi vstop v mednarodni svet znanosti. Bil je v uredniškem odboru pri nastajanju knjige Bibliografija slovenskih geologov v projektih IGCP – UNESCO 1976-2001, med letoma 2000 in 2006 pa je bil tudi predsednik Društva prijateljev mineralov in fosilov Slovenije.

Svoje dolgoletne raziskave njemu najljubše tematike je strnil tudi v monografiji Mikrofacies mezozojskih karbonatnih kamnin Slovenije, ki je izšla leta 2011. Mikro svet je znal preliti v izvirne poglede na okolje nastanka karbonatnih kamnin slovenskega prostora. Poleg tega je objavil več kot 80 znanstvenih in strokovnih člankov, iz katerih bodo lahko črpali ideje in znanje še mnoge prihodnje generacije geologov. Njegova bibliografija šteje skupno več kot 300 enot. V času njegovega delovanja na Zavodu ni bilo niti enega večjega projekta, v katerem ne bi tvorno sodeloval. Prav tako obsežno pa je delo, ki ga ni mogoče pokazati in ga lahko vrednotijo le njegovi sodelavci, namreč nasveti, sugestije, korekcije in recenzije, s čimer je rešil prenekatero težavo mlajših in starejših kolegov. Zavzemal se je za vključevanje izsledkov raziskav v reševanje praktičnih problemov in hkrati skrbel, da se je razvijalo slovensko strokovno izrazoslovje.

Vrline njegovega značaja in nadarjenost za reševanje zapletenih problemov so se izkazali pri njegovem uspešnem vodenju skupinskih projektov. Omenimo zlasti njegovo uspešno usklajevanje delovanja med seboj težko združljivih osebnosti, ki jih je z veliko potrpežljivostjo in izjemno veščino vpletel v skupno delo vse do uspešnega zaključka.

Spoštovanje do Bojanovega dela in znanja pa se ni končalo v mejah Slovenije. K sodelovanju so ga vabili iz vseh sosednjih držav, kjer se na meji stika enaka geološka problematika. Svoje dosežke je predstavil na številnih mednarodnih in domačih znanstvenih srečanjih.

Težke razmere, ki so nastopile za raziskovalno dejavnost po letu 1992, je vzel zelo resno in tudi osebno. Tako je po daljšem razmišljanju in tehtanju v začetku leta 2000 prevzel najprej mesto vršilca dolžnosti direktorja, od julija 2000 dalje pa tudi formalno direktorja Geološkega zavoda Slovenije, v katerega se je takrat preoblikoval iz Inštituta za geologijo, geotehniko in geofiziko. Med odgovornim vodenjem Geološkega zavoda ni vrgel puške v koruzo, ampak je vzdrževal živ stik z raziskovalno dejavnostjo. S svojimi dolgoletnimi izkušnjami in preudarnimi potezami ga je uspešno vodil do aprila 2006, ko je vajeti prepustil mlajšim. Sam se je posvetil vodenju oddelka ter zaključevanju svoje dolge in uspešne znanstveno-raziskovalne kariere. Zadnje desetletje je skupaj s soavtorji pripravil za tisk rezultate mnogih raziskav, ki so bile »pozabljene« v arhivskih poročilih, in jih objavil v vrsti člankov in monografij, pogosto nadgrajene s sodobnejšimi interpretacijami.

Ob vsem naštetem ni pozabil na dejstvo, da nobena znanstvena disciplina ne more uspevati in rasti brez dobrega mladega kadra. Tako je bil dolga leta vključen v učni proces na Naravoslovnotehniški fakulteti v Ljubljani na Oddelku za geologijo. Sprva je sodeloval na podiplomskem študiju, od leta 1992 dalje pa kot docent pri predavanjih iz predmeta Sedimentologija in občasno pri predavanjih iz predmeta Facialna analiza. Leta 2005 je prevzel predavanja pri predmetu Regionalna geologija na dodiplomskem študiju, ki jih je vodil do svoje upokojitve. Hkrati je pomagal pri izvedbi številnih terenskih vaj, diplom, magisterijev in doktoratov. Pod njegovim mentorstvom ali z njegovim sodelovanjem je nastalo nekaj izrednih magistrskih in doktorskih del. Vse to in njegovi znanstveni dosežki so botrovali, da je bil leta 2008 izvoljen v naziv izrednega profesorja. Tako študentom, kot tudi vsem kolegom, ki smo se kadarkoli obrnili nanj s svojimi vprašanji, je znal geološke procese razložiti na enostaven način, pa vendar na visokem strokovnem nivoju. Rad jih je popestril z anekdotami, ki so se nabrale tekom njegovega dolgoletnega dela. Nikdar ni pozabil stavka, ki ga je izrekel šofer avtobusa, ko je bil na terenu na Hrvaškem: »Vi, koji proučavate utrobu matere Zemlje…«. Primerjal ga je s suhoparnim strokovnim izrazoslovjem in se pri tem pomenljivo zasmejal.

Ustvarjalno pot vrhunskega raziskovalca in znanstvenika izr. prof. dr. Bojana Ogorelca je kronala prestižna nagrada, Lipoldova medalja, ki jo je prejel leta 2011.

Polno je popisana knjiga mnogo prekratke življenjske poti našega cenjenega kolega in prijatelja Bojana. Neustavljiva bolezen je nasilno pretrgala niti njegove bogate ustvarjalnosti. S svojimi deli bo za vedno zapisan v zgodovino slovenske geologije in široke strokovne javnosti. Njegova blaga narava, neposrednost in šegavost pa bosta ostala del naše zavesti in našega kolektiva.

Mirka Trajanova
Marko Komac

Prof. dr. Bojan Ogorelec – tiskana bibliografija 1974 – 2012

Kuščer, D., Grad, K., Nosan, A. & Ogorelec, B. 1974: Geološke raziskave soške doline med Bovcem in Kobaridom. Geologija 17, 426-476.

Ogorelec, B. & Premru, U. 1975: Sedimentne oblike triadnih karbonatnih kamenin v osrednjih Posavskih gubah. Geologija 18, 187-196.

Ogorelec, B. 1976: Stromatoliti, njihova klasifikacija in pojavljanje. Rud.- met. zb. 23/1, 53-60.

Ogorelec, B., Šribar, L. & Buser, S. 1976: O litologiji in biostratigrafiji volčanskega apnenca. Geologija 19, 125-151.

Premru, U., Ogorelec, B. & Šribar, L. 1977: O geološki zgradbi Dolenjske. Geologija 20, 167-192.

Molnar, F. M., Rothe, P., Förstner, U., Štern, J., Ogorelec, B., Šercelj, A. & Culiberg, M. 1978: Lakes Bled and Bohinj: origin, composition, and pollution of recent sediments. Geologija 21, 93-164.

Ogorelec, B. & Rothe, P. 1979: Diagenetische Entwicklung und faziesabhängige Na-Verteilung in Karbonat-Gesteinen Sloweniens. Geol. Rundschau 68/3, 965-978.

Grad, K. & Ogorelec, B. 1980: Zgornjepermske, skitske in anizične kamenine na žirovskem ozemlju. Geologija 23/2, 189-220.

Orehek, A. & Ogorelec, B. 1980: Sedimentološke značilnosti jurskih in krednih karbonatnih kamenin na Trnovskem gozdu. Geol. Vjesnik 32, 185-192.

Čar, J., Gregorič, V., Ogorelec, B. & Orehek, S. 1980: Sedimentološki razvoj skitskih plasti v idrijskem rudišču. Rud.-met. zb. 27, 3-20.

Ogorelec, B., Mišič, M., Šercelj, A., Cimerman, F., Faganeli, J. & Stegnar, P. 1981: Sediment sečoveljske soline. Geologija 24, 179-216.

Dolenec, T., Ogorelec, B. & Pezdič, J. 1981: Zgornjepermske in skitske plasti pri Tržiču. Geologija 24/2, 217-238.

Orehek, A. & Ogorelec, B. 1981: Korelacija mikrofacijalnih i geohemijskih osobina jurskih i krednih stena južne karbonatne platforme Slovenije. Glas Repub. zavoda zašt prir. Prirod. muzej Titograd, 14, 161-181.

Faganeli, J., Fanuko-Kovačič, N., Lenarčič, M., Malej, A., Mišič, M., Ogorelec, B., Vrišer, B., Vukovič, A. & Župan, J. 1981: Zasledovanje vpliva začasnega izpusta komunalnih odplak mesta Koper na morje v Koprskem zalivu. Slov. morje in zaledje 4-5, 177-198.

Čar, J., Skaberne, D., Ogorelec, B., Turnšek, D. & Placer, L. 1981: Sedimentological characteristics of Upper Triassic (Cordevolian) circular quiet water coral bioherms in western Slovenia, northwestern Yugoslavia. V: Toomey, D. F. (ed.): European fossil reef models, SEPM Spec. Publ. 30, Tulsa, 233-240.

Turnšek, D., Buser, S. & Ogorelec, B. 1981: Un Upper Jurassic reef complex from Slovenia, Yugoslavia. V: Toomey, D. F. (ed.): European fossil reef models, SEPM Spec. Publ. 30, Tulsa, 361-369.

Pungartnik, M., Brumen, S. & Ogorelec, B. 1982: Litološko zaporedje karnijskih plasti v Mežici. Geologija 25/2, 237-250.

Turnšek, D., Buser, S. & Ogorelec, B. 1982: Carnian coral-sponge reefs in the Amphiclina beds between Hudajužna and Zakriž (western Slovenia). Razpave SAZU, Razr. IV., 24/2, 51-98.

Ogorelec, B., Mišič, M., Cimerman, F. & Faganeli, J. 1983: Sédiments quaternaires du forage effectué dans la Baie de Koper, Adriatique du nord, Yugoslavie. Rapp. P-V. Réun. Comm. Int. Explor. Sci. Mer Mediterr. 28/4, 251-253.

Drobne, K., Cimerman, F. & Ogorelec, B. 1983: The vertical distribution of smaller benthic Foraminifera on submarine cliff in the Adriatic Sea. Thalass. Jugosl. 19, 121-122.

Turnšek, D., Buser, S. & Ogorelec, B. 1983: The role of corals in Ladinian reef communities of Slovenia, Yugoslavia. Palaeontogr. Amer. 54, 201-209.

Jelaska, V. & Ogorelec, B. 1983: The Upper Cretaceous depositional environments of the carbonate platform on the island of Brač. V: Babić, Lj. (ed.): Contributions to Sedimentology of Some Carbonate and Clastic Units of the Coastal Dinarides: Excursion Guide Book. Zagreb, IAS, 99-124.

Jurkovšek, B., Ogorelec, B., Kolar-Jurkovšek, T., Jelen, B., Šribar, L. & Stojanovič, B. 1984: Geološka zgradba ozemlja južno od Vršiča s posebnim ozirom na razvoj karnijskih plasti. Rud.-met. zb., 31, 3/4, 301-334.

Ogorelec, B., Mišič, M., Faganeli, J., Šercelj, A., Cimerman, F., Dolenec, T. & Pezdič, J. 1984: Kvartarni sediment vrtine V-3 v Koprskem zalivu. Slov. morje in zaledje, 7/6-7, 165-186.

Faganeli, J., Fanuko, N., Lenarčič, M., Malej, A., Mišič, M., Ogorelec, B., Vrišer, B., Vukovič, A. & Župan, J. 1984: Zasledovanje vpliva začasnega izpusta komunalnih odplak mesta Koper na morje v Koprskem zalivu. Slov. morje in zaledje, 7, 6/7, 179-198.

Dolenec, T., Pezdič, J., Ogorelec, B. & Mišič, M. 1984: Izotopska sestava kisika in ogljika v recentnem sedimentu iz Blejskega jezera in v pleistocenski jezerski kredi Julijskih Alp. Geologija 27, 161-170.

Ogorelec, B., Jurkovšek, B., Šribar, L., Jelen, B., Stojanovič, B. & Mišič, M. 1984: Karnijske plasti v Tamarju in pri Logu pod Mangartom. Geologija 27, 107-158.

Ogorelec, B. 1984: Postajališče št. 8: Kaninsko pogorje in Bovška kotlina. V: Orehek, A. (ur.). 6. Sed. plenum Jugosl. Bovec, 39-45.

Jelaska, V., Ogorelec, B. & Prohić, E. 1984: Facial variability and geochemistry in sediments nearly the Cretaceous-Tertiary boundary (Island of Brač, Yugoslavia). 5ème Congrès Européen de Sedimentologie, Marseille 1984 (Absract).

Faganeli, J., Mišič, M., Ogorelec, B., Dolenec, T. & Pezdič, J. 1985: Organic matter in two 41-m boreholes from the Gulf of Trieste (Northern Adriatic). Rapp. P-V. Réun. - Comm. Int. Explor. Sci. Mer Mediterr., 29/2, 139-142.

Ogorelec, B. 1985: Sečoveljske soline v očeh geologa. Proteus, 48/3, 93-98.

Buser, S., Grad, K., Ogorelec, B., Ramovš, A. & Šribar, L. 1986: Stratigraphical, paleontological and

sedimentological characteristics of Upper Permian beds in Slovenia, NW Yugoslavia. Mem. Soc. Geol. Ital. 34, 195-210.

Faganeli, J., Dolenec, T., Pezdič, J., Ogorelec, B. & Mišič, M. 1987: Nutrients in sediment pore water of the Gulf of Trieste (Northern Adriatic). Boll. oceanol. teor. appl., 5/2, 95-108.

Buser, S. & Ogorelec, B. 1987: Carnian Amphiclina beds – Hudajužna. V: Colizza, E. (ed.): E. Friuli, Karst of Gorizia and of W. Slovenia: Guidebook. Trieste, 13-18.

Ogorelec, B., Buser, S. & Šribar, L. 1987: Volče limestone – Podsela (Upper Cretaceous). V: Colizza, E. (ed.): E. Friuli, Karst of Gorizia and of W. Slovenia: Guidebook. Trieste, 31-35.

Buser, S., Ogorelec, B. & Orehek, S. 1987: Upper Malm limestone - Krnica on Mt. Trnovski gozd. V: Colizza, E. (ed.): E. Friuli, Karst of Gorizia and of W. Slovenia: Guidebook. Trieste, 49-51.

Buser, S., Turnšek, D. & Ogorelec, B. 1987: Lower Malm reef limestone – Selovec on Mt. Trnovski gozd. V: Colizza, E. (ed.): E. Friuli, Karst of Gorizia and of W. Slovenia: Guidebook. Trieste, 53-55.

Ogorelec, B., Orehek, A., Buser, S. & Pleničar, M. 1987: Komen beds - Skopo at Dutovlje (Upper Cretaceous). V: Colizza, E. (ed.): E. Friuli, Karst of Gorizia and of W. Slovenia: Guidebook, Trieste, 61-66.

Koch, R. & Ogorelec, B. 1987: Albian - Cenomanian beds - Kreplje at Dutovlje. V: Colizza, E. (ed.): E. Friuli, Karst of Gorizia and of W. Slovenia: Guidebook, Trieste, 67-69.

Drobne, K., Ogorelec, B., Pavlovec, R. & Pavšič, J. 1987: Section Golež, Danian-Cuisian. V: Colizza, E. (ed.): E. Friuli, Karst of Gorizia and of W. Slovenia: Guidebook. Trieste, 75-88.

Faganeli, J., Ogorelec, B., Mišič, M., Dolenec, T. & Pezdič, J. 1987: Organic geochemistry of two 40-m sediment cores from the Gulf of Trieste (Northern Adriatic). Estuar. coast. Shelf sci. 25, 157-167.

Drobne, K., Ogorelec, B., Pleničar, M., Barattolo, F., Turnšek, D. & Zucchi-Stolfa, M. L. 1987: The Dolenja vas section, a transition from Cretaceous to Paleocene in the NW Dinarides, Yugoslavia. Mem. Soc. Geol. Ital. 40, 73-84.

Turnšek, D., Buser, S. & Ogorelec, B. 1987: Upper Carnian reef limestone in clastic beds at Perbla near Tolmin (NW Yugoslavia). Razpave SAZU, Razred I., 27, 37-64.

Ogorelec, B., Mišič, M., Faganeli, J., Stegnar, P., Vrišer, B. & Vukovič, A. 1987: Recentni sediment Koprskega zaliva. Geologija 30, 87-121.

Brezigar, A., Ogorelec, B., Rijavec, J. & Mioč, P. 1987: Geološka zgradba predpliocenske podlage Velenjske udorine in okolice. Geologija 30, 31-65.

Pavlovec, R., Pleničar, M., Drobne, K., Ogorelec, B. & Šušteršič, F. 1987: History of geological investigations of the Karst (Kras) region and the neighbouring territory (Western Dinarides). Mem. Soc. Geol. Ital. 40, 9-20.

Faganeli, J., Planinc, R., Pezdič, J. & Ogorelec, B. 1988: Marine geology of the Gulf of Trieste (Northern Adriatic) B: Geochemical properties. Rapp. P-V. Réun. - Comm. Int. Explor. Sci. Mer Mediterr. 31, 93-94.

Drobne, K., Ogorelec, B., Pleničar, M., Zucchi-Stolfa, M. L. & Turnšek, D. 1988: Maastrichtian, Danian and Thanetian Beds in Dolenja vas (NW Dinarides, Yugoslavia) Mikrofacies, foraminifers, rudists and corals. Razprave SAZU, Razred IV, 27, 37-64.

Ogorelec, B. 1988: Mikrofazies, Geochemie und Diagenese des Dachsteinkalkes und Hauptdolomits in Süd-West-Slowenien, Jugoslawien. Dissertation, Natur. Mathemat. Gesamtfakultät, Heidelberg, 173 p.

Cimerman, F., Drobne, K. & Ogorelec, B. 1988: L'association de foraminiferes benthiques des vases de la baie de Veliko jezero sur l'ile de Mljet et de la falaise Lenga, ouverte vers la mer (Adriatique moyenne). Rev. paléobiol., Vol. spec. 2, 741-753.

Placer, L., Ogorelec, B., Čar, J. & Mišič, M. 1989: Nekaj novih podatkov o Ravenski jami na Cerkljanskem. Acta Carsol. 18, 129-138.

Koch, R., Ogorelec, B. & Orehek, A. 1989: Microfacies and diagenesis of Lower and Middle Cretaceous carbonate rocks of NW-Yugoslavia (Slovenia, Trnovo area). Facies 21, 135-170.

Jurkovšek, B., Šribar, L., Ogorelec, B. & Kolar-Jurkovšek, T. 1989: Pelagične jurske in kredne plasti v zahodnem delu Julijskih Alp. Geologija 31/32 (1988), 285-328.

Faganeli, J., Pezdič, J., Ogorelec, B. & Mišič, M. 1990: Sources of sedimentary organic matter in the Adriatic Sea. 32. Cong. C.I.E.S.M., Perpignan. 32, 283-284.

Koch, R. & Ogorelec, B. 1990: Biogenic constituents, cement types and sedimentary fabrics: their interrelations in Lower Cretaceous (Valanginian to Hauterivian) peritidal carbonate sediments (Trnovo, NW Slovenia). V: Heling, D. et al. (eds.): Sediments and environmental geochemistry: Selected aspects and case histories. Berlin: Springer, 95-123.

Dozet, S. & Ogorelec, B. 1990: Mikrofacije noričkih i retijskih naslaga u južnoj Sloveniji. Kongres geologa SFRJ, Ohrid.

Ogorelec, B., Mišič, M. & Faganeli, J. 1991: Marine geology of the Gulf of Trieste (northern Adriatic): Sedimentological aspects. Marine Geol. 99, 79-92.

Faganeli, J., Planinc, R., Pezdič, J., Smodiš, B., Stegnar, P. & Ogorelec, B. 1991: Marine geology of the Gulf of Trieste (Northern Adriatic): Geochemical aspects. Marine Geol. 99, 93-108.

Faganeli, J., Pezdič, J., Ogorelec, B., Herndl, G. J. & Dolenec, T. 1991: The role of sedimentary biogeochemistry in the formation of hypoxia in shallow coastal waters (Gulf of Trieste, northern Adriatic). V: Tyson, R. V. & Pearson, T. H. (eds.): Modern and ancient continental shelf anoxia, Geol. Soc. Spec. Publ. 58, London, 107-117.

Ogorelec, B. & Rothe, P. 1992: Mikrofazies, Diagenese und Geochemie des Dachsteinkalkes und Hauptdolomits in Süd-West-Slowenien. Geologija 35, 81-181.

Koch, R. & Ogorelec, B. 1992: Biogenic constituents, cement types and sedimentary fabrics: their interrelations in Lower Cretaceous (Valanginian to Hauterivian) peritidal carbonat sediments (Trno-

vo, SW Slovenia). Zentralbl. Geol. Paläontol., Teil 1/ 5, 561-568.

Pleničar, M., Drobne, K. & Ogorelec, B. 1992: Rudists and larger foraminifera below the Cretaceous - Tertiary boundary in the Dolenja vas section. V: Kollmann, H. A. & Zapfe, H. (eds.): New aspects on Tethyan Cretaceous fossil assemblages, Schrift. d. Erdwiss. Kommiss. 9, Wien, Springer, 231-240.

Buser, S. & Ogorelec, B. 1992: Evolution and microfazies of Mesozoic sedimentary rocks in Slovenia. V: 13th Reg. Meet. Sedimentol. Jena, 4-5 (Abstr.)

Faganeli, J., Pezdič, J., Ogorelec, B., Mišič, M. & Najdek, M. 1994: The origin of sedimentary organic matter in the Adriatic. Continent. shelf res. 14/ 4, 365-384.

Jelaska, V., Gušić, I., Jurkovšek, B., Ogorelec, B., Ćosović, V., Šribar, Lu. & Toman, M. 1994: The Upper Cretaceous geodynamic evolution of the Adriatic - Dinaric carbonate platform(s). V: 1st Int. Meet. Premediterran. Carb. Platforms, Marseille, 1994, 89-91 (Abstr.).

Dolenec, T., Veler, J., Pezdič, J., Ogorelec, B. & Faganeli, J. 1994: Oxygen and carbon isotopic composition of holocene sediment from the salt marsh of Sečovlje (Gulf of Trieste). V: IAS Int. Assoc. of Sedimentology, Ischia, 160-161 (Abstr.).

Dolenec, T., Pezdič, J., Ogorelec, B. & Lojen, S. 1994: Mineralogy and stable isotope composition of the surface sediment of the Lake Bled (Slovenia). V: IAS Int. Assoc. of Sedimentology, Ischia, 158-159 (Abstr.).

Aničić, B. & Ogorelec, B. 1995: Badenijski rodolit na Kozjanskem. Geologija 37/38 (1994), 225-249.

Dolenec, T., Ogorelec, B. & Pezdič, J. 1995: The Permian-Triassic boundary in the Karavanke Mountains (Slovenia): stable isotope variations. V: Velić, I. & Šparica, M. (ur.): 1. Hrv. Geol. Kongr., Opatija, Zbornik radova. Zagreb: IGI, 163-165.

Ogorelec, B., Dolenec, T., Cucchi, F., Giacomich, R., Drobne, K. & Pugliese, N. 1995: Sedimentological and geochemical characteristics of carbonate rocks from the K/T boundary to Lower Eocene in the Karst area (NW Adriatic platform). V: Velić, I. & Šparica, M. (ur.): 1. Hrv. Geol. Kongr., Opatija, Zbornik radova. Zagreb: IGI, 415-421.

Dolenec, T. & Ogorelec, B. 1995: The Permian – Triassic boundary in the Karavanke Mountains (Slovenia): Carbonate isotope variations. IAS -16th Regional Meeting of Sedimentology, Paris, Book of Abstracts, 170.

Drobne, K.Ogorelec, B., Barattolo, F., Dolenec, T., Pleničar, M., Turnšek, D., Zucchi-Stolfa, M.L. & Marton, E. 1995: Stop 1: The Dolenja Vas section (Upper Maastrichtian, lower and Upper Danian, Thanetian). Atti Mus. Geol. Paleontol. Monfalcone, Quaderno Speciale 3, 99-115.

Čermelj, B., Faganeli, J., Ogorelec, B., Dolenec, T., Pezdič, J. & Smodiš, B. 1996: The origin and recycling of sedimented biogenic debris in a subalpine eutrophic lake (Lake Bled, Slovenia). Biogeochemistry 32, 69-91.

Jurkovšek, B., Toman, M., Ogorelec, B., Šribar, Lu., Šribar, Lj. & Poljak, M. & Drobne, K. 1996: Formacijska geološka karta južnega dela Tržaško-komenske planote 1 : 50.000, kredne in paleogenske karbonatne kamnine, IGGG, Ljubljana, 143 p.

Jurkovšek, B., Ogorelec, B., Šribar, Lu. & Drobne, K. 1996: New results of the geological researches of the Trieste-Komen Plateau and comparison with other areas of the Dinaric Carbonate Platform. V: Drobne, K. et al. (ur.): The role of impact processes in the geological and biological evolution of planet Earth: Intern. workshop, Postojna, ZRC SAZU, 125-132.

Drobne, K., Ogorelec, B., Dolenec, T., Marton, E. & Palinkaš, L. 1996: Biota and abiota at the K/T boundary in the Dolenja vas sections, Slovenia. V: Drobne, K. et al. (ur.): The role of impact processes in the geological and biological evolution of planet Earth: Intern. workshop, Postojna, ZRC SAZU, 163-181.

Ogorelec, B., Jurkovšek, B. & Šribar, Lu. 1996: Škrbina (Komen limestone), the first pelagic episode (Cenomanian-Turonian transgression). V: Drobne, K. et al. (ur.): The role of impact processes in the geological and biological evolution of planet Earth : Intern. workshop, Postojna, ZRC SAZU, 183-188.

Ogorelec, B. & Buser, S. 1996: Dachstein limestone from Krn in Julian Alps (Slovenia). Geologija 39, 133-157.

Ogorelec, B., Jurkovšek, B., Šatara, D., Barić, G., Jelen, B. & Kapović, B. 1996: Potencialnost karbonatnih kamnin za nastanek ogljikovodikov v zahodni Sloveniji. Geologija 39, 215-237.

Jurkovšek, B., Kolar-Jurkovšek, T. & Ogorelec, B. 1997: Geologija avtocestnega odseka Divača - Kozina. Annales, Ser. hist. nat. 7/11, 161-186.

Ogorelec, B., Faganeli, J., Mišič, M. & Čermelj, B. 1997: Reconstruction of paleoenvironment in the Bay of Koper: (Gulf of Trieste, northern Adriatic). Annales, Ser. hist. nat. 7/11, 187-200.

Ogorelec, B. & Dozet, S. 1997: Upper Triassic, Jurassic and Lower Cretaceous beds in eastern Sava Folds - Section Laze at Boštanj (Slovenia). Rud.-metal. zb. 44, 3/4, 223-235.

Caffau, M., Pleničar, M. & Ogorelec, B. 1998: Remarks on the morphological variability of Biradiolites angulosus d'Orbigny in a sector of the Trieste Karst (Italy). Geobios 22, 29-36.

Pavlovec, R. & Ogorelec, B. 1998: Geological characteristics of Istrian coast and the Trieste bay. Flows in the Northern Adriatic Sea, Coast Wise Europe Inter. Conf. ž98. Izola, Book of Abstracts).

Ogorelec, B., Pezdič, J. & Dolenec, T. 1998: Mesozoic carbonate rocks in Slovenia : a case study for isotope composition. V: Pezdič, J. (ur.). IV Isotope Workshop of the Europ. Soc. Isotope Res., Portorož, RMZ – Mater. Geoenvir. 45/1-2,132-135.

Jurkovšek, B., Ogorelec, B. & Kolar-Jurkovšek, T. 1999: Spodnjetriasne plasti pri Tehovcu (Polhograjsko hribovje). Geologija 41 (1998), 29-40.

Belocky, R., Slapansky, P., Ebli, O., Ogorelec, B. & Lobitzer, H. 1999: Die Uran-Anomalie in der Trias-Deckscholle des Gaisberg / Kirchberg in Tirol (Österreich) - geophysikalische, geochemische und mikrofazielle Untersuchungen. Abh. Geol. Bundesanst. 56, 2, 13-33.

Ogorelec, B., Orehek, A. & Budkovič, T. 1999: Lithostratigraphy of the Slovenian part of the Ka-

ravanke road tunnel. Abh. Geol. Bundesanst. 56, 2, 99-112.

Turnšek, D., Dolenec, T., Siblik, M., Ogorelec, B., Ebli, O. & Lobitzer, H. 1999: Contributions to the fauna (corals, brachiopods) and stable isotopes of the Late Triassic Steinplatte reef / basin - complex, Northern Calcareous Alps, Austria. Abh. Geol. Bundesanst, 56/2, 121-140.

Jurkovšek, B. Pleničar, M., Ogorelec, B. & Kolar-Jurkovšek, T. 1999: Palaeogeographic development of the Dinaric carbonate platform in western Slovenia. V: Höfling, R. & Steuber, Th. (eds.): V. Int. Cong. on Rudists: abstracts and field trip guides, 3, Univ. Erlangen, 114-118.

Ogorelec, B., Dolenec, T. & Pezdič, J. 2000: Izotopska sestava O in C v mezozojskih karbonatnih kamninah Slovenije - vpliv faciesa in diageneze. Geologija 42 (1999), 171-205.

Dolenec, T., Ogorelec, B., Lojen, S. & Buser, S. 1999: Meja perm - trias v Masorah pri Idriji. RMZ - Mater. Geoenviron. 46/ 3, 449-452.

Faganeli, J., Pezdič, J., Ogorelec, B., Dolenec, T. & Čermelj, B. 1999: Salt works of Sečovlje (Gulf of Trieste, northern Adriatic) - a sedimentological and biogeochemical laboratory for evaporitic environments. RMZ-Mater. Geoenviron. 46/3, 491-499.

Placer, L., Rajver, D., Trajanova, M., Ogorelec, B., Skaberne, D. & Mlakar, I. 2000: Vrtina Ce-2/95 v Cerknem na meji med Južnimi Alpami in Zunanjimi Dinarid. Geologija 43/2, 251-266.

Ogorelec, B., Mišič, M. & Faganeli, J. 2000: Sečoveljske soline - geološki laboratorij v naravi. Ann, Ser. hist. nat., 10/2, 243-252.

Cimerman, F., Ogorelec, B. & Drobne, K. 2000: Foraminifere iz finozrnatih sedimenata Velikog jezera i sedimenata otvorenog mora na rtu Lenga (Otok Mljet, Jadransko more). V: Vlahović, I. & Biondić, R. (ur.): 2. Hrvat. geol. kong., Cavtat, Zbornik radova, Zagreb, IGI, 499 (Abstr.).

Ogorelec, B. & Dozet, S. 2000: Oolitic limestone and dolomite in Mesozoic beds of Slovenia. V: Vlahović, I. & Biondić, R. (ur.): 2. Hrvat. geol. kongr., Cavtat, Zbornik radova, Zagreb, IGI, 509-511.

Ogorelec, B., Drobne, K., Jurkovšek, B., Dolenec, T. & Toman, M. 2001: Paleocene beds of the Liburnia Formation in Čebulovica (Slovenia, NW Adriatic-Dinaric platform). Geologija 44/1, 15-65.

Dolenec, M. & Ogorelec, B. 2001: Organic carbon isotope variability across the P/Tr boundary in the Idrijca Valley section (Slovenia: a high resolution study. Geologija 44/2, 331-340.

Ogorelec, B. 2001: Karbonatne kamnine: njihov nastanek in razširjenost v Sloveniji. Društv. novice (Tržič), 26, 15-20.

Ogorelec, B. & Dozet, S. 2001: V spomin dr. Peru Mioču. Geologija 44/2, 213-216.

Koch, R., Moussavian, E., Ogorelec, B., Skaberne, D. & Bucur, I. I. 2002: Development of a Lithocodium (syn. Bacinella irregularis)-reef-mound - a patch reef within Middle Aptian lagoonal limestone sequence near Nova Gorica (Sabotin Mountain, W-Slovenia). Geologija 45/1, 71-90.

Aničić, B., Ogorelec, B., Kralj, P. & Mišič, M. 2002: Litološke značilnosti terciarnih plasti na Kozjanskem. Geologija 45/1, 213-246.

Ogorelec, B. 2002: Vloga in perspektive geologije v Sloveniji: uvodni referat na 1. Slov. geol. kongr., Črna na Koroškem 9.-11.10.2002. Geologija 45/2, 623-628.

Dolenec, M., Ogorelec, B. & Lojen, S. 2003: Upper Carboniferous to Lower Triassic carbon isotopic signature in carbonate rocks of the Westeren Tethys (Slovenia). Geol. Carpath. 54/4, 217-228.

Dolenec, M., Ogorelec, B. & Lojen, S. 2002: A high resolution study of carbonate and organic carbon isotope variability across the P/Tr boundary in the Idrijca Valley section (Slovenia). IAS Conf., Johanesburg, (Book of Abstracts).

Skaberne, D. & Ogorelec, B. 2003: Žažar Formation, Upper Permian marine transgression over the Val Gardena Formation (Javorjev dol, SW from Cerkno, Western Slovenia). V: Vlahović, I. & Tišljar, J. (eds.): Evolution of depositional environments from the Palaeozoic to the Quaternary in the Karst Dinarides and the Pannonian Basin: field trip guidebook, Zagreb, IGI, 123-125.

Aničić, B., Ogorelec, B. & Dozet, S. 2004: Geološka karta Kozjanskega 1: 50.000. Geol. zav. Slovenije.

Dolenec, T., Ogorelec, B., Dolenec, M. & Lojen, S. 2004: Carbon isotope variability and sedimentology of the Upper Permian carbonate rocks and changes across the Permian-Triassic boundary in the Masore section (Western Slovenia). Facies 50/ 2, 287-299.

Poljak, M., Lapanje, A., Gušić, I., Bole, B. & Ogorelec, B. 2005: Vrtina MET-1/04 pri Metliki na meji med Zunanjimi in Notranjimi Dinaridi. Geologija 48/1, 53-72.

Ogorelec, B., Bole, B., Mišič, M., Leonidakis, J., Faganeli, J. & Čermelj, B. 2005: Recent sediment of Lake Bled (NW Slovenia). RMZ - Mater. geoenviron., 52/1, 1-4.

Ogorelec, B., Baratollo, F. & Drobne, K. 2005: Cretaceous/Tertiary boundary and Paleocene deposits of Trieste Karst and Slovenia, Paleocene marine algae of SW Slovenia (Dolenja vas and Čebulovica). V: Field excursion. Guide book, (Studi Trent. Sci. Nat., Acta Geol. 80, 2003). Trento, 39-64.

Ogorelec, B. 2005: Akademik prof. dr. Mario Pleničar - osemdesetletnik: razpet med Prekmurjem in Krasom. Društv. novice (Tržič), 32, 4-5

Ogorelec, B., Buser, S. & Mišič, M. 2006: Manganovi gomolji v jurskem apnencu Južnih Alp Slovenije. Geologija 49/1, 69-84.

Ogorelec, B., Bole, B., Leonidakis, J., Čermelj, B., Mišič, M. & Faganeli, J. 2006: Recent sediment of Lake Bled (NW Slovenia): sedimentological and geochemical properties. Water, air & soil pollution, Focus, 6, 5/6, 505-513.

Ogorelec, B. 2006: Mikrofacies in diageneza mezozojskih karbonatnih kamnin Slovenije. V: Režun, B. (ur.): 2. slov. geol. kongr., Idrija, Zbornik povzetkov, 70-71.

Drobne, K. & Ogorelec, B. 2006: Geologic oveview of the Paleogene in SW Slovenia. V: Melis, R. et al. (eds.): Giorn. Paleont., Trieste, Guida alle escursioni, Ed. Univ. Trieste, 35-42, 58-61.

Ogorelec, B. & Komac, M. 2006: V spomin prof. dr. Stanku Buserju. Geologija 49/2, 195-203.

Ogrinc, N., Faganeli, J., Ogorelec, B. & Čermelj, B. 2007: The origin of organic matter in holocene sediments in the bay of Koper (Gulf of Trieste, nothern Adriatic sea). Geologija 50/1, 179-188.

Ogorelec, B., Dolenec, T. & Drobne, K. 2007: Cretaceous-Tertiary boundary problem on shallow carbonate platform: carbon and oxygen excursions, biota and microfacies at the K/T boundary sections Dolenja vas and Sopada in SW Slovenia, Adria CP. Palaeogeogr. palaeoclimatol. palaeoecol. 255, 1/2, 64-76.

Drobne, K., Ogorelec, B. & Riccamboni, R. 2007: *Bangiana hanseni* n.gen n.sp. (Forminifera), an index species of Danian age (Lower Paleocene) from the Adriatic carbonate platform (SW Slovenia, NE Italy, Herzegovina). Razpr. - SAZU, Razr. IV, 48/1, 5-71.

Ogorelec, B. 2007: V spomin Karlu Gradu. Geologija 50/1, 5-7.

Ćosović, V., Drobne, K.atica, Ogorelec, B., Moro, A., Koić, M., Šoštarko, I., Tarlao, A. & Tunis, G. 2008: *Decastronema barattoloi* (De Castro), characterisc fossil of the Paleocene and the Eocene peritidal sediments from the Adriatic carbonate platform. Geologia Croatica 61, 2/3, 321-332.

Buser, S. & Ogorelec, B. 2008: Globljevodne triasne in jurske plasti na Kobli. Geologija 51/2, 181-189.

Drobne, K., Ogorelec, B., Pavšič, J. & Pavlovec, R. 2008: Palaeogene and Neogene, Slovenian Tethys basins. V: McCann, T. (ed.): The Geology of Central Europe. London: Geol. Soc., 1093-1098.

Ogorelec, B. 2009: Spodnje jurske plasti v Preserju pri Borovnici. Geologija 52/2, 193-204.

Pleničar, M., Ogorelec, B. & Novak, M. (ur./eds.) 2009: Geologija Slovenije (The Geology of Slovenia). Geološki zavod Slovenije, 612 p., Ljubljana (2011).

Pleničar, M., Ogorelec, B. & Novak, M. 2009: Uvod (Introduction). V: Pleničar, M. et al. (ur./eds.): Geologija Slovenije (The Geology of Slovenia). Geološki zavod Slovenije, 3-20, Ljubljana (2011).

Skaberne, D., Ramovš, A. & Ogorelec, B. 2009: Srednji in zgornji perm (Middle and Upper Permian). V: Pleničar, M. et al. (ur./eds.): Geologija Slovenije (The Geology of Slovenia). Geološki zavod Slovenije, 137-154, Ljubljana (2011).

Drobne, K., Ogorelec, B., Pavšič, J. & Pavlovec, R. 2009: Paleocen in eocen v jugozahodni Sloveniji (Paleocene and Eocene in South-Western Slovenia). V: Pleničar, M. et al. (ur./eds.): Geologija Slovenije (The Geology of Slovenia). Geološki zavod Slovenije, 311-372, Ljubljana (2011).

Ogorelec, B. & Mikuž, V. 2010: V spomin mag. Bogoljubu Aničiću. Geologija 53/2, 114-118.

Kovacs, S. et al. 2010: Triassic environments in the Circum-Pannonian Region related to the initial Neotethyan rifting stage. In: Vozar, J. et al. (eds.): Variscian and Alpine terranes of the Circum-Pannonian Region. Slovak .Acad. Sci. Geol. Inst., 87-156, Bratislava.

Haas, J. et al. 2010: Jurassic environments in the Circum-Pannonian Region. In: Vozar, J. et al. (eds.): Variscian and Alpine terranes of the Circum-Pannonian Region. Slovak .Acad. Sci. Geol. Inst., 157-201, Bratislava.

Tunis, G., Pugliese, N., Jurkovšek, B., Ogorelec, B., Drobne, K., Riccamboni, R. & Tewari, W.C. 2011: Microbialites as Markers of Biotic and Abiotic Events in the Karst District, Slovenia and Italy. In: Tewari, V. & Seckbach, J. (eds.): Stromatolites: Interaction of Microbes with Sediments. Cellular Origin, Life in Extreme Habitats and Astrobiology, Vol. 18/2, Springer Verl., 251-272.

Jež, J., Otoničar, B., Fuček, L. & Ogorelec, B. 2011: Late Cretaceous sedimentary evolution of a northern sector of the Adriatic Carbonate Platform (Matarsko Podolje, SW Slovenia). Facies 57/3, 447-468.

Kovacs, S., Sudar, M., Gradinaru, E., Gawlick, H.-J., Karamata, S., Haas, J., Pero, Cs., Gaetani, M., Mello, J., Polak, M., Aljinović, D., Ogorelec, B., Kolar-Jurkovšek, T., Jurkovšek, B. & Buser, S. 2011: Triassic Evolution of the Tectonostratigraphic Units of the Circum-Pannonian Region. Jb. Geol. B.-A., 151/3+4, Wien, 199-280.

Haas, J., Kovacs, S., Gawlick, H.-J., Gradinaru, E., Karamata, S., Sudar, M., Pero, Cs., Mello, J., Polak, M., Ogorelec, B. & Buser, S. 2011: Jurassic Evolution of the Tectonostratigraphic Units of the Circum-Pannonian Region. Jb. Geol. B.-A., 151/3+4, Wien, 281-353.

Ogorelec, B. 2011: Mikrofacies mezozojskih karbonatnih kamnin Slovenije (Microfacies of Mesozoic Carbonate Rocks of Slovenia). Geologija, 54/2(dod./suppl.), 135 p.

Dozet, S. & Ogorelec, B. 2012: Younger Paleozoic, Mesozoic and Tertiary oolitic and oncolitic beds in Slovenia – An Overview. Geologija, 55/2, 181-208.

Navodila avtorjem

GEOLOGIJA objavlja znanstvene in strokovne članke s področja geologije in sorodnih ved. Revija od leta 2000 izhaja dvakrat letno. Članke recenzirajo domači in tuji strokovnjaki z obravnavanega področja. Ob oddaji člankov avtorji predlagajo **tri recenzente**, vendar pa si uredništvo pridržuje pravico do izbire recenzentov po lastni presoji. Avtorji morajo članek popraviti v skladu z recenzentskimi pripombami ali utemeljiti zakaj se z njimi ne strinjajo.

Avtorstvo: Za izvirnost podatkov, predvsem pa mnenj, idej, sklepov in citirano literaturo so odgovorni avtorji. Z objavo v GEOLOGIJI se tudi obvežejo, da ne bodo drugje objavili prispevka z isto vsebino.

Jezik: Članki naj bodo napisani v angleškem, izjemoma v slovenskem jeziku, vsi pa morajo imeti slovenski in angleški izvleček. Za prevod poskrbijo avtorji prispevkov sami.

Vrste prispevkov:

Izvirni znanstveni članek
Izvirni znanstveni članek je prva objava originalnih raziskovalnih rezultatov v takšni obliki, da se raziskava lahko ponovi, ugotovitve pa preverijo. Praviloma je organiziran po shemi IMRAD (**I**ntroduction, **M**ethods, **R**esults, **A**nd **D**iscussion).

Pregledni znanstveni članek
Pregledni znanstveni članek je pregled najnovejših del o določenem predmetnem področju, del posameznega raziskovalca ali skupine raziskovalcev z namenom povzemati, analizirati, evalvirati ali sintetizirati informacije, ki so že bile publicirane. Prinaša nove sinteze, ki vključujejo tudi rezultate lastnega raziskovanja avtorja.

Strokovni članek
Strokovni članek je predstavitev že znanega, s poudarkom na uporabnosti rezultatov izvirnih raziskav in širjenju znanja.

Diskusija in polemika
Prispevek, v katerem avtor ocenjuje ali dokazuje pravilnost nekega dela, objavljenega v GEOLOGIJI ali z avtorjem strokovno polemizira.

Recenzija, prikaz knjige
Prispevek, v katerem avtor predstavlja vsebino nove knjige.

Oblika prispevka: Besedilo pripravite v urejevalniku Microsoft Word. Prispevki naj praviloma ne bodo daljši od 20 strani formata A4, v kar so vštete tudi slike, tabele in table. Le v izjemnih primerih je možno, ob predhodnem dogovoru z uredništvom, tiskati tudi daljše prispevke.

Članek oddajte uredništvu vključno z vsemi slikami, tabelami in tablami v elektronski obliki po naslednjem sistemu:

- *Naslov članka (do 12 besed)*
- *Avtorji (ime in priimek, naslov, e-mail naslov)*
- *Ključne besede (do 7 besed)*
- *Izvleček (do 300 besed)*
- *Besedilo*
- *Literatura*
- *Podnaslovi k slikam in tabelam*
- *Tabele, Slike, Table*

Citiranje: V literaturi naj avtorji prispevkov praviloma upoštevajo le tiskane vire. Poročila in rokopise naj navajajo le v izjemnih primerih, z navedbo kje so shranjeni. V seznamu literature naj bodo navedena samo v članku omenjena dela. Citirana dela, ki imajo DOI identifikator, morajo imeti ta identifikator izpisan na koncu citata. Za citiranje revije uporabljamo standardno okrajšavo naslova revije. Med besedilom prispevka citirajte samo avtorjev priimek, v oklepaju pa navajajte letnico izida navedenega dela in po potrebi tudi stran. Če navajate delo dveh avtorjev, izpišite med tekstom prispevka oba priimka (npr. Pleničar & Buser, 1967), pri treh ali več avtorjih pa napišite samo prvo ime in dodajte et al. z letnico (npr. Mlakar et al., 1992). Citiranje virov z medmrežja v primeru, kjer avtor ni poznan zapišemo (Internet 1). V seznamu literaturo navajajte po abecednem redu avtorjev.

Imena fosilov (rod in vrsta) naj bodo napisana poševno, imena višjih taksonomskih enot (družina, razred, itn.) pa normalno. Imena avtorjev taksonov naj bodo prav tako napisana normalno, npr. *Clypeaster pyramidalis* Michelin, *Galeanella tollmanni* (Kristan), Echinoidea.

Primeri citiranja članka:

Mali, N., Urbanc, J. & Leis, A. 2007: Tracing of water movement through the unsaturated zone of a coarse gravel aquifer by means of dye and deuterated water. Environ. geol., 51/8: 1401–1412, doi:10.1007/s00254-006-0437-4.

Pleničar, M. 1993: *Apricardia pachiniana* Sirna from lower part of Liburnian beds at Divača (Triest-Komen Plateau). Geologija, 35: 65–68.

Primer citirane knjige:

Flügel, E. 2004: Mikrofacies of Carbonate Rocks. Springer Verlag, Berlin: 976 p.

Jurkovšek, B., Toman, M., Ogorelec, B., Šribar, L., Drobne, K., Poljak, M. & Šribar, Lj. 1996: Formacijska geološka karta južnega dela Tržaško-komenske planote – Kredne in paleogenske kamnine 1 : 50.000 = Geological map of the southern part of the Trieste-Komen plateau – Cretaceous and Paleogene carbonate rocks. Geološki zavod Slovenije, Ljubljana: 143 p., incl. Pls. 23, 1 geol. map.

Primer citiranja poglavja iz knjige:

Turnšek, D. & Drobne, K. 1998: Paleocene corals from the northern Adriatic platform. In: Hottinger, L. & Drobne, K. (eds.): Paleogene Shallow Benthos of the Tethys. Dela SAZU, IV. Razreda, 34/2: 129-154, incl. 10 Pls.

Primer citiranja virov z medmrežja:

Če sta znana avtor in naslov citirane enote zapišemo: Čarman, M. 2009: Priporočila lastnikom objektov, zgrajenih na nestabilnih območjih. Internet: http://www.geo-zs.si/UserFiles/1/File/Nasveti_lastnikom_objektov_na_nestabilnih_tleh.pdf (17. 1. 2010)

Če avtor ni poznan zapišemo tako:
Internet: http://www.geo-zs.si/ (22.10.2009)

Če se navaja več enot z medmrežja, jim dodamo še številko
Internet 1: http://www.geo-zs.si/ (15.11.2000)
Internet 2: http://www.geo-zs.si/ (10.12.2009)

Slike, tabele in table: Slike (ilustracije in fotografije), tabele in table morajo biti zaporedno oštevilčene in označene kot sl. 1, sl. 2 itn., oddane v formatu TIFF, JPG ali EPS z ločljivostjo 300 dpi. Le izjemno je možno objaviti tudi barvne slike, vendar samo po predhodnem dogovoru z uredništvom. Obvezno je treba upoštevati zrcalo revije **172 x 235 mm**. Večjih formatov od omenjenega zrcala GEOLOGIJE ne tiskamo na zgib, je pa možno, da večje oziroma daljše slike natisnemo na dveh straneh (skupaj na levi in desni strani) z vmesnim »rezom«. V besedilu prispevka morate omeniti vsako sliko po številčnem vrstnem redu. Dovoljenja za objavo slikovnega gradiva iz drugih revij publikacij in knjig, si pridobijo avtorji sami. Table pripravite v formatu zrcala naše revije.

Če je članek napisan v slovenskem jeziku mora imeti celotno besedilo, ki je na slikah in tabelah tudi v angleškem jeziku. Podnaslovi naj bodo čim krajši.

Korekture: Te opravijo avtorji člankov, ki pa lahko popravijo samo tiskarske napake. Krajši dodatki ali spremembe pri korekturah so možne samo na avtorjeve stroške.

Avtorji prejmejo 25 separatov brezplačno, sicer pa so prispevki dostopni tudi na internetnih straneh http://www.geo-zs.si/slo-text/geologija.htm.

Oddajanje prispevkov:

Avtorje prosimo, da prispevke pošljejo na naslov uredništva:
GEOLOGIJA
Geološki zavod Slovenije
Dimičeva ulica 14, 1000 Ljubljana
bernarda.bole@geo-zs.si ali urednik@geologija-revija.si

Uredništvo Geologije

Instructions for authors

Scope of the journal: GEOLOGIJA publishes scientific papers which contribute to understanding of the geology of Slovenia or to general understanding of all fields of geology. Some shorter contributions on technical or conceptual issues are also welcome. Occasionally, a collection of symposia papers is also published.
All submitted manuscripts are sent for review by at least two specialists. When submitting their paper, authors should recommend at least **three reviewers**. Note that the editorial office retains the sole right to decide whether or not the suggested reviewers are used. Authors should correct their papers according to the instructions given by the reviewers. Should you disagree with any part of the reviews, please explain why. Revised manuscript will be reconsidered for publication.

Author's declaration: Submission of a paper for publication in Geologija implies that the work described has not been published previously, that it is not under consideration for publication elsewhere and that, if accepted, it will not be published elsewhere.

Language: Papers should be written in English or Slovene, and should have both English and Slovene abstracts.

Types of papers:

Original scientific paper
In an original scientific paper, original research results are published for the first time and in such a form that the research can be repeated and the results checked. It should be organised according to the IMRAD scheme (**I**ntroduction, **M**ethods, **R**esults, **A**nd **D**iscussion).

Review scientific paper
In an overview scientific paper the newest published works on specific research field or works of a single researcher or a group of researchers are presented in order to summarise, analyse, evaluate or synthesise previously published information. However, it should contain new information and/or new interpretations.

Professional paper
Technical papers give information on research results that have already been published and emphasise their applicability.

Discussion paper
A discussion gives an evaluation of another paper, or parts of it, published in GEOLOGIJA or discusses its ideas.

Book review
This is a contribution that presents a content of a new book in the field of geology.

Style guide:
Submitted manuscripts should not exceed 20 pages of A4 format (12 pt typeface, 1 line-spacing, left justification) including figures, tables and plates. Only exceptionally and in agreement with the editorial board longer contributions can also be accepted.
Manuscripts submitted to the editorial office should include figures, tables and plates in electronic format ordered according to the following scheme:

- *Title (maximum 12 words)*
- *Authors (full name and family name, postal address and e-mail address)*
- *Key words (maximum 7 words)*
- *Abstract (maximum 300 words)*
- *Text*
- *References*
- *Figure and Table Captions*
- *Tables, Figures, Plates*

References: References should be cited in the text as follows: (Flügel, 2004) for a single author, (Pleničar & Buser, 1967) for two authors and (Mlakar et al., 1992) for multiple authors. Pages and figures should be cited as follows: (Pleničar, 1993, p. 67) and (Pleničar, 1993, fig. 1). Anonymous internet resources should be cited as (Internet 1). Only published references should be cited. Manuscripts should be cited only in some special cases in which it also has to be stated where they are kept. Cited reference list should include only publications that are mentioned in the paper. Authors should be listed alphabetically. Journal titles should be given in standard abbreviated form. A doi identifier, if there is any, should be placed at the end as shown in the first case.
Taxonomic names should be in italics, while names of the authors of taxonomic names should be in normal, such as *Clypeaster pyramidalis* Michelin, *Galeanella tollmanni* (Kristan), Echinoidea.

Articles should be listed as follows:

Mali, N., Urbanc, J. & Leis, A. 2007: Tracing of water movement through the unsaturated zone of a coarse gravel aquifer by means of dye and deuterated water. Environ. geol., 51/8: 1401–1412, doi:10.1007/s00254-006-0437-4.

Pleničar, M. 1993: *Apricardia pachiniana* Sirna from lower part of Liburnian beds at Divača (Triest-Komen Plateau). Geologija, 35: 65–68.

Books should be listed as follows:

Flügel, E. 2004: Mikrofacies of Carbonate Rocks. Springer Verlag, Berlin: 976 p.

Jurkovšek, B., Toman, M., Ogorelec, B., Šribar, L., Drobne, K., Poljak, M. & Šribar, Lj. 1996: Formacijska geološka karta južnega dela Tržaško-komenske planote – Kredne in paleogenske kamnine 1 : 50.000 = Geological map of the southern part of the Trieste-Komen plateau – Cretaceous and Paleogene carbonate rocks. Geološki zavod Slovenije, Ljubljana: 143 p., incl. Pls. 23, 1 geol. map.

Book chapters should be listed as follows:

Turnšek, D. & Drobne, K. 1998: Paleocene corals from the northern Adriatic platform. In: Hottinger, L. & Drobne, K. (eds.): Paleogene Shallow Benthos of the Tethys. Dela SAZU, IV. Razreda, 34/2: 129-154, incl. 10 Pls.

Internet resources should be listed as follows:
Known author and title:
Čarman, M. 2009: Priporočila lastnikom objektov, zgrajenih na nestabilnih območjih. Internet: http://www.geo-zs.si/UserFiles/1/File/Nasveti_lastnikom_objektov_na_nestabilnih_tleh.pdf (17. 1. 2010)
Unknown authors and title:
Internet: http://www.geo-zs.si/ (22.10.2009)
When more than one unit from the internet are cited they should be numbered:
Internet 1: http://www.geo-zs.si/ (15.11.2000)
Internet 2: http://www.geo-zs.si/ (10.12.2009)

Figures, tables and plates: Figures (illustrations and photographs), tables and plates should be numbered consequently and marked as Fig. 1, Fig. 2 etc., and saved as TIFF, JPG or EPS files and submitted at 300 dpi. Colour pictures will be published only on the basis of previous agreement with the editorial office. The maximum size of full-page illustrations and tables is **172 x 235 mm**. Larger formats can only be printed as a double-sided illustration (left and right) with a cut in the middle. All figures should be referred to in the text and should normally be numbered in the sequence in which they are cited. The approval for using illustrations previously published in other journals or books should be obtained by each author.
When a paper is written in Slovene it has to have the entire text which accompanies illustrations and tables written both in Slovene and English. Figure and table captions should be kept as short as possible.

Proofs: One set of page proofs (as pdf files) will be sent by e-mail to the corresponding author. Corrections are made by the authors. They should correct only typographical errors. Short additions and changes are possible but should paid by the authors.

Offprints: Authors receive 25 offprints free of charge. As Geologija is an open access journal, all pdfs can be downloaded from its website: http://www.geo-zs.si/slo-text/geologija.htm.

Submission: Authors should submit their papers to the address of the editorial office:

GEOLOGIJA
Geological Survey of Slovenia
Dimičeva ulica 14, 1000 Ljubljana, Slovenia
bernarda.bole@geo-zs.si or urednik@geologija-revija.si

The Editorial Office

GEOLOGIJA

št.: 56/1, 2013

www.geologija-revija.si

ISSN 0016-7789

Geološki zavod Slovenije
Geological Survey of Slovenia
www.geo-zs.si